

**Stable iron isotope variations in higher plants -  
systematics and controls**

Von der Naturwissenschaftlichen Fakultät der  
Gottfried Wilhelm Leibniz Universität Hannover

zur Erlangung des Grades

Doktorin der Naturwissenschaften

Dr. rer. nat.

genehmigte Dissertation

von

**Dipl.-Geow. Monika Stelling** (geb. Gülke)

geboren am 10.11.1979 in Hannover

**2010**

Referent: Prof. Dr. Friedhelm von Blanckenburg (GFZ Potsdam)

Koreferenten: Prof. Dr. Hartmut Stützel (Leibniz Universität Hannover)

Prof. Dr. Nicolaus von Wirén (IPK Gatersleben)

Mitglieder der Prüfungskommission:

Prof. Dr. Jürgen Böttcher (Vorsitzender)

Prof. Dr. Friedhelm von Blanckenburg

Prof. Dr. Hartmut Stützel

Tag der Promotion: 22.12.2010

## **Erklärung zur Dissertation**

Hiermit versichere ich, dass ich die Dissertation „Stable iron isotope variations in higher plants - systematics and controls“ selbstständig verfasst und alle benutzten Hilfsmittel und Quellen sowie evtl. zur Hilfeleistung herangezogene Institutionen vollständig angegeben habe. Die Dissertation wurde nicht schon als Diplomarbeit oder ähnliche Prüfungsarbeit verwendet.

Walzbachtal, den 21.09.2010

Monika Stelling



*If we knew what it was we were doing,  
It would not be called research, would it?*

Albert Einstein

---

# Ich danke...

**Prof. Dr. Friedhelm von Blanckenburg** für die Initiierung des DFG-Projekts, die Möglichkeit in diesem innovativen und interdisziplinären Projekt arbeiten zu können, für seine Betreuung des Projekts, sein Vertrauen, seine Geduld, seine fachliche Kompetenz, seine immerwährende Motivation und die vielen produktiven Diskussionen und Anregungen!

**Prof. Dr. Nicolaus von Wirén** für sein Interesse an meiner Arbeit, die Möglichkeit so viele Experimente an seinem Institut machen zu können, das Vertrauen, die vielen produktiven Gespräche, fachlichen Tipps und für das Übernehmen des Ko-Referats.

**Prof. Dr. Hartmut Stützel** für das Interesse an meiner Arbeit, die Möglichkeit des Pflanzenanbaus an seinem Institut, die Diskussionen, die stetige Hilfsbereitschaft und für das Übernehmen des Ko-Referats.

**Dr. Enrico Scheuermann** für die gute Zusammenarbeit, die Pflanzenanzucht in Hohenheim, die vielen netten und produktiven Treffen, Diskussionen und Telefonate.

**Elke Neitzel-Rode** für die Hilfe bei der Pflanzenanzucht in Hannover und die guten Tipps.

**Prof. Dr. Ronny Schönberg** für die Einweisung an der Neptune, das Interesse an meiner Arbeit, die vielen Tipps und Tricks und die Motivation.

**Dr. Ingo Horn** für die Hilfe an der Neptune.

**Prof. Dr. Michael Staubwasser** für die Hilfe im Labor und die vielen fachlichen Ratschläge.

**Florian, Sonja und Michaela**, meinen HiWis im Laufe der Jahre, die mir bei der Ernte und im Labor so gut und zuverlässig geholfen haben.

**Alexandra Tangen** für ihre Hilfe im Labor, die vielen Tipps, das Zuhören und die guten Gespräche (nicht nur über die Arbeit).

**Allen Mitarbeitern des Instituts für Mineralogie** für die schöne Arbeits-Atmosphäre, die netten Mi-Frei-Tee Runden, das Interesse an meiner Arbeit und die gemeinsamen Feiern.

**Der ehemaligen „Isotopengeochemie-Gruppe“**, insbesondere den ehemaligen Doktoranden Jan Sch., Hella, Kevin, Grit und Sonja für anregende Diskussionen, gemeinsame Aktivitäten und für die lustige Atmosphäre im und außerhalb des *clean lab*.

**Meinen Büromädels Grit und Sonja** (!) für die vielen schönen gemeinsamen Stunden, das Tee-trinken, diskutieren (nicht nur über die Arbeit), die Motivation, die vielen Tipps vor allem die Neptune und Chemie-Fragen betreffend und alle gemeinsamen Aktivitäten!

**Andrea und Stephan** für das Tjede-hüten in den letzten Wochen.

**Meiner Familie (Gülke und Stelling) und meinen Freunden** für die Unterstützung und Motivation in allen Lebenslagen.

**Jan** für seine Unterstützung, seine Motivation, seine Tipps, den Glauben an meine wissenschaftlichen Fähigkeiten und vieles mehr.

**Tjede**, dafür dass sie da ist, für ihr Lachen, und dass sie mir gezeigt hat, was wirklich wichtig ist.

*Diese Arbeit ist für Dich!*

# Table of Contents

<b>Table of Contents .....</b>	<b>i</b>
<b>Abstract.....</b>	<b>1</b>
<b>Zusammenfassung.....</b>	<b>5</b>
<b>1 Introduction .....</b>	<b>9</b>
1.1 Objectives.....	9
1.2 Organization of the thesis.....	11
1.3 Iron in plants.....	13
1.4 Stable iron isotopes .....	22
1.4.1 Principles of stable isotope fractionation .....	22
1.4.2 Stable iron isotopes .....	29
<b>2 Fractionation of stable iron isotopes in higher plants.....</b>	<b>39</b>
2.1 Abstract .....	39
2.2 Introduction .....	39
2.3 Materials and methods .....	41
2.3.1 Plant growth .....	41
2.3.2 Soils.....	42
2.3.3 Sample preparation.....	42
2.3.4 Iron isotope measurements.....	43
2.4 Results and discussion.....	43
2.5 Conclusions .....	50
<b>3 Determining the stable Fe isotope signature of plant-available iron in soils .....</b>	<b>53</b>
3.1 Abstract .....	53
3.2 Introduction .....	53
3.2.1 Iron and its isotopes in soil.....	55
3.2.2 Experimental strategies for the extraction of iron pools from soils .....	57
3.3 Materials and Methods .....	60
3.3.1 Soil characteristics and plant samples.....	60
3.3.2 Iron extraction from soil fractions.....	62
3.3.3 Digestion of plant samples .....	65

3.3.4	Iron separation.....	65
3.3.5	Iron isotope ratio measurements and reproducibility.....	66
3.4	Results.....	67
3.4.1	Iron concentrations in the different mineral pools.....	67
3.4.2	Iron isotope signature of bulk soils.....	68
3.4.3	Iron isotope signature of the different Fe pools in soils.....	70
3.5	Discussion.....	72
3.5.1	Comparison between the two extraction procedures.....	72
3.5.2	Determination of the iron isotope signature of plant-available soil iron.....	77
3.6	Conclusions.....	81
<b>4</b>	<b>Identification of differences in iron metabolism between strategy I and II plants as revealed by the distribution of stable iron isotopes during plant growth.....</b>	<b>83</b>
4.1	Abstract.....	83
4.2	Introduction.....	84
4.3	Principles of iron uptake and transport by plants and iron isotope systematics.....	85
4.4	Materials and Methods.....	89
4.4.1	Plant growth with nutrient solution.....	89
4.4.2	Sample decomposition and iron separation.....	89
4.4.3	Iron isotope measurements.....	91
4.5	Results.....	92
4.5.1	Bean.....	93
4.5.2	Oat.....	97
4.6	Discussion.....	99
4.6.1	Iron isotope fractionation in strategy I plants.....	99
4.6.2	Iron isotope fractionation in strategy II plants.....	102
4.7	Conclusions and potential applications.....	105
<b>5</b>	<b>Deciphering mechanisms of iron acquisition and retranslocation in maize using stable iron isotope fractionation.....</b>	<b>107</b>
5.1	Aim of the study.....	107
5.2	Materials and Methods.....	107
5.2.1	Experiments.....	107
5.2.2	Nutrient solution.....	111



5.2.3	SPAD value .....	112
5.2.4	Sample decomposition and iron separation.....	113
5.2.5	Iron isotope measurements.....	113
5.3	Results .....	114
5.3.1	Experiment 1: Maize sequential harvest .....	114
5.3.2	Experiment 2: Maize supplied with phytosiderophores from wheat.....	116
5.3.3	Experiment 3: Maize plants for Bienfait solution (Fe(III)-EDTA).....	117
5.3.4	Experiment 4: Maize supplied with phytosiderophores from wheat, <sup>58</sup> Fe tracer experiment.....	119
5.3.5	Experiment 5: Maize grown on a soil substrate .....	122
5.4	Discussion .....	124
5.4.1	Isotope fractionation during acquisition of iron.....	124
5.4.2	Isotope fractionation during (re-)translocation of iron.....	126
5.5	Conclusion.....	128
5.6	Tables .....	130
<b>6</b>	<b>References .....</b>	<b>139</b>
	<b>Lebenslauf.....</b>	<b>153</b>
	<b>Publikationen.....</b>	<b>154</b>



## Abstract

Iron is the fourth-most abundant element in the Earth's crust and an essential nutrient for all living organisms. The mass-dependent shift in the relative abundances of the stable iron isotopes  $^{54}\text{Fe}$ ,  $^{56}\text{Fe}$ ,  $^{57}\text{Fe}$  and  $^{58}\text{Fe}$  is induced by changes in the binding energy and by kinetic effects. With the advent of multiple-collector inductively coupled plasma mass spectrometers (MC-ICP-MS) it became possible to determine the natural variations of iron isotope ratios with a precision of better than 0.05 ‰ in  $\delta^{56}\text{Fe}$  ( $\delta^{56}\text{Fe}/\text{‰} = [({}^{56}/{}^{54}\text{Fe}_{\text{sample}}/{}^{56}/{}^{54}\text{Fe}_{\text{IRMM-014}}) - 1] \cdot 10^3$ ). In nature variations of up to 5 ‰ have been found so far. Up to now the research of stable iron isotope fractionation has mainly taken place in the domain of Geosciences. Little is known about the nature and extent of iron isotope fractionation in the biosphere, especially in higher plants. Consequently, the objective of this thesis is to identify the stable iron isotope variations in higher plants and the determination of the isotopic difference between plants and the substrate they grow on, as well as to identify isotope distribution patterns and fractionation factors. Another aim of this thesis is to elucidate the mechanisms which lead to Fe isotope variations in plants and to test whether stable iron isotopes are an adequate tool to study uptake and translocation processes in higher plants.

Several studies were designed to address these issues. In the first study several legumes were grown on two types of soil, different plant organs were harvested and the  $\delta^{56}\text{Fe}$  values were determined. It appeared that strategy I plants, which rely on reduction of iron before uptake, are enriched in the lighter iron isotopes by up to 1.6 ‰ compared to the standard IRMM-014, and show the trend that younger plant organs obtain lighter iron than older parts. In contrast, strategy II plants, which rely on chelation of iron by exuded phytosiderophores, are only slightly enriched in the heavier iron isotopes and show uniform compositions in all plant organs.

In the second study the iron isotope composition of the iron of the soils where these plants grew on was determined that is most likely available to supply the plants. The iron isotope ratio of bulk soils was measured and two different sequential extraction methods, designed to resolve the iron isotope signature of various soil fractions, were tested. The pools which contribute most to plant nutrition are about 0.3 ‰ lighter than the bulk soils. The isotope composition of this supposedly plant-available iron was compared to that of the plants grown on the soils. While redox and other transformation processes in the rhizosphere enrich

strategy I plants to varying degrees in light iron isotopes, strategy II plants exhibit a uniform iron isotopic composition and are only slightly enriched in the heavier iron isotopes by about 0.3 ‰ compared to the plant-available soil iron. Therefore these plants may record the iron isotope composition of plant-available iron in soils, to which the composition of strategy I plants can be compared to.

Next it was examined how the iron isotope compositions of plants evolve during growth. For this reason bean and oat as representatives of strategy I and II plants were grown on a nutrient solution supplied with Fe(III)-EDTA and were harvested at least at three different points in time. Total bean plants are enriched in the light iron isotopes. Younger leaves contain lighter iron than older ones, and during growth younger leaves further accumulate the lighter isotopes whereas older leaves and the total roots are simultaneously depleted in light iron isotopes. This indicates that isotope fractionation is a result of translocation or re-translocation processes. Oat plants are also enriched in the light iron isotopes. An explanation for this enrichment of light iron isotopes, which is in contrast with that found in strategy II plants grown on soil in the previous study is the prevalence of a constitutive reductive uptake mechanism of iron in the nutrient solution used as this is non-deficient in iron. In contrast iron availability in the natural aerated soils used in the previous study was low. However, during growth of the oat plants the initial isotope ratio obtained during the first uptake is maintained in all organs at all growth stages, including the roots. The absence of fractionation of iron isotopes during the translocation of iron in strategy II plants hints at a difference in translocation mechanisms between strategy I and II plants.

Results of these studies provide support to the hypothesis that stable metal isotopes potentially serve as a new tool to identify the physiological mechanisms of metal uptake and translocation in plants.

This tool of stable iron isotope fractionation was applied to identify the mechanisms of iron translocation in maize. Iron isotope data of various experiments with maize as a representative of strategy II plants are presented. Maize was grown in a nutrient solution with known iron isotopic signature as well as in an isotopically spiked nutrient solution, without iron in the nutrient solution and on a soil substrate. The obtained  $\delta^{56}\text{Fe}$  values clearly reveal that maize retranslocates iron from older leaves into younger plant parts independent from the iron status of the plant. Furthermore it is shown that the direction and the extent of iron isotope

fractionation during iron acquisition by maize plants depends on the form of iron supply and therefore iron availability.

The results of this thesis demonstrate that the uptake of iron by plants from soil and its translocation inside the plant are important sources of isotopic variations in the biogeochemical cycle of iron. In addition it is shown that stable iron isotopes can serve as an adequate tool in plant physiology.

**Keywords:** Iron isotope fractionation, higher plants, MC-ICP-MS



## Zusammenfassung

Eisen ist das vierthäufigste Element der Erdkruste und essentieller Nährstoff für alle lebenden Organismen. Die massenabhängige Verschiebung in den relativen Häufigkeiten der stabilen Eisenisotope  $^{54}\text{Fe}$ ,  $^{56}\text{Fe}$ ,  $^{57}\text{Fe}$  und  $^{58}\text{Fe}$  wird durch Änderungen in der Bindungsenergie und durch kinetische Effekte hervorgerufen. Seit der Einführung von Multikollektor-Plasma-Massenspektrometern (MC-ICP-MS) ist es möglich, die natürlichen Variationen im Eisenisotopenverhältnis bis auf eine Genauigkeit von 0,05 ‰ zu bestimmen. Bislang wurden in der Natur Variationen von etwa 5 ‰ für das  $^{56}\text{Fe}/^{54}\text{Fe}$  Verhältnis (dargestellt als  $\delta^{56}\text{Fe}/[\text{‰}] = \left( \frac{^{56}\text{Fe}_{\text{sample}}}{^{56}\text{Fe}_{\text{IRMM-014}}} - 1 \right) \cdot 10^3$ ) beobachtet. Diese Entdeckung wurde bislang hauptsächlich von Geowissenschaftlern genutzt. Bisher ist wenig über die Art und das Ausmaß der Eisenisotopenfraktionierung in der Biosphäre, vor allen in höheren Pflanzen, bekannt. Daher ist es Ziel dieser Arbeit, die Variationen in den stabilen Eisenisotopenverhältnissen in höheren Pflanzen zu identifizieren. Dabei soll die isotopische Differenz zwischen Pflanzen und dem Substrat, auf dem sie wachsen, bestimmt, sowie Muster und Fraktionierungsfaktoren identifiziert werden. Außerdem sollen die Mechanismen, die zur Eisenisotopenfraktionierung führen, herausgestellt werden und es soll gezeigt werden, ob stabile Eisenisotope ein geeignetes Werkzeug darstellen, mit dem man die Aufnahme- und Translokationprozesse in Pflanzen untersuchen kann.

Diese Themen wurden in mehreren Studien behandelt. In der ersten Studie wurden ausgewählte Gemüse- und Getreidesorten auf zwei Bodenarten angepflanzt, verschiedene Pflanzenteile geerntet und der  $\delta^{56}\text{Fe}$  Wert bestimmt. Dabei zeigte sich, dass Strategie I Pflanzen, die Eisen mithilfe einer vorherigen Reduktion aufnehmen, um bis zu 1,6 ‰ in den leichten Isotopen angereichert sind und dass tendenziell jüngere Pflanzenteile leichteres Eisen beinhalten als ältere. Im Gegensatz dazu sind Strategie II Pflanzen, die Phytosiderophore ausscheiden, welche dreiwertiges Eisen zur Aufnahme chelatisieren, nur leicht in den schweren Eisenisotopen angereichert und alle Pflanzenteile zeigen ähnliche  $^{56/54}\text{Fe}$  Verhältnisse.

In einer weiteren Studie wurde die eisenisotopische Zusammensetzung des Eisens der Böden bestimmt, auf denen die Pflanzen gewachsen sind und das am wahrscheinlichsten von Pflanzen aufgenommen wird. Dazu wurde das  $^{56/54}\text{Fe}$  Verhältnis der Gesamtböden gemessen und zwei verschiedene sequentielle Extraktionsmethoden getestet, um die

Eisenisotopenzusammensetzung verschiedener Eisen-Fractionen in den Böden zu bestimmen. Die Eisen-Fractionen, die den größten Anteil an pflanzenverfügbaren Eisens ausmachen, sind um 0,3 ‰ in den leichten Eisenisotopen gegenüber dem Gesamtboden angereichert. Diese Eisenisotopenzusammensetzung wurde mit der der Pflanzen verglichen, die auf den Böden gewachsen sind. Strategie I Pflanzen werden durch Redox- und andere Transformationsprozesse in der Rhizosphäre verschieden stark in den leichten Eisenisotopen angereichert. Strategie II Pflanzen hingegen sind um 0,3 ‰ in den schweren Isotopen angereichert und zeigen ähnliche  $^{56/54}\text{Fe}$  Verhältnisse in allen Pflanzenteilen. Es kann daher geschlossen werden, dass Strategie II Pflanzen die Eisenisotopenzusammensetzung des pflanzenverfügbaren Eisens im Boden anzeigen können, mit der dann die der Strategie I Pflanzen verglichen werden kann.

Des Weiteren wurde untersucht, wie sich die Eisenisotopenzusammensetzung von Pflanzen während des Wachstums entwickelt. Zu dem Zweck wurden Bohne und Hafer als Vertreter von Strategie I und II Pflanzen auf einer Fe(III)-EDTA enthaltenden Nährlösung angepflanzt und bei verschiedenen Wachstumsstadien geerntet. Dabei konnte beobachtet werden, dass Bohnen-Pflanzen in den leichten Eisenisotopen gegenüber der Nährlösung angereichert sind und dass tendenziell jüngere Pflanzenteile leichteres Eisen enthalten als ältere. Während des Wachstums werden die älteren Blätter in den schwereren Eisenisotopen angereichert, während Eisen in den jüngeren Blättern immer leichter wird. Das lässt darauf schließen, dass jüngere Blätter ihr Eisen nicht nur aus der Nährlösung, sondern auch aus Speichermolekülen älterer Blättern beziehen. Es wird vermutet, dass die beobachteten Muster aus einer Eisen Reduktion vor der Aufnahme in die Pflanze und aus Reduktion von Eisen bei der nicht quantitativen Mobilisierung aus Speichermolekülen resultieren. Da diese Muster in der Strategie II Pflanze Hafer nicht sichtbar sind, kann geschlossen werden, dass die Translokationsmechanismen von Eisen innerhalb der beiden Pflanzentypen, zumindest bei ausreichender Eisernahrung, unterschiedlich sind. Des Weiteren ist Hafer, im Gegensatz zu den Ergebnissen der bisherigen Studie, in den leichten Isotopen um 0,4 ‰ angereichert. Dieser Unterschied wird mit dem Einfluss der Eisenspeziation im Boden oder der Nährlösung, und damit der Eisenverfügbarkeit, erklärt. Dies verdeutlicht, dass die Eisenisotopensignatur von Pflanzen nicht nur von der jeweiligen Aufnahmestrategie abhängt, sondern auch von der Eisenverfügbarkeit im Substrat. All diese Resultate führten zu der Idee, dass stabile Eisenisotopenfraktionierung als ein neues Werkzeug in der Pflanzenphysiologie eingesetzt werden könnte.



Mit diesem neuen Werkzeug der Eisenisotopenfraktionierung sollten dann die Eisen-Aufnahme- und Translokations-Mechanismen in Mais identifiziert werden. Dazu wurde Mais in einer Nährlösung mit bekanntem Isotopenverhältnis, ohne Eisen in der Nährlösung, in einer im Isotop  $^{58}\text{Fe}$  angereicherten Nährlösung und auf Boden angezogen. Die gemessenen Eisenisotopenverhältnisse zu verschiedenen Erntezeitpunkten zeigen deutlich, dass Mais Eisen unabhängig vom Eisenstatus der Pflanze von Blattstufe zu Blattstufe umlagert und dass die Richtung und das Ausmaß der Eisenisotopenfraktionierung während der Eisenaufnahme von der angebotenen Eisenform und damit der Eisenverfügbarkeit abhängt.

Die Ergebnisse dieser Arbeit zeigen, dass die pflanzliche Eisenaufnahme und die Eisenumlagerung in der Pflanze bedeutende Quellen isotopischer Variationen im biogeochemischen Zyklus des Eisens darstellen. Es wird außerdem gezeigt, dass stabile Eisenisotope als neues Werkzeug in der Pflanzenphysiologie dienen können.

Schlagwörter: Eisenisotopenfraktionierung, höhere Pflanzen, MC-ICP-MS



# 1 Introduction

## 1.1 Objectives

Fractionation of the stable iron isotopes provides a new geochemical tool that promises to be useful for many basic and applied research questions in the Earth, Environmental and Biological Sciences. The analytical methods to resolve mass-dependent variations in the abundances of iron isotopes in nature have only been developed about a decade ago.

Although iron is the fourth-most abundant element in the Earth's crust, after O, Si and Al (Wedepohl, 1995), and the sufficient supply with iron is essential for all living organisms, precious little effort has been dedicated towards the study of iron isotopes in higher organisms.

Iron occurs in different oxidation states, participates in many abiotic and biotically mediated redox processes and has a variety of ligands and bonding partners. These reactions lead to mass-dependent fractionation of stable iron isotopes between different phases if transfer is incomplete. Most studies of stable iron isotopes were undertaken by the Earth Science community and iron isotope fractionation by microbes in the environment was the major biological application focused on (e.g. Brantley et al., 2001; Croal et al., 2004, Johnson et al., 2004b). Walczyk and von Blanckenburg (2002; 2005) first showed that it is in fact higher organisms that produce the largest iron isotope fractionations in nature. Results from the present thesis support this finding and demonstrate that the iron isotope effects caused by plant growth present the most significant and systematic shifts of geosphere - biosphere interaction. Furthermore iron isotopes present a novel tool for studying Fe metabolism in plants which is required for a better understanding of intracellular redox state, binding forms and Fe transport processes in plants, as will be shown in this thesis. Using the stable iron isotope fingerprint has the advantage in that no high and physiologically unrealistic iron concentrations or artificially enriched isotopes are required.

The need for knowledge of iron metabolism processes in plants arises from efforts to biofortify herbal human food with iron. This is a scientific challenge with global implications. The World Health Organization (WHO) estimates that worldwide around 2 billion people are iron-deficient of which approximately 50% suffer from iron deficiency anaemia (WHO,

2003). Iron deficiency and anaemia lead first to decreased work performance, and at higher levels to lower resistance to infection, and growth deficits (Edison et al., 2008).

To combat against iron deficiency is so difficult because even though plants are primary sources of iron in the human diet, iron concentration in plants is often below the dietary requirements or the bioavailability is low. In addition, many people of the developing world do not have access to animal sources of iron. The usual strategy to compensate for this deficit is fortification of plant foods. But often this fortified iron is not highly bioavailable or poor people from the rural areas cannot afford these fortified plant foods (Boccio and Iyengar, 2003). Therefore, another approach is to enhance the iron content of plant foods through biofortification. In this process the plant uses its own mechanisms to fortify or increase the density or bioavailability of nutrients (like iron) in its edible parts. Two strategies among several to develop iron biofortified plants are the alteration of pathways of iron metabolism, and the modification of iron bioavailability.

When choosing to alter a plant by targeting its iron acquisition system, it is crucial to fully understand the iron metabolic processes significant to that plant. But many aspects of iron uptake, transport and remobilization in higher plants are still not well known.

Due to insufficient methods it is yet not possible to figure out the physiological significance of remobilization and characterize underlying reactions. Radioactively labelled Fe isotopes are used as markers for translocation/retranslocation processes in plants (Zhang et al., 1996) so far but they are only able to provide information on uptake rates and transferred amounts from a synthetic Fe substrate. A new tool is demanded to identify underlying processes. As proposed by Álvarez-Fernández (2006) this could be stable iron isotopes in the future.

This thesis supports this statement. I show that stable iron isotopes are an adequate tool to study uptake and translocation processes in higher plants and that biochemical reactions like redox-changes or ligand exchange can be elucidated. The findings presented here show an approach that promises to be of general interest to trace the behaviour of metals in biological systems. This thesis provides more evidence that the heavy metal isotope systems are emerging as indicators of geosphere-biosphere metal transfer processes. Therefore this work is interdisciplinary and provides applications not only in geo-, but also in plant- and nutrition sciences.

## 1.2 Organization of the thesis

This thesis is subdivided into five chapters: an introduction section and four main chapters. The introduction section provides the aim of the thesis and introduces the reader into the general concepts of iron-metabolism in plants. The principles of stable isotope fractionation are then presented as well as the current state-of-the-art of iron isotope research in the geo- and biosphere. The chapters 2 to 4 contain separate introduction and conclusion sections and therefore present independent units without the context of other chapters. Manuscripts that represent these chapters are either already published (chapter 2 and 3) in international journals or aimed at being submitted for publication in international journals (chapter 4). Chapter 5 is a summary of several experiments, their results and main points of discussion.

**Chapter 2** provides the first data which show that the plant-specific iron uptake mechanisms for plants (strategy I: reduction of iron, strategy II: chelation to iron and uptake of Fe-phytosiderophores) can be fingerprinted with stable iron isotope compositions. For this study different species of strategy I and II plants were grown on two different types of soil. Parts of plants were harvested at two different times. First direct evidence is found that translocation mechanisms have to be different in both types of plants. This study is the first showing that stable iron isotopes are likely to present a novel tool for studying iron metabolism in plants. This work is published in the international journal “Environmental Science and Technology” in April 2007 (Guelke, M. & von Blanckenburg, F. (2007): Fractionation of stable iron isotopes in higher plants. *Environmental Science & Technology*, 41 (6), 1896-1901).

In **Chapter 3** the stable iron isotope composition of the plant-available iron pool in soils are identified. For the interpretation of a plant's iron isotope ratios the knowledge of the fractionation factor between the plant and the soil on which it grows is essential. To determine this fractionation factor the exact iron isotope composition of iron which can be taken up by plants needs to be known. In this chapter it is stated that the stable iron isotope composition of strategy II plants (grasses) has a potential capability as indicator of the mobile plant-available iron fraction in soils. I determined the stable iron isotope signature of the plant-available iron pools in two agronomic soils with two different sequential extraction methods. This isotopic signature was compared to that of typical strategy I and II plants grown on the soils. Strategy II plants exhibited uniform iron isotopic composition and only little fractionation occurred during uptake of iron by these plants when compared to the composition of the most mobile iron fraction in soil. An apparent fractionation factor could be determined. This work is

published in the international journal “Chemical Geology” (Guelke, M., von Blanckenburg, F., Staubwasser, M., Schoenberg, R. & Stuetzel, H. (2010): Determining the stable iron isotope signature of plant-available iron in soils. *Chemical Geology*, 277 (3-4), 269-280).

In **Chapter 4** it is shown how the iron isotope ratios changed in different organs of both a strategy I and a strategy II plant during growth in a nutrient solution supplied with Fe(III)-EDTA. It is demonstrated that the stable iron isotope patterns evolve not only in the uptake mechanisms of these plants but also in the translocation mechanisms. The distribution of iron isotopes inside the strategy I plant indicates remobilization of iron from older plant organs and points to iron isotope fractionation during reduction of iron before membrane transport and reduction of iron during mobilization from storage molecules. In contrast to our previous results (chapter 2) the complete strategy II plant was enriched in the light iron isotopes, too, although there was no significant change in the iron isotope ratios during growth and in the different plant organs. This divergence can be explained with the influence of iron speciation in the growth media, suggesting that the iron isotope signature of plant biomass depends not only on the iron uptake strategy but also on the iron availability in the growth substrate. The measured stable isotope compositions also indicate that in addition to the different uptake mechanisms, strategy I and II plants have different iron translocation mechanisms, which is consistent with the hypothesis that strategy I plants may more frequently change the redox state of iron during translocation, while in strategy II plants, iron may remain to a larger extent in its ferric form, also during ligand exchange.

In **Chapter 5** iron isotope data of various experiments with the strategy II plant maize are given. The experiments were conducted together with Dr. Enrico Scheuermann of the Institute for Plant Nutrition at the University of Hohenheim. Maize plants were grown under controlled conditions in a nutrient solution with known iron isotopic signature as well as in a nutrient solution which was enriched in the isotope  $^{58}\text{Fe}$ . Plant growth and the determination of the chlorophyll contents were performed by Dr. Scheuermann whereas iron concentration and stable iron isotope measurements were done by me. In this chapter the results and a preliminary interpretation of using stable iron isotopes to investigate the specific processes of iron metabolism of strategy II plants are reported. In addition this chapter contains isotope data of maize grown on a soil substrate. This experiment was conducted in Hannover at the Institute of Biological Production Systems. The obtained data of all maize experiments clearly reveal that the iron isotope signature of maize depends on the iron availability of the growth substrate. Furthermore it is shown that maize retranslocated iron from older leaves into

younger plant organs, regardless of the iron status of the plant. In addition the obtained data allow hypothesizing that reduction of iron is a main factor in translocation mechanisms in maize.

### 1.3 Iron in plants

Besides nitrogen and phosphorous iron is one of the nutrients that mostly inhibits plant growth. But unlike the other nutrients iron supply cannot easily be increased by fertilization because the supplied iron becomes unavailable in the form of insoluble iron hydroxides. Consequently, it is fundamental to understand the metabolism of iron in plants.

Although iron comprises approximately 5 % of the earth's crust and is the fourth most abundant element in the lithosphere (Wedepohl, 1995), the bioavailability of iron for plants is usually low (Lindsay and Schwab, 1982). In the earth's crust iron is prominent in the ferrous and ferric form in minerals like biotite, amphibole, pyroxene or olivine. During weathering iron oxides and hydroxides are formed from these minerals which have different solubilities in the following order (Lindsay and Schwab, 1982):

$\text{Fe}(\text{OH})_3$  poorly crystalline >  $\text{FeOOH}$  lepidocrocite >  $\text{Fe}_2\text{O}_3$  hematite >  $\text{Fe}_2\text{O}_3$  maghemite >  $\text{FeOOH}$  goethite.

For plant nutrition the poorly crystalline Fe(III)-precipitates play a particularly significant role as they have the highest solubility. For the dissolution of these Fe compounds the pH and the redox-potential of the soil are important. The solubility of Fe minerals decreases exponentially for each pH unit increase (Lindsay and Schwab, 1982). Reducing conditions lead to the reduction of Fe(III) to Fe(II)-oxides/hydroxides and the release of dissolved Fe(II) which has a higher solubility (Sah and Mikkelsen, 1986).

The low solubility of iron under aerobic conditions is not sufficient to provide enough free iron for optimal plant growth. Plants require  $10^{-9} - 10^{-4}$  mol Fe/ L soil (Guerinot and Yi, 1994). Free Fe(III) in an aerobic, aqueous environment is limited to an equilibrium concentration of approximately  $10^{-17}$  M, a value far below that required for optimal plant (Guerinot and Yi, 1994; Marschner, 1995).

Although there are organic compounds like siderophores, produced by fungi and bacteria, in the soil which are able to bind Fe(III) and therefore enhance iron concentration, there are only

$10^{-10}$  M dissolved iron available on calcareous soils (Briat and Lobreaux, 1997) which comprise one third of all world's surface soils. Thus, Fe-deficiency often limits plant growth causing agricultural problems.

### Functions of iron in plants

Iron is a transition element and can easily change its redoxstate between Fe(III) and Fe(II). It can form octahedral complexes with various ligands. This variability in the oxidation state is the reason for the special role of iron in biological redox systems. However, usually most Fe in plants is in the ferric form (Goodman and Dekock, 1982). There are two major groups of Fe containing proteins in plants: heme proteins (e.g. cytochrome, catalase, nitrate reductase) and Fe-S proteins (e.g. ferredoxin, nitrite reductase) which take part in many metabolic processes, including the electron transfer chains of respiration and photosynthesis (cytochromes), the biosynthesis of DNA (ribonucleotide reductase), lipids (lipoxygenase) and hormones (1-aminocyclopropane 1-carboxylic acid (ACC) oxidase) and nitrogen assimilation (nitrate reductase) (Curie et al., 2009). The heme-bound enzyme catalase catalyses the reaction from  $\text{H}_2\text{O}_2$  to  $\text{H}_2\text{O}$  and  $\text{O}_2$  and thus makes  $\text{H}_2\text{O}_2$  innocuous, an important process to avoid the occurrence of the cell damaging radical  $\text{O}_2^{\cdot-}$ . Under Fe-deficiency, visual symptoms firstly appear in the young leaves caused by an inhibition of several Fe-dependent steps on chlorophyll biosynthesis.

### Iron acquisition by the roots

Plant roots preferentially take up iron in its ferrous form and under non-limiting Fe supplies, Fe uptake is mediated via a constitutive acquisition system that consists of a membrane-bound ferric reductase which is linked to a divalent metal ion transporter and an ATP-driven proton extrusion pump. This means that plants reduce iron and take up the ferrous form when they are grown on soils with a high Fe availability (Chaney et al., 1972). However, this rarely occurs. High Fe(II) concentrations are found only in flooded, anaerobic soils which lead to excessive Fe uptake and consequently to Fe toxicity (Bienfait et al., 1985). But as Fe in soils is normally present as hardly soluble Fe(III) compounds which are not available for plant use, higher plants were forced to evolve different strategies to make iron in soil available for their needs. There is general agreement of at least two strategies of plants for iron acquisition (Marschner et al., 1986) (Figure 1.1).



**Strategy I** is used by all dicotyledonous plants and the non-graminaceous monocots. Under iron deficiency, roots of these plants exude protons into the rhizosphere via a plasmalemma P-type ATPase, lowering the pH of the soil solution and promoting dissolution of Fe(III) precipitates. Fe becomes more available by reducing Fe<sup>3+</sup> to the more soluble Fe<sup>2+</sup>. Fe(III)chelates reductases have been identified in several plants at the molecular level. Iron is reduced in the apoplast and subsequently transported as Fe<sup>2+</sup> into the root by the membrane transporter protein IRT1, a member of the ZIP metal transporter family. Genes encoding Fe<sup>3+</sup>-chelate reductase (FRO1) have been cloned from *Arabidopsis thaliana* (Robinson et al., 1999) and pea (Waters et al., 2002). The iron transporter gene IRT1 has been cloned from *Arabidopsis thaliana* (Eide et al., 1996) as well as its orthologs from pea and from tomato (Cohen et al., 1998; Eckhardt et al., 2001).

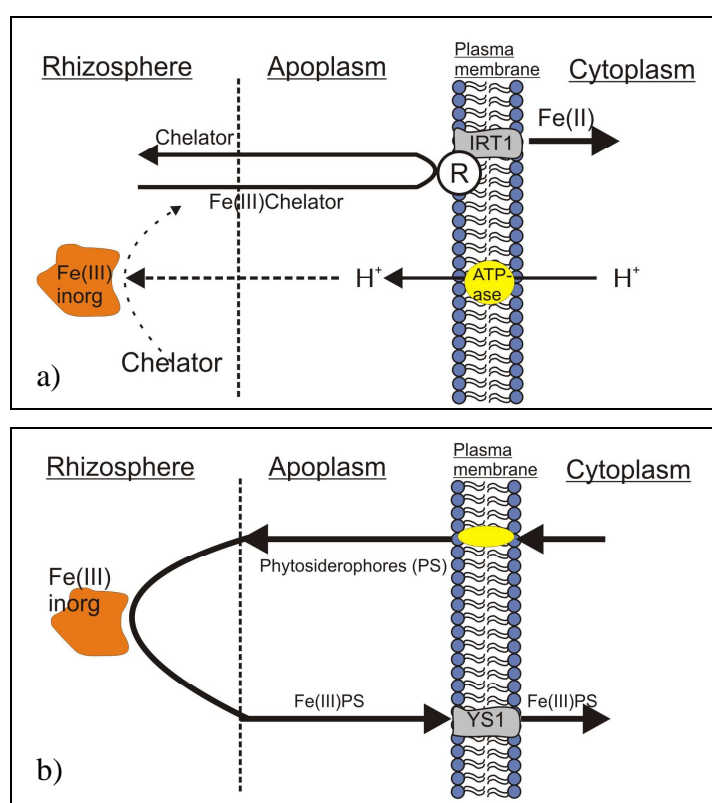


Figure 1.1 Iron uptake of roots according to strategy I (a) and strategy II (b) and the membrane transport processes involved. R: Fe(III)chelate reductase, IRT1: Fe(II) transporter, YS1: phytosiderophore–Fe(III) (PS) transporter. The process of PS secretion has not been finally resolved (yellow ellipse). After Hell and Stephan (2003).

All three components of strategy I (proton extrusion, reduction, uptake by transporters) increase their activities during iron deficiency. Further adaptive mechanisms include root morphology changes, root hair and transfer cell development.

**Strategy II** is used by the monocotyledonous plants (the grasses) and employs ferric chelators called phytosiderophores (PS) which are exuded under iron deficiency. Phytosiderophores belong to the mugineic acid (MA) family which are non-proteinogenic secondary amino acids with a molecular weight of around 320. They can effectively chelate ferric iron via their amino and carboxyl groups. The family of mugineic acids includes several species. One of them is 2 deoxy-mugineic acid (Figure 1.2). Each grass produces its own set of MAs and increases the production and secretion of MAs in response to iron deficiency. Tolerance to Fe-deficiency is therefore correlated with the amounts and the types of PS secreted (Marschner, 1995).

PS have a high affinity for Fe(III) to which they are bound efficiently in the rhizosphere. Fe(III)–PS complexes are then transported into the plant roots via a specific transport system. The uptake of the Fe(III)–PS complex was elucidated by cloning of the mutant allele of the transport-defective YS1 mutant from maize (Curie et al., 2001). This chelation strategy is more efficient than the reduction strategy used by the other plants and thus allows grasses to survive more drastic iron-deficiency conditions (Curie and Briat, 2003).

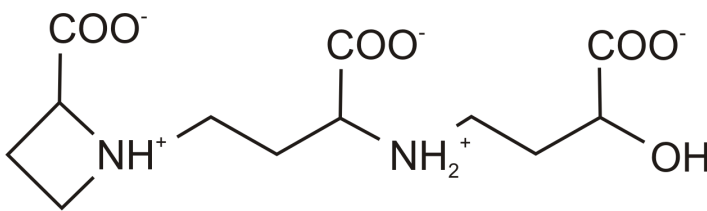


Figure 1.2 Structure of the phytosiderophore 2 deoxy-mugineic acid.

When plants of either strategy are confronted with Fe-deficiency stress, the strategy-specific processes are upregulated in the plant's root system (Grusak and DellaPenna, 1999).

### Iron transport in plants

The acquisition of iron and other micronutrients in the plant actually starts in the apoplast of the root epidermal cells (Sattelmacher, 2001). Iron diffuses through the free apoplastic space

to the plasmalemma but, once it is reduced or de-chelated, may not be completely imported by the different uptake systems. Under aerated conditions part of the iron is oxidized and precipitates as hydroxide or phosphate salt, forming an apoplastic iron pool (Bienfait et al., 1985). This pool comprises up to 95 % of total root iron content in hydroponic culture and can be used when conditions of iron deficiency are applied (Becker et al., 1995). Apoplastic iron may be less important in roots of soil-grown plants as evidenced by specific determination of iron concentrations in cross-sections of barley roots (Strasser et al., 1999). Iron enters the roots' epidermal cells through either the uptake of Fe(III)-phytosiderophore complexes used by the grasses or the strategy I acidification, reduction, and ferrous transport pathway present in all other plants (Figure 1.1; Figure 1.3 inlet).

Iron moves through the root to the central vascular cylinder, which contains the xylem and the phloem, where it can be loaded into the xylem and translocated to other parts of the plant.

All solutes must enter the vascular cylinder through a symplastic (intra-cellular) pathway because the casparian strip, a layer of waxy coated endodermal cells, forms an impermeable barrier for water and solutes. This casparian strip separates the soil solution and the apoplast of the outer root from the apoplast of the inner root and the vascular cylinder. In the symplast iron is bound by chelating compounds. Fe-chelator complexes then move through intercellular connections into the stele along the diffusion gradient. It is proposed that nicotianamine (NA) (Figure 1.4) functions as iron chelator. NA is produced by the enzymatic condensation of three amino-carboxylpropyl groups of three S-adenosyl-methionine molecules by nicotianamine synthase. This leads to the formation of a hexadentate co-ordination which results in the formation of very stable octahedral chelates with a central metal ion. NA is a precursor of phytosiderophores. It is present in all plants and has the ability to bind various metals including  $\text{Fe}^{2+}$  and  $\text{Fe}^{3+}$  (von Wirén et al., 1999), whereby the kinetic stability is higher for the Fe(II)-NA complex and lower for the Fe(III)-NA complex. NA is not secreted and it is suggested that it plays a role in intra-and intercellular metal transport in both strategy I and II plants.

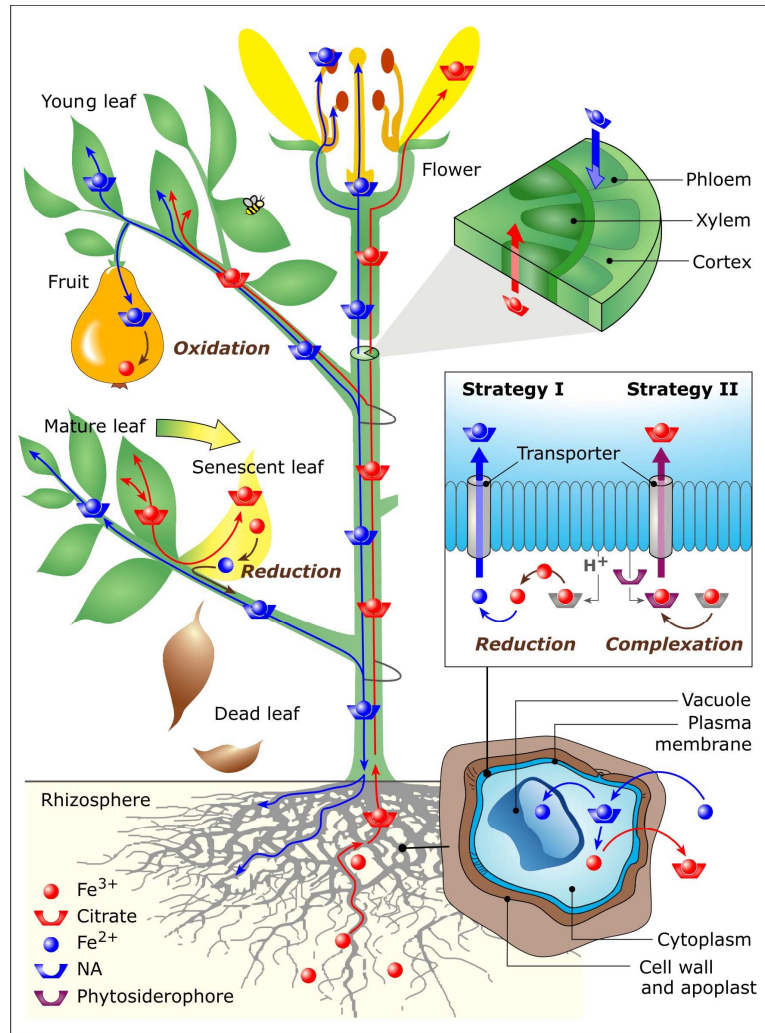


Figure 1.3 Iron uptake and translocation pathways in higher plants. Arrows represent the long-distance circulation of iron chelates within a flowering plant (after Briat et al. 2007). Uptake into the root is mediated by transporter proteins; this occurs either after reduction (strategy I) or after complexation (strategy II). Complex formation by organic acids or, in particular, nicotianamine (“NA”, blue arrows) moves Fe between cells. Transport in the xylem is as an Fe(III)-citrate complex, and in graminaceous plants, also an Fe(III)-phytosiderophore complex (red arrows). Transfer of Fe from the xylem into leaf cells requires Fe(III)-citrate reduction, followed by transport across the membrane as  $\text{Fe}^{2+}$  or as a ferric complex with nicotianamine or phytosiderophores (the latter only in strategy II plants). Within leaf and root cells, most of the physiologically active Fe is found as Fe(II) or Fe(III) in the protein fraction, as heme-bound Fe, or fixed in Fe–S clusters (Briat et al. 2007). When the plant enters the generative growth phase, root activity usually decreases, so elements become translocated to sink tissues (brown arrows). Fe can be reduced again before reaching the sink organs (Curie et al. 2009). From von Blanckenburg et al. (2009).

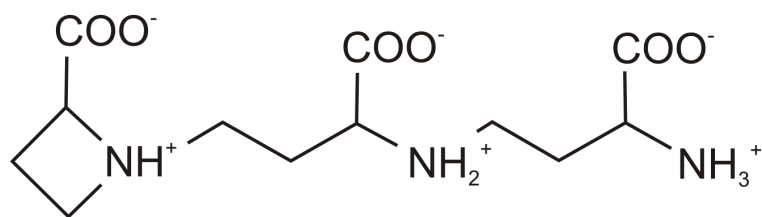


Figure 1.4 Structure of nicotianamine (NA).

Fe has to be discharged from the symplast to be released into the xylem but the mechanism is not yet clearly understood (Kim and Guerinot, 2007). In the xylem, where the pH is around 5.5-6, Fe is present as Fe(III)-citrate (Hell and Stephan, 2003). Unpublished studies show that Fe-PS might be transported in the xylem as well (von Wirén, pers. comm). The mechanism of Fe uptake from the xylem vessels into leaf tissues (xylem unloading to symplast and re-absorption to apoplast) is not clear (Kim and Guerinot, 2007). However, it is believed that strategy I mechanisms play a role when Fe moves across the plasma membrane of leaf cells and it has to be mediated by transporters of iron–citrate, NA–iron or other iron complexes or free  $\text{Fe}^{2+}$ . The photoreduction of xylem-transported ferric carboxylates like citrate seems to play an important role in the reduction of iron in the shoots. The driving force for this reaction is provided by light energy (Bienfait and Scheffers, 1992). The idea of enzymatic iron reduction in leaves has been controversial (Schmidt, 1999), but plasmalemma activity of Fe(III)-chelate reductase has been clearly demonstrated (Larbi et al., 2001).

Fe has also to be transported by the phloem, for example to the seeds. The pH in the phloem is above 7, so Fe must be bound to chelators to stay soluble. It is believed that Fe is transported as Fe-ITP (iron transporter protein) in the phloem. ITP binds Fe(III) as shown by *in vivo* labelling experiments. In addition nicotianamine (Figure 1.4) has been proposed to be another Fe-transporter in the phloem as it is ubiquitous in plant tissues and at the relatively higher pH of the phloem, both Fe(III) and Fe(II) are predicted to be complexed with NA (von Wirén et al., 1999). The presence of a small amount of Fe(II) in the phloem sap has led to the idea that NA can act as a shuttle by chelating Fe(II) from Fe(III)-ITP during phloem loading and unloading (Kim and Guerinot, 2007). However, it is supposed that NA plays an essential role as principal chelator of free iron in cells whenever iron is not bound to target structures such as heme or stored as phytoferritin. It is not clear if transport within the plant differs significantly between strategy I and II plants. The fate of the imported Fe(III)-PS complex is currently unclear. But since NA forms complexes with Fe(III) as well, iron might just be

chelated by NA as a default mechanism until it is channelled into further transport, storage sites or functional target molecules (Hell and Stephan, 2003).

### Iron storage in plants

Plants can suffer from iron deficiency but also from an excess of iron despite strict control by the root uptake systems. Iron can be stored in the apoplast, but inside the cells plastids and vacuoles are important iron stores. To bind excess free iron in the cells, the synthesis of phytoferritin is induced. Ferritins are ubiquitous multimeric protein complexes that are able to store up to 4000 iron atoms in a central cavity. Their abundance is controlled by precise regulatory mechanisms (Briat, 1999). In plant cells Fe is stored as phytoferritin in the stroma of plastids. The mechanism of Fe uptake into the chloroplasts is not well understood. Fe uptake studies with isolated barley chloroplasts indicated that this process is light-dependent, and requires Fe(III)chelate reductase activity (Buglio et al., 1997). More than 90 % of leaf Fe is located in the chloroplasts (Terry and Abadia, 1986).

It is proposed that NA (Figure 1.4) is involved in the regulation, delivery and distribution of Fe between several organelles in the cytoplasm (the symplastic department). It is not yet clear how plants regulate cellular Fe homeostasis and intracellular Fe transport, but several observations have suggested that vacuoles play a significant role in storing excess Fe and releasing Fe into the cytosol under iron deficiency. It has been observed that upon Fe overload NA concentrations are increased in tomato and pea and most of the NA is found in the vacuoles whereas under normal or Fe-deficient conditions it is detected mostly in the cytosol (Pich et al., 2001). Current knowledge is limited whether Fe translocates into the vacuole as Fe-NA complex (Fe(II) or Fe(III)) or whether specific transporters for NA are present and the Fe-NA complexes then form inside the vacuole (Kim and Guerinot, 2007). In comparison to the cytoplasm the vacuole is relatively acidic and therefore oxidizing which means that vacuolar iron is likely to be stored as Fe(III) in ferric (hydr)oxides or phosphates. Kim et al. (2006) showed that vacuolar Fe storage plays an important role for the growth of germinating seedlings. They identified VIT1 (Vacuolar Iron Transporter 1) in *Arabidopsis* which functions as a Fe<sup>2+</sup> transporter in vacuolar Fe storage. It remains to be shown what contribution ferritin in plastids and vacuoles have in buffering cellular iron in leaves and roots. However, results of Pich et al. (2001) together with the finding that the Fe(II)-NA complex is a poor Fenton reagent (von Wirén et al., 1999) indicate that at the cellular level NA could be involved in the

detoxification of high Fe concentrations by chelation and sequestration in the vacuole. Therefore cytosolic iron homeostasis apparently requires NA to mediate between different forms of iron storage (Stephan and Scholz, 1993; Stephan et al., 1996; Curie et al., 2009).

### Iron remobilization in plants

The term “remobilization” was defined as a decrease in the net content of mineral nutrients, in amount per organ, e.g. leaf. Remobilization is especially important for seed germination and periods of insufficient Fe-supply to the roots during vegetative or reproductive growth (Marschner et al., 1986). The translocation of mineral nutrients from roots to shoots is strongly affected, especially by the demand of the shoot (Engels and Marschner, 1992). If the shoot demand exceeds the mineral nutrient supply to the roots and transport from roots to shoot, remobilization from mature leaves is increased and their amount per leaf decreases for mineral nutrients such as N or K. It is quite clear how roots respond to iron deficiency and how Fe is remobilized in the rhizosphere and then taken up by the plant roots. However, there is only little information about iron remobilization from older leaves. Zhang et al. (1996) showed with <sup>59</sup>Fe labelled iron that bean plants (*Phaseolus vulgaris L.*) are able to remobilize iron from older leaves when grown under Fe-deficiency. For strategy II plants remobilization has not been demonstrated to date. Remobilization of vacuolar iron stores to meet cellular needs has been shown to occur in yeast requiring the reduction of Fe(III) to Fe(II) (Singh et al., 2007).

### Probable iron isotope effects in plants

As can be seen from the previous sections of this chapter iron metabolism in plants involves many changes of the redox state of iron and of the ligand it is bound to. These metal conversion processes in plants are expected to result in isotope fractionation whenever they are not quantitative (see chapter 1.4). These preconditions for iron isotope fractionation are given in the rhizosphere, in the cell apoplast, during passage across the plasma membrane, in the cytoplasm involving storage of iron in vacuoles or plastids, during export from the cytoplasm into xylem vessels, in the membrane passage from the xylem fluid into the cytoplasm of leaf cells, during loading into the phloem vessel and during transfer from the phloem into the seed or fruit (von Blanckenburg et al., 2009).

## 1.4 Stable iron isotopes

### 1.4.1 Principles of stable isotope fractionation

#### General characteristics

Atoms whose nuclei have the same number of protons but a different number of neutrons are called isotopes. The term “isotope” originated from the Greek and means “at the same place”, indicating that isotopes occupy the same position in the periodic table. Isotopes are usually symbolized in the form  ${}^m_n\text{E}$  where the superscript “m” is the mass number and the subscript “n” is the atomic number of an element E. The atomic weight of each naturally occurring element is the average of the weights given by its various isotopes.

Isotopes can be divided into stable and unstable isotopes, depending on the ratio of protons and neutrons in the nucleus. Unstable isotopes are radioactive species. Variations in the abundances of radiogenic isotopes derive from radioactive decay which occurs if the ratio of protons and neutrons is disadvantageous to the nuclear binding energy (Hoefs, 2009). The related isotope will decay under emission of high-energy radiation and change into a different element, depending on the kind of decay. A large number of natural radioactive isotopes have decayed since they were formed. Those with a very high half-life (e.g.  ${}^{238}\text{U}$ ) are still existent as well as the shorter-lived ones that are permanently created by cosmic radiation (e.g.  ${}^{14}\text{C}$ ) or due to decay of high half-life isotopes (e.g.  ${}^{230}\text{Th}$ ).

Isotopes with a favorable proton/neutron ratio do not decay and are called stable isotopes. But stable isotopes can also vary in their abundances. The partitioning of isotopes between two substances or two phases of the same substance with different isotope ratios is called “isotope fractionation” and is caused by small chemical and physical differences between the isotopes of an element. The main phenomena producing isotope fractionations are isotope exchange reactions (equilibrium isotope fractionation) and kinetic processes, the latter depending primarily on differences in reaction rates of isotopic molecules. The theory of isotopes effects and a related isotope fractionation mechanism will be presented here briefly.

Variations in the atomic mass of an element result in differences in the chemical and physical properties of the given isotopes. These differences arise from quantum mechanical effects. Quantum theory says that the energy of a molecule is restricted to certain discrete energy levels. The lowest level does not correspond to the minimum of the energy curve, but is



located slightly above it with an amount of  $\frac{1}{2} h\nu$ , where  $h$  is the Planck's constant ( $6.626 \times 10^{-34}$  J·s) and  $\nu$  the frequency with which atoms in the molecule vibrate with respect to one another. This fundamental vibration frequency depends on the mass of the substituted atoms. As a consequence of the relation of equation 1.1 and 1.2 the zero point energy (ZPE) of a bond involving a light isotope is greater than the zero point energy of a bond involving a heavy isotope (Figure 1.5).

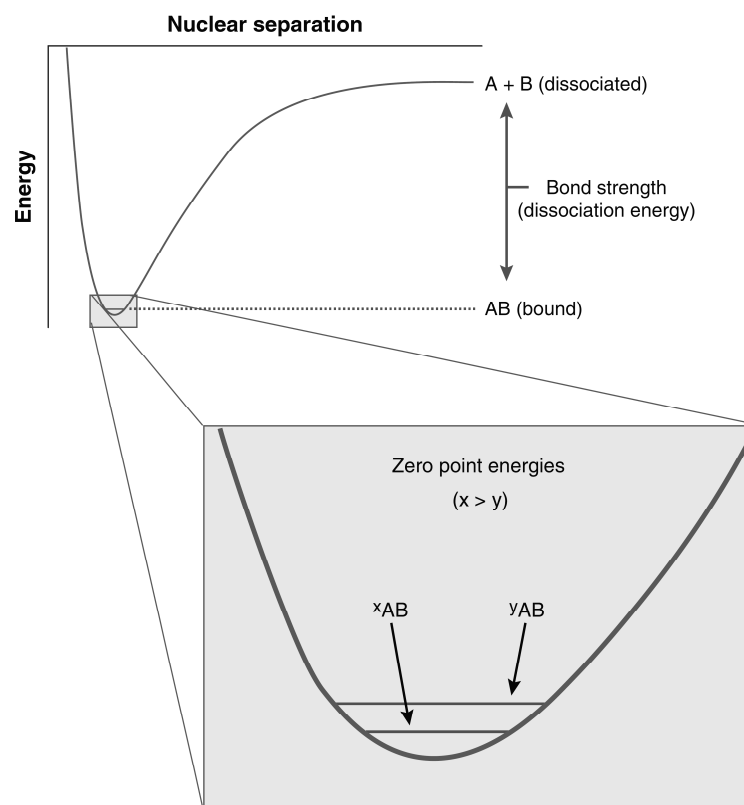


Figure 1.5 Schematic illustration of how isotope substitution affects zero point energies (ZPEs) and bond strengths. (Inset) Detail of the potential energy well that describes the diatomic bond between two atoms, A and B. If there are two isotopes of A,  ${}^x\text{A}$  and  ${}^y\text{A}$ , they will have different ZPEs and hence different bond strengths (from Anbar and Rouxel, 2007).

Therefore, molecules bearing the light isotopes will generally react a little more readily than those with the heavy isotope during a chemical reaction (Hoefs, 2009):

$$E_{\text{vibr}} = \left(n + \frac{1}{2}\right)h\nu \quad 1.1$$

$$\text{with } \nu = \frac{1}{2\pi} \sqrt{k \left( \frac{1}{m_1} + \frac{1}{m_2} \right)} \quad 1.2$$

Thereby  $n$  is the quantum number for the respective degree of freedom,  $h$  is the Planck's constant,  $\nu$  the vibration frequency and  $k$  the effective constant of power of the bond between the two molecules. The masses of the two atoms of the molecule are represented with  $m_1$  and  $m_2$  (Schauble, 2004). With the binding of the heavier isotope the mass  $m_1$  is increased in the molecule, consequently the vibration frequency is reduced and therefore the vibration energy  $E_{\text{vibr}}$  is also diminished.

### Equilibrium isotope fractionation

Equilibrium fractionation can take place at isotope exchange reactions. These are a special case of general chemical equilibrium and can be written like



where  $x$  and  $y$  are two isotopes and  $A$  and  $B$  two phases. The equilibrium constant for this reaction is

$$K_{eq} = \frac{({}^y A)({}^x B)}{({}^y B)({}^x A)} \quad 1.4$$

defined as the quotient of the thermodynamic activities of the products and reactants. Assuming exchange of one atom of the element and ideal mixing of isotopes in both phases (Polyakov, 1993),  $K_{eq}$  is the same as the equilibrium isotope fractionation factor  $\alpha$  (see equation 1.18).

Equivalent to any chemical reaction the equilibrium constant is related to the change in standard Gibbs free energy:

$$\Delta G^0_R(T, P) = \Delta H^0_R - T\Delta S^0_R + \Delta V^0_R = -RT \ln K_{eq} \quad 1.5$$

In principle, the free energy change and the equilibrium constant can be calculated for isotope exchange reactions from thermodynamic data of molar enthalpy ( $\Delta H^0_R$ ), entropy ( $\Delta S^0_R$ ) and volume ( $\Delta V^0_R$ ) as a function of pressure ( $P$ ) and absolute temperature ( $T$ ), but the changes in  $\Delta G^0_R$  on isotopic substitution would be too small (less than a few tens of joules) for precise classical thermodynamic calculations which makes a quantum mechanical approach

necessary. Except for some light elements the change in volume and bond structure for isotope exchange reactions is very small, particularly for condensed phases like minerals. Therefore, following  $G = F + PV$ ,  $\Delta G$  of the reaction is equivalent to the Helmholtz free energy ( $\Delta F$ ) and the equilibrium constant is

$$K_{\text{eq}} = e^{\left(\frac{-\Delta F}{RT}\right)} \quad 1.6$$

Approximating the atomic motion by a harmonic oscillator,  $\Delta F$  is roughly the same as the difference in the zero-point energy ( $\Delta ZPE$ ), which can be calculated with equation 1.1:

$$\Delta F \approx \Delta ZPE = \sum_{\text{products}} \left(\frac{1}{2} h\nu\right) - \sum_{\text{reactants}} \left(\frac{1}{2} h\nu\right) = \frac{1}{2} h\Delta\nu \quad 1.7$$

Therefore, the difference in the vibrational frequency  $\Delta\nu$  which is correlated to the masses of substances (equation 1.2) drives equilibrium isotope fractionation.

More precisely, the sum of energy of motion of a molecule includes vibrational, rotational and translational energies and can be described by statistical mechanics using partition functions  $Q$ . Partition functions consider all energy states of a molecule and the probability to occupy particular states.  $Q$  is related to the Helmholtz free energy according to

$$F = -RT \ln Q \quad 1.8$$

The vibrational partition function,  $Q_{\text{vib}}$ , for harmonic vibrations, describes the sum over all vibrational energies,  $E_n$  in a molecule:

$$Q_{\text{vib}} = \sum_n \exp(-E_n/kT) \text{ with } E_n = \left(n + \frac{1}{2}\right) h\nu \quad 1.9$$

$k$  is the Boltzmann's constant ( $1.38 \times 10^{-23} \text{ J K}^{-1}$ ) and  $n$  describes the energy state, i.e. the quantum number, of the vibrational degree of freedom. For a molecule in the ground state,  $n=0$ , which defines the zero-point energy, the partition functions for rotation ( $Q_{\text{rot}}$ ) and translation ( $Q_{\text{trans}}$ ) in a molecule can be calculated according to:

$$Q_{\text{rot}} = \frac{8\pi^2 I kT}{h^2} \text{ and} \quad 1.10$$

$$Q_{\text{trans}} = V \left(\frac{2\pi m kT}{h^2}\right)^{3/2} \quad 1.11$$

$I$  is the moment of inertia of the molecule,  $V$  is the volume of the molecule and  $m$  is its mass. Therefore the total energy of atomic motion is

$$F = -RT \ln(Q_{trans} \cdot Q_{rot} \cdot Q_{vib}) \quad 1.12$$

From this the following expression for  $k_{eq}$  and therefore  $\alpha$  result:

$$\begin{aligned} k_{eq} = \alpha &= \exp\left(\frac{-\Delta F}{RT}\right) = \exp\left[\frac{-(F_{products} - F_{reactants})}{RT}\right] \\ &= \exp\left\{\sum_{products} \ln(Q_{trans} \cdot Q_{rot} \cdot Q_{vib}) - \sum_{reactants} \ln(Q_{trans} \cdot Q_{rot} \cdot Q_{vib})\right\} \\ &= \frac{\prod_{products} (Q_{trans} \cdot Q_{rot} \cdot Q_{vib})}{\prod_{reactants} (Q_{trans} \cdot Q_{rot} \cdot Q_{vib})} \end{aligned} \quad 1.13$$

In contrast to most cation exchange reactions, where  $\Delta G$  is approximately constant over a specific range of temperatures, the free energy change of isotope exchange reactions varies significantly with  $T$ . Therefore isotope fractionation often depends on higher orders of inverse temperature ( $T^{-2}$ ).

Isotope fractionation between two compounds at room temperature can be roughly estimated from the difference in vibrational energy of the participating reactants according to

$$\alpha = K_{eq} = \exp(-\Delta G_0/kT) \approx \exp(-\Delta E_{vib}/kT) \quad 1.14$$

A rule of thumb predicts a fractionation of 1 ‰ for a difference in vibrational energy of 2.5 J/mol (Schauble, 2004). This rule is valid for reactions at moderate temperatures only, e.g. at room temperature. Equilibrium isotope effects are strongest at low temperature and decrease with rising temperature (Urey, 1947). However, isotope fractionations do not decrease to zero monotonously with increasing temperature. At intermediately high temperatures, they may change sign and increase in magnitude, but they will approach zero for very high temperatures (Hoefs, 2009).

Some qualitative predictions have been made by Schauble (2004) which govern the equilibrium fractionation:

- Usually the magnitude of isotope fractionation decreases with increasing temperature, approximately with  $1/T^2$ . Exceptions are the direct binding of an element to hydrogen.

- The magnitude of isotope fractionation decreases with increasing element mass ( $m$ ) and decreasing mass difference ( $\Delta m$ ) between the isotopes, roughly scaling with

$$\frac{m_{heavy} - m_{light}}{m_{heavy} \times m_{light}} \gg \frac{\Delta m}{m^2} \quad 1.15$$

- At equilibrium the heavy isotopes are concentrated in the molecules with the more strongly bonds. Bond strength is positively correlated with a high oxidation state of the element of interest, presence of highly covalent bonds, a low coordination number and low-spin electronic configuration.

### Kinetic isotope fractionation

Kinetic isotope effects are the second reason for isotope fractionations. Kinetic isotope fractionation between different phases can occur during incomplete isotope exchange reactions due to differences in the reaction rate constants of different isotopes of an element. These differences result from the mass-dependence of bond strength, i.e.  $^{heavy}AB$  reacts more slowly than  $^{light}AB$ . Incomplete unidirectional reactions or processes like evaporation, diffusion, dissociation- or biologically mediated reactions can produce isotope fractionations.

Quantitatively, many observed deviations from simple equilibrium processes can be interpreted as consequences of the various isotopic components having different rates of reactions (Hoefs, 2009). The mass of a molecule or atom affects its velocity ( $v$ ). This can be shown for an ideal gas, where the translational kinetic energy ( $K_E$ ) is the same for all molecules or atoms:

$$K_E = \frac{1}{2} m \times v^2 = \frac{3}{2} k_R \times T \quad 1.16$$

Thereby  $k$  is the Boltzmann's constant,  $T$  the absolute temperature and  $m$  the mass of the molecule or atom, whose velocities differ according to:

$$\frac{m_{light}}{m_{heavy}} = \frac{v_{heavy}^2}{v_{light}^2} \quad 1.17$$

Thus, in many kinetic reactions, the light isotopes are enriched in the reaction product.

Reporting isotope fractionation

The isotope fractionation factor  $\alpha$  for isotopes  $^{\text{light}}\text{X}$  and  $^{\text{heavy}}\text{X}$  between two substances XA and XB, not considering if equilibrium fractionation or kinetic fractionation is usually expressed:

$$\alpha_{\text{XA-XB}} = \frac{\left( \frac{\text{heavy X}}{\text{light X}} \right)_{\text{XA}}}{\left( \frac{\text{heavy X}}{\text{light X}} \right)_{\text{XB}}} \quad 1.18$$

Analogous to equation 1.13,  $\alpha$  can be expressed as partition function ratios:

$$\alpha_{\text{A-B}} = \frac{Q_{\text{light A}}/Q_{\text{heavy A}}}{Q_{\text{light B}}/Q_{\text{heavy B}}} \quad 1.19$$

Usually calculated partition function ratios are expressed as reduced partition functions ( $\beta$ -factors), ignoring translational and rotational energies. From these  $\beta$ -factors, the equilibrium fractionation factor can be calculated according to:

$$a_{\text{A-B}} = \frac{\beta_{\text{A}}}{\beta_{\text{B}}} \text{ or } 1000 \ln \alpha_{\text{A-B}} = 1000 \ln \beta_{\text{A}} - 1000 \ln \beta_{\text{B}} \quad 1.20$$

Fractionations are usually very small, in the order of parts per thousand or parts per ten thousand, so expressions like  $1000 \cdot \ln \alpha$  or  $1000 \cdot (\alpha - 1)$  are common that magnify the difference between  $\alpha$  and 1.  $\alpha = 1.001$  is equivalent with 1 ‰.

The delta notation is a general way to express shifts in isotope ratios between two compartments. It gives the permil deviation of the isotopic ratio of the sample relative to that of a standard:

$$\frac{\delta^{\text{heavy X}}_{\text{sample}}}{[\text{‰}]} = \left( \frac{\text{heavy X}/\text{light X}_{\text{sample}}}{\text{heavy X}/\text{light X}_{\text{standard}}} - 1 \right) \times 1000 \quad 1.21$$

The fractionation between two phases is often expressed as  $\Delta_{\text{A-B}} = \delta_{\text{A}} - \delta_{\text{B}}$ , thereby

$$\Delta \approx 10^3 \ln \alpha. \quad 1.22$$

## 1.4.2 Stable iron isotopes

Stable isotope fractionation is known for the light elements such as H, O or C since a long time and the phenomenon is utilized for many applications (Hoefs, 2009) like the origin of life, the evolution of the solar system or for climate research.

Fractionation effects for the heavier elements such as iron are not long known. The expected isotope fractionations are very small as the magnitude of maximally possible isotope fractionation depends on the mass of an element and the mass difference between the two isotopes of interest. Relatively large isotopic variations of tens to hundreds of permil are observed in nature for isotope systems of light elements like H, Li or O. For heavier elements like iron which has a mass difference of about 4 % in  $^{56}\text{Fe}/^{54}\text{Fe}$ , natural isotopic variations are smaller ( $< 5 \text{ ‰}$ ) and therefore analytically more ambitious. Until recently the precision of mass-spectrometric methods was not enough to resolve these small variations in isotopic abundances. But this changed with the advent of double spike thermal ionisation mass spectrometry (TIMS) and multi-collector inductively coupled plasma mass spectrometry (MC-ICP-MS). Now it is possible to determine the natural occurring isotope variations of metals with a precision of better than 0.1 ‰. For iron a reproducibility of 0.05 ‰ was achieved (Schoenberg and von Blanckenburg, 2005). In situ techniques, such as secondary ion mass spectrometry (SIMS) (e.g. Woodhead, 2006) and laser ablation coupled to MC-ICP-MS (e.g. Horn and von Blanckenburg, 2007) for these heavy stable isotope systems were also developed.

Iron has four naturally occurring isotopes:  $^{54}\text{Fe}$  (5.85 %),  $^{56}\text{Fe}$  (91.75 %),  $^{57}\text{Fe}$  (2.12 %) and  $^{58}\text{Fe}$  (0.28 %) (Rosman and Taylor, 1998). Iron isotope fractionation is expressed in the delta notation, which gives the permil deviation of the isotopic ratio (e.g.  $^{56}\text{Fe}/^{54}\text{Fe}$  or  $^{57}\text{Fe}/^{54}\text{Fe}$ ) of the sample relative to that of the IRMM-014 standard (Taylor et al., 1992) of which the isotopic composition is close to that of various igneous rock reservoirs (Beard et al., 2003; Poitrasson and Freydier, 2005; Schoenberg and von Blanckenburg, 2006):

$$\frac{\delta^{56}\text{Fe}_{\text{sample}}}{[\text{‰}]} = \left( \frac{\left( \frac{^{56}\text{Fe}}{^{54}\text{Fe}} \right)_{\text{sample}}}{\left( \frac{^{56}\text{Fe}}{^{54}\text{Fe}} \right)_{\text{IRMM-014}}} - 1 \right) \times 1000 \quad 1.23$$

Thereby conversion between  $^{57}\text{Fe}/^{54}\text{Fe}$  and  $^{56}\text{Fe}/^{54}\text{Fe}$  isotope ratios is according to  $\delta^{57}\text{Fe} = \delta^{56}\text{Fe} \cdot 1.48$ , based on the mass fractionation law

$$\left(\alpha^{57/54}\text{Fe}\right) = \left(\alpha^{56/54}\text{Fe}\right)^\beta, \text{ with } \beta_a = \frac{\left(\frac{\ln M^{57}\text{Fe}}{\ln M^{54}\text{Fe}}\right)}{\left(\frac{\ln M^{56}\text{Fe}}{\ln M^{54}\text{Fe}}\right)} \text{ or } \beta_b = \frac{\left(\frac{1}{M^{57}\text{Fe}} - \frac{1}{M^{54}\text{Fe}}\right)}{\left(\frac{1}{M^{56}\text{Fe}} - \frac{1}{M^{54}\text{Fe}}\right)} \quad 1.24$$

whereby  $\beta_a$  is relating to kinetic fractionation and  $\beta_b$  is relating to equilibrium fractionation (Young et al., 2002). The conversion factor in equation 1.23 is derived from the kinetic law. These mass dependent fractionation laws have shown to be helpful to differentiate between equilibrium and kinetic isotope fractionation in nature (Young et al., 2002).

#### ***1.4.2.1 Stable iron isotope geochemistry: state of the art***

Iron is an abundant element that participates in many biotically and abiotically-controlled redox processes in different geochemical environments. Iron has a variety of important bonding partners and ligands, forming sulfide, oxide and silicate minerals as well as complexes with water. Bacteria can use Fe during both dissimilatory and assimilatory redox processes. Due to its high abundance and its important role in many processes, isotope studies of iron are of substantial interest (Hoefs, 2009).

Iron isotope fractionation was first described for meteorite inclusions using a thermal ionization mass spectrometry (TIMS) technique (Voelkening and Papanastassiou, 1989). In the following years the TIMS technique was improved and the absolute isotope composition and atomic weight of an iron reference material by calibration with synthetic isotope mixtures was determined (Taylor et al., 1992; Taylor et al., 1993). It was now possible to compare measured isotope effects between laboratories by the commercially available iron reference material known as IRMM-014. This standard is a pure iron metal which is certified and supplied by the Institute for Reference Materials and Measurements in Geel, Belgium.

In 1999, a TIMS technique with a double-spike approach led to a better correction of instrumental mass bias and in the late 1990s the multi-collector inductively coupled plasma mass spectrometry (MC-ICP-MS) was established to investigate iron isotope ratios in geological samples (Halliday et al., 1995; Halliday et al., 1998; Belshaw et al., 2000).

A decade ago only a few abstracts had been published on Fe isotope geochemistry. This number rose almost exponentially with the analytical development in mass spectrometry. Although the quantity and quality of the first obtained data was unsatisfactory, scientists were



enthusiastic as they wanted to evolve new tools for understanding the biological cycling of iron, specifically microbial  $\text{Fe}^{3+}$  reduction, which was recognized in the late 1980s as a main process by which iron is cycled in the surface environments of the Earth (Lovely and Philipps, 1988; Myers and Nealson, 1988). Beard et al. (1999) hypothesized that iron isotopes may be a biosignature for microbial Fe cycling, but others were unconvinced (Anbar et al., 2000, Bullen et al., 2001). In the early 2000s there were many experimental and theoretical studies into the mechanisms of Fe isotope fractionation in abiologic and biologic systems (e.g. Anbar et al., 2000; Polyakov and Mineev, 2000; Brantley et al., 2001, Schauble et al., 2001; Johnson et al., 2002). Up to now a number of reviews has been published on experimental obtained fractionation factors and Fe isotope compositions found in nature (Anbar, 2004; Beard and Johnson, 2004; Johnson et al., 2004b; Dauphas and Rouxel, 2006; Johnson and Beard, 2006; Anbar and Rouxel, 2007; Johnson et al., 2008).

The general variation in  $\delta^{56}\text{Fe}$  observed in natural systems is about 5 ‰ (Figure 1.6), excluding variations of several hundreds of permil due to mass-independent fractionation in extraterrestrial materials (e.g. Voelkening and Papanastassiou, 1989; Tripa et al., 2002; Engrand et al., 2005).

A largely homogenous Fe isotope composition of the solar system is suggested due to the narrow range of  $\delta^{56}\text{Fe}$  found in chondrites, meteorites from Mars and Vesta, lunar rocks, and igneous rocks from Earth. Only small variations possibly exist between planetary bodies (e.g. Schoenberg and von Blanckenburg, 2006; Poitrasson, 2007). The Earth's basaltic crust is expected to have a  $\delta^{56}\text{Fe}$  value of about 0.1 ‰ relative to the reference material IRMM-014 (Beard et al., 2003; Schoenberg and von Blanckenburg, 2006).

Fe isotopes have become promising useful tracers of the biogeochemical redox cycling of Fe. Biotic and abiotic redox processes are among the principal factors that fractionate Fe isotopes. These redox processes include dissimilatory iron reduction (Beard et al., 1999; Icopini et al., 2004), anaerobic photosynthetic Fe(II) oxidation (Croal et al., 2004), abiotic Fe(II) oxidation and precipitation of ferric hydroxides (Bullen et al., 2001; Balci et al., 2006), and sorption of aqueous Fe(II) onto ferric hydroxides (Icopini et al., 2004; Teutsch et al., 2005). Equilibrium isotope fractionations of 3 ‰ between coexisting Fe(III) and Fe(II) aqueous species have been observed and theoretically calculated (Welch et al., 2003; Anbar et al., 2005).

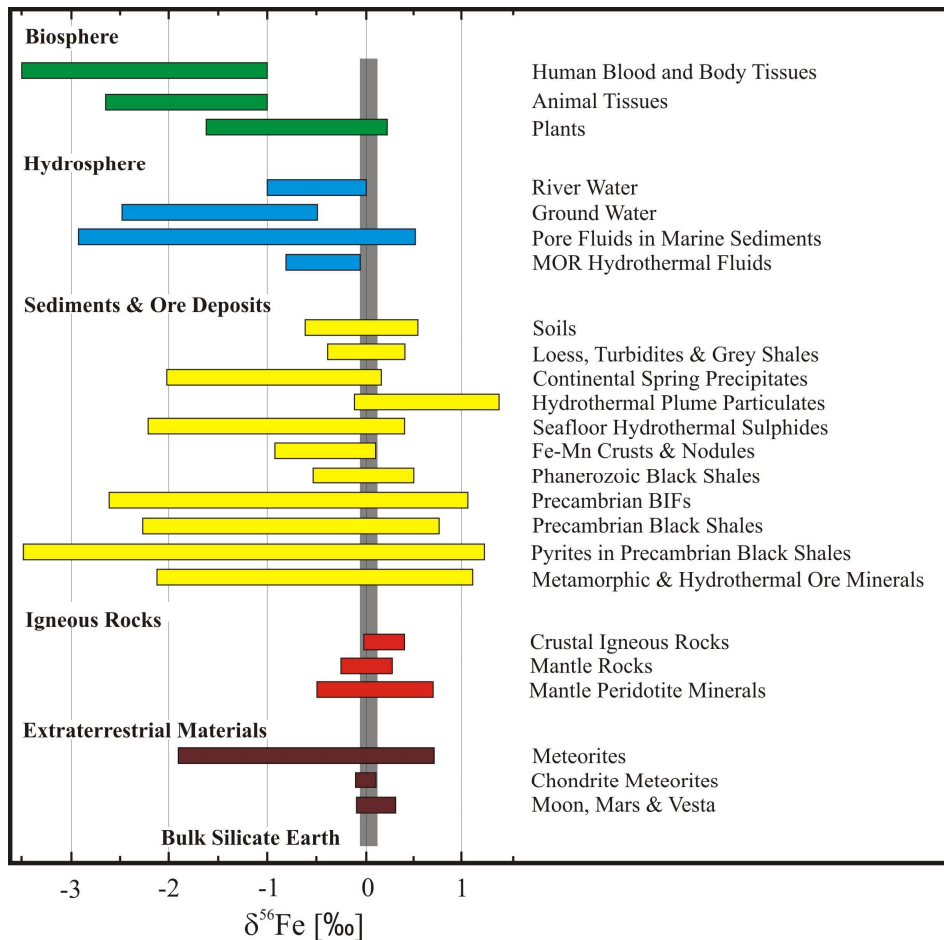


Figure 1.6 Natural iron isotope variations. Data of “biosphere” from Walczyk and von Blanckenburg (2002; 2005), Guelke and von Blanckenburg (2007) and Noordmann (2008). Other data from Anbar (2004), Beard and Johnson (2004), Johnson and Beard (2004), Dauphas and Rouxel (2006) and references therein. Grey bar: bulk silicate earth.

Also nonredox processes can result in significant kinetic and /or equilibrium Fe isotope fractionation (up to 1 ‰), for example inorganic mineral precipitation of Fe oxides (Skulan et al., 2002), carbonates (Wiesli et al., 2004), and sulfides (Butler et al., 2005). Considerable Fe isotope fractionation (up to  $-0.8$  ‰) can also take place during dissolution of silicates and ferric oxides in the presence of simple organic ligands such as oxalate (Brantley et al., 2001; 2004; Wiederhold et al., 2006) and during the dissolution of siderophores produced by soil bacteria (Brantley et al., 2001; 2004). Fractionation might also occur during ligand exchange reactions (Anbar et al., 2000; Roe et al., 2003; Schauble, 2004; Dideriksen et al., 2008).

Therefore it is not surprising that large variations in the Fe isotope compositions have been found so far in the biosphere where many redox reactions, ligand exchange, precipitation and dissolution of iron take place. The range of found isotopic variation in nature in general is

about 5 ‰, in the biosphere (plants, animals, humans) it is about 3.7 ‰ to date, indicating that the biosphere is the reservoir on earth with the largest variations besides BIFs and pyrites in Precambrian black shales (Figure 1.6).

Unfortunately up to now there are only a small number of studies concerning natural iron isotope signatures in the biosphere including plants and animals/humans although it is a very promising field and great variations in  $\delta^{56}\text{Fe}$  have been found in nature so far (Walczyk and von Blanckenburg, 2002; 2005). In the following part of the chapter I will focus on the state of art of iron isotope fractionations found in the biosphere.

To interpret iron isotope variations in plants it is crucial to know the iron isotope composition of the soil where the plants grow on. Regrettably iron isotope data from natural soil environments are still rare. Bulk soils were measured in the study of Walczyk and von Blanckenburg (2005) and gave values of +0.3 ‰ to -0.2 ‰ in  $\delta^{56}\text{Fe}$ , indicating that the iron isotope composition of bulk soils is around zero. Significant iron isotope fractionation during lateral iron translocation at the landscape scale was investigated by Wiederhold and von Blanckenburg (2002) but the correlation of the observed data to specific pedogenic processes was limited. Fantle and DePaolo (2004) studied iron isotope variations in four selected horizons of a soil profile in northern California and found variations of about 0.7 ‰ in  $\delta^{56}\text{Fe}$  between bulk soil samples from different depths. Brantley et al. (2001; 2004) reported a strong enrichment of light isotopes in the exchangeable iron fraction compared to oxide-bound iron in a soil sample from the B horizon of a hornblende-containing soil. Emmanuel et al. (2005) reported variations of about 0.35 ‰ in  $\delta^{57}\text{Fe}$  (approximating 0.24 ‰ in  $\delta^{56}\text{Fe}$ ) in bulk soil samples of a Czech forest soil and an Israeli semi-arid soil. In their study a least-squares method was used to estimate the Fe isotopic composition of the end-members representing the three main Fe reservoirs in the Czech soil (silicates, organically bound Fe and pedogenic Fe-oxides). Wiederhold et al. (2007a, 2007b) showed that different iron pools (poorly-crystalline iron oxyhydroxides, crystalline iron oxides, and silicate bound iron) of different types of soil (Podzol, Cambisol, redoximorphic soil) have different iron isotope signatures and that podzolation leads to a preferential translocation of lighter iron isotopes within the soil. Thompson et al. (2007) measured the iron isotopic composition of surface and subsurface basaltic soil horizons and found different Fe isotopic signatures at different soil depths and in different soil fractions ranging from +1 ‰ to -0.3 ‰ in  $\delta^{56}\text{Fe}$ . Schuth et al. (2009) determined the iron isotope composition of horizons of a gleysol from NW Germany and found  $\delta^{57}\text{Fe}$  values ranging from +0.3 ‰ in the Ah horizon and -0.2 ‰ in the Gor

horizon. Additionally they conducted an experimental study where suspensions of gleysol horizons were subjected to controlled redox conditions. The experiments yielded values from about  $-0.4\text{ ‰}$  in  $\delta^{57}\text{Fe}$  for moderately reducing conditions to  $-1\text{ ‰}$  for reducing conditions and  $+0.3\text{ ‰}$  for oxidising conditions. Fe concentrations increased substantially at reducing conditions, indicating a preferential mobilisation of lighter iron into aqueous solutions at reducing conditions, leaving a residue enriched in heavy iron isotopes.

With the start of this work actually no iron isotope data were available on natural grown or greenhouse plants and even up to now our study (Guelke and von Blanckenburg, 2007) is the only one giving iron isotope data of greenhouse plants. However, very recently Kiczka et al. (2010b) found an enrichment of the lighter iron isotopes by  $-1.0$  to  $-1.7\text{ ‰}$  in  $\delta^{56}\text{Fe}$  in three alpine plant species, two of them being strategy I plants and one potentially a strategy II plant, grown under natural growth conditions.

The usefulness of stable iron isotopes as tracers in plant biology has been recognized (Álvarez-Fernández, 2006; Rodríguez-Castrillon et al., 2008; Stuerup et al., 2008). For other elements like Si (Opfergelt et al., 2006a; 2006b), Zn (Weiss et al., 2005; Viers et al., 2007; Moynier et al., 2009), Ca (Wiegand et al., 2005; Page et al., 2008; Centi-Tok et al., 2009) or Mg (Black et al., 2008; Bolou Bi et al., 2008) isotope data of plants are available. Thereby it has been shown that plants favour the heavy isotope of Si and the Si-isotopic compositions of the various plant parts indicate that heavy isotopes discrimination occurs at three levels in the plant (at the root epidermis, for xylem loading and for xylem unloading) (Opfergelt et al., 2006b). Plants seem also to favour the heavier isotopes of Mg as roots of rye-grass and clover are significantly enriched in the heavier Mg isotopes but shoots are systematically lighter than roots (Bolou Bi et al., 2008). Black et al. (2008) reported that wheat plants grown hydroponically preferentially took up the heavy Mg isotopes from the growth solution as well. The uptake of Zn by roots grown in nutrient solution leads to an enrichment of heavier Zn isotopes in the roots but lighter Zn isotopes in the shoots (Weiss et al., 2005). During Zn transport within the plant, both diffusion and active uptake of heavy isotopes by cells out of the xylem favour the mobility of light isotopes to the most aerial parts of the plants (Viers et al., 2007). Additionally Moynier et al. (2009) showed that translocation within the plant favours the lighter Zn isotopes. Results of Wiegand et al. (2005) and Page et al. (2008) propose a converse systematic behaviour of stable Ca isotopes in trees: tree tissues contain lighter Ca than the soil fractions whereby roots and stem wood contain the lightest Ca, while leaves hold the heaviest Ca. Centi-Tok et al. (2009) also demonstrated increasingly heavy Ca

in the order roots – stem wood – leaves for spruce and beech at a watershed in Northern France.

First data on the stable iron isotope composition of plants were given by Walczyk and von Blanckenburg (2002). These authors measured stable iron isotope signatures in human blood, human body tissues and in the human diet, including animal and plant food sources. Plant food was purchased from conventional supermarkets and comprised cereals like wheat, rye and rice as well as vegetables like spinach, lentils, green beans, soybeans and peas. All plant foods were found to be enriched in the lighter iron isotopes up to  $-1.5$  ‰ in  $\delta^{56}\text{Fe}$  compared to IRMM-014, only spinach had a  $\delta^{56}\text{Fe}$  value of near zero. Except for fish samples animal food products were even more enriched in the light iron isotopes, up to  $-2.5$  ‰ and the lightest values for stable iron isotopes were found in human blood and human tissues (Figure 1.7). Human blood covers a range of  $-2.0$  to  $-3.1$  ‰ in  $\delta^{56}\text{Fe}$ , human liver is heavier with  $-0.9$  to  $-1.6$  ‰ and human muscle tissue has similar values as human blood with  $-2.1$  to  $-3.4$  ‰. The lowest  $\delta^{56}\text{Fe}$  was measured for human hair with  $-3.3$  ‰.

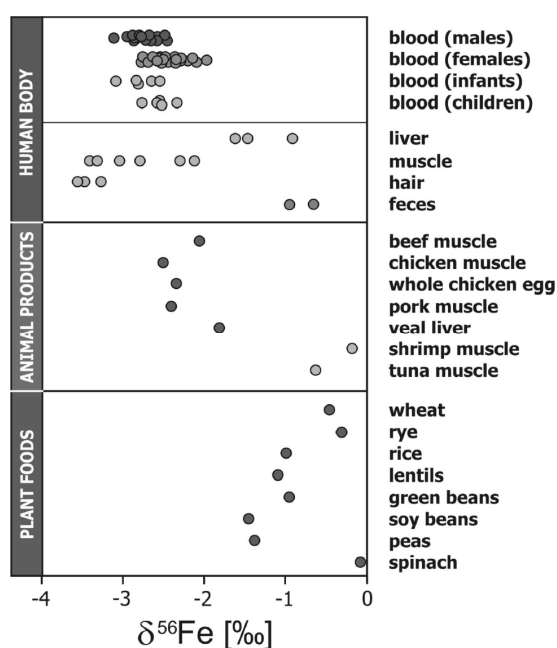


Figure 1.7 Fe isotope variations in the human body and in different food samples covering the most relevant dietary food sources (from Walczyk and von Blanckenburg, 2002).

All these first values show that the lighter iron isotopes are enriched along the food chain, decreasing with 1 ‰ with each trophic level (Figure 1.8). Iron in the human diet is isotopically heavier than iron in the human body but lighter than iron in the geosphere.

Thereby animal food sources like meat and eggs are more enriched in the lighter iron isotopes compared to plant food sources.

The question arose why human blood has such a light iron isotope composition. As only 10-20 % of iron in the daily human diet derive from animal products (Ziegler and Filer, 1996), these products can't be responsible for the light iron isotope ratios in human blood. Additionally most of dietary iron leaves our body unabsorbed; this can be seen as well in the  $\delta^{56}\text{Fe}$  values of human feces (Figure 1.7) which are similar to that of the human diet.

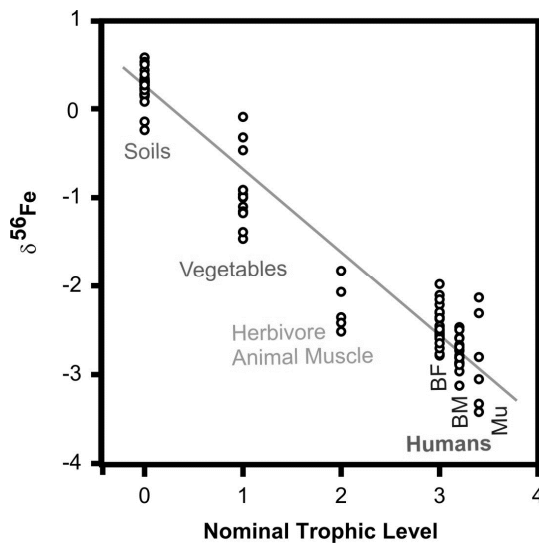


Figure 1.8 Fractionation of stable iron isotopes along the food chain. BF: Blood female; BM: Blood male; Li: Liver tissue; Mu: Muscle tissue (from Walczyk and von Blanckenburg, 2005).

It was suggested that blood iron isotopic shifts either originate from preferential losses of heavy iron isotopes from the body via skin exfoliation, sweat, hair, bile or urine; from fractionation processes during absorption in the intestine, or from isotope effects during distribution between body tissues. The first idea was excluded immediately since losses were too small and hair for instance has an even lighter iron isotope composition than human blood (Figure 1.7). The authors concluded that the iron isotope effect in the human blood results from the preferential uptake of light iron isotopes in the human intestine. In the food sources iron is mostly prominent in its ferric form and has to be reduced in the small intestine to be absorbed by the human body. This reduction could lead to a fractionation effect, favouring the uptake of the lighter iron isotopes. The authors also concluded that the different iron isotope signature in the blood reflects each individual's efficiency of iron absorption (Krayenbuehl et al., 2005; Walczyk and von Blanckenburg, 2005). After Ohno et al. (2004) these signatures stay stable for at least one year. This finding reflects directly the slowly turn-over of iron in the human body. The hypothesis of a preferential absorption of lighter iron isotopes in the

intestine was confirmed by analyzing blood of patients, suffering from hereditary hemochromatosis, a disease that is characterized by excessive iron uptake in the intestine (Krayenbuehl et al., 2005). The iron isotopic composition of blood obtained from patients undergoing regular phlebotomies (blood-lettings) for iron removal was compared to that of the blood of untreated hemochromatic patients as well as an age matched control group. Patients suffering from iron overload tend to have a higher proportion of the heavier iron isotopes in blood relative to healthy controls when treated with regular phlebotomies. It was concluded that the rate of iron absorption in the intestine is determining the isotopic signature in blood as under hemochromatosis the fractionation effect is lower as iron absorption is higher.

Besides absorption efficiency as a main determining factor for the isotopic composition of blood iron, potential isotope effects during distribution and relocation of iron within organs and tissues were considered. It was found out that liver tissue is much less enriched in the light iron isotopes than blood (Walczyk and von Blanckenburg, 2002). A reinterpretation of the observation in haemochromatotics was done. In fact, the release of liver iron rather enriched in heavy isotopes could be responsible for the changes in blood iron isotopic composition rather than a further increase in absorption efficiency in response to the acute blood loss. The question arose whether the enrichment of light iron isotopes in human blood could just be a consequence of the storage of heavy iron in the liver, leaving a light residue. But liver iron was not substantially depleted in light iron isotopes compared to dietary iron; therefore this could not be the only reason. The question remained open whether there might be other complementarily fractionated organs besides liver that could be responsible for the observed effects. Hotz (2009) addressed this question in her dissertation. In one of her studies a Goettingen minipig was used as a model of human physiology and the iron isotope composition of body tissues relevant to iron metabolism was determined. The author found an enrichment of light iron isotopes in the gastric and intestinal mucosa of the minipig and a correlation of iron isotopic signatures of the mucosa with known and suggested sites of iron absorption of mammals. This is a direct proof for a preferential uptake of light iron isotopes from the diet. A detected enrichment of heavier iron isotopes in the liver and other ferritin-rich organs (red bone marrow, spleen) indicate that both iron absorption and iron deposition in body tissues are mass-sensitive and determine the individual iron isotope composition in blood. To confirm this statement Hotz (2009) observed the changes in blood iron isotope signatures of four iron-overloaded subjects undergoing phlebotomy treatment (blood-letting).

She detected a measurable effect on the iron isotopic composition of blood resulting from blood lettings and therefore mobilization of storage iron. The evolution of blood loss was quantitatively visible in the iron isotopic composition of blood. The author concludes that iron absorption efficiency and partitioning of iron between blood and body iron stores are determinants of the iron isotopic composition of human blood.

Recently a systematic study of the iron isotope composition of middle-European human food sources showed a mean  $\delta^{56}\text{Fe}$  of  $-0.5\text{‰}$  in a normal human diet with slight variations for men and women. For a vegetarian diet a  $\delta^{56}\text{Fe}$  of  $-0.2\text{‰}$  could be determined (Noordmann, 2008). These values together with the data for human blood obtained by Walczyk and von Blanckenburg (2002) make the calculation of a  $\Delta^{56}\text{Fe}_{\text{diet-human body}}$  possible. This yields a  $\Delta^{56}\text{Fe}_{\text{diet-human body}}$  of  $-2.0\text{‰}$  for women and  $-2.2\text{‰}$  for men when a “normal” European diet is followed. A vegetarian diet leads to a  $\Delta^{56}\text{Fe}_{\text{diet-human body}}$  of  $-2.2\text{‰}$  for women and  $-2.6\text{‰}$  for men.

The first attempt of Walczyk and von Blanckenburg (2002; 2005) and also the work of Kiczka et al. (2010b) only showed that plants seem to be enriched in the lighter iron isotopes but systematic studies are missing up to now. In the following chapters of this thesis many open questions are addressed concerning the iron isotopic signature of different plant species grown on agricultural soil or in nutrient solution, the development of  $\delta^{56}\text{Fe}$  during translocation of Fe inside the plant, as well as elucidating the mechanisms which lead to iron isotope fractionation in plants and establishing stable iron isotopes as a tool to study uptake and translocation mechanisms in plants.



## 2 Fractionation of stable iron isotopes in higher plants

### 2.1 Abstract

Although the fractionation of stable iron isotopes by biological processes in the environment is currently a matter of intense debate, the isotope fractionation associated with the growth of higher plants has, to date, not been characterized. Here it is shown that iron isotope fractionation induced by higher plants is substantial and also generates systematic plant-specific patterns. A hypothesis is suggested in which these patterns mirror the two different strategies that plants have developed to incorporate iron from the soil: reduction of Fe(III) in soils by strategy I plants resulted in the uptake of iron, which is depleted in  $^{56}\text{Fe}$  by up to 1.6 per mil relative to  $^{54}\text{Fe}$  when compared to the available Fe in soils; complexation with siderophores by strategy II plants resulted in the uptake of iron that is 0.2 per mil heavier than that in soils. Furthermore, younger parts of strategy I plants became increasingly depleted in heavy isotopes as the plant was growing, while strategy II plants incorporated nearly the same isotope composition throughout. This points to entirely different translocation mechanisms between strategy I and II plants. Such presumably redox-related differences in translocation have been under debate up to now. It is concluded that plant metabolism represents an important cause of isotopic variation in the biogeochemical cycling of Fe. Therefore, heavy stable metal isotope systems now start to be viable indicators of geosphere - biosphere metal transfer processes.

### 2.2 Introduction

The isotopic composition of an element is changed if the element is transported from a source compartment to a target compartment given that element transfer is both incomplete and mass-sensitive (Walczyk and von Blanckenburg, 2002). Stable isotope ratios are routinely used in studying the biogeochemical cycling of light elements in the environment, including studies of the mechanisms of photosynthesis and of nutrient uptake and translocation in plants (Taiz and Zeiger, 2002). However, until very recently, equivalent methods have not been available for heavier elements with atomic masses above 40 amu due to instrumental limitations. Sophisticated mass-spectrometric techniques now allow the measurement of small

changes in heavy metal stable isotope ratios resulting from equilibrium and kinetic reactions in both biotic and abiotic processes (Johnson et al., 2004b; Dauphas and Rouxel, 2006). Due to its importance in natural systems, iron has attracted particular attention and iron isotopes now provide a new tool to trace the biogeochemical iron cycle (Walczyk and von Blanckenburg, 2002; Johnson et al., 2005; Walczyk and von Blanckenburg, 2005; Dauphas and Rouxel, 2006).

While biogeochemists have mainly used this new isotope tool to focus on the work of microbes in the environment it is in fact the higher organisms that produce the largest isotope fractionations. Recent studies on iron isotope fractionation in the human body and of human food sources revealed that large fractionations of stable iron isotopes take place in higher animals and plants (Walczyk and von Blanckenburg, 2002). The lighter iron isotopes are enriched along the food chain and each individual human being bears a distinct Fe isotope signature in blood, pointing at the possibility that Fe uptake efficiency results in an isotope fingerprint, and that iron isotopes can be used to quantify the uptake efficiency (Walczyk and von Blanckenburg, 2005). Plants are the principal source of iron in most human diets (Guerinot and Salt, 2001) but they have not yet been characterized isotopically in a systematic manner (Walczyk and von Blanckenburg, 2002). For human nutrition studies it is important to determine a representative fractionation factor between the human diet and the human body. In plant research stable isotopes potentially offer an excellent and safe tool to study the uptake and the metabolic processes of iron (Álvarez-Fernández, 2006).

The sufficient supply of iron is essential for all living organisms to maintain cellular homeostasis. In plants Fe is required for iron-sulfur proteins and as a catalyst in enzyme-mediated redox reactions (Taiz and Zeiger, 2002). Although abundant in soil, iron is one of the most limiting nutrients for plant growth (Guerinot and Salt, 2001) because it exists primarily in the ferric form [Fe(III)] which is of extremely low solubility (Lindsay and Schwaab, 1982). Iron excess occurs on waterlogged soils with anaerobic conditions such as rice fields. The excess accumulation of Fe(II) in plants results in the well-known bronzing phenomenon, caused by oxidative stress (Briat and Lobreaux, 1997). To utilize iron efficiently for growth, two distinct iron acquisition mechanisms known as strategy I and strategy II have evolved in higher plants (Roemheld and Marschner, 1986). Strategy I plants, which comprise the dicots and non-grass monocots, excrete protons via a plasmalemma H<sup>+</sup>-ATPase to acidify the rhizosphere, thus making Fe(III) more soluble. The inducible ferric chelate reductase activity of FRO2 reduces Fe(III) to Fe(II) (Robinson et al., 1999). Fe(II) is

subsequently transported into the plant by IRT1, which is the major iron transporter of the plant root (Vert et al., 2002). Within the cells the production of highly toxic hydroxyl radicals through iron redox changes is avoided by sophisticated chelation mechanisms (Hell and Stephan, 2003). The grasses use the strategy II response, which relies on chelation of Fe(III) rather than reduction (Takagi et al., 1984). In this case, phytosiderophores are released into the soil where they chelate Fe(III); the complexed Fe(III) is then internalized via specific transporters (Curie et al., 2001; Schaaf et al., 2004). A better understanding of intracellular redox state, binding forms and Fe transport processes in plants is required for biofortification (Roemheld and Schaaf, 2004). Although numerous studies with radioactively marked Fe isotopes have examined Fe partitioning in plants (Roemheld and Marschner, 1986; Roemheld and Schaaf, 2004), methods based on stable isotope fractionation have the potential to shed additional light on the behaviour of iron in plants (Álvarez-Fernández, 2006). Unlike radioactively labelled Fe isotopes, which provide information on uptake rates and transferred amounts from a synthetic Fe substrate, stable iron isotopes identify the underlying processes and, potentially, the fractions transferred from natural soil substrates.

### **2.3 Materials and methods**

Using multi-collector inductively coupled plasma mass spectrometry (MC-ICP-MS), it was investigated whether plants discriminate between Fe isotopes. The isotopic composition of dietary plant iron was determined and it was elaborated whether Fe isotope effects can be used to trace uptake and translocation mechanisms in strategy I and strategy II plants. Stable Fe isotope compositions were analyzed in different kinds of vegetables including graminaceous and non-graminaceous species and in the soils where they were grown.

#### **2.3.1 Plant growth**

About five individuals of different kinds of legumes were sown in 5–10 L pots on a sandy and a loamy soil. Plants grew in a daylight climate chamber with a temperature of 16 – 18 °C and were only watered with deionised water without fertilizer. About ten individual plants were taken from each soil after approximately 60 days, and, where possible, at a full growth period after approximately 180 days. Plants were washed with deionised water and separated into stem, leaves, and seeds. The original seeds were also examined. To investigate whether the Fe

isotopic composition changes with the age of plant sections, bean plants were sampled for the lower and upper parts of the stem and for the first to fourth fully expanded leaf. Plant samples were dried at 80 °C for at least 3 days in an oven and ground to mince and homogenize them.

### 2.3.2 Soils

Two types of soils were used as substrate for plant growth under field conditions: (1) a Cambisol from glacial sand of the Drenthe stadium of the Saaleian glaciation (profile Hannover-Herrenhausen; location Rp 3548 / Hp 5807) located in the “Geest”, the moraine landscape prevalent in Lower Saxony,  $\text{pH}_{\text{H}_2\text{O}} = 7.5$ ; and (2) a Stagni-Haplic Luvisol from loess of the Weichselian glaciation (profile Ruthe; location Rp 3556 / Hp 5790) located at the NW margin of the main European loess belt in the centre of Germany,  $\text{pH}_{\text{H}_2\text{O}} = 7.8$ . Both soils are used as agricultural soils; the Ap horizon (0-30 cm depth) was sampled.

To estimate the Fe isotopic composition of the iron pool in the soils that is available to plants, the  $^{56}\text{Fe}/^{54}\text{Fe}$  ratio of the exchangeable iron fraction (exchanged with 1 M  $\text{MgCl}_2$ ), iron of amorphous iron oxides and in organic complexes (extracted with a mixture of 30 %  $\text{H}_2\text{O}_2$  and 0.03 M  $\text{HNO}_3$ ) were determined using the extraction methods after Tessier et al. (1979), and iron in the soil solution (saturated with deionised water, followed by shaking, centrifugation and filtration). The  $\delta^{56}\text{Fe}$  of the bulk soils was determined as well.

### 2.3.3 Sample preparation

Samples were prepared for isotopic analysis according to the procedure of Schoenberg and von Blanckenburg (2005). Approximately 250 mg of each plant sample was digested via a microwave digestion system in 4 mL of concentrated  $\text{HNO}_3$ , evaporated on a hotplate in Teflon beakers and treated with a mixture of 30 %  $\text{H}_2\text{O}_2$  and concentrated  $\text{HNO}_3$  to oxidize the organic compounds and ferrous iron to ferric iron. Subsequently the samples were redissolved in 6 M  $\text{HCl}$  and centrifuged to eliminate any remaining solids. Iron was separated from other elements by anion-exchange chromatography (resin DOWEX AG<sup>®</sup> 1x8 100-200 mesh) with quantitative recovery, evaporated, and dissolved in 1 mL 0.3 M  $\text{HNO}_3$  (Schoenberg and von Blanckenburg, 2005). It has been shown that Fe separates of samples with high transition metal contents or organic matrices may not be entirely matrix-free after anion-exchange chromatography and require further purification (Schoenberg and von Blanckenburg, 2005). Therefore, an additional precipitation step was employed that ensures

quantitative precipitation of all Fe(III) as Fe(III)OOH while Cu, Zn, Co, Cd, Mn and V as well as organic compounds remain in solution. The samples were precipitated at pH 10 with NH<sub>4</sub>(OH) and solutions were allowed to equilibrate for 1 h before centrifugation. The supernate solutions were discarded and the precipitates were washed with pure H<sub>2</sub>O. The precipitate was redissolved in HNO<sub>3</sub>. Quantitative recovery during precipitation, essential to avoid Fe isotope fractionation, was assured by determining the Fe concentration before and after the precipitation step. Finally the samples were diluted to 3-8 ppm Fe in 0.3 M HNO<sub>3</sub> for isotopic analysis.

### 2.3.4 Iron isotope measurements

Iron isotope compositions were determined using a multiple-collector inductively coupled plasma mass spectrometer (MC-ICP-MS; Neptune, *ThermoFinnigan*). The sample-standard bracketing approach commonly used to correct for mass discrimination was applied (Schoenberg and von Blanckenburg, 2005) using the Fe isotopic reference material IRMM-014. Sample and standard solutions were introduced into the mass spectrometer in 0.3 M HNO<sub>3</sub> at concentrations of 3-8 ppm Fe. All values are reported as  $\delta^{56}\text{Fe}$  relative to the IRMM-014 standard of which the isotopic composition is close to that of rocks at the Earth's surface (Johnson et al., 2004a; Dauphas and Rouxel, 2006; Schoenberg and von Blanckenburg, 2006) (defined as  $\delta^{56}\text{Fe} = 0$  with  $\delta^{56}\text{Fe}/[\text{‰}] = [({}^{56}/{}^{54}\text{Fe}_{\text{sample}}/{}^{56}/{}^{54}\text{Fe}_{\text{standard}}) - 1] \cdot 10^3$  where  ${}^{56}\text{Fe}/{}^{54}\text{Fe}_{\text{sample}}$  is the  ${}^{56}\text{Fe}/{}^{54}\text{Fe}$  ratio of the measured sample and  ${}^{56}\text{Fe}/{}^{54}\text{Fe}_{\text{standard}}$  is the average  ${}^{56}\text{Fe}/{}^{54}\text{Fe}$  ratio of the IRMM-014 standards measured before and after each sample).

$\delta^{56}\text{Fe}$  and  $\delta^{57}\text{Fe}$  of all samples were plotted against each other and were found to follow a mass-dependent fractionation law which demonstrates the absence of molecular or elemental interferences. A precision of  $\pm 0.05 \text{ ‰}$  (2SD) for the  $\delta^{56}\text{Fe}$  and  $\pm 0.08 \text{ ‰}$  (2SD) for the  $\delta^{57}\text{Fe}$  (Schoenberg and von Blanckenburg, 2005) was achieved.

## 2.4 Results and discussion

The observed isotope shifts were mass-dependent. The obtained precision allowed to resolve differences in the isotopic composition of Fe of the different parts of the plant species and in different soil fractions. The sandy and loamy soils had a bulk Fe isotopic composition of  $\delta^{56}\text{Fe} = 0.03 \pm 0.1 \text{ ‰}$  and  $\delta^{56}\text{Fe} = -0.07 \pm 0.1 \text{ ‰}$ , respectively. If a mean of the  $\delta^{56}\text{Fe}$  values

## 2 Fractionation of stable iron isotopes in higher plants

---

of the extracted soil fractions which mostly tend to be mobilized by plants (Inoue et al., 1993; Bertrand and Hinsinger, 2000) is taken, an approximate  $\delta^{56}\text{Fe}$  value of  $-0.14 \pm 0.07$  ‰ (2SD) for the plant-available iron in the sandy and  $-0.08 \pm 0.06$  ‰ (2SD) for the plant-available iron in the loamy soil is obtained. The absence of Fe released from silicates and clay minerals was assured by measuring Si and Al concentrations in the solutions.

Iron isotope compositions of different parts of strategy I and strategy II plants varied from  $\delta^{56}\text{Fe} = +0.17$  ‰ to  $-1.64$  ‰ (Table 2-1) and displayed some consistent features: strategy I plants usually yielded lower  $\delta^{56}\text{Fe}$  than the plant-available iron in both types of soil, whereas strategy II plants usually yielded slightly higher  $\delta^{56}\text{Fe}$  than the plant-available soil iron (Figure 2.1). The isotope fractionation was not dependent on the type of soil as plants experienced similar isotope shifts on both soils. Fractionation of iron in strategy I plants was more pronounced in plant samples grown on the sandy soil, however.

Reduction, sorption to Fe oxides, precipitation, complexation with organic ligands and a change in the dissolved inorganic Fe species has been shown to affect the isotopic composition of iron (e.g. Bullen et al., 2001; Welch et al., 2003; Brantley et al., 2004; Croal et al., 2004; Icopini et al., 2004; Johnson and Beard, 2004; Anbar et al., 2005; Staubwasser et al., 2006; Wiederhold et al., 2006). Redox reactions result in the largest fractionations. For example aqueous solutions at equilibrium (22°C) contained Fe(III) that had  $\delta^{56}\text{Fe}$  values which were 3 ‰ higher than that of dissolved Fe(II) (Welch et al., 2003). Conversely, reduction of a ferric solid led to  $\delta^{56}\text{Fe}$  that was approx. 1.0 - 1.5 ‰ lower in the resulting reduced species (Johnson et al., 2005; Staubwasser et al., 2006).

These iron isotope fractionation patterns allow to conclude that the main fractionation in strategy I plants occurs during reduction of Fe in the rhizosphere prior to absorption by the root cells. Since only a small fraction of the mobile iron in the soil is reduced, an equilibrium fractionation allows for a partitioning of isotopes, resulting in a lower  $\delta^{56}\text{Fe}$  value in the plants than in the soil. In contrast to redox-related isotope shifts, release of ferric iron from Fe oxides by complexation results in only minute isotope shifts, and is usually associated with a small shift towards heavy compositions. Little fractionation (a slight enrichment of heavy Fe isotopes) was observed in the study of Brantley et al. (2004) between abiotically DFAM (siderophore desferrioxamine mesylate) dissolved Fe and goethite ( $\delta^{56}\text{Fe}_{\text{goethite}} = -0.23$  ‰,  $\delta^{56}\text{Fe}_{\text{in solution}} = -0.14$  to  $0.11$  ‰; mean:  $\Delta_{\text{Fe solution-Fe goethite}} = 0.2$  ‰, where  $\Delta_{\text{Fe solution-Fe goethite}}$  describes the isotope fractionation between a source compartment containing Fe in

## 2 Fractionation of stable iron isotopes in higher plants

goethite and target compartment containing Fe(III) in solution, in this case  $\Delta = \delta^{56}\text{Fe}_{\text{Fe solution}} - \delta^{56}\text{Fe}_{\text{Fe goethite}}$ ).

Table 2-1 Iron concentrations and  $\delta^{56}\text{Fe}$  of all plant parts

Sample	$\delta^{56}\text{Fe} \pm *2\sigma$	$\delta^{57}\text{Fe} \pm *2\sigma$	Fe conc. [ $\mu\text{g/g}$ ]	Sample	$\delta^{56}\text{Fe} \pm *2\sigma$	$\delta^{57}\text{Fe} \pm *2\sigma$	Fe conc. [ $\mu\text{g/g}$ ]
<i>sandy soil</i>				<i>loamy soil</i>			
<b>Bean (<i>Phaseolus vulgaris</i> L.)</b>							
701 (original seed)	-0.581 $\pm$ 46	-0.870 $\pm$ 74	55				
711B (leaf first harvest)	-0.552 $\pm$ 46	-0.847 $\pm$ 99	114	721B (leaf first harvest)	-0.611 $\pm$ 47	-0.937 $\pm$ 90	100
711S (stem first harvest)	-0.400 $\pm$ 46	-0.567 $\pm$ 73	29	721S (stem first harvest)	-0.224 $\pm$ 46	-0.383 $\pm$ 73	86
712B (leaf second harvest)	-1.131 $\pm$ 46	-1.662 $\pm$ 73	85	722B (leaf second harvest)	-0.535 $\pm$ 46	-0.749 $\pm$ 73	71
712S (stem second harvest)	-0.625 $\pm$ 46	-0.939 $\pm$ 79	46	722S (stem second harvest)	-0.281 $\pm$ 46	-0.430 $\pm$ 73	31
712F (new grown seed)	-1.462 $\pm$ 46	-2.113 $\pm$ 73	92	722F (new grown seed)	-0.966 $\pm$ 46	-1.400 $\pm$ 92	56
<b>Bean growth experiment</b>							
B1F (fruit)	-1.635 $\pm$ 46	-2.380 $\pm$ 73	60				
B1S1 (older part of stem)	-0.503 $\pm$ 46	-0.709 $\pm$ 73	70				
B1S2 (younger part of stem)	-0.852 $\pm$ 46	-1.194 $\pm$ 73	30				
B1B1 (first fully grown leaf)	-0.404 $\pm$ 46	-0.613 $\pm$ 73	104				
B1B2 (second fully grown leaf)	-0.901 $\pm$ 46	-1.288 $\pm$ 73	77				
B1B3 (third fully grown leaf)	-1.048 $\pm$ 46	-1.499 $\pm$ 73	72				
B1B4 (fourth fully grown leaf)	-1.112 $\pm$ 46	-1.605 $\pm$ 73	62				
<b>Lettuce (<i>Valerianella locusta</i> L.)</b>							
901 (original seed)	-0.379 $\pm$ 46	-0.562 $\pm$ 73	150				
911B (leaf first harvest)	-0.306 $\pm$ 46	-0.470 $\pm$ 73	175	921B (leaf first harvest)	-0.201 $\pm$ 46	-0.316 $\pm$ 73	223
<b>Spinach (<i>Spinaci oleracea</i> L.)</b>							
1001 (original seed)	-1.054 $\pm$ 46	-1.566 $\pm$ 87	76				
1011B (leaf first harvest)	-0.211 $\pm$ 46	-0.363 $\pm$ 80	164	1021B (leaf first harvest)	-0.185 $\pm$ 46	-0.318 $\pm$ 75	174
1011S (stem first harvest)	-0.132 $\pm$ 46	-0.195 $\pm$ 76	190	1021S (stem first harvest)	-0.102 $\pm$ 46	-0.170 $\pm$ 76	191
<b>Rape (<i>Brassica napus</i> L.)</b>							
501 (original seed)	-1.176 $\pm$ 46	-1.791 $\pm$ 81	118				
511B (leaf first harvest)	-1.011 $\pm$ 46	-1.480 $\pm$ 84	61	521B (leaf first harvest)	-0.836 $\pm$ 46	-0.128 $\pm$ 73	70
511S (stem first harvest)	-0.301 $\pm$ 46	-0.386 $\pm$ 99	107	521S (stem first harvest)	-0.337 $\pm$ 46	-0.419 $\pm$ 88	67
512F (new grown seed)	-1.535 $\pm$ 46	-2.007 $\pm$ 99	31				
<b>Pea (<i>Pisum sativum</i> L.)</b>							
601 (original seed)	-1.196 $\pm$ 48	-1.779 $\pm$ 73	64				
611B (leaf first harvest)	-0.914 $\pm$ 46	-1.352 $\pm$ 73	116	621B (leaf first harvest)	-0.690 $\pm$ 46	-1.010 $\pm$ 73	122
611S (stem first harvest)	-0.750 $\pm$ 46	-1.081 $\pm$ 73	70	621S (stem first harvest)	-0.433 $\pm$ 46	-0.646 $\pm$ 73	72
<b>Amaranth (<i>Amaranthus hybridus</i> L.)</b>							
401 (original seed)	-1.490 $\pm$ 46	-2.217 $\pm$ 75	72				
411B (leaf first harvest)	-1.151 $\pm$ 46	-1.730 $\pm$ 73	153	421B (leaf first harvest)	-0.433 $\pm$ 46	-0.639 $\pm$ 73	122
411S (stem first harvest)	-0.970 $\pm$ 46	-1.464 $\pm$ 73	126	421S (stem first harvest)	-0.277 $\pm$ 46	-0.381 $\pm$ 79	75
412B (leaf second harvest)	-0.406 $\pm$ 46	-0.589 $\pm$ 73	164	422B (leaf second harvest)	-0.220 $\pm$ 46	-0.359 $\pm$ 73	60
412S (stem second harvest)	-0.139 $\pm$ 46	-0.245 $\pm$ 75	50	422S (stem second harvest)	-0.216 $\pm$ 46	-0.292 $\pm$ 78	8
412F (new grown seed)	-1.029 $\pm$ 46	-1.549 $\pm$ 73	109	422F (new grown seed)	-0.900 $\pm$ 46	-1.256 $\pm$ 73	48
<b>Soybean (<i>Glycine max.</i> L.)</b>							
801 (original seed)	-0.732 $\pm$ 90	-1.100 $\pm$ 73	53				
811B (leaf first harvest)	-0.643 $\pm$ 46	-0.934 $\pm$ 73	142	821B (leaf first harvest)	-0.687 $\pm$ 46	-0.971 $\pm$ 73	81
811S (stem first harvest)	-0.506 $\pm$ 46	-0.804 $\pm$ 75	44	821S (stem first harvest)	-0.716 $\pm$ 46	-1.058 $\pm$ 73	32
812B (leaf second harvest)	-0.296 $\pm$ 46	-0.400 $\pm$ 73	110	822B (leaf second harvest)	-0.476 $\pm$ 46	-0.623 $\pm$ 73	84
812S (stem second harvest)	-0.241 $\pm$ 46	-0.377 $\pm$ 73	40	822S (stem second harvest)	-0.700 $\pm$ 46	-1.010 $\pm$ 73	30
812F (new grown seed)	-0.931 $\pm$ 46	-1.384 $\pm$ 73	50	822F (new grown seed)	-1.523 $\pm$ 46	-2.229 $\pm$ 73	84

## 2 Fractionation of stable iron isotopes in higher plants

Table 2-1 continuation

Sample	$\delta^{56}\text{Fe} \pm *2\sigma$	$\delta^{57}\text{Fe} \pm *2\sigma$	Fe conc. [ $\mu\text{g/g}$ ]	Sample	$\delta^{56}\text{Fe} \pm *2\sigma$	$\delta^{57}\text{Fe} \pm *2\sigma$	Fe conc. [ $\mu\text{g/g}$ ]
<i>Maize (Zea mays L. convar. Saccharata)</i>							
101 (original seed)	-0.100 $\pm$ 46	-0.159 $\pm$ 73	68				
111B (leaf first harvest)	0.018 $\pm$ 53	0.059 $\pm$ 99	121	121B (leaf first harvest)	0.058 $\pm$ 65	0.025 $\pm$ 82	59
<i>Oat (Avena sativa L.)</i>							
301 (original seed)	0.094 $\pm$ 46	0.219 $\pm$ 89	30				
311B (leaf first harvest)	0.005 $\pm$ 99	-0.023 $\pm$ 98	69	321B (leaf first harvest)	0.071 $\pm$ 46	0.154 $\pm$ 73	50
311S (stem first harvest)	0.136 $\pm$ 99	0.169 $\pm$ 99	39	321S (stem first harvest)	0.071 $\pm$ 46	0.076 $\pm$ 73	39
312B (leaf second harvest)	0.087 $\pm$ 46	0.057 $\pm$ 73	82	322B (leaf second harvest)	-0.009 $\pm$ 46	-0.057 $\pm$ 73	99
312S (stem second harvest)	0.064 $\pm$ 46	0.098 $\pm$ 73	3	322S (stem second harvest)	0.072 $\pm$ 46	0.107 $\pm$ 73	7
312F (new grown seed)	0.003 $\pm$ 46	0.016 $\pm$ 73	20	322F (new grown seed)	0.096 $\pm$ 46	0.124 $\pm$ 73	25
<i>Wheat (Triticum aestivum L.)</i>							
201 (original seed)	-0.109 $\pm$ 46	-0.118 $\pm$ 73	25				
211B (leaf first harvest)	0.021 $\pm$ 46	0.030 $\pm$ 79	70	221B (leaf first harvest)	0.076 $\pm$ 46	0.090 $\pm$ 73	63
212B (leaf second harvest)	-0.046 $\pm$ 46	-0.028 $\pm$ 73	51	222B (leaf second harvest)	-0.018 $\pm$ 46	0.018 $\pm$ 73	65
212S (stem second harvest)	0.172 $\pm$ 46	0.236 $\pm$ 73	1	222S (stem second harvest)	0.091 $\pm$ 46	0.103 $\pm$ 73	2
212F (new grown seed)	-0.051 $\pm$ 46	-0.078 $\pm$ 73	92	222F (new grown seed)	-0.022 $\pm$ 46	-0.040 $\pm$ 73	50

\* given as the 2 standard deviation reproducibility of replicate measurements. This is determined from the internal measuring precision for single analysis, or external reproducibility of our JM standard (Schoenberg and von Blanckenburg, 2005), whichever was largest. Numbers refer to the last digits given for the  $\delta$ -values.

A similar minor enrichment of 0.3 ‰ in  $\delta^{56}\text{Fe}$  was observed for the solution of ligand-bound Fe(III) after goethite dissolution by oxalate (Wiederhold et al., 2006). Indeed our results showed a slight enrichment ( $\Delta^{56}\text{Fe} \approx 0.2$  ‰) of the heavy Fe isotopes in strategy II plants compared to the plant-available iron in the soils. However, leaves showed no resolvable further fractionation; only seeds tended to be slightly lighter than leaves (Figure 2.1).

Efficient acquisition of iron in graminaceous plant species relies on the synthesis and release of phytosiderophores (PS). Siderophores bind Fe(III) more effectively than do low-molecular weight organic acids, especially at neutral to alkaline conditions (Powell et al., 1980). The small enrichment of heavy isotopes is likely to be due to an equilibrium fractionation during complexation of Fe(III) to phytosiderophores in the rhizosphere. The Fe(III)-PS complexes are subsequently taken up by YS1-type membrane proteins that energize root uptake by the cotransport of metal-phytosiderophores with protons (Curie et al., 2001). As the Fe(III)-PS complex is too big for fractionation itself (relative mass differences are too small), the Fe(III)-PS uptake should not result in any further fractionation. This is the case even if uptake is not quantitative which is due to the degradation of Fe(III)-PS-complexes by microbes or absorption by the soil matrix. In summary, the reductive uptake of light iron by strategy I



plants, and the non-fractionating Fe(III) complexing by strategy II plants is entirely compatible with Fe isotope fractionation theory and known fractionation factors.

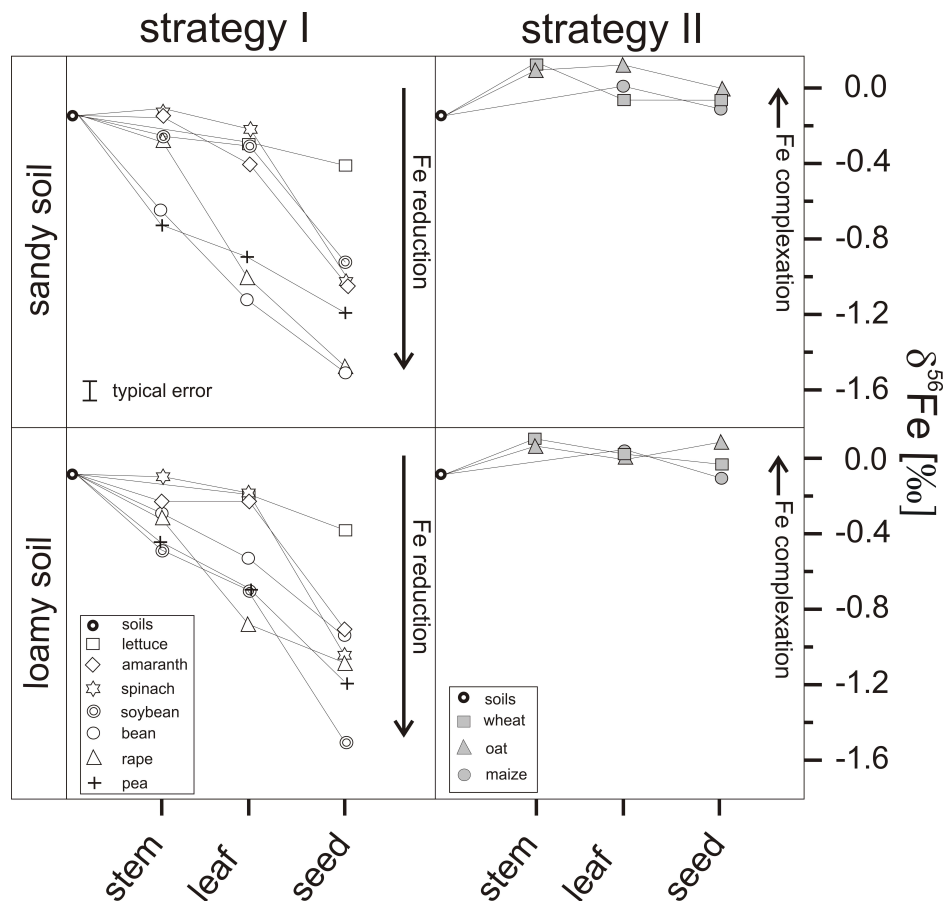


Figure 2.1  $\delta^{56}\text{Fe}$  of plant-available iron in the two soils and of different parts of strategy I and strategy II plants. Samples of stems, leaves and grown seeds were taken after approximately 60 days and, where possible, at full growth period after approximately 180 days. In almost all cases final compositions are plotted, unless an earlier growth stage is indicated in Table 2-1. For illustration purposes typical fractionation factors for reduction and complexation to siderophores (Brantley et al., 2004; Johnson et al., 2005; Staubwasser et al., 2006) are also given as arrows.

After identifying the feasibility of uptake-related fractionations, it is proceeded to apply similar concepts to iron translocation in plants. The theory of iron translocation in both strategy I and II plants is disputed much more than that of iron uptake (Hell and Stephan, 2003; Álvarez-Fernández, 2006). Stable iron isotope fractionations potentially provide new insight into this debate and it is possible to argue that substantial differences between translocation in strategy I and II plants are plausible based on the observed isotope shifts. All parts of strategy I plants were enriched in the lighter Fe isotopes throughout plant growth. The

## 2 Fractionation of stable iron isotopes in higher plants

---

$\delta^{56}\text{Fe}$  values decreased from soils to stems (mean  $-0.15$  to  $-0.6$  ‰), from stems to leaves (mean  $-0.2$  to  $-0.9$  ‰) and from leaves to seeds, which were fractionated up to  $-1.6$  ‰ relative to the soil Fe (Table 2-1). In addition, stem and leaves of a bean plant (strategy I) showed decreasing  $\delta^{56}\text{Fe}$  during growth. This was particularly true in the step of first ( $\delta^{56}\text{Fe}$  of  $-0.4$  ‰) to fourth fully grown leaves ( $\delta^{56}\text{Fe}$  of  $-1.1$  ‰) (Table 2-1).

The question now arises whether this successive enrichment of light isotopes in strategy I plants resulted from iron isotope fractionation during uptake, during translocation, or both. A plausibility test of the potential causes of this phenomenon along four possible end member scenarios provides evidence for iron translocation being the governing process. For illustration purposes it is assumed that in all cases iron reduction is associated with a fractionation  $\Delta_{\text{reduced species-oxidized species}}$  of  $-1.5$  ‰ (Johnson et al., 2005; Staubwasser et al., 2006), and that plant-available iron in soils has a composition of  $-0.1$  ‰.

1. *Closed-system fractionation during uptake.* In this case the Fe-pool available for uptake is successively depleted in light iron isotopes which are extracted into the strategy I plant by reduction. A Rayleigh-type mass balance (Walczyk and von Blanckenburg, 2002) dictates that this source compartment will develop towards heavier iron isotope compositions which in turn would also lead to a development towards heavier compositions in strategy I plants during growth. This has not been observed.

2. *Open system fractionation during uptake.* In this case an infinite iron pool supplies the roots and the Fe isotope fractionation will always be  $\Delta_{\text{reduced species-oxidized species}}$  ( $-1.5$  ‰). This would lead to the same  $\delta^{56}\text{Fe}$  values throughout all parts of strategy I plants if the fractionation occurs exclusively during uptake. Again, such uniform compositions have not been observed.

3. *Closed-system fractionation during translocation.* Here a series of Rayleigh steps supplying light iron from older into younger plant parts with concomitant reduction leads to fractionation during growth of the plant. For example translocation of about 50 % will result in translocated iron of which  $\delta^{56}\text{Fe}$  is 1.1 ‰ lower than the original  $\delta^{56}\text{Fe}$ , while the Fe(III) remaining in the source compartment will change by 1.04 ‰ towards heavier compositions. This translocation scenario predicts the observed sense of fractionations, while the magnitude is difficult to assess given that at present neither exact values of  $\Delta_{\text{reduced species-oxidized species}}$  nor of fractions translocated are known.

4. *Fractionation during uptake and translocation as an open system.* This scenario is similar to scenario (3), but since it is unlikely that younger parts of a plant receive all their iron from their first-generation leaves, fresh Fe from uptake is continuously mixed into the plant. This again leads to a decrease of the  $\delta^{56}\text{Fe}$  value during growth of the plants, but due to binary mixing the resulting isotope effect will be damped over that predicted for the closed-system scenario (3). Regardless of the actual details of the process, fractionation during translocation is the mechanism that best fits the decrease in  $\delta^{56}\text{Fe}$  from older to younger parts of strategy I plants.

This prediction is compatible with the mechanisms that have been suggested for translocation of iron in strategy I plants. The current view is that within the cell of strategy I plants, Fe(II) is chelated by nicotianamine (NA) and then transported to the xylem vessels (Hell and Stephan, 2003). Iron is oxidized when released into the xylem vessels and then transported as a Fe(III)-citrate complex (Tiffin, 1966). No isotope fractionation is expected during this step as loading is presumably quantitative. The further distribution of iron from the cells adjacent to the veins of the leaf lamina is probably again mediated by the Fe(II)-NA complex, so for non-quantitative xylem-unloading another reduction and therefore isotopic fractionation favoring the lighter isotopes occurs. Excess iron is stored as a phytoferritin complex, localized in the plastids of shoots and also roots (Briat and Lobreaux, 1997). Non-quantitative oxidative phytoferritin fixation, for example, would result in light residual Fe(II)-NA. When remobilized from older leaves for iron import into seeds, iron might be transported within the phloem as Fe(III) by nicotianamine (Le Jean et al., 2005). Whenever these redoxchanges are non-quantitative, light mobile Fe(II) will develop and heavy Fe(III) is stored. Successive oxidation-reduction cycling during translocation will gradually increase the ensuing fractionations. Kinetic fractionation is also possible, when Fe is loaded to or unloaded from the chelators. The chelators themselves are too big for kinetic fractionation, however (molecular mass of NA approximately 350 amu). In light of the obtained results, which indicate preferred translocation of light iron into the younger parts of the strategy I plant, the explanation is that the heavier iron is locked into phytoferritin or other target molecules leaving a light reduced residue, or mobilizing light iron upon reduction.

The fate of imported Fe(III) as part of a PS complex in strategy II plants is currently unclear. Redox changes during translocation similar to that in strategy I plants have been traditionally suggested (Hell and Stephan, 2003), but an alternative scenario invokes Fe(III) that is chelated by NA rather than Fe(II), since NA forms complexes with Fe(III) as well (von Wirén et al.,

1999). In this case Fe(III)-NA complexation would be the default mechanism until Fe is channelled into further transport and storage sites or functional target molecules without redox changes (Hell and Stephan, 2003). Unlike strategy I plants our strategy II plants show virtually no Fe isotope fractionation throughout growth. Hence we can speculate that Fe does not change its redox state during translocation or that reduction/oxidation is quantitative in all steps. If kinetic fractionation during ligand exchange played a role, fractionations would be visible in both strategy I and II plants. As fractionation is not detectable throughout growth of strategy II plants, kinetic fractionation is probably negligible. However, a minute decrease in  $\delta^{56}\text{Fe}$  from leaves to seeds is observed in strategy II plants. This decrease might be due to the reduction step required for the release of Fe(III) stored in phytoferritin for import into seeds (Chasteen, 1998). The resulting fractionation will be small if this release is almost quantitative. With this exception we infer that the theory of ligand exchange without redox changes (Hell and Stephan, 2003) during translocation is the currently best explanation of the strategy II results. In fact it now seems possible that stable Fe isotopes provide the first direct evidence for a difference in iron translocation mechanisms between strategy I and strategy II plants.

### 2.5 Conclusions

The findings of this study have several implications. First, it is worth noting that although to date emphasis in the characterization of iron isotope fractionation in the biosphere has been on microbial metabolism (Johnson et al., 2005) the isotope effects caused by plant growth provide the most substantial, and also the most systematic shifts of geosphere - biosphere interaction. Second, it has been suggested that the iron isotope composition of human blood is light relative to the human diet (Walczyk and von Blanckenburg, 2002), and that  $\delta^{56}\text{Fe}$  is reduced by 1 per mil with each trophic level within the human food chain (Walczyk and von Blanckenburg, 2005). To accurately quantify these mechanisms, differences in the Fe isotopic composition between strategy I and II plants that have previously been overlooked (Walczyk and von Blanckenburg, 2002) need to be taken into account. For example, the fractionation factor in the human intestine (Walczyk and von Blanckenburg, 2005) would be even larger if the individuals' diet contained more cereals (strategy II plants) than legumes (strategy I plants) or meat. Furthermore, the Fe isotope ratio of an individuals' blood might also depend on the ratio of strategy I to strategy II plants in the diet. The full characterization of human

and animal diet is essential in the application of metal isotopes in nutrition studies. Third, and most importantly, our results show that isotopic fractionation of iron will emerge as a complementary tool in the study of Fe uptake and translocation in plants, as previously suggested (Álvarez-Fernández, 2006). The advantage of stable isotopes is that soil iron including the non-soluble fractions is intrinsically labelled isotopically, and that the fingerprint of the fractions taken up can be traced without the requirement of adding artificial tracers. In addition, studies on iron translocation in plants can be conducted under field conditions which is difficult or impossible to achieve with radiotracers. These applications are important as a better understanding of intracellular redox state, binding forms and Fe transport processes in plants is required for biofortification (increasing the Fe content of food crops) (Briat and Lobreaux, 1997). This is a scientific challenge of global significance since iron deficiency affects more than 2 billion people worldwide (WHO, 2003).



### 3 Determining the stable Fe isotope signature of plant-available iron in soils

#### 3.1 Abstract

The isotope composition of iron in soils can display the environmental conditions that formed this soil. But plants extract only the mobile iron from soil, which is a small fraction of the soils total iron. Yet this fraction is notoriously difficult to extract experimentally. Here it is shown that this signature is provided readily in the form of strategy II plants (grasses). The stable Fe isotope signature of iron pools in two agronomic soils was determined with two different sequential extraction methods. The Fe isotopic composition of the following soil mineral pools was measured: exchangeable iron, iron of poorly-crystalline (oxyhydr)oxides, iron in organic matter, iron of crystalline oxides and silicate bound iron. Variations of about 1 per mil in  $\delta^{56}\text{Fe}$  ( $\delta^{56}\text{Fe}/[\text{‰}] = [({}^{56}/{}^{54}\text{Fe}_{\text{sample}}/{}^{56}/{}^{54}\text{Fe}_{\text{IRMM-014}}) - 1] \cdot 10^3$ ) were found in the iron isotopic composition between the different soil mineral pools. The pools that contribute most to plant nutrition are water-extractable- and exchangeable iron, iron in organic matter and iron of poorly-crystalline (oxyhydr)oxides. These fractions were about 0.3 per mil lighter than the bulk soils. Silicates in our soils had a  $\delta^{56}\text{Fe}$  of up to 0.4 ‰, suggesting preferential loss of light Fe during weathering. The isotope composition of the plant-available Fe was compared to that of typical strategy I and strategy II plants, grown on the soils. While redox and other transformation processes in the rhizosphere enriched strategy I plants to varying degrees in light Fe isotopes, strategy II plants exhibited a uniform Fe isotopic composition and were only slightly enriched in the heavier iron isotopes by about 0.3 ‰. Therefore these plants may record the Fe isotope composition of plant-available iron in soils, to which the composition of strategy I plants can be compared to.

#### 3.2 Introduction

Iron is an essential nutrient supplied to plants from soil. Yet iron availability in the rhizosphere is limited by the very low solubility and slow dissolution rates of inorganic iron compounds which are beneath those required for plant and microbial growth (Lindsay and Schwab, 1982). To increase iron supply according to their demand, plants can induce

chemical reactions in the rhizosphere that increase iron solubility from iron pools in soil. Identifying which of these pools is available to plants, however, is important because iron deficiency is a major problem in plant nutrition that can lead to a dramatic loss in crop yield (Briat and Lobreaux, 1997). It is crucial to fully assess the bioavailability of Fe for plants in soils, as well as its biogeochemical cycling (Yang et al., 2007). Stable iron isotopes potentially provide a tool suited to provide this understanding. Stable Fe isotopes have been used to study the biogeochemical iron cycle in geologic systems (reviews by Anbar, 2004; Johnson et al., 2004b; Dauphas and Rouxel, 2006; Johnson et al., 2008), and in humans and higher plants (Walczyk and von Blanckenburg, 2002, 2005; Guelke and von Blanckenburg, 2007). Iron isotope fractionation is usually expressed in the delta notation, which gives the permil deviation of the isotopic ratio (e.g.  $^{56}\text{Fe}/^{54}\text{Fe}$  or  $^{57}\text{Fe}/^{54}\text{Fe}$ ) of the sample relative to that of the IRMM-014 standard (Taylor et al., 1992):  $\delta^{56}\text{Fe}/[\text{‰}] = [(\frac{^{56/54}\text{Fe}_{\text{sample}}}{^{56/54}\text{Fe}_{\text{IRMM-014}}}) - 1] \cdot 10^3$ .

With regard to plants it has recently been discovered that iron in higher plants was isotopically fractionated compared to the iron in the soil the plants grew on. These stable Fe isotope signatures are plant-specific (Guelke and von Blanckenburg, 2007; Chapter 2 of this thesis). Strategy I plants, which have to reduce iron before uptake, incorporated light iron, while strategy II plants, which take up iron as Fe(III)siderophore complexes, incorporated virtually unfractionated iron relative to bulk iron in soils. However, many details in the iron metabolism of higher plants are still unclear. An increased understanding of these processes is necessary for biofortifying herbal human food with Fe. This is a scientific challenge with global implications since the World Health Organization (WHO) estimates that worldwide around 2 billion people are iron-deficient (WHO, 2003). Stable iron isotopes carry the potential to be a new tool in plant biology and to shed light on mechanisms that would not be detectable with other means (Álvarez-Fernández, 2006). Radioactively labelled Fe isotopes are used as markers for translocation/retranslocation processes in plants so far but they are only able to provide information on uptake rates and transferred amounts from a synthetic Fe substrate. As redox reactions (inorganic and biologically mediated) induce the largest fractionation, stable iron isotopes are a powerful tool for identifying, monitoring, and quantifying redox processes in the Fe metabolism of plants (Weiss et al., 2008; von Blanckenburg et al., 2009).

An important starting point for any field experiment that makes use of stable iron isotope composition in plants is knowledge of the isotope composition of the iron pools in soils that



are available to plants. Therefore experiments were conducted in which the iron isotope signature in different chemical soil extracts of typical Ap horizons (homogenized by plowing) from agriculturally used soils was determined and compared to that of the plants that grew on the soils. The Fe isotope signature of bulk soils was determined and two different sequential extraction methods designed to determine the Fe isotope signature of the various soil fractions were tested.

#### **3.2.1 Iron and its isotopes in soil**

The solubility of inorganic iron is controlled by both the pH and the redox potential of the soils pore water. Dissolution of iron involves a multitude of possible hydrolysis species that are in equilibrium with iron-bearing minerals. These minerals have different solubilities that are a function of their crystallinity and stability. The most soluble iron bearing mineral in soils is amorphous iron hydroxide and the least soluble is goethite (Lindsay and Schwab, 1982). This differential solubility has led to its description by a series of iron reservoirs in soils which are: a) ionic and complexed form in solution; b) exchangeable; c) organically complexed but water insoluble; d) insoluble inorganic precipitates; e) held in primary minerals. Reservoirs a and b are the most soluble and thus the Fe pools in soils which are most likely to be plant-available. However, these are very small in most cases so that the organically bound Fe forms and poorly-crystalline Fe(III) precipitates are likely to play the major role in plant nutrition (Lindsay and Schwab, 1982; Borggaard, 1992; Bertrand and Hinsinger, 2000, and many other workers). In contrast the crystalline oxides like goethite or hematite do not appear to provide an important mobile Fe pool. For example Bertrand and Hinsinger (2000) found that dissolution of goethite by maize was insignificant. Although it was shown that plants are able to dissolve minor amounts of goethite (Bertrand and Hinsinger, 2000; Reichard et al., 2005), plant-available iron is defined here without crystalline Fe oxides.

Several authors have explored the range of stable iron isotopes in soils. Most of these studies use selective extraction procedures to identify the composition of the iron pools in soils. These procedures are described in section 3.2.2. A common denominator of these previous studies is that selective chemical extractions are used that are attributed to distinct operationally defined pools of both isotopically heavy and light Fe in soils.

In the first studies of this kind, Brantley and co-workers (2001, 2004) reported a strong enrichment of light isotopes in the exchangeable iron fraction compared to oxide-bound iron in a soil sample from the B horizon of a hornblende-containing soil. Fantle and DePaolo (2004) studied iron isotope variations in four selected horizons of a soil profile in northern California using leaches in water and 0.5 M HCl on their samples and found variations of about 0.7 ‰ in  $\delta^{56}\text{Fe}$  between bulk soil samples from different depths. Emmanuel et al. (2005) reported variations of about 0.35 ‰ in  $\delta^{57}\text{Fe}$  (approximating 0.24 ‰ in  $\delta^{56}\text{Fe}$ ) in bulk soil samples of a Czech forest soil and an Israeli semi-arid soil. In their study a least-squares method was used to estimate the Fe isotopic composition of the end-members representing the three main Fe reservoirs in the Czech soil (silicates, organically bound Fe and pedogenic Fe-oxides). Wiederhold et al. (2007a, 2007b) showed that different iron pools (poorly-crystalline iron (oxyhydr)oxides, crystalline iron oxides, and silicate bound iron) of different types of soil (Podzol, Cambisol, redoximorphic soil) had different iron isotope signatures and that podzolization led to a preferential translocation of lighter iron isotopes within the soil. They applied a three-step sequential extraction procedure to separate the iron mineral pools from the soil samples. Thompson et al. (2007) also performed different soil extraction procedures to determine the iron isotopic composition of surface and subsurface basaltic soil horizons. Besides bulk digestion they extracted the most readily soluble Fe using 0.5 M HCl, 0.1 M acid ammonium oxalate and Na-pyrophosphate and found different Fe isotopic signatures at different soil depths and in different soil fractions ranging from +1 ‰ to -0.3 ‰ in  $\delta^{56}\text{Fe}$ . In a conference abstract Schuth et al. (2009) presented the iron isotope composition of horizons of a gleysol from NW Germany and found  $\delta^{57}\text{Fe}$  values ranging from +0.3 ‰ in the Ah horizon and -0.2 ‰ in the Gor horizon. Additionally they conducted an experimental study where suspensions of gleysol horizons were subjected to controlled redox conditions. Buss et al. (2010) determined the iron isotopic composition of 0.5 M HCl extracts of soil and saprolite samples in the Luquillo Mountains of Puerto Rico. They found that iron in the HCl extracts of saprolite samples is enriched in the light iron isotopes relative to the igneous rocks in the profile by only 0.1 ‰ in  $\delta^{56}\text{Fe}$ . Iron in the soil samples and bottom of the saprolite directly overlying the bedrock, where biological activity is highest, is more enriched in the lighter iron isotopes by -0.4 to -0.6 ‰. Poitrasson et al. (2008) examined two lateritic profiles and found a very limited range in iron isotope compositions, with  $\delta^{57}\text{Fe}$  values ranging from 0.06 ‰ relative to IRMM-014 in a saprolite, to 0.27 ‰ in a soft clayed horizon.

All these data indicate that different iron pools in soils carry distinct iron isotope signatures and show that labile iron pools in soils are mostly enriched in the lighter iron isotopes.

#### **3.2.2 Experimental strategies for the extraction of iron pools from soils**

A suitable technique had to be developed to identify the isotopic composition of the plant-available iron pool in the two soils. A variety of methods exist to extract distinct mineral iron pools from soils. Physical methods like sieving, density separation or handpicking under a microscope are unsuitable because the size of the relevant particles in soils is usually too small. Therefore, chemical separation methods, based on the sequential dissolution of specific iron phases from soil samples are used (Wiederhold et al., 2007b).

Many sequential extraction methods have been developed (e. g. Borggaard, 1988; Heron et al., 1994; La Force and Fendorf, 2000) but for stable isotope studies they require testing for artefacts during sample preparation. First, the isotope ratio of both the solution and the solid residue can be biased if an isotope fractionation takes place during incomplete dissolution. A second potential challenge is to avoid alteration of the sample during treatment or dissolution of phases during leaching that are not considered soluble in the aqueous environment. For example, Fantle and DePaolo (2004) and Wiederhold et al. (2007b) used 0.5 M HCl in their step to extract poorly-crystalline (oxyhydr)oxides. Wiederhold et al. (2007b) then used 1 M HCl in conjunction with hydroxylamine-hydrochloride in their step to extract crystalline iron oxides. Such strong HCl, however, is likely to also partially dissolve the silicate minerals present and may potentially induce an iron isotope fractionation in the process (Chapman et al., 2009; Kiczka et al., 2010a). A third serious issue in sequential extraction methods is the generation of secondary precipitation or adsorption products. Partial precipitation or adsorption reactions of iron-containing phases from the solution used for the extraction potentially introduce fractionation artefacts that would seriously bias the results (Icopini et al., 2004; Mikutta et al., 2009). A fourth, equally important aspect is the potential matrix effects in the mass spectrometer resulting from incomplete purification of Fe from the solvent used for the extraction. Since both the quantitative retention of Fe on an anion exchange column, employed to separate iron from its matrix, and isotope ratio measurements by MC-ICP-MS are very sensitive to matrix effects, they require solutions from which organic compounds have been destroyed.

In soil science a common method to characterize the pool of poorly-crystalline Fe (oxyhydr)oxides (“Fe<sub>o</sub>”), and thus to estimate plant-available Fe, is the extraction with ammonium-oxalate in an acidic solution (pH 3) (Schwertmann, 1991). Its ratio Fe<sub>o</sub>/Fe<sub>d</sub> to the dithionite-extractable Fe (“Fe<sub>d</sub>”), also termed “activity ratio”, is often used in soil science to describe the extent of pedogenesis or to differentiate soils (e.g., Cornell and Schwertmann, 2003). Since oxalate is light-sensitive the extraction must be carried out in the dark. Unfortunately, despite the short exposure times, oxalate attacks also minor amounts of well-crystallized iron oxides, particularly maghemite, magnetite and lepidocrocite (Schwertmann, 1973). Since small amounts of iron dissolved from crystallized oxides by oxalate can result in large fractionations (Wiederhold et al., 2006) the oxalate method is not applicable for isotopic analysis.

Using a modified dithionite extraction method (Canfield, 1993), Staubwasser et al. (2006) were able to accurately measure Fe isotope ratios in Fe oxides and oxy-hydroxides leached from marine sediments. In this study two sequential extraction methods were chosen that have been shown to extract distinct Fe reservoirs and that do not significantly bias their stable Fe isotope signature during extraction. The first of these two complementary methods (method S-mod) was adapted from Staubwasser et al. (2006) with additional leaching of exchangeable and organically bound iron (Tessier et al., 1979). The second method (method W) was based on a sequential extraction designed by Wiederhold et al. (2007b) to determine the Fe isotope composition of various Fe reservoirs in soils.

#### ***3.2.2.1 First sequential extraction procedure (Method S-mod)***

In method S-mod exchangeable ions were extracted with MgCl<sub>2</sub> (1 M, 2h, 25°C). Brantley et al. (2004) stated that this extraction step (fraction Fe<sub>ex</sub>) is not causing any isotope fractionation. This was concluded from the similarity between two MgCl<sub>2</sub> extractions of the same sample after 1h and 10h.

In a second step, organically bound iron including Fe sorbed to organic surfaces, complexed by organic ligands or incorporated into organic macromolecules was dissolved with weak HNO<sub>3</sub> and H<sub>2</sub>O<sub>2</sub> (Tessier et al., 1979; Emmanuel et al., 2005). In the third step all iron oxides were extracted with a dithionite-citrate solution as used by Staubwasser et al. (2006) to determine the Fe isotope composition of Fe oxyhydroxides in marine sediments. The term “Fe oxides” is used throughout this paper to refer to both Fe oxides and hydrous Fe oxides that are not associated with organic matter. Dithionite dissolves all poorly-crystalline and crystalline

iron oxides except magnetite together with minor amounts of silicate-bound Fe(III) and acid soluble sulfides (Haese, 2000). Small amounts of Fe leached from silicates do not significantly affect isotope ratios (Staubwasser et al., 2006). Leaching experiments performed on a synthetic mixed haematite-goethite sample demonstrated the absence of unwanted fractionation during sample separation and measurement (Staubwasser et al., 2006). The extraction solvent can be completely removed by oxidation and quantitative precipitation of sulfur as BaSO<sub>4</sub> (Staubwasser et al., 2006). In the final step all remaining soil material was dissolved by a microwave digestion with HF-HNO<sub>3</sub>.

#### ***3.2.2.2 Second sequential extraction procedure (Method W)***

In method W hydrochloric acid (0.5 M, 24 h, 25 °C) dissolved the poorly-crystalline Fe oxyhydroxides like ferrihydrite and both adsorbed and organically bound iron. Wiederhold et al. (2006) showed that the stepwise dissolution of goethite with 0.5 M HCl does not cause any iron isotope fractionation. In another study Skulan et al. (2002) showed that the partial dissolution of hematite by HCl produced no significant isotopic fractionation (within 0.1 ‰ (2SD) in  $\delta^{56}\text{Fe}$ ). The lack of iron isotope fractionation may be due to a different bond breaking mechanism when compared to ligand-controlled dissolution and indicates bond breakage between oxygen and adjacent iron atoms during detachment (Wiederhold et al., 2006). On the other hand, HCl can etch silicate minerals from granite. Chapman et al. (2009) reported that after 48 hours of cold leaching with 0.5 M HCl around 40  $\mu\text{g/mL}$  Fe were in the leachate of granite (bulk 14078  $\mu\text{g/mL}$ ), but up to 600  $\mu\text{g/mL}$  Fe in the leachate of basalt (bulk 103663  $\mu\text{g/mL}$ ), which means that 0.5 M HCl leaches around 0.5 % of silicates within 48 hours, which is negligible even if leaching leads to iron isotope fractionation of up to  $-1$  ‰ (Chapman et al., 2009). However, Kiczka et al. (2010a) showed that nearly 20 % of the Fe from biotite and chlorite were released within 24h in 0.01 M HCl. Thus, the amount of Fe which is released from silicates during dissolution in HCl is highly dependent on the mineralogy of the soils and might not always be insignificant. In addition, other factors such as grain size may have an effect on the dissolution kinetics of different mineral phases. Hence, HCl is able to partially attack silicate minerals in soil extractions but the influence on Fe isotope data will not be significant in most cases and needs to be accepted as a potential small bias. As a test for silicate dissolution during our HCl extraction Al concentrations were also measured. The second step used hydroxylamine-hydrochloride in 1 M HCl. Wiederhold et al. (2007b) showed that hydroxylamine-hydrochloride breaks up all crystalline iron oxides like goethite and hematite by complete reductive dissolution. However these authors reported

that minor amounts of clay minerals or other silicate minerals might also be etched and a small bias has to be taken into account when interpreting the iron isotope data. In the third step all remaining soil material was dissolved by a microwave digestion with HF-HNO<sub>3</sub>. The sequential extractions were performed in parallel to the total soil digests, which allowed performing an isotope mass balance between the sum of the extractions and the total digests.

## 3.3 Materials and Methods

### 3.3.1 Soil characteristics and plant samples

Ap horizons of two soil types from two characteristic landscapes prevalent in NW Germany were used as substrate for plant growth under field conditions: (1) a Cambisol from glacial sand of the Drenthe stadium of the Saaleian glaciation (profile Hannover-Herrenhausen; location 9.705237° west/ 52.395613° north (UTM projection WGS84)) located in the “Geest”, the moraine landscape prevalent in Lower Saxony; and (2) a Stagni-Haplic Luvisol from loess of the Weichselian glaciation (profile Ruthe; location 9.819935° west/ 52.242075° north (UTM projection WGS84)) located at the NW margin of the main European loess belt in the centre of Germany. Usually the measurement of soil pH takes place in 0.01 M CaCl<sub>2</sub> solution. Here sorbed H<sup>+</sup>-ions can be exchanged with CaCl<sub>2</sub> ions, therefore the measured pH is 0.3 to 1.0 pH units lower as the pH measured in aqueous solution (pH<sub>H<sub>2</sub>O</sub>). The pH<sub>H<sub>2</sub>O</sub> of the two soils was 7.5 and 7.8, respectively, thus the pH is slightly acidic to neutral.

The Ap horizons are well-aerated and exhibit oxic conditions all year round. No redoximorphic features such as iron and manganese mottles or concretions, which are characteristic for hydromorphic soils, are present. The matrix colour of the samples is dark brown to ochre. For the Stagni-Haplic Luvisol formed on loess the texture is unknown, for the Cambisol it is 75 % sand, 19 % silt and 6 % clay. The organic carbon content is 2.8 and 1.8 %, respectively (Table 3-1). In both samples, quartz is the most abundant mineral. The <2mm fine soil fraction the sample from glacial sands contains 11 % feldspar and the sample from loess 16 %, whereby the feldspars are composed of nearly equal amounts of Orthoclase and Albit phases (50 and 40 % of whole feldspar), the amounts of the Anorthite phase are smaller (Dultz, 2002). The mineralogical composition of the clay fraction is similar for both

### 3 Determining the stable Fe isotope signature of plant-available iron in soils

profiles with illite as the most common mineral in amounts of 60–80 % (Niederbudde and Schwertmann, 1980) and goethite as the predominant iron oxide.

The Ap horizon (0–30 cm depth) was sampled at both sites; samples were dried at 40 °C in the laboratory and sieved through a 1.6 mm mesh. Aliquots of the samples were ground to a fine powder in an agate mortar. Selected properties of the two soils including oxalate-soluble iron concentrations are presented in Table 3-1. The soils are commonly used by plant and soil scientists at the Leibniz Universitaet Hannover. All information of Table 3-1 is internal and unpublished.

Table 3-1 Characteristics of the two soils

<b>Soil</b>	<b>Location</b>	
	<i>Herrenhausen</i>	<i>Ruthe</i>
	Cambisol	Stagni-Haplic Luvisol
<b>Parent material</b>	glacial sand	loess
<b>Horizon</b>	Ap	Ap
<b>pH<sub>H2O</sub></b>	7.50	7.80
<b>P<sub>2</sub>O<sub>5</sub> [g/kg]</b>	0.36	0.04
<b>K<sub>2</sub>O [g/kg]</b>	0.17	0.04
<b>MgO [g/kg]</b>	0.08	0.09
<b>NaCl [%]</b>	0.03	0.08
<b>Organic compounds [%]*</b>	2.80	1.80
<b>Oxalate-soluble Fe [g/kg]</b>	1.50	1.20

\*organic compounds determined by dry combustion, 1000°C

In the previous study (Guelke and von Blanckenburg, 2007; chapter 2 of this thesis) different kinds of plants (all vegetables and grasses) were sown in pots filled with the unsieved Cambisol and Stagni-Haplic Luvisol respectively. Plants grew in a daylight climate chamber with a temperature of 16 – 18 °C and were only watered with deionised water without the addition of fertilizer. About ten individual plants were harvested after approximately 60 days, washed with deionised water and separated into stem, leaves and seeds. Plant samples were dried in an oven at 80 °C for at least three days and subsequently ground to mince and homogenize them. For details of plant growth, plant species, harvest times, and the resulting iron isotope composition the reader is referred to chapter 2 of this thesis.

#### 3.3.2 Iron extraction from soil fractions

The iron pools described in section 3.2.2 and also water-extractable and total Fe were extracted from both soils as follows. All reagents used during sample preparation were *suprapure* grade and prepared with ultrapure water (Milli Q, >18.2 MΩ cm). Hydrochloric and nitric acids were *pro analysi* grade and were further purified by sub-boiling distillation measured by ICP-OES after distillation in our laboratory. Fe concentrations of these chemicals were checked and were only used if they were below detection limit. Hydrofluoric acid used during digestions was suprapure quality (MERCK, Germany). All preparation work was carried out in a metal-free clean chemistry laboratory class 1000 in laminar-flow hoods, class 10.

**Bulk soil Fe ( $Fe_{\text{bulk}}$ ).** Approximately 50 mg of the powdered samples was dissolved in a concentrated HF-HNO<sub>3</sub> (mixture 1:2) on a hotplate with 160 °C for about 24 hours. After decomposition of samples the solutions were evaporated and 5 mL aqua regia was added to redissolve fluoride complexes. After an additional microwave digestion the clear solutions were evaporated in Teflon beakers on a hotplate. The residue was redissolved in concentrated HNO<sub>3</sub> to ensure complete oxidation of ferrous to ferric iron. This solution was evaporated anew and the residue was taken up in 6 M HCl.

**Water-extractable Fe ( $Fe_{\text{H}_2\text{O}}$ ).** An aliquot of about 25 g of the dried and sieved soils was used to extract the ionic and complexed iron forms in solution. The soil samples were water-saturated with approximately 40 mL ultrapure water and were shaken over-head for about 12 hours. Samples were then centrifuged and the supernate was filtered through 0.2 μm PTFE membrane filters. Throughout this study Whatman Puradisc™ 25 TF filters were used which were wetted before filtering with ultrapure H<sub>2</sub>O. After drying down on a hotplate the evaporated sample was treated with concentrated HNO<sub>3</sub> to convert all ferrous into ferric iron and was then taken up into 1 mL 6 M HCl.

##### 3.3.2.1 First sequential extraction procedure (method S-mod)

**Exchangeable iron ( $Fe_{\text{ex}}$ ).** 3 g of soil samples were weighted into six 50 mL centrifuge tubes and 30 mL 1 M MgCl<sub>2</sub> solution was added to each tube. Analytical grade MgCl<sub>2</sub> was additionally cleaned before use by anion exchange chromatography (see section 3.3.4) to remove all traces of iron. The Fe concentration in the cleaned MgCl<sub>2</sub> was checked by ICP-OES and was found to be 0.001 μg/mL.



The samples were placed into an over-head shaker for 2 hours at room temperature. Then the tubes were centrifuged (15 min, 5000 rpm, 4472 x g) and the supernates decanted. The centrifugate of the MgCl<sub>2</sub> extraction was washed twice with ultrapure water, centrifuged, and the wash water was pooled with the extraction sample which was then filtered through 0.2 µm PTFE membrane filters. After drying down on a hotplate the evaporated supernates were treated with concentrated HNO<sub>3</sub> to convert all ferrous iron into the ferric form and were then taken up into 10 mL 6 M HCl. After washing the centrifugate of the MgCl<sub>2</sub> extraction was gently dried on a hotplate at about 80 °C.

**Organically bound iron (Fe<sub>org</sub>).** The centrifugate from the extraction with exchangeable Fe was used for the second extraction step, in which 3 mL 0.01 M HNO<sub>3</sub> and 5 mL H<sub>2</sub>O<sub>2</sub> (30 %) were added to 0.2 g of the dried and homogenized residue. The solution was transferred to savillex<sup>®</sup> beakers, closed, and then placed on a hotplate at 80 °C. Two hours later another mL of H<sub>2</sub>O<sub>2</sub> was added to the solutions, they were heated for another hour, after which 7.5 mL 0.01 M HNO<sub>3</sub> were added and after a few minutes the solutions were transferred into 50 mL centrifuge tubes and centrifuged (15 min, 5000 rpm, 4472 x g). The supernates were decanted; the centrifugate was washed twice with ultrapure water, centrifuged and the wash water pooled with the extraction samples, which were then filtered through 0.2 µm PTFE membrane filters. The evaporated samples were treated with concentrated HNO<sub>3</sub> to oxidise all ferrous iron and were then taken up in 5 mL 6 M HCl.

**Iron oxides (Fe<sub>oxide</sub>).** The cleaned centrifugate of the HNO<sub>3</sub>-H<sub>2</sub>O<sub>2</sub> extraction was gently dried on a hotplate at about 80 °C in 25 mL Erlenmeyer flasks. 10 mL of a dithionite-citrate solution, consisting of 0.35 M acetic acid, 50 g/L Na-dithionite and 0.2 M Na-citrate, was added to about 50 mg of the dried and homogenized soil samples. After 12 hours the samples were centrifuged, the supernates were decanted; the centrifugate was washed twice with ultrapure water, centrifuged and the wash water was pooled with the extraction samples, which were then filtered through 0.2 µm PTFE membrane filters. The separation of Fe from the leach solution was preceded by hot oxidation in *aqua regia* via microwave digestion followed by oxidation in ammonia and H<sub>2</sub>O<sub>2</sub>. The solution was then transferred into vials and Fe hydroxide was precipitated after adding ammonia and H<sub>2</sub>O<sub>2</sub>. Next the precipitate was dissolved in 1 M HCl and 1 M HNO<sub>3</sub> and a 0.1 M BaCl<sub>2</sub> solution was added to precipitate all remaining sulfate as barite. After centrifugation the supernate was decanted and Fe was precipitated by adding ammonia and H<sub>2</sub>O<sub>2</sub>. The solution was centrifuged, the supernate decanted and the centrifugate finally dissolved in 6 M HCl for further analysis.

**Silicates and clay minerals ( $Fe_{sil}$ ).** Silicate-bound Fe is present within the crystalline structure of the primary and secondary silicate minerals. The residues of the third extraction in the Erlenmeyer flasks were dried at 80 °C and homogenized. Approximately 40 mg of the powdered samples was dissolved in a 1:2 mixture of concentrated HF-HNO<sub>3</sub> followed by microwave digestion with 5 mL *aqua regia*. After evaporation on a hotplate the residues were redissolved in concentrated HNO<sub>3</sub> to ensure complete oxidation of ferrous to ferric iron. These solutions were evaporated and the residues were taken up in 6 M HCl.

#### 3.3.2.2 Second sequential extraction procedure (method W)

**Poorly-crystalline Fe (oxyhydr)oxides ( $Fe_{am.oxide}$ ).** In the first extraction step 2 g of the soil samples were weighed into 50 mL centrifuge tubes and 40 mL 0.5 M HCl was added. The samples were placed into an over-head shaker at room temperature. After 24 hours of shaking the tubes were centrifuged (15 min, 5000 rpm, 4472 x g) and the supernates were decanted. The centrifugate was washed twice with ultrapure water, centrifuged and the wash water was pooled with the extraction samples, which were then filtered through 0.2 µm PTFE membrane filters.

**Crystalline iron oxides ( $Fe_{cryst.oxide}$ ).** The cleaned residue in the 50 mL tubes of the first extraction step was treated with 40 mL of a 1 M hydroxylamine-hydrochloride solution in 1 M HCl. The tubes were shaken and placed into a hot-water bath (90 °C, 4 hours) with manual overhead-shaking every 10 minutes. Afterwards the tubes were centrifuged (15 min, 5000 rpm, 4472 x g) and the supernates were decanted. The centrifugate was washed twice with ultrapure water, centrifuged again and the wash water was pooled with the extraction samples, which were then filtered through 0.2 µm PTFE membrane filters.

**Silicates and clay minerals ( $Fe_{sil}$ ).** The residues of the previous extraction step contained the remaining dissolved silicates and clay minerals of the soils. The cleaned residues of the  $Fe_{cryst.oxide}$  extraction were filled into Erlenmeyer flasks, dried at 80 °C and homogenized. Approximately 60 mg of the powdered sample was dissolved in a 1:2 mixture of concentrated HF-HNO<sub>3</sub> followed by microwave digestion with 5 mL *aqua regia*. After evaporation on a hotplate the residues were redissolved in concentrated HNO<sub>3</sub> to ensure complete oxidation of ferrous to ferric iron. These solutions were again evaporated and the residues taken up in 6 M HCl.

The extracted solutions  $Fe_{am.oxide}$  and  $Fe_{cryst.oxide}$  were taken to dryness on a hot plate after which concentrated H<sub>2</sub>O<sub>2</sub> and concentrated HNO<sub>3</sub> were added and samples were subjected to

a microwave agitation at 200 °C for about an hour to destroy any remaining organic matter, or hydroxylamine, and to oxidise ferrous into ferric iron. After drying down the residues were dissolved in 6 M HCl.

#### **3.3.3 Digestion of plant samples**

Approximately 250 mg dry weight of each plant sample was digested via microwave agitation in 5 mL of concentrated HNO<sub>3</sub> at 200 °C, evaporated on a hotplate and treated with a mixture of 30 % H<sub>2</sub>O<sub>2</sub> and concentrated HNO<sub>3</sub> to oxidize remaining organic compounds and ferrous iron to ferric iron. Subsequently the samples were redissolved in 6 M HCl and centrifuged before Fe separation.

#### **3.3.4 Iron separation**

Iron of the soil and plant samples was separated from other elements by anion exchange chromatography following the method of Schoenberg and von Blanckenburg (2005). In a few words, after a cleaning procedure and conditioning of the resin, samples, dissolved in 6 M HCl, were loaded on the columns. Matrix elements were washed out with 6 M HCl and afterwards Fe was extracted with 5 M HNO<sub>3</sub>. Samples were dried down and redissolved in a drop of 15 M HNO<sub>3</sub>. After nearly drying down samples were dissolved in 0.3 M HNO<sub>3</sub>.

As it has been shown that even after anion exchange chromatography solutions might be not entirely free of Zn, Cu or organic complexes (Schoenberg and von Blanckenburg, 2005), an additional precipitation step was applied that ensures quantitative precipitation of all Fe(III) as Fe(III)OOH while Cu, Zn, Co, Cd, Mn and V as well as organic compounds remain in solution. For this purpose the samples were precipitated at pH 10 with ammonia (Schoenberg and von Blanckenburg, 2005). After one hour the samples were centrifuged, the supernate solutions were discarded and the precipitates were washed with ultrapure H<sub>2</sub>O. The precipitate was redissolved in 0.3 M HNO<sub>3</sub>.

Iron concentrations of all samples were measured by optical emission spectroscopy with inductively coupled plasma (ICP–OES: *Varian Vista PRO CCD Simultaneous*) after decomposition or extraction and after the iron separation column/precipitation to ensure quantitative recovery and the absence of remaining matrix elements. This is important to avoid artificial isotope fractionation (Anbar et al., 2000; Roe et al., 2003) and matrix effects during isotope measurement. The post-purification iron yield was measured on volumetrically

determined aliquot amounts and was found to be better than 95 %. Al concentrations in the soil samples were also measured to test for etching of clay minerals during the sequential extractions (Barker et al., 2003). Procedural blanks were checked regularly and ranged between 17 and 120 ng Fe ( $n=10$ ).

#### 3.3.5 Iron isotope ratio measurements and reproducibility

A detailed description of iron isotope measurements by multiple-collector inductively coupled plasma mass spectrometry (MC-ICP-MS; *ThermoFinnigan Neptune*) in the geochemistry-laboratory at the Institute for Mineralogy of the Leibniz Universitaet Hannover can be found in Schoenberg and von Blanckenburg (2005). A sample-standard bracketing approach with the standard material IRMM-014 was used to correct for instrumental mass bias. Standards and samples were diluted to 3–7 ppm with 0.3 M HNO<sub>3</sub>, depending on the daily status of the machine. Obtained isotope ratios are expressed in the delta notation, which gives the permil deviation of the isotopic ratio (e.g. <sup>56</sup>Fe/<sup>54</sup>Fe or <sup>57</sup>Fe/<sup>54</sup>Fe) of the sample relative to that of the IRMM-014 standard: ( $\delta^{56}\text{Fe}/\text{‰} = [(\frac{^{56}\text{Fe}_{\text{sample}}}{^{56}\text{Fe}_{\text{standard}}}) - 1] \cdot 10^3$ ). The  $\delta^{57}\text{Fe}$  values were also determined and it was checked in a three isotope plot that all data follow the theoretical mass-dependant fractionation law which demonstrates the absence of molecular or elemental interferences. The external reproducibility of the internal house standard JM (Johnson&Matthey, Fe Puratronic wire) was determined by Schoenberg and von Blanckenburg (2005) using different instrumental settings. It was found to be 0.046 ‰ for  $\delta^{56}\text{Fe}$  and 0.073 ‰ for  $\delta^{57}\text{Fe}$  (2SD, respectively). In this study the internal reproducibility for a single analysis of the JM standard was slightly inferior with  $\pm 0.05$  to  $\pm 0.07$  ‰ (2SD) in  $\delta^{56}\text{Fe}$ . External reproducibilities of stable Fe isotope determinations of natural samples in the laboratory were determined by Schoenberg and von Blanckenburg (2005) who tested a variety of natural samples with different matrices (inorganic and organic). The excellent agreement of  $\delta^{56}\text{Fe}$  reproducibilities between chemical replicates of the same dissolution allows for an assessment of an overall external reproducibility of 0.049 ‰ (2SD). The reproducibility of replicate measurements and chemical replicates of individual dissolutions was also determined according to Schoenberg and von Blanckenburg (2005) of the samples processed in this and the previous study (Chapter 2 of this thesis). It was found to be 0.07 ‰ (2SD;  $n=29$ ) for the  $\delta^{56}\text{Fe}$  of chemical replicates of individual dissolutions and 0.11 ‰ (2SD) for replicate measurements ( $n=108$ ). Considering only soil samples the reproducibility was better with 0.09 ‰ (2SD;  $n=12$ ) for replicates measurements and 0.05 ‰ (2SD;  $n=3$ ) for chemical

replicates. Nevertheless, the external reproducibility is slightly inferior to that obtained by Schoenberg and von Blanckenburg (2005).

To compare the iron concentration and iron isotope results of the different soil fractions measured with bulk iron and bulk iron isotope composition a mass balance approach was used which was calculated according to the following formula, where  $Fe_n$  is the fraction of the iron concentration in pool n and  $\delta^{56}Fe_n$  the isotopic composition of pool n:

$$\delta^{56}Fe_{total-calculated} = \sum_n (\delta^{56}Fe_n \times [Fe]_n) \quad 3.1$$

while the errors of the calculated total Fe concentrations were the propagated errors of the individual fractions, and errors of the calculated total  $\delta^{56}Fe$  the propagated errors of the individual fractions and their corresponding  $\delta^{56}Fe$ .

## 3.4 Results

### 3.4.1 Iron concentrations in the different mineral pools

Iron concentrations of the different Fe pools in the soils are given in Table 3-2. The Cambisol had a total Fe concentration of 8860 mg/kg (0.9 %) and the Stagni-Haplic Luvisol of 13190 mg/kg (1.3 %). These are common values as soils contain between 0.2 and 5 % Fe (Sparks, 2003; Essington, 2004). Wiederhold et al. (2007b) found similar values in a Cambisol with 1.1 % total iron concentration. For the Cambisol, calculated bulk Fe concentrations (Table 3-2) showed good agreement between the summed Fe of the extraction procedures and bulk Fe. For the Stagni-Haplic Luvisol calculated bulk Fe concentrations were lower than measured Fe concentrations by about 20 % for the first and 10 % for the second extraction procedure, when  $Fe_{bulk\ calculated}$  was compared to  $Fe_{bulk}$ . This could be due to uncertainties for the Fe calibration during the ICP-OES measurement (about 5 %), or inhomogeneity of the soil material. Blanks of chemicals and obtained blanks during processing cannot account for this big discrepancy (see section 3.3.2). As Al concentrations showed excellent agreement between measured and calculated Al (Table 3-2) probably no sample material was lost during extraction procedures and no significant inaccuracies were introduced during dilution.

The concentrations of iron resulting in the water-extractable solution were 0.1 and 0.02 mg per kg soil in the Cambisol and Stagni-Haplic Luvisol, respectively. This equals 2.5 and 0.5 mg/L in solution ( $4.5 \cdot 10^{-4}$  and  $8.9 \cdot 10^{-6}$  mol/L) as 25 mg soil was weighed in for this extraction. The values are not surprising as the solubility of all Fe(III) oxides is very low (ferrihydrite has a solubility of about  $10^{-7}$  mol/L) and common iron concentrations in soil solutions of Ap horizons at near neutral pH are 0.005 to 8 mg/L (Bradford et al., 1971; Campbell and Becket, 1988), mostly comprising soluble organic complexes. At near-neutral pH under oxic conditions, the predicted activity of free iron in solution would be even smaller (Kraemer, 2004).

The extraction of exchangeable iron revealed similarly low iron concentrations with less than 1 mg/kg soil (which equals 1.8 and 0.1 mg/L solution as 3 g of soil were weighed in). More Fe was associated with organic matter which accounts for 4 % and 0.5 % of total iron for the Cambisol and Stagni-Haplic Luvisol, respectively. The organic matter fraction did not represent a significant reservoir for Fe as only a small amount of organic matter is present in these soils (Table 3-1).

Most Fe was contained in the oxide fraction. With method S-mod the extracted fraction contained around 55 % of total Fe and comprised both crystalline and poorly-crystalline Fe oxides. Method W yielded even higher Fe amounts in the oxide fraction for the Cambisol. The fraction  $Fe_{am.oxide}$  contained Fe from the poorly-crystalline oxides, adsorbed iron, and some of the organically bound iron which amounted to 11 and 16 % of the total iron in the Cambisol and Stagni-Haplic Luvisol. The crystalline oxides ( $Fe_{cryst.oxide}$ ) contained an additional 52 and 35 %, respectively.

#### **3.4.2 Iron isotope signature of bulk soils**

The sandy Cambisol and the loamy Stagni-Haplic Luvisol soils yielded a bulk Fe isotope composition of  $\delta^{56}Fe = -0.04 \pm 0.05$  ‰ (2SD) and  $\delta^{56}Fe = -0.01 \pm 0.05$  ‰ (2SD), respectively (Table 3-2, Figure 3.1). This is in agreement with Wiederhold et al. (2007b) who found similar values for bulk soils within error in all horizons in a Cambisol profile on basaltic tuff. The bulk soil values were virtually identical to those of various igneous rock reservoirs (Beard et al., 2003; Poitrasson and Freydier, 2005; Weyer et al., 2005; Schoenberg and von Blanckenburg, 2006).

### 3 Determining the stable Fe isotope signature of plant-available iron in soils

Table 3-2 Fe and Al concentrations and  $\delta^{56}\text{Fe}$  values of bulk soils and all soil fractions

soil	fraction	Fe concentration [mg/kg] <sup>1</sup>	% of total Fe	Al concentration [mg/kg] <sup>1</sup>	% of total Al	$\delta^{56}\text{Fe}$ [‰]	error (2SD) <sup>3</sup>
<b>First sequential extraction procedure (method S-mod)</b>							
Cambisol	<i>Fe<sub>bulk</sub></i>	<b>8860 ± 310</b>		<b>18355 ± 642</b>		<b>-0.04</b>	<b>0.06</b>
	Fe <sub>bulk</sub> calculated	<b>8310 ± 210<sup>2</sup></b>	100.00	18128 ± 453 <sup>2</sup>	100.00	<b>-0.07</b>	0.11 <sup>4</sup>
	Fe <sub>H2O</sub>	<b>0.109 ± 0.004</b>	0.00	0.07 ± 0.00	0.00	<b>-0.48</b>	0.05
	Fe <sub>ex</sub>	<b>0.61 ± 0.02</b>	0.01	9.1 ± 0.3	0.10	<b>-0.05</b>	0.05
	Fe <sub>org</sub>	<b>290 ± 10</b>	3.51	266 ± 9	1.50	<b>-0.14</b>	0.05
	Fe <sub>oxide</sub>	<b>4720 ± 170</b>	56.86	39.2 ± 1.4	0.20	<b>-0.28</b>	0.06
	Fe <sub>sil</sub>	<b>3290 ± 120</b>	39.62	17814 ± 641	98.30	<b>0.25</b>	0.06
Stagni-Haplic Luvisol	<i>Fe<sub>bulk</sub></i>	<b>13190 ± 460</b>		<b>26924 ± 942</b>		<b>-0.01</b>	<b>0.05</b>
	Fe <sub>bulk</sub> calculated	<b>10220 ± 260<sup>2</sup></b>	100.00	26526 ± 663 <sup>2</sup>	100.00	<b>0.01</b>	0.12 <sup>4</sup>
	Fe <sub>H2O</sub>	<b>0.023 ± 0.001</b>	0.00	0.02 ± 0.0	0.00		
	Fe <sub>ex</sub>	<b>0.035 ± 0.001</b>	0.00	1.8 ± 0.1	0.01	<b>0.03</b>	0.05
	Fe <sub>org</sub>	<b>49.1 ± 1.7</b>	0.48	98.9 ± 3.6	0.37	<b>-0.17</b>	0.06
	Fe <sub>oxide</sub>	<b>5370 ± 190</b>	52.58	92.2 ± 3.3	0.35	<b>-0.34</b>	0.07
	Fe <sub>sil</sub>	<b>4800 ± 170</b>	46.94	26333 ± 948	99.27	<b>0.41</b>	0.06
<b>Second sequential extraction procedure (method W)</b>							
Cambisol	<i>Fe<sub>bulk</sub></i>	<b>8860 ± 310</b>		<b>18355 ± 642</b>		<b>-0.04</b>	<b>0.06</b>
	Fe <sub>bulk</sub> calculated	<b>8400 ± 190<sup>2</sup></b>	100.00	18245 ± 456 <sup>2</sup>	100.00	<b>-0.04</b>	0.11 <sup>4</sup>
	Fe <sub>am.oxide</sub>	<b>1370 ± 50</b>	16.25	847 ± 30	4.64	<b>-0.22</b>	0.07
	Fe <sub>cryst.oxide</sub>	<b>4320 ± 150</b>	51.50	1759 ± 62	9.64	<b>-0.12</b>	0.07
	Fe <sub>sil</sub>	<b>2710 ± 100</b>	32.25	15639 ± 547	85.71	<b>0.18</b>	0.06
Stagni-Haplic Luvisol	<i>Fe<sub>bulk</sub></i>	<b>13190 ± 460</b>		<b>26924 ± 942</b>		<b>-0.01</b>	<b>0.05</b>
	Fe <sub>bulk</sub> calculated	<b>11950 ± 280<sup>2</sup></b>	100.00	26161 ± 654 <sup>2</sup>	100.00	<b>0.00</b>	0.11 <sup>4</sup>
	Fe <sub>am.oxide</sub>	<b>1320 ± 50</b>	11.04	946 ± 33	3.61	<b>-0.27</b>	0.06
	Fe <sub>cryst.oxide</sub>	<b>4170 ± 150</b>	34.85	1851 ± 65	7.07	<b>-0.03</b>	0.07
	Fe <sub>sil</sub>	<b>6470 ± 230</b>	54.12	23364 ± 818	89.31	<b>0.07</b>	0.06

<sup>1</sup> Errors are combined from weighing, dilution, instrumental count statistics and calibration error.

<sup>2</sup> Errors are propagated from absolute errors of the individual fractions.

<sup>3</sup> given as the 2 standard deviation for a single analysis, or external reproducibility of our JM standard (Schoenberg and von Blanckenburg, 2005), whichever was largest.

<sup>4</sup> propagated from all individual errors of fractions.

### 3.4.3 Iron isotope signature of the different Fe pools in soils

#### 3.4.3.1 First sequential extraction procedure (method S-mod)

Results from the sequential extraction method S-mod are shown in Figure 3.1 and 3.2 and Table 3-2. It is obvious that the range of iron isotope ratios was much broader than that of bulk soil signatures as it covered about 0.7 ‰ in  $\delta^{56}\text{Fe}$ .

The  $\text{MgCl}_2$ -extractable iron in the Cambisol had an isotopic composition of  $\delta^{56}\text{Fe} = -0.05 \pm 0.05$  ‰ (2SD), the Stagni-Haplic Luvisol of  $0.03 \pm 0.05$  ‰ (2SD). Within error both were identical to their respective bulk soil. The blank of the used  $\text{MgCl}_2$  solution was found to contain  $0.001 \mu\text{g/mL}$  Fe, and 30 mL of this solution were used. The total Fe content of the extraction was 1.8 and 0.1  $\mu\text{g}$ , respectively. For the Cambisol the Fe content of the  $\text{MgCl}_2$  represented 1.6 % of the extracted Fe, but for the Stagni-Haplic Luvisol it represented 30 %, which could have resulted in a significant bias of measured isotope ratios.

The Fe isotopic composition of water-extractable iron (fraction  $\text{Fe}_{\text{H}_2\text{O}}$ ) was difficult to measure because iron concentrations were very low and therefore a determination of  $\delta^{56}\text{Fe}$  was only possible for the Cambisol. This measurement yielded a  $\delta^{56}\text{Fe}$  of  $-0.48$  ‰, indicating that light iron was dissolved within the soil solution, presumably in the form of soluble organic complexes.

The  $\delta^{56}\text{Fe}$  of the  $\text{Fe}_{\text{org}}$  fraction in the Cambisol was  $-0.14$  ‰ and in the Stagni-Haplic Luvisol it was  $-0.17$  ‰. According to Borggaard (1992), this fraction is the major reservoir of Fe that was particularly available for uptake by plants. The third extraction step ( $\text{Fe}_{\text{oxide}}$ ) yielded a  $\delta^{56}\text{Fe}$  value for Fe-oxides in the Cambisol of  $-0.28$  ‰ and in the Stagni-Haplic Luvisol of  $-0.34$  ‰. The iron oxides exhibited the lightest Fe isotope signature found in all fractions except the water-extractable fraction.

Fe in silicates (fraction  $\text{Fe}_{\text{sil}}$ ) yielded a higher  $\delta^{56}\text{Fe}$  with  $+0.25$  ‰ for the Cambisol and  $+0.40$  ‰ for the Stagni-Haplic Luvisol. Both values point to an iron isotope composition similar or even heavier than that contained in the most highly differentiated silicate rocks (Poitrasson and Freydier, 2005; Schoenberg and von Blanckenburg, 2006).

Mass balance calculations (equation 3.1) showed excellent agreement between the Fe isotope signature of the soil extracts (Figure 3.1 and 3.2) and bulk soil digests.



### 3.4.3.2 Second sequential extraction procedure (method W)

Results from the second sequential extraction procedure as adapted from Wiederhold et al. (2007b) are shown in Figures 3.1 and 3.2 and Table 3-2. The range of iron isotope ratios between the different fractions covered about 0.4 ‰ in  $\delta^{56}\text{Fe}$  but it was not as large as that of the S-mod extraction procedure.

The  $\delta^{56}\text{Fe}$  of Fe extracted with HCl (fraction  $\text{Fe}_{\text{am.oxide}}$ ) in the Cambisol was  $-0.22$  ‰, in the Stagni-Haplic Luvisol it was  $-0.27$  ‰. The  $\delta^{56}\text{Fe}$  of the  $\text{Fe}_{\text{cryst.oxide}}$  fraction in the Cambisol was  $-0.12$  ‰, in the Stagni-Haplic Luvisol it was  $-0.03$  ‰. At the third step all remaining soil material containing iron in primary silicates and clay minerals was completely dissolved with HF-HNO<sub>3</sub>. Fe in silicates (fraction  $\text{Fe}_{\text{sil}}$ ) yielded a  $\delta^{56}\text{Fe}$  of  $+0.18$  ‰ for the Cambisol and  $+0.07$  ‰ for the Stagni-Haplic Luvisol.

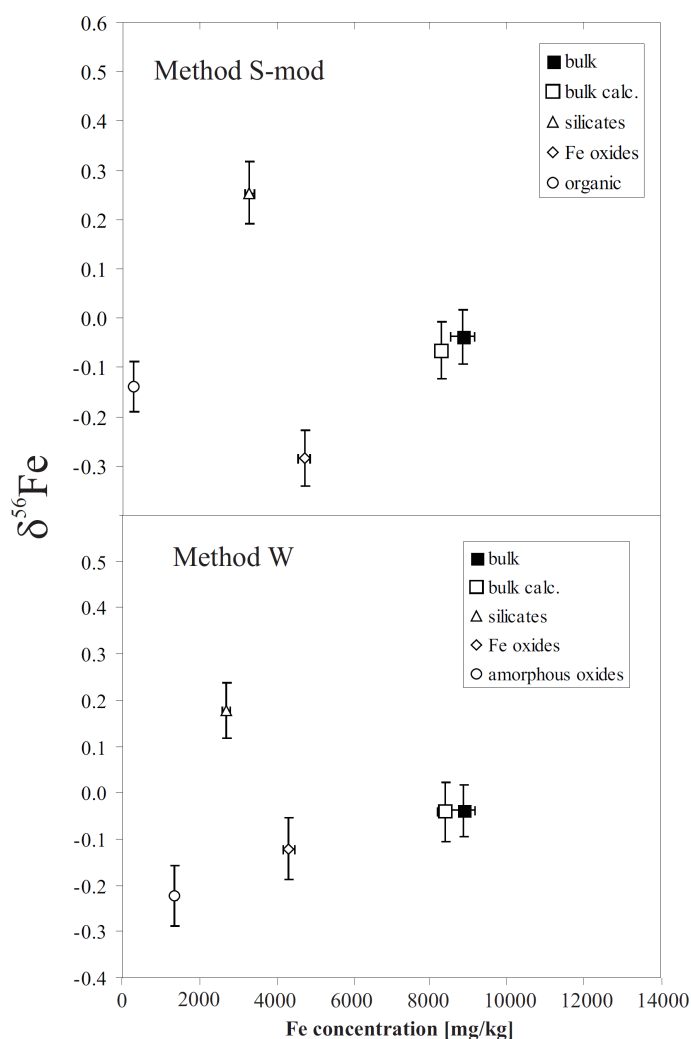


Figure 3.1 Fe concentration and  $\delta^{56}\text{Fe}$  values for the sequential extraction methods for the Cambisol.

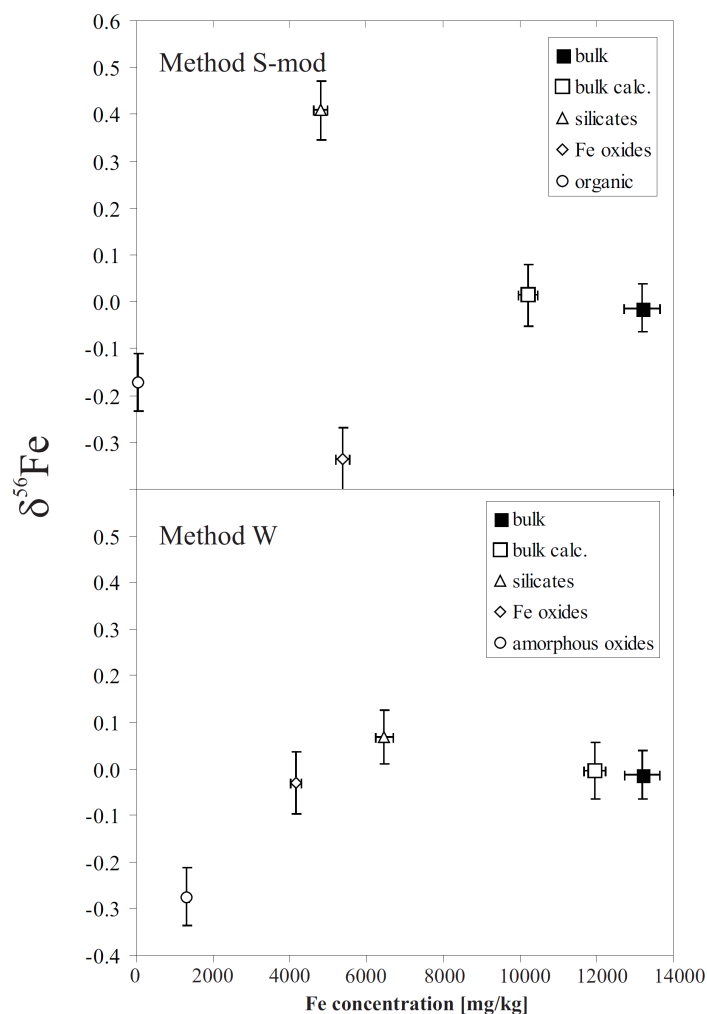


Figure 3.2 Fe concentration and  $\delta^{56}\text{Fe}$  values for the sequential extraction methods for the Stagni-Haplic Luvisol.

## 3.5 Discussion

### 3.5.1 Comparison between the two extraction procedures

#### 3.5.1.1 Water-extractable and exchangeable iron

In method S-mod the exchangeable iron fraction was extracted with  $\text{MgCl}_2$ . This fraction consists of ions that are bound to surfaces by outer-sphere binding. As free ion  $\text{Fe}^{2+}$  and  $\text{Fe}^{3+}$  is expected in inner-sphere binding, Fe released during this stage is likely to have been bound to the surface of solid phases via organic complexes. The  $\text{MgCl}_2$ -extractable iron in the Cambisol had an isotopic composition of  $\delta^{56}\text{Fe} = -0.05 \pm 0.05 \text{‰}$  (2SD), in the Stagni-Haplic Luvisol of  $0.03 \pm 0.05 \text{‰}$  (2SD). For two reasons it is hesitated to attribute much significance

to this ratio: first, due to a significant blank of the used and cleaned  $\text{MgCl}_2$  and a very low Fe concentration in these soil extracts one has to consider a blank, biasing the measured isotope ratios. Second, although Brantley et al. (2004) stated that the extraction with  $\text{MgCl}_2$  does not lead to artificial fractionation of Fe isotopes; Wiederhold et al. (2007b) considered the measurement of “exchangeable Fe” in oxic soils to be very difficult because of the very slow solubility of ferric iron at neutral pH. In their opinion it is difficult to demonstrate that iron atoms which were displaced by the excess of Mg ions from soil exchange sites did not oxidize and re-precipitate during the 2 h extraction.

Similar to the findings of Brantley et al. (2001; 2004)  $\delta^{56}\text{Fe}$  as light as  $-0.48\text{‰}$  were found, indicating that light iron was dissolved within the soil solution, presumably in the form of soluble organic complexes. Although it is not known which plants grew on the soils, this could be due to light plant debris in the organic litter of the Ap horizon, which is expected to contain light iron if strategy I plants grew on the soil (Guelke and von Blanckenburg, 2007; chapter 2 of this thesis), or can be due to a bias in the form of an oxidation step associated with reprecipitation from solutions, or a fractionation during adsorption (Icopini et al., 2004) occurring in nature and leading to a higher  $\delta^{56}\text{Fe}$  in the exchangeable fraction. Nevertheless, fractionation during extraction cannot be excluded.

#### ***3.5.1.2 Organically bound iron***

In method S-mod organically bound iron including Fe sorbed to organic surfaces, complexed by organic ligands or incorporated into organic macromolecules was dissolved with weak  $\text{HNO}_3$  and  $\text{H}_2\text{O}_2$  after Tessier et al. (1979) and Emmanuel et al. (2005). The  $\delta^{56}\text{Fe}$  of the  $\text{Fe}_{\text{org}}$  fraction in the Cambisol was  $-0.14\text{‰}$  and in the Stagni-Haplic Luvisol it was  $-0.17\text{‰}$ . According to Borggaard (1992), this fraction is the major reservoir of Fe that is particularly available for uptake by plants. Table 3-2 shows that 1.5 % of total Al was dissolved during this extraction step for the Cambisol and 0.4 % of total Al for the Stagni-Haplic Luvisol. This is likely to result from the dissolution of Al-oxyhydroxides (Berggren and Mulder, 1995), as  $\text{Al}(\text{OH})_3$  has a solubility of more than 3 mg/L at the pH of the examined soils ( $K_{\text{sp}} \approx 10^{-34}$  at pH 5) and the amorphous forms have an even higher solubility ( $K_{\text{sp}} \approx 10^{-32}$ ) (Dixon and Weed, 1989). It is therefore concluded that the extraction with weak  $\text{HNO}_3$  and  $\text{H}_2\text{O}_2$  is an adequate method to extract organically bound iron from soils.

#### **3.5.1.3 Iron bound in oxides**

In method S-mod, the exchangeable, the water-extractable and the organic iron pool were each extracted separately from each other. In method W this was not the case. These pools were extracted together with iron of poorly-crystalline iron oxides with HCl and yielded a  $\delta^{56}\text{Fe}$  of  $-0.22$  ‰ for the Cambisol and  $-0.27$  ‰ for the Stagni-Haplic Luvisol. The extraction with HCl for iron isotope analyses is controversial. On the one hand it has been shown that proton-promoted dissolution of iron oxides does not fractionate iron isotopes (Skulan et al., 2002; Wiederhold et al., 2006), probably due to a different bond breaking mechanism when compared to ligand-controlled dissolution, indicating bond breakage between oxygen and adjacent iron atoms during detachment (Wiederhold et al., 2006). On the other hand it has also been shown that HCl can etch silicate minerals. Obviously the extent depends on the mineralogy of the soil. However, the possibility of a bias in measured iron isotope ratios in the HCl extracted iron pool of method W resulting from silicate dissolution has to be taken into account. Checks of Al concentrations in this fraction show that these amounted to several wt%. While some of this Al might be derived from dissolution of silicate minerals, some is equally likely derived from dissolution of Al-hydroxides, Al substitution in iron oxide structures and adsorbed Al. By mass balance, it can be assumed however, that the silicate dissolution effect is small and introduces at best an artefact of 0.1 ‰. This number results from the percentage of Al present in the respective fractions. If half of this percentage was derived from silicate dissolution 2–2.5 % silicate Fe in the method W fractions of poorly crystalline oxides can be assumed. If this silicate Fe has a  $\delta^{56}\text{Fe}$  of  $+1$  ‰ (which is an extreme upper bound) and the oxide fraction of  $-2$  ‰ (which is similarly a low bound) this would result in a bias of less than 0.1 ‰ which is approximately the obtained reproducibility. It is therefore concluded that the extraction with HCl is an adequate method to extract poorly-crystalline iron oxides from soils.

In method S-mod all iron oxides (poorly-crystalline and crystalline) were extracted with a dithionite-citrate solution as used by Staubwasser et al. (2006) to determine the Fe isotope composition of Fe oxyhydroxides in marine sediments. Leaching experiments performed on a synthetic mixed haematite-goethite sample demonstrated the absence of artificial fractionation during sample separation and measurement (Staubwasser et al., 2006). Small amounts of Fe leached from silicates did not significantly affect isotope ratios of Staubwasser et al. (2006). This extraction step ( $\text{Fe}_{\text{oxide}}$ ) yielded a  $\delta^{56}\text{Fe}$  value for Fe-oxides in the Cambisol of  $-0.28$  ‰ and in the Stagni-Haplic Luvisol of  $-0.34$  ‰ which were identical within error to the values

obtained for poorly-crystalline Fe oxides of method W (fraction  $\text{Fe}_{\text{am.oxide}}$ ) (Table 3-2). The iron oxides exhibited the lightest Fe isotope signature found in all fractions except the water-extractable fraction. Fe-oxides/hydroxides are, besides clay minerals, the major product of weathering reactions in soils (Cornell and Schwertmann, 2003). The obtained values indicate that during weathering light iron isotopes have been preferentially removed from silicate minerals (Fantle and DePaolo, 2004).

Table 3-2 shows that no significant Al was contained in the  $\text{Fe}_{\text{oxide}}$  fraction. While the presence of Al in the extractions does not necessarily imply silicate dissolution, its absence certainly shows that silicates were not dissolved in this step.

While the  $\text{Fe}_{\text{oxide}}$  fraction of method S-mod extracts both poorly-crystalline and crystalline oxides like goethite, the  $\text{Fe}_{\text{am.oxide}}$  fraction of method W only comprises the poorly-crystalline Fe (oxyhydr)oxides as well as organically bound iron which is extracted separately in method S-mod. Therefore the sum of iron concentrations in the fractions  $\text{Fe}_{\text{org}}$  and  $\text{Fe}_{\text{oxide}}$  of method S-mod should be equal to the sum of iron concentrations of the fractions  $\text{Fe}_{\text{am.oxide}}$  and  $\text{Fe}_{\text{cryst.oxide}}$ . Indeed, the sum of fractions containing organically bound iron and iron oxides (poorly-crystalline and crystalline) are identical within error for the Stagni-Haplic Luvisol, for the Cambisol they differ by ca. 500 mg/kg. As the sum of poorly crystalline and crystalline iron oxides and organically bound iron is similar, also Fe concentration in the silicate fraction should be similar for both methods for the respective soil, as the exchangeable and water-extractable fraction are negligibly small. However, for the Cambisol they differ by 600 mg/kg, in the Stagni-Haplic Luvisol by 1670 mg/kg. Nevertheless, mass balance between the measured and calculated  $\text{Fe}_{\text{bulk}}$  concentration showed good agreement for the Cambisol with both extraction procedures but for the Stagni-Haplic Luvisol a discrepancy of about 20 % for the first and 10 % for the second extraction procedure exists. There, calculated bulk Fe concentrations are lower than measured Fe concentrations. This could be due to uncertainties for the Fe calibration during the ICP-OES measurement (about 5 %), or inhomogeneity of the soil material. Blanks of chemicals and obtained blanks during processing cannot account for this big discrepancy (see section 3.3.2). As explained above Al mass balances show that sample recovery from extractions was quantitative and no significant inaccuracies during dilution occurred.

However, the  $\delta^{56}\text{Fe}$  of the  $\text{Fe}_{\text{cryst.oxide}}$  fraction (leached with hydroxylamine-hydrochloride in 1M HCl) in the Cambisol was  $-0.12\text{ ‰}$ , in the Stagni-Haplic Luvisol it was  $-0.03\text{ ‰}$ . Within

error the  $\delta^{56}\text{Fe}_{\text{cryst.oxide}}$ ,  $\delta^{56}\text{Fe}_{\text{am. oxide}}$  and  $\delta^{56}\text{Fe}_{\text{oxide}}$  values were similar for the Cambisol but for the Stagni-Haplic Luvisol they differed significantly. Checks of Al concentrations in the method W fractions of crystalline oxides show that these were nearly 10 wt%. Besides dissolution of Al-hydroxides, desorption of Al substituted in iron oxide structures and that adsorbed, some Al might derive from silicate and clay mineral dissolution.

With mass balance it can be calculated that this silicate dissolution effect can introduce at most an artefact of 0.3 ‰ in  $\delta^{56}\text{Fe}$  if a hypothetical  $\delta^{56}\text{Fe}$  of +1 ‰ for silicates and of -2 ‰ for oxides and an extreme upper bound of 10 % Fe input through silicate dissolution is assumed. With the obtained values (assuming 5 % silicate dissolution,  $\delta^{56}\text{Fe}$  of silicates +0.4 ‰ and  $\delta^{56}\text{Fe}$  for oxides -0.4 ‰) this would result in an offset of at least 0.04 ‰ which is within error. Therefore the obtained  $\delta^{56}\text{Fe}$  values for crystalline oxides of method W cannot be explained by the presence of silicate-bound Fe, confirmed by the Fe concentrations which are identical within error for the oxide fractions ( $\text{Fe}_{\text{org}} + \text{Fe}_{\text{oxide}} = \text{Fe}_{\text{am. oxide}} + \text{Fe}_{\text{cryst.oxide}}$ ) of the two extraction procedures.

At this stage no explanation for the differences between the various Fe oxide fractions in the Stagni-Haplic Luvisol can be made.

#### **3.5.1.4 Iron of silicates**

Fe in silicates (fraction  $\text{Fe}_{\text{sil}}$ ) of method S-mod yielded a higher  $\delta^{56}\text{Fe}$  with +0.25 ‰ for the Cambisol and +0.40 ‰ for the Stagni-Haplic Luvisol. Both values point to an iron isotope composition similar or even heavier than that contained in the most highly differentiated silicate rocks (Poitrasson and Freydier, 2005; Schoenberg and von Blanckenburg, 2006). These relatively heavy compositions indicate that during weathering light iron isotopes have been preferentially removed from silicate minerals (Fantle and DePaolo, 2004). This observation is consistent with the light Fe found in oxides. Similar observations were made by Wiederhold et al. (2007a; 2007b) and Thompson et al. (2007) who both found enrichments of heavy Fe isotopes in weathering residues.

Nearly 100 weight% Al was found in the  $\text{Fe}_{\text{sil}}$  fractions of the two soils (Table 3-2) extracted with method S-mod indicating that no silicates were dissolved during the other extractions. Mass balance calculations (equation 3.1) showed excellent agreement between the Fe isotope signature of the soil extracts (Figures 3.1 and 3.2) and bulk soil digests.

Silicates measured after the method W procedure showed a similarly high  $\delta^{56}\text{Fe}$  value for the Cambisol with 0.18 ‰, but only 0.07 ‰ for the Stagni-Haplic Luvisol which differs significantly by more than 0.3 ‰ from that obtained with method S-mod.

#### ***3.5.1.5 A preferred extraction procedure***

As mass balance calculations showed excellent agreement between the Fe isotope signature of the soil extracts and bulk soil digests (Figures 3.1 and 3.2) with both extraction procedures, it is difficult to evaluate the sequential extraction procedure method that is more suitable for Fe isotope analyses. Although slightly more demanding in terms of laboratory steps and reagent preparation, the extraction with dithionite for the isotopic analysis of Fe from iron oxides and iron from the residual silicates is preferred in our study as Al concentrations were considerably lower. However, the HCl step appears to be the currently best available to extract poorly-crystalline Fe (oxyhydr)oxides from soils. An improved sequential extraction procedure for the determination of the iron isotopic signature of different mineral pools in soils is suggested that involves an extraction with  $\text{H}_2\text{O}_2\text{-HNO}_3$  for Fe bound to organic complexes, an extraction with HCl for Fe of poorly-crystalline (oxyhydr)oxides, a dithionite-citrate extraction for the extraction of iron from crystalline iron oxides and dissolution with  $\text{HF-HNO}_3$  of the residue (silicates, clay minerals). For the determination of the plant-available iron pool it is sufficient to determine the organically bound iron and iron of poorly-crystalline (oxyhydr)oxides, therefore an extraction with  $\text{H}_2\text{O}_2\text{-HNO}_3$  followed by HCl is preferred.

#### **3.5.2 Determination of the iron isotope signature of plant-available soil iron**

Now that the iron budgets, the iron pools in the soils, and their respective isotope ratios are established, it can be proceeded to identify those that are available to plants. First, observations from plant iron budgets are used to single out those compartments that are the most likely to be available. Plants are estimated to require Fe concentrations in the soil of up to  $10^{-9}\text{-}10^{-4}$  M which approximates less than 5 mg Fe/L to avoid iron deficiency (Guerinot and Yi, 1994). In the soil samples the amounts of oxalate-soluble iron were 1500 and 1200 mg/kg (Table 3-1). Therefore it can be concluded that the plants were not iron deficient as iron of poorly-crystalline (oxyhydr)oxides, which can be extracted with ammonium-oxalate, is the most likely to be mobilized (Borggaard, 1992). The concentration of iron extracted from the soils with HCl of method W contains similar Fe amounts to the ammonium-oxalate soluble iron (about 1300 mg/kg) and, like the ammonium-oxalate leach, contains iron from

### 3 Determining the stable Fe isotope signature of plant-available iron in soils

---

poorly-crystalline Fe (oxyhydr)oxides. The extraction with HCl is regarded useful to determine the iron isotope signature of poorly-crystalline Fe (oxyhydr)oxides in soils. Furthermore, Fe bound to organic complexes, exchangeable iron, and water-extractable iron contribute to plant Fe nutrition (Lindsay and Schwab, 1982; Borggaard, 1992; Bertrand and Hinsinger, 2000, and many other workers). As the extraction of exchangeable iron with  $MgCl_2$  for our soils is considered to be very difficult and probably erroneous and the Fe pool is very small, one can calculate the isotopic signature of plant-available iron in the two soils according to

$$\delta^{56}Fe_{\text{plant-available}} = f_{\text{am.oxide}} \cdot \delta^{56}Fe_{\text{am.oxide}} + f_{\text{org}} \cdot \delta^{56}Fe_{\text{org}} + f_{\text{H}_2\text{O}} \cdot \delta^{56}Fe_{\text{H}_2\text{O}} \quad 3.2$$

where  $f_x$  is the proportion each fraction  $x$  and  $\delta^{56}Fe_x$  the isotopic composition of the extracted fraction. This results in a  $\delta^{56}Fe_{\text{plant-available}}$  of  $-0.206$  ‰ for the Cambisol and  $-0.266$  ‰ for the Stagni-Haplic Luvisol. Note that these values differ from the ones given in Chapter 2 of this thesis for the same soils, as those were merely mean values of different soil extracts and no  $\delta^{56}Fe$  of Fe extracted with HCl was available in that study. Obviously, the equation combines extractions of the two methods and the  $Fe_{\text{am.oxide}}$  fraction of method W contains also organically bound and water-extractable iron. But a revised extraction procedure for the determination of plant-available iron is suggested in section 3.5.1.5 with the extraction of organically bound iron followed by the extraction of the poorly-crystalline Fe oxides with HCl. For the soils of this study the Fe concentration in the  $Fe_{\text{org}}$  fraction is low and values would not change significantly if one left out the fraction in the calculation of the  $\delta^{56}Fe$  of plant-available iron, but it is very likely that in other soil types this fraction has a much larger influence.

Clearly the obtained values are just estimates. For example, plants might first extract their Fe from organic complexes before they proceed to dissolve the poorly-crystalline Fe (oxyhydr)oxides. Regardless the plant-available iron in the studied soils is enriched in the light iron isotopes when compared to bulk soils.

Now the question arises on the way in which the iron isotope ratio is modified from that calculated to be plant-available in soil iron as iron is taken up by plants. Because of the low free iron concentration in soils, plants have two special strategies to mobilize iron from the soil and make it available to absorption by their roots (Roemheld and Marschner, 1986). Most plants are strategy I plants. These plants are able to excrete protons via a plasmalemma  $H^+$ -ATPase to acidify the rhizosphere, thus making Fe(III) more soluble. A reductase then



reduces Fe(III) to Fe(II) (Robinson et al., 1999) as strategy I plants can only take up ferrous iron, which is subsequently transported into the plant by an iron transporter (Vert et al., 2002). Strategy II is used by the grasses which are able to exude phytosiderophores (PS), large organic molecules that can bind the Fe(III) from the soil solution (Takagi et al., 1984), and transport the Fe(III)-PS complexes through the plasma membrane of the root cells via specific transporters without the need for reduction (Curie et al., 2001; Schaaf et al., 2004).

As plants have totally different ways to mobilize and incorporate iron it is not surprising that strategy I and II plants vary in their iron isotopic signature and differ from that in the soil (Guelke and von Blanckenburg, 2007; chapter 2 of this thesis). Redox reactions result in large fractionation (Welch et al., 2003; Anbar et al., 2005; Johnson et al., 2005; Staubwasser et al., 2006) where light iron isotopes are fractionated into the ferrous dissolved pool. Crosby et al. (2007) have shown a fractionation of  $-3$  ‰ from a solid Fe(III) substrate into Fe(II)<sub>aq</sub> using dissimilatory iron reducing bacteria. This value is similar to the inorganic fractionation factor (Welch et al., 2003; Anbar et al., 2005) but it can be lowered by readsorption of Fe(II)<sub>aq</sub> as adsorption processes are known to preferentially sequester the heavier isotope at soil particle surfaces (Icopini et al., 2004). These predictions have been confirmed for reduction of ferric iron in marine sediments (Severmann et al., 2006; Staubwasser et al., 2006). In contrast, complexation of Fe from goethite to siderophores resulted in minor fractionations (Brantley et al., 2004; Dideriksen et al., 2008), enriching the heavier isotopes in the solution. Recently it was shown that plant Fe indeed reflects these fractionations (Guelke and von Blanckenburg, 2007; chapter 2 of this thesis). It was hypothesized that reduction of Fe(III) in soils by strategy I plants led to a decrease of up to 1.6 ‰ in  $\delta^{56}\text{Fe}$  in seeds compared to the bulk soils. Complexation with siderophores by strategy II plants led to iron in these plants that is 0.2 ‰ heavier than that in soils (Figure 3.3).

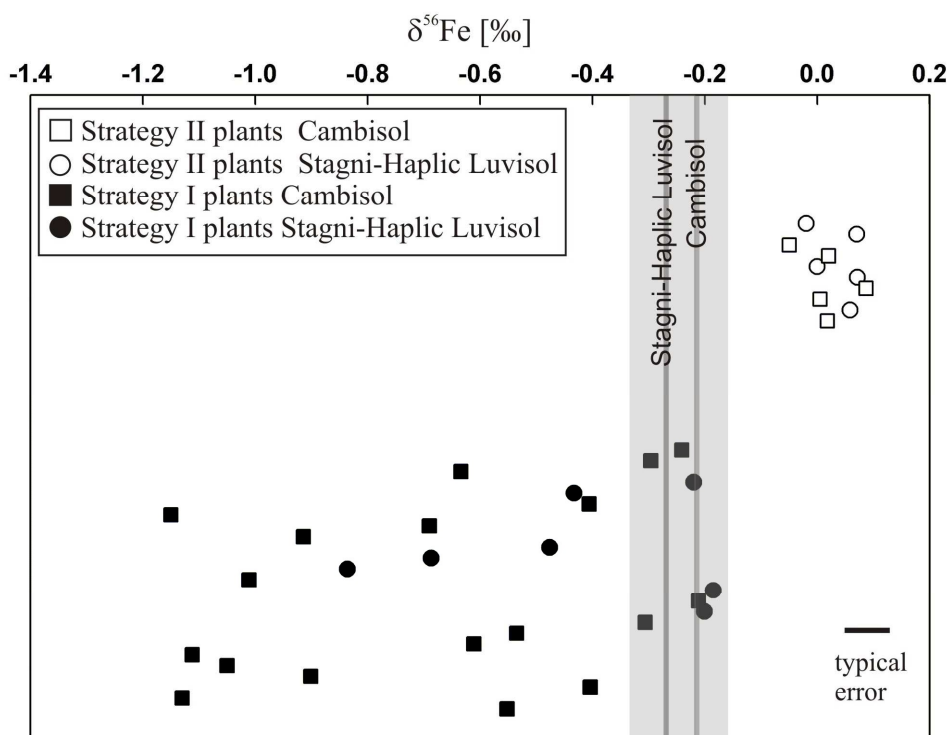


Figure 3.3  $\delta^{56}\text{Fe}$  for leaves from different strategy I and strategy II plants grown on the two agronomic soils (Guelke and von Blanckenburg, 2007, chapter 2 of this thesis). Grey bars:  $\delta^{56}\text{Fe}$  of plant-available iron of the two soils measured. Grey areas: uncertainties of these values.

In Figure 3.3 the  $\delta^{56}\text{Fe}$  values of leaves of different strategy I and II plants are plotted. Strategy I plants scattered in their  $\delta^{56}\text{Fe}$  but strategy II plants covered only a small range from  $-0.05$  ‰ to  $+0.1$  ‰. In chapter 2 it has been shown that strategy I plants also evolved isotopically during growth whereas strategy II plants appear to use a uniform mechanism to transport Fe through the plant as they displayed unvarying  $\delta^{56}\text{Fe}$  at all growth stages. Only one fractionation step is required during the complexation of Fe from iron bearing minerals in the soil onto phytosiderophores (Guelke and von Blanckenburg, 2007; Chapter 2 of this thesis). This fractionation factor can be calculated as follows. The iron isotopic composition of the plant-available iron of the Cambisol was about  $-0.21$  ‰ in  $\delta^{56}\text{Fe}$ . Leaves of strategy II plants grown on the Cambisol yielded a  $\delta^{56}\text{Fe}$  of approximately  $0.02$  ‰. This yields an apparent fractionation factor  $\Delta^{56}\text{Fe}_{\text{plant-soil}}$  of circa  $+0.2$  ‰. For the Stagni-Haplic Luvisol strategy II plants yielded a  $\delta^{56}\text{Fe}$  of  $0.03$  ‰ and the apparent fractionation factor  $\Delta^{56}\text{Fe}_{\text{plant-soil}}$  is circa  $0.3$  ‰. These values are very similar to the ones Brantley et al. (2004) found for the dissolution of goethite by siderophores ( $\Delta^{56}\text{Fe}_{\text{solution-goethite}} = 0.2$  ‰), Dideriksen et al. (2008)

found for the equilibrium isotope fractionation between complexes of the siderophore Fe(III)-desferrioxamine B (FeDFOB) and inorganic aqueous Fe(III) complexes ( $\Delta^{56}\text{Fe}_{\text{DFOB-inorg}} = 0.5 \text{ ‰}$ ) and Wiederhold et al. (2006) found for the ligand controlled dissolution of goethite with oxalate ( $\Delta^{56}\text{Fe}_{\text{solution-goethite}}$  about 0.3 ‰). Siderophores form multi-dentate and very stable complexes with dissolved Fe(III), with stability constants up to  $\sim 10^{50}$  (Hider, 1984). They attach to Fe at mineral surfaces, destabilizing Fe-bonding within the mineral structure, thereby causing ligand-promoted dissolution (e.g. Kalinowski et al., 2000). The extent of equilibrium fractionation depends on the strength of the bonding environment (Schauble, 2004; Hill and Schauble, 2008). Therefore it is expected that differences in the various organic ligands' mode of bonding can lead to a range of isotope fractionation factors.

### 3.6 Conclusions

It is concluded that the extraction with  $\text{H}_2\text{O}_2\text{-HNO}_3$  for organically bound iron and HCl for iron of poorly-crystalline Fe (oxyhydr)oxides is at the moment most suitable for the determination of the plant-available iron pool and thus to determine its iron isotopic signature. These extraction steps induce complete dissolution of the respective pool and therefore do not cause any isotope fractionation. A small bias can account from silicate dissolution but will in most cases be negligible. Variations of up to 0.7 ‰ in  $\delta^{56}\text{Fe}$  were found for the different soil mineral pools of a Cambisol and a Stagni-Haplic Luvisol. Light Fe isotopes were enriched in the oxide fractions, indicating preferential weathering of light isotopes from silicates. This hypothesis is confirmed by analysis of the silicate minerals, dissolved with HF-HNO<sub>3</sub> after prior exposure to all other extraction steps of method S-mod, which yielded a  $\delta^{56}\text{Fe}$  of +0.25 and +0.4 ‰, respectively. This ratio is higher than that expected for unweathered minerals. An iron isotope composition of about -0.21 ‰ and -0.27 ‰ for the plant available soil iron was calculated. Strategy II plants which grew on these soils contained Fe with  $\delta^{56}\text{Fe}$  of virtually 0 ‰ which is about 0.2 to 0.3 ‰ heavier than the measured plant-available Fe in soils. It is proposed that these values represent the apparent fraction factors  $\Delta^{56}\text{Fe}_{\text{plant-soil}}$  during uptake of Fe by strategy II plants. Therefore it is concluded that these plants are most likely to be suitable indicators for the composition of plant-available iron in soils. If so, the measurement of a strategy II plant is sufficient to calculate the composition of plant-available Fe in soil, to which the iron isotope evolution of strategy I plants can be compared to. Such iron isotope studies of plants contain an intrinsic advantage that is not available in other

methods. This advantage can, for example, be applied in chronosequences when the aim is to determine the change in the soils isotope composition through time (von Blanckenburg et al., 2009). The potential of the approach suggested here is that in each soil site grasses can be measured for their Fe isotope composition to determine the composition of the soils mobile iron fraction without relying in elaborate soil sampling and extraction methods, while strategy I plants, potentially driving the change in isotope composition through time by multiply fractionation cycles, unveil the driving force of this Fe isotope composition.

Although it is now possible to bracket the  $\Delta^{56}\text{Fe}_{\text{strategy II plant-soil}}$  to a narrow range, more sophisticated experiments should be performed to elucidate whether there is really only one fractionation step during the incorporation of iron by strategy II plants and if in fact all strategy II plants show the same Fe isotope pattern. Hence this study can be seen as only a first attempt providing a basis that should accompany evolution of these methods. Nevertheless an improved sequential extraction procedure is suggested to extract plant-available iron from soils, and these results show great promise that strategy II plants can serve as proxies of available soil iron isotope composition.

## **4 Identification of differences in iron metabolism between strategy I and II plants as revealed by the distribution of stable iron isotopes during plant growth**

### **4.1 Abstract**

Multiple-collector ICP-MS now routinely allows resolving small differences in metal stable isotope compositions of plants. Using this method, in an earlier study it was found that strategy I plants, which rely on reduction of iron before uptake, were enriched in stable  $^{54}\text{Fe}$  relative to  $^{56}\text{Fe}$  when grown on soil. In contrast strategy II plants, which rely on chelation of Fe(III) by phytosiderophores before uptake, were slightly enriched in the heavier iron isotopes.

The new study here explores the iron isotope fractionation caused by translocation during growth of a plant. As representatives of strategy I and II plants bean and oat were grown in a nutrient solution supplemented with Fe(III)-EDTA and were harvested at least at three different points in time. Total bean plants were found to be enriched in the light iron isotopes. Younger leaves contained lighter iron than older ones, and during growth younger leaves further accumulated the lighter isotopes whereas older leaves and the total roots were simultaneously depleted in light iron isotopes. This indicates that isotope fractionation is a result of translocation or re-translocation processes.

Oat plants, grown in a Fe(III)-EDTA-containing nutrient solution, were also enriched in the light iron isotopes. An explanation for this enrichment of light iron isotopes, which is in contrast with that found in strategy II plants grown on soil in the previous study (see chapter 2), is the prevalence of a constitutive reductive uptake mechanism of iron in the nutrient solution used as this is non-deficient in iron. In contrast iron availability in the natural aerated soil used in the previous study was low. However, during growth of the oat plants the initial isotope ratio obtained during the first uptake is maintained in all organs at all growth stages, including the roots. The absence of fractionation of iron isotopes during the translocation of iron in strategy II plants hints at a difference in translocation mechanisms between strategy I and II plants.

Results of the present study provide further support to the hypothesis that stable metal isotopes potentially serve as a new tool to identify the physiological mechanisms of metal uptake and translocation in plants.

## 4.2 Introduction

Even though iron is the fourth most abundant element in the Earth's crust and is essential for all living organisms including humans, animals and plants, iron deficiency is a major agronomical and health problem in many parts of the world. Plant's iron uptake and homeostasis controls the plant iron content and therefore the quality of edible plant parts. The major goal in studies of iron uptake by plants is biofortification. Biofortification means that the plant uses its own mechanisms to fortify or enhance the density or bioavailability of nutrients in its edible tissues. But the mechanisms for plant uptake and transport of iron are not completely understood. Besides molecular biological methods other tools are required to address open questions in the iron metabolism of plants. Recently, the use of stable iron isotopes as one possible tool has been recognized (e.g. Álvarez-Fernández 2006; Stuerup et al. 2008).

The research of stable iron isotope fractionation has mainly taken place in the domain of the Geosciences (reviews e.g. Dauphas and Rouxel 2006; Johnson and Beard 2006; Anbar and Rouxel 2007; Johnson et al. 2008). In the studies undertaken to date, variations in the minor, but well-resolvable  $^{56}\text{Fe}/^{54}\text{Fe}$  ratios are expressed in permil relative to a reference material and are reported in the delta notation ( $\delta^{56}\text{Fe}$ ). Efforts in studying stable iron isotope fractionation in the biosphere were mostly directed at detecting microbial iron isotope fractionation (Beard et al. 1999; Crosby et al. 2007). In higher animals the iron isotope composition in human blood and human tissues has been examined (Walczyk and von Blanckenburg 2002; Ohno et al. 2004; Krayenbuehl et al. 2005; Walczyk and von Blanckenburg 2005). In the first study of the stable iron isotope signature of higher plants the  $\delta^{56}\text{Fe}$  values in vegetables and crops grown on two distinct soil substrates were determined (Guelke and von Blanckenburg 2007). It was found that strategy I and strategy II plants differ in their stable iron isotope composition. Iron in strategy I plants was found to yield significantly lower  $\delta^{56}\text{Fe}$  values than the plant-available iron pool in the soil substrates, whereas iron in strategy II plants yielded slightly heavier  $\delta^{56}\text{Fe}$  values than the soil substrates. The first observation was explained with

the preferential reduction of the lighter iron isotopes during uptake (e.g. Welch et al. 2003; Staubwasser et al. 2006) while the latter could be due to the preferential chelation of heavier iron isotopes during complexation to phytosiderophores (Brantley et al. 2004; Dideriksen et al. 2008). In addition it was found that  $\delta^{56}\text{Fe}$  values in strategy I plants decreased from soils to stems, from stems to leaves and from leaves to seeds with seeds having the lowest  $\delta^{56}\text{Fe}$  value of  $-1.6\text{‰}$ . In contrast, all measured parts of strategy II plants displayed similar  $\delta^{56}\text{Fe}$  values. This finding led to the assumption that these plant types differ in the numbers of oxidation and reduction cycles during translocation as these processes are known to induce significant iron isotope fractionation (e.g. Welch et al. 2003).

Very recently Kiczka et al. (2010) found a  $\delta^{56}\text{Fe}$  of  $-1.0$  to  $-1.7\text{‰}$  in three Alpine plant species, two of them being strategy I plants and one being possibly a strategy II plant, grown under natural growth conditions. Mass balance calculations revealed that fractionation towards lighter Fe isotopic composition occurred before uptake, probably during mineral dissolution, and during selective uptake of iron at the plasma membrane. Iron isotopes were further fractionated during remobilization from old into new plant tissue, which changed the isotopic composition of leaves and flowers over the season.

However, these previous studies pose several questions. First, the transport mechanisms responsible for the fractionation processes need to be identified. Second, the question arises whether the fractionation during uptake depends on the iron speciation in the growth medium. For example, the observed trends might be characteristic of plants grown on soil substrates, and might differ in plants grown in nutrient solutions.

To address these open questions a strategy I plant (bean: *Phaseolus vulgaris* L.) and a strategy II plant (oat: *Avena sativa* L.) were planted on purified quartz sand, watered with a nutrient solution of known iron isotopic signature, and different plant organs were harvested at several growth stages. The iron concentration and the iron isotopic signature were determined and compared to that of the nutrient solution.

### **4.3 Principles of iron uptake and transport by plants and iron isotope systematics**

Iron from the soil or nutrient solution diffuses into the apoplast of plant roots. The apoplast represents an extracytosolic compartment of plant cells and is defined by the space that is

influenced by the properties of the cell wall. Under non-limiting iron supplies, iron uptake is mediated via a constitutive acquisition system that consists of a membrane-bound ferric reductase which is linked to a divalent metal ion transporter and an ATP-driven proton extrusion pump. This means that plants reduce iron and take up the ferrous form when they are grown on soils with a high iron availability. However, this rarely occurs. In soils iron is present in sparingly soluble Fe(III) compounds which are not directly available for root uptake. Therefore higher plants were forced to develop different strategies to make iron in soil available for their needs (Figures 1.1 and 1.2 in introductory section). Strategy I plants, which comprise the dicots and non-grass monocots, excrete protons via a plasmalemma H<sup>+</sup>-ATPase to acidify the rhizosphere, thus making Fe(III) more soluble. The inducible ferric chelate reductase activity of FRO2 reduces Fe(III) to Fe(II) (Robinson et al., 1999). Fe(II) is subsequently transported into the plant by IRT1, which is the major iron transporter of the plant root (Vert et al., 2002). This strategy is induced under Fe-deficiency. Strategy II plants, which are represented by graminaceous plant species, acquire iron by exuding phytosiderophores (PS). Phytosiderophores belong to the mugenic acid (MA) family which are non-proteinogenic secondary amino acids with a molecular weight of around 320. PS have a high affinity for Fe(III) and efficiently chelate Fe(III) in the rhizosphere via their amino and carboxyl groups. Fe(III)-PS complexes are then transported into plant roots via a specific membrane transport system. This chelation strategy is more efficient than reduction of ferric iron via a membrane-associated ferrireductase (strategy I) used by the other plants and thus allows grasses to survive more drastic iron-deficiency conditions (Curie and Briat, 2003).

The mechanisms of iron transport in plants, once taken up by the roots, are less clear. It has recently been suggested that younger leaves receive their iron primarily from the phloem whereas older leaves receive iron from the xylem (Morrissey and Guerinot, 2009). In the xylem iron is transported as Fe(III)-citrate, in the phloem as Fe(III)-ITP (Iron Transporter Protein) or Fe-nicotianamine (NA). The species of Fe-NA transported in the phloem has still to be identified. NA is a precursor of phytosiderophores. It is present in all plants and has the ability to bind various metals including Fe<sup>2+</sup> and Fe<sup>3+</sup> (von Wirén et al., 1999) but the kinetic stability is higher for the Fe(II)-NA complex than for the Fe(III)-NA complex. NA is not secreted and it is suggested that it plays a role in intra-and intercellular metal transport in both strategy I and II plants.

Developing seeds receive iron from the roots and from senescent leaves. At daylight iron moves to the seeds most likely via the phloem, because the flow of the xylem is driven by



transpiration and seeds hardly transpire. At night, iron is also transported to the seeds through the xylem due to root pressure. The level of remobilization from shoot to seed varies by species (Morrissey and Guerinot, 2009). It has also been shown that Fe-NA is essential for flower and seed development. In the seed, iron is thought to be stored mainly in the vacuoles of the embryo and endosperm as Fe(III) (Morrissey and Guerinot, 2009). Thus, iron metabolism in plants involves many changes in its binding forms and most likely also changes in the redox state (Figure 4.1).

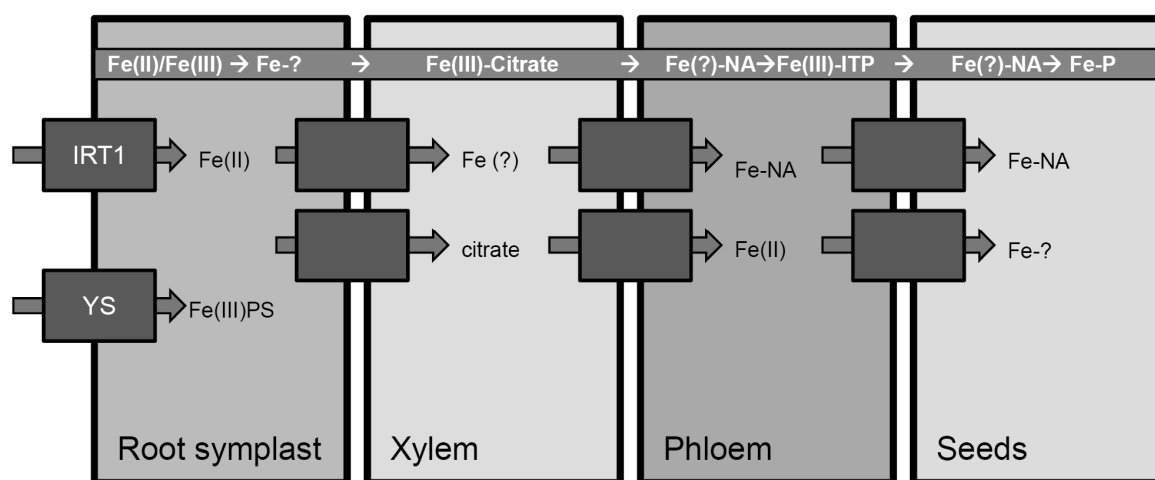


Figure 4.1 Fe chelation and long-distance iron transport in strategy I and II plants. The grey boxes symbolize transporters. The blue band represents redox- and ligand changes of iron.

Iron enters the root epidermal cells as Fe(II) (Strategy I plants) or Fe(III)-PS (strategy II plants). It is certainly chelated but it is unclear by which ligand. Once in the xylem iron is known to be bound by citrate. In the phloem iron is thought to be bound to nicotianamine (NA) or iron transport protein (ITP), whereby NA could act as a shuttle between the transporter and ITP. NA is an essential part of long distance movement to the seeds, although it is unclear in what form the iron is held, once it is loaded to the seeds. Inside the seeds iron is stored in the vacuole as Fe-phytate (P) or Fe-NA and in the plastides as phytoferritin (Fe(III)). After Morrissey and Guerinot (2009).

Stable iron isotopes are an excellent tool to study biogeochemical pathways of iron. Stable iron isotopes can be used in two different approaches. These are on the one hand isotope fractionation studies, utilizing minute natural isotopic shifts in the isotopic ratios of iron isotopes as driven by binding form and reaction kinetics, and on the other hand tracing studies, using artificial compounds enriched in a specific isotope. Both approaches permit to track the natural cycles of iron and to study metabolic processes, e.g. in humans or plants.

Iron has four naturally occurring stable isotopes with the following approximate composition:  $^{54}\text{Fe}$  (5.8 %),  $^{56}\text{Fe}$  (91.8 %),  $^{57}\text{Fe}$  (2.1 %) and  $^{58}\text{Fe}$  (0.3 %) (Rosman and Taylor, 1998). The

relative abundances are virtually constant in nature but tiny differences due to small chemical or physical differences between the iron isotopes can now be identified using advanced mass-spectrometric techniques (Weyer and Schwieters, 2003; Schoenberg and von Blanckenburg, 2005). The partitioning of isotopes between two substances or two phases of the same substance with different isotope ratios is called isotope fractionation. The main phenomena producing isotope fractionations are isotope exchange reactions (equilibrium isotope fractionation) and kinetic processes, the latter depending primarily on differences in reaction rates of isotopic molecules. Iron isotope fractionation is expressed in the delta notation, which provides the permil deviation of the isotopic ratio (e.g.  $^{56}\text{Fe}/^{54}\text{Fe}$  or  $^{57}\text{Fe}/^{54}\text{Fe}$ ) of the sample relative to that of the IRMM-014 standard (Taylor et al., 1992):  $\delta^{56}\text{Fe}/ [\text{‰}] = [(\frac{^{56/54}\text{Fe}_{\text{sample}}}{^{56/54}\text{Fe}_{\text{standard}}}) - 1] \cdot 10^3$ .

Iron metabolism in plants involves several changes of the binding form and redox state of iron (Briat et al., 2007). These metal conversion processes are expected to result in isotope fractionation whenever they are not quantitative. Crosby et al. (2007) have shown a fractionation of  $-3 \text{ ‰}$  from a solid Fe(III) substrate into Fe(II)<sub>aq</sub> using dissimilatory iron-reducing bacteria. This value is similar to the abiotic fractionation factor (Welch et al., 2003; Anbar et al., 2005). In soil  $\delta^{56}\text{Fe}$  of the Fe(II)<sub>aq</sub> taken up can still be lowered by re-adsorption of Fe(II)<sub>aq</sub> as adsorption processes are known to preferentially sequester the heavier isotope at soil particle surfaces (Icopini et al., 2004). These predictions have been confirmed for reduction of ferric iron in marine sediments (Severmann et al., 2006; Staubwasser et al., 2006). Additionally it has been shown that iron isotope fractionation might occur during ligand exchange reactions. Dideriksen et al. (2008) described the equilibrium isotope fractionation between complexes of the siderophore Fe(III)-desferrioxamine B (FeDFOB) and inorganic aqueous Fe(III) complexes with a  $\Delta^{56}\text{Fe}_{\text{DFOB-inorg}}$  of  $0.5 \text{ ‰}$ , which is similar to what Wiederhold et al. (2006) found for the ligand-controlled dissolution of goethite with oxalate ( $\Delta^{56}\text{Fe}_{\text{solution-goethite}}$  about  $0.3 \text{ ‰}$ ).

Preconditions for iron isotope fractionation in plants are given in the rhizosphere, in the apoplast, during passage across the plasma membrane, in the cytoplasm when considering storage of iron in vacuoles or plastids, during export from the cytoplasm into xylem vessels, in the membrane passage from the xylem fluid into the cytoplasm of leaf cells, during loading into the phloem vessel and during transfer from the phloem into the seed or fruit (von Blanckenburg et al., 2009).

## 4.4 Materials and Methods

### 4.4.1 Plant growth with nutrient solution

Seeds of *Avena sativa* L. (oat) and *Phaseolus vulgaris* L. (bean) were immersed into deionised water on a tissue for two days and then planted onto approximately 5 L quartz sand at a density of 6 plants in 5 L pots. Plants were watered as needed with deionised water. Every two days a nutrient solution with the following composition was added until the quartz-sand was fully covered with solution: 1000  $\mu\text{M}$   $\text{Ca}(\text{NO}_3)_2$ , 375  $\mu\text{M}$   $\text{K}_2\text{SO}_4$ , 325  $\mu\text{M}$   $\text{MgSO}_4$ , 100  $\mu\text{M}$   $\text{KH}_2\text{PO}_4$ , 8  $\mu\text{M}$   $\text{H}_3\text{BO}_3$ , 0.2  $\mu\text{M}$   $\text{CuSO}_4$ , 0.2  $\mu\text{M}$   $\text{ZnSO}_4$ , 0.2  $\mu\text{M}$   $\text{MnSO}_4$ , 10  $\mu\text{M}$   $\text{NaCl}$ , 0.05  $\mu\text{M}$   $\text{MoNa}_2\text{O}_4$  and 20  $\mu\text{M}$  Fe(III)-EDTA, all dissolved in deionised water. The Fe(III)-EDTA solution was not part of the nutrient solution containing the other elements, but was added separately before every watering. Plants grew in a daylight climate chamber with a temperature of 16 – 18 °C. At different points in time, one pot of plants was harvested; plants in the other pots continued to grow. Bean plants were harvested 17 days, 30 days, 47 days and 74 days after germination. Oat plants were harvested 14, 28 and 50 days after germination.

The plants were rinsed with ultrapure water and separated into roots, stem, the different leaves and fruits/buds. Roots were rinsed to remove adherent nutrient solution. Since apoplastic iron was not removed (Bienfait et al., 1985) measured roots concentration and isotope data integrate over both, intracellular iron and apoplastic iron.

The pedicel from the leaves was removed prior to cleaning. The plant parts were dried in an oven for at least 3 days at 80 °C and their dry weight was determined afterwards. Finally they were ground to mince and homogenize them. The same procedure was applied for original seeds.

### 4.4.2 Sample decomposition and iron separation

All reagents used during sample preparation were *suprapure* grade and prepared with ultrapure water. Hydrochloric and nitric acids were *pro analysi* grade and were further purified by sub-boiling distillation. All preparation work was carried out in a clean lab class 1000 in laminar-flow hoods, class 10.

Approximately 200 mg of each dried plant sample was digested via microwave digestion in 7 mL concentrated  $\text{HNO}_3$  and 1 mL concentrated  $\text{H}_2\text{O}_2$  at 200 °C for more than half an hour.

The Fe(III)-EDTA solution given to the bean and oat plants was also digested in order to determine its isotopic signature. The EDTA complex breaks down completely at temperatures of about 200 °C after 2 hours (Martell et al., 1975). 10 mL of the Fe(III)-EDTA solution (3 repetitions) were dried down, the residues were dissolved in 7 mL concentrated HNO<sub>3</sub> and 1 mL concentrated H<sub>2</sub>O<sub>2</sub> followed by microwave digestion at 220 °C for two hours. After this procedure the Fe(III)-EDTA solutions were clear, indicating that all EDTA was destroyed. As an additional test for the initial composition the nutrient solution (including Fe(III)-EDTA) was digested in the same way.

As it is also possible that plants mobilize small amounts of iron from the quartz sand which does contain traces of adsorbed iron, the iron concentration in a quartz leach which best represents the mobilization of iron by plants was determined. In three replicates 2 g of the quartz sand were weighed into 50 mL centrifuge tubes and 40 mL 0.5 M HCl were added. The samples were placed into an over-head shaker at room temperature. After 24 hours of shaking the tubes were centrifuged (15 min, 5000 rpm, 4472 x g) and the supernates decanted and filtered through 0.2 µm PTFE membrane filters wetted with ultrapure water. This procedure is thought to extract all poorly-crystalline iron (oxyhydr)oxides and iron bound to organic compounds (Wiederhold et al., 2007, chapter 3 of this thesis) which are most likely to be available for plant nutrition (e.g. Borggaard, 1992; Bertrand and Hinsinger, 2000). The total iron concentration and stable iron isotope composition of the quartz sand was also determined. For this purpose the quartz sand was digested via microwave agitation with a 1:2 HF/HNO<sub>3</sub> mixture at 200 °C for about an hour. Fluoride complexes that form in silicate samples were destroyed by treating the evaporated sample with concentrated aqua regia and heating to 170 °C for several hours. After digestion all samples were dried down on a hotplate and full oxidation of iron to its trivalent state was achieved by adding a drop of concentrated HNO<sub>3</sub> to the samples, heating them to 150 °C and careful drying them down. Afterwards all samples were dissolved in 1 mL of 6 M HCl for iron purification by anion-exchange chromatography following the procedure described by Schoenberg and von Blanckenburg (2005). As iron concentrations in plant materials are quite low (50-100 µg/g) microcolumns were used for iron separation, filled with ca. 300 µL DOWEX AG<sup>®</sup> 1x8 (100-200 mesh) resin. For the Fe(III)-EDTA- and nutrient solution samples 7.5 mL Spectrum<sup>®</sup> 104704 polypropylene columns filled with 1 mL of the resin were used. The exchange capacity of 1 mL wet resin is 1.2 mmol FeCl<sub>4</sub><sup>-</sup> corresponding to approximately 90 mg iron (Schoenberg and von Blanckenburg, 2005). After a cleaning procedure and conditioning of the resin, samples,

dissolved in 6 M HCl, were loaded to these columns. Matrix elements were washed out with 6 M HCl and afterwards iron was eluted with 5 M HNO<sub>3</sub>. Samples were dried down and redissolved in a drop of 15 M HNO<sub>3</sub>. After taking samples almost to dryness, they were dissolved in 1 mL of 0.3 M HNO<sub>3</sub>.

An additional precipitation step was applied for the plant samples that ensures quantitative precipitation of all Fe(III) as Fe(III)OOH while e.g. Zn as well as organic compounds stay in solution (Schoenberg and von Blanckenburg, 2005). The samples were precipitated at pH 10 with ammonia. After one hour the samples were centrifuged, the supernate solutions were discarded and the precipitates washed twice with ultrapure H<sub>2</sub>O before they were redissolved in 0.3 M HNO<sub>3</sub>. Quantitative recovery and removal of matrix elements during iron separation and precipitation was controlled by iron concentration measurements with small aliquots of the samples before and after each step by optical emission spectroscopy with inductively coupled plasma (ICP-OES: *Varian Vista PRO CCD Simultaneous*). This check is important because non-quantitative recovery could result in artificial isotope fractionation (Anbar et al., 2000; Roe et al., 2003). Additionally the iron concentrations of the plant samples were obtained and total procedural iron blanks were measured with mostly less than 60 ng. This was less than 1 % of the processed iron (with a minimum measureable Fe content of 6 µg) and was considered to be insignificant.

### 4.4.3 Iron isotope measurements

The iron isotope compositions of the Fe(III)-EDTA-solution, and for comparison also that of the nutrient solution, the quartz sand, and the different plant tissues were determined with the use of a multiple-collector inductively coupled plasma mass spectrometer (MC-ICP-MS; Neptune, *ThermoFinnigan*) by means of a high-mass resolution mode. Molecular interferences were resolved routinely by increasing mass resolution on this instrument (Weyer and Schwieters, 2003). The mass discrimination was corrected with the sample-standard bracketing approach (Schoenberg and von Blanckenburg, 2005) using the iron isotopic reference material IRMM-014 (Institute of Reference Material and Measurement, Geel, Belgium).

Sample and standard solutions were introduced into the mass spectrometer in 0.3 M HNO<sub>3</sub> at concentrations of 5-7 ppm Fe. All values are reported as  $\delta^{56}\text{Fe}$  and  $\delta^{57}\text{Fe}$  relative to the

IRMM-014 standard of which the isotopic composition is close to that of rocks at the Earth's surface (Schoenberg and von Blanckenburg, 2006 and others).

$\delta^{56}\text{Fe}$  and  $\delta^{57}\text{Fe}$  of all samples were plotted against each other and were found to follow a mass-dependent fractionation law which demonstrates the absence of molecular or elemental interferences. Within each analytical session the internal laboratory standard JM (Johnson & Matthey, Fe Puratronic wire) was measured to test the accuracy of the measurements. During the course of this study the measured Fe isotope composition of the JM standard was  $\delta^{56}\text{Fe} = 0.421 \pm 0.050 \text{ ‰}$  and  $\delta^{57}\text{Fe} = 0.625 \pm 0.090 \text{ ‰}$  ( $2\sigma$ ,  $n = 62$ ), which is in agreement with previous measurements ( $\delta^{56}\text{Fe} = 0.423 \pm 0.046 \text{ ‰}$  and  $\delta^{57}\text{Fe} = 0.624 \pm 0.073 \text{ ‰}$ ) given by Schoenberg and von Blanckenburg (2005). The reproducibility of replicate measurements and chemical replicates according to Schoenberg and von Blanckenburg (2005) of the samples processed in this and the previous studies (chapter 2 and 3 of this thesis) were determined as well. It was found to be  $0.07 \text{ ‰}$  ( $2\sigma$ ;  $n = 29$ ) for the  $\delta^{56}\text{Fe}$  of chemical replicates and  $0.11 \text{ ‰}$  for replicate measurements ( $2\sigma$ ;  $n = 108$ ). These values are less reproducible than those obtained by Schoenberg and von Blanckenburg (2005).

A mass balance approach is used to determine the  $\delta^{56}\text{Fe}$  of bulk plants and above-ground organs (without the roots) which is calculated according to the following formula, where  $Fe_n$  is the fraction of the iron amount of plant tissue  $n$  (dry weight multiplied with Fe concentration) and  $\delta^{56}Fe_n$  the isotopic composition of plant tissue  $n$ :

$$\delta^{56}Fe_{total} = \sum_n (\delta^{56}Fe_n \times [Fe]_n) \quad 4.1$$

Errors of the calculated total  $\delta^{56}\text{Fe}$  are the propagated errors of the  $\delta^{56}\text{Fe}$  of the individual plant tissues.

## 4.5 Results

The iron isotopic composition of the Fe(III)-EDTA solution, the nutrient solution and the quartz sand is shown in Table 4-1. The iron concentration for the quartz sand leachate was about  $60 \text{ ng/g}$ . As this comprised only about  $5 \%$  of the iron contained in the Fe(III)-EDTA it is considered to be negligible. The iron concentration leached from quartz was too low for iron isotope measurements. However, even if the  $\delta^{56}\text{Fe}$  of leached Fe and Fe(III)-EDTA

#### 4 Identification of differences in iron metabolism between strategy I and II plants

differed significantly, this would result in a bias of less than 0.1 ‰, which is within the 2 standard deviation of the analysis (assuming a  $\delta^{56}\text{Fe}$  of the leached Fe of  $-2$  ‰, which is an upper bound).

Table 4-1 Iron concentration and  $\delta^{56}\text{Fe}$  of the Fe(III)-EDTA solution, nutrient solution and quartzsand

	Fe concentration [ $\mu\text{g/g}$ ]	$\delta^{56}\text{Fe}$ [‰]	2SD [‰] <sup>1</sup>
Fe(III)-EDTA	1.10	0.56	0.11
nutrient solution	1.10	0.55	0.11
quartz sand HCl leach	0.06	-----	
quartz sand	2.50	0.25	0.11

<sup>1</sup> given as the 2 standard deviation reproducibility of replicate measurements

Total quartz sand had a Fe concentration of 2.5  $\mu\text{g/g}$ . About 2.5 % of this Fe was available for the plants in form of mobile Fe (leached with HCl). The residual Fe contained in the quartz sand is considered to be negligible as plants are not able to extract iron of crystalline oxides or silicates (Bertrand and Hinsinger, 2000).

Iron in Fe(III)-EDTA had a  $\delta^{56}\text{Fe}$  of  $0.56 \pm 0.11$  ‰. For comparison, the isotopic composition of a small aliquot of the nutrient solution (after Fe(III)-EDTA was added) was also determined. It is in agreement with the value found for Fe(III)-EDTA. In the following discussion the isotopic difference between plant parts and the Fe(III)-EDTA of the nutrient solution will be expressed as:  $\Delta^{56}\text{Fe}_{\text{plant-Fe(III)-EDTA}} = (\delta^{56}\text{Fe})_{\text{plant}} - (\delta^{56}\text{Fe})_{\text{Fe(III)-EDTA}}$  (Figures 4.2 and 4.3). The precision on the  $\delta^{56}\text{Fe}$  values was better than 0.11 ‰ (2SD) (Table 4-2). The error of the nutrients'  $\delta^{56}\text{Fe}$  value was not propagated into  $\Delta^{56}\text{Fe}_{\text{plant-Fe(III)-EDTA}}$  since this error was the same during the entire growth experiment, assuming uniform iron composition in the growth solution.

##### 4.5.1 Bean

All parts of bean plants except for the roots exhibited iron concentrations in the range expected for green plant tissues (Marschner, 1995). Seeds and fruits showed the lowest iron concentrations of approx. 50 ppm (Table 4-2). Roots had the highest Fe concentrations of mostly more than 200 ppm and differed between the harvests which might be explained by the lack of apoplastic iron removal prior to sample digestion. Therefore the  $\delta^{56}\text{Fe}$  of roots

#### 4 Identification of differences in iron metabolism of strategy I and II plants

---

includes apoplastic iron, precipitated in the “free space” after reduction. This pool was potentially available for plants; precipitated iron could be re-reduced and taken up. As roots were washed with ultrapure water after harvesting and Fe(III)-EDTA was easily washed out it is assumed that the apoplast comprises only iron which was reduced once and then precipitated again.

The concentration of iron in the cotyledon and first leaf decreased during growth. The iron concentration of the stem decreased from the first to the second harvest but then increased again. Shells of fruits had lower iron concentrations than fruits. Together they showed similar values as the original seeds.

All measured tissues of the bean plants were found to be enriched in the lighter iron isotopes compared to the Fe(III)-EDTA solution by up to  $-2.5\text{ ‰}$ . Iron in the different plant tissues became increasingly lighter from older to younger plant parts, i.e. from roots to cotyledon, to stem, to leaves and to fruits. At every harvest point this trend was visible. It is also obvious that during first growth the earlier leaves accumulated iron with high  $\delta^{56}\text{Fe}$  while the young leaves of the later growth stages obtained iron with lower  $\delta^{56}\text{Fe}$  than that obtained by the earlier leaves during their growth. Iron in roots and the cotyledon shifted to slightly higher compositions during growth. Iron in the stem and the first leaf evolved towards heavier compositions from the third harvest point on. The second and third leaf shifted to heavier isotopes during growth as well, whereas the fruits developed towards a lighter iron isotope composition when they grew further (Figures 4.2 and 4.3).



#### 4 Identification of differences in iron metabolism between strategy I and II plants

Table 4-2 Iron concentrations and stable Fe isotope compositions of plant tissues and total bean plants

Bean							
number of harvest	plant part	dry mass [g]	Fe concentration [ $\mu\text{g/g}$ ]	error <sup>1</sup>	$\delta^{56}\text{Fe}$ [‰]	2SD [‰] <sup>2</sup>	$\Delta^{56}\text{Fe}_{\text{plant-FeEDTA}}$ [‰]
<b>1<sup>st</sup> harvest</b>	seeds		53	± 2	-0.53	0.11	
	roots	0.4	205	± 7	-0.45	0.11	-1.00
	cotyledon	6	128	± 4	-0.57	0.11	-1.12
	stem	2.2	38	± 1	-0.76	0.11	-1.31
	leaf 1	5.7	133	± 4	-1.19	0.11	-1.74
	above-ground organs <sup>4</sup>				-0.72	0.19 <sup>3</sup>	-1.27
	<b>Total plant<sup>4</sup></b>				<b>-0.70</b>	<b>0.22<sup>3</sup></b>	<b>-1.25</b>
<b>2<sup>nd</sup> harvest</b>	roots	1.5	199	± 7	-0.35	0.11	-0.90
	cotyledon	5.0	70	± 3	-0.44	0.11	-0.99
	stem	5.5	22	± 1	-0.87	0.11	-1.42
	leaf 1	1.6	57	± 2	-1.32	0.11	-1.87
	leaf 2	7.9	64	± 2	-1.63	0.11	-2.18
	bud	0.4	62	± 2	-1.69	0.11	-2.24
	above-ground organs <sup>4</sup>				-0.96	0.24 <sup>3</sup>	-1.51
<b>Total plant<sup>4</sup></b>				<b>-0.70</b>	<b>0.27<sup>3</sup></b>	<b>-1.25</b>	
<b>3<sup>rd</sup> harvest</b>	roots	3.0	311	± 11	-0.27	0.11	-0.82
	cotyledon	1.2	99	± 3	-0.21	0.11	-0.76
	stem	5.0	44	± 2	-0.54	0.11	-1.09
	leaf 1	3.1	63	± 2	-0.86	0.11	-1.41
	leaf 2	0.5	56	± 2	-1.14	0.11	-1.69
	leaf 3	11.6	78	± 2	-1.38	0.11	-1.93
	fruit 1	0.9	52	± 2	-1.59	0.11	-2.14
	fruit 2	3.5	48	± 2	-1.65	0.11	-2.20
above-ground organs <sup>4</sup>				-0.85	0.29 <sup>3</sup>	-1.40	
<b>Total plant<sup>4</sup></b>				<b>-0.62</b>	<b>0.31<sup>3</sup></b>	<b>-1.17</b>	
<b>4<sup>th</sup> harvest</b>	roots	6.0	433	± 15	-0.25	0.11	-0.80
	stem	1.5	81	± 3	-0.31	0.11	-0.86
	leaf 2	1.3	59	± 2	-0.38	0.11	-0.93
	leaf 3	8.0	68	± 2	-0.69	0.11	-1.24
	fruit 1	3.1	49	± 2	-1.83	0.11	-2.38
	fruit 2	19.6	43	± 2	-1.90	0.11	-2.45
	shell of fruit 1	1.8	24	± 1	-1.15	0.11	-1.70
	shell of fruit 2	6.7	17	± 1	-1.05	0.11	-1.60
	above-ground organs <sup>4</sup>				-1.2	0.29 <sup>3</sup>	-1.75
<b>Total plant<sup>4</sup></b>				<b>-0.65</b>	<b>0.31<sup>3</sup></b>	<b>-1.20</b>	

<sup>1</sup> Errors are combined from weighing, dilution, instrumental count statistics and calibration error. Numbers refer to the last digits given for the concentration values

<sup>2</sup> given as the 2 standard deviation reproducibility of replicate measurements

<sup>3</sup> propagated from the 2 standard deviation reproducibilities of replicate measurements from all plant parts

<sup>4</sup> calculated with wt% fractions of the different plant tissues (equation 4.1)

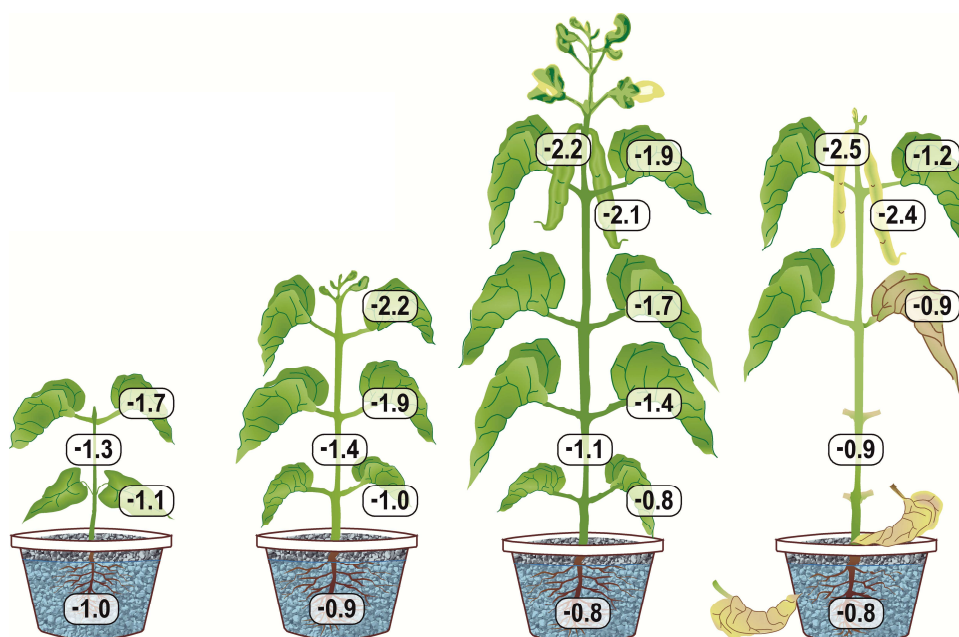


Figure 4.2 Schematic illustration of development of the  $\Delta^{56}\text{Fe}_{\text{plant-Fe(III)-EDTA}}$  of bean plant tissues during growth.

With mass balance (equation 4.1) above-ground organs' and bulk plant isotope compositions were calculated for each point of harvest (Table 4-2). Complete bean plants were found to be lighter by about 1.2 ‰ than Fe(III)-EDTA at all three growth stages. In contrast, the composition of the above-ground plant changed from  $-1.2$  ‰ at stage 1 to  $-1.75$  ‰ at stage 4 when compared to the growth solution.

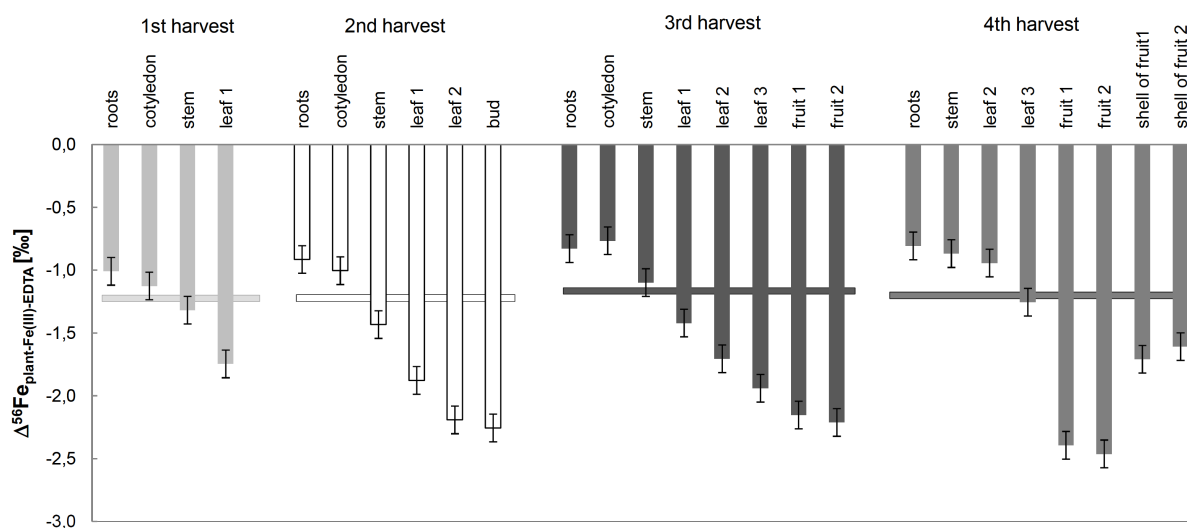


Figure 4.3  $\Delta^{56}\text{Fe}_{\text{plant-Fe(III)-EDTA}}$  of bean plant parts. The error bars denote the standard reproducibilities obtained for the  $\delta^{56}\text{Fe}_{\text{plant}}$  part. Horizontal grey bars show  $\Delta^{56}\text{Fe}$  between bulk plants (eq. 4.1) and the Fe(III)-EDTA for each growth experiment.

### 4.5.2 Oat

Similar to the bean plants, oat roots showed very high iron concentrations (Table 4-3) which can be explained by the lack of apoplastic iron removal prior to digestion.

The iron concentration in the cotyledon decreased from 77  $\mu\text{g/g}$  at the first point of harvest to 62  $\mu\text{g/g}$  at the second point of harvest. In the stem it decreased from 42 to 15  $\mu\text{g/g}$  whereas in the first leaf and fourth leaf the iron concentration increased during growth. In the second and third leaf the iron concentration was slightly diminished.

All  $\delta^{56}\text{Fe}$  values of the oat plants covered a small range of (Table 4-3). All measured tissue samples of the oat plants were enriched in the lighter iron isotopes compared to the nutrient solution ( $\Delta^{56}\text{Fe}_{\text{plant-Fe(III)EDTA}}$  0.34 to 0.62 ‰), a range which is only vaguely above the 2 standard deviation. In contrast to the bean plant, this finding does not change when roots are involved in the calculation or when only the above-ground organs are taken into account (Figures 4.4 and 4.5).

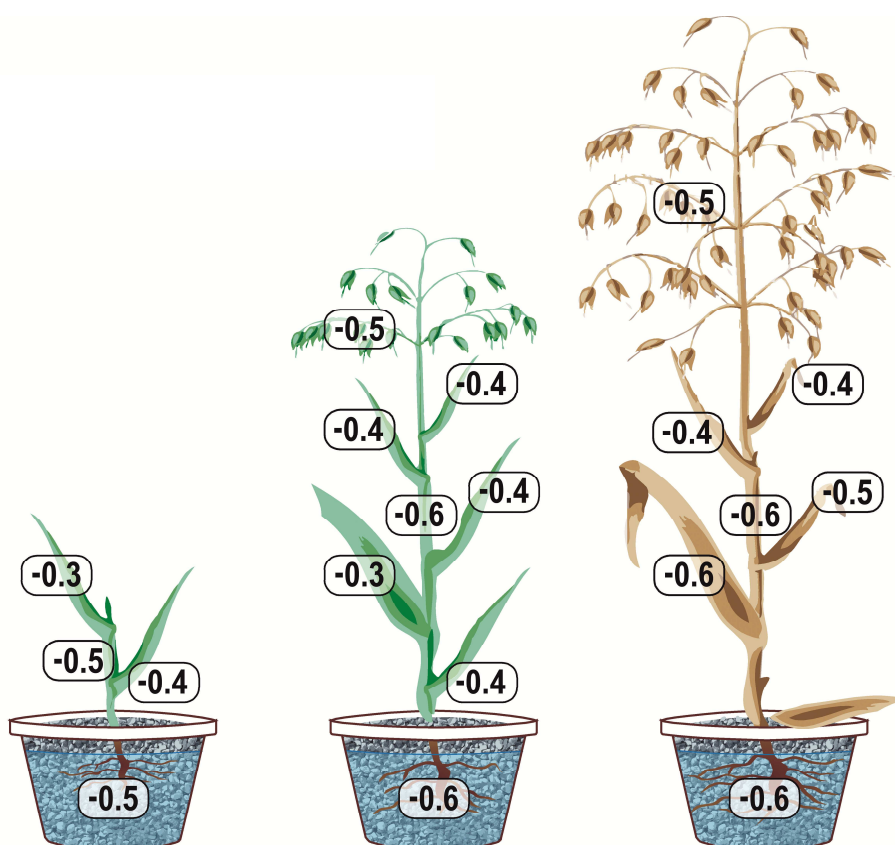


Figure 4.4 Schematic illustration of development of the  $\Delta^{56}\text{Fe}_{\text{plant-Fe(III)-EDTA}}$  of oat plant tissues during growth.

#### 4 Identification of differences in iron metabolism of strategy I and II plants

At all three harvests the roots, stems and the cotyledons had identical iron isotopic compositions within the 2 standard deviations. From the second to the third point of harvest the first leaf evolved towards a lighter iron isotope composition by 0.3 ‰, at the same time the iron concentration doubled. The iron isotopic composition of the second and third leaf and the fruit stayed the same during growth whereas leaf 4 evolved towards slightly lighter compositions.

Table 4-3 Iron concentrations and stable iron isotope compositions of plant tissues and total oat plants

Oat							
number of harvest	plant part	dry mass [g]	Fe concentration [ $\mu\text{g/g}$ ]	error <sup>1</sup>	$\delta^{56}\text{Fe}$ [‰]	2SD [‰] <sup>2</sup>	$\Delta^{56}\text{Fe}_{\text{plant-FeEDTA}}$ [‰]
	seeds		33	$\pm 1$	0.22	0.11	
<b>1<sup>st</sup> harvest</b>	roots	0.4	1053	$\pm 37$	0.04	0.11	-0.51
	cotyledon	1.2	77	$\pm 3$	0.18	0.11	-0.37
	stem	0.6	42	$\pm 2$	0.04	0.11	-0.51
	leaf 1	2.3	48	$\pm 2$	0.21	0.11	-0.34
	<i>above-ground organs</i> <sup>4</sup>				0.09	0.19 <sup>3</sup>	-0.46
	<b>Total plant</b> <sup>4</sup>					0.06	0.22 <sup>3</sup>
<b>2<sup>nd</sup> harvest</b>	roots	1	405	$\pm 14$	-0.05	0.11	-0.60
	cotyledon	0.1	62	$\pm 2$	0.14	0.11	-0.41
	stem	5.3	24	$\pm 1$	-0.06	0.11	-0.61
	leaf 1	0.7	55	$\pm 2$	0.27	0.11	-0.28
	leaf 2	0.5	67	$\pm 2$	0.19	0.11	-0.36
	leaf 3	0.5	63	$\pm 2$	0.18	0.11	-0.37
	leaf 4	0.2	55	$\pm 2$	0.19	0.11	-0.36
	fruit	2.7	27	$\pm 1$	0.05	0.11	-0.50
<i>above-ground organs</i> <sup>4</sup>				0.03	0.29 <sup>3</sup>	-0.52	
<b>Total plant</b> <sup>4</sup>					-0.01	0.31 <sup>3</sup>	-0.56
<b>3<sup>rd</sup> harvest</b>	roots	2	469	$\pm 16$	-0.01	0.11	-0.56
	stem	3.6	15	$\pm 1$	-0.05	0.11	-0.60
	leaf 1	0.1	120	$\pm 4$	-0.07	0.11	-0.62
	leaf 2	0.5	52	$\pm 2$	0.09	0.11	-0.46
	leaf 3	0.1	53	$\pm 2$	0.14	0.11	-0.41
	leaf 4	0.1	62	$\pm 2$	0.03	0.11	-0.52
	fruit	3.3	11	$\pm 0$	0.07	0.11	-0.48
	<i>above-ground organs</i> <sup>4</sup>				-0.04	0.27 <sup>3</sup>	-0.59
<b>Total plant</b> <sup>4</sup>					-0.02	0.29 <sup>3</sup>	-0.57

<sup>1</sup> Errors are combined from weighing, dilution, instrumental count statistics and calibration error. Numbers refer to the last digits given for the concentration values

<sup>2</sup> given as the 2 standard deviation reproducibility of replicate measurements

<sup>3</sup> propagated from the 2 standard deviation reproducibilities of replicate measurements from all plant parts

<sup>4</sup> calculated with wt% fractions of the different plant tissues (equation 4.1)

With mass balance (equation 4.1) the total iron isotopic composition of the oat plants for each point of harvest was calculated (Table 4-3). It was found that oat plants were uniformly lighter by about 0.5 ‰ than Fe(III)-EDTA at all three growth stages.

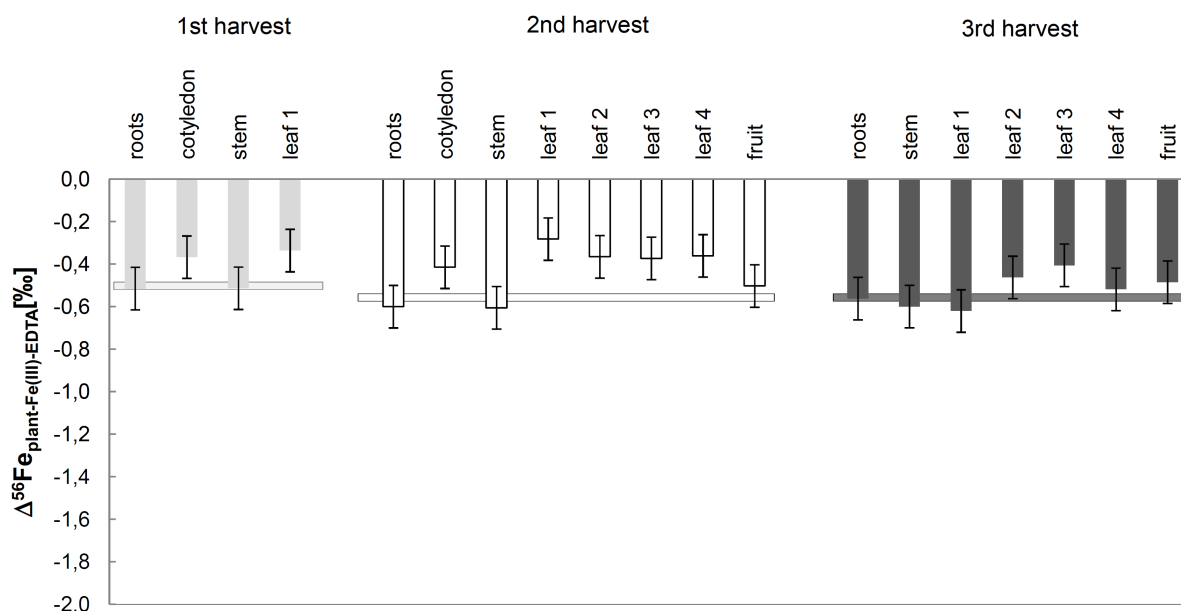


Figure 4.5  $\Delta^{56}\text{Fe}_{\text{plant-Fe(III)-EDTA}}$  of oat plant parts. The error bars denote the standard reproducibilities obtained for the  $\delta^{56}\text{Fe}_{\text{plant}}$  part. Horizontal grey bars show  $\Delta^{56}\text{Fe}$  between bulk plants (eq. 4.1) and the Fe(III)-EDTA for each growth experiment.

## 4.6 Discussion

### 4.6.1 Iron isotope fractionation in strategy I plants

#### 4.6.1.1 Fractionation during uptake of iron in strategy I plants

Mass balance (equation 4.1) shows that iron of the complete strategy I plant bean was about  $1.2 \pm 0.11$  ‰ lighter than the Fe(III)-EDTA and  $0.2 \pm 0.11$  ‰ lighter than iron of the original seeds at every point of harvest. Therefore (i) uptake of iron by the bean plants from a Fe(III)-EDTA solution led to an enrichment of light iron isotopes, (ii) the fractionation factor for iron uptake by bean plants grown in nutrient solution was constant during all growth stages and (iii) this enrichment of light iron isotopes is compatible with a reduction step before uptake.

A similar enrichment of light iron isotopes has been found in strategy I plants grown on two distinct types of soil substrate (Guelke and von Blanckenburg, 2007, chapter 2 of this thesis),

where iron in some plant parts was up to 1.6 ‰ lighter than the plant-available iron in the respective soil substrate. This similarity indicates that fractionation patterns of strategy I plants do not depend on the type of the growth medium or iron availability. Further evidence for reductive uptake of light iron isotopes is provided by the roots, which were all depleted in heavy iron isotopes when compared to the growth solution. However, in contrast to the bulk plants, the root's composition also changed during growth. Roots of bean plants were enriched in the light iron isotopes by 1 ‰ compared to the Fe(III)-EDTA at the first point of harvest, by 0.9 ‰ at the second point of harvest and 0.8 ‰ at the third and fourth point of harvest. With 200-400 ppm the roots furthermore contained much more iron than the plant tissues with 60-80 ppm. Therefore, this iron is also included in iron-containing solids ( $\text{FePO}_4$  or  $\text{Fe}(\text{OH})_3$ ) that were precipitated in the apoplast. The change of the root  $\delta^{56}\text{Fe}$  cannot be attributed to a change in the  $\delta^{56}\text{Fe}$  of the nutrient solution over time as the nutrient solution was renewed every 2 days. Thus, iron isotope fractionation by bacterial growth within the nutrient solution is unlikely. Reduction of iron by the reductase in the plasma membrane of root cells most likely leads to the observed enrichment in  $^{54}\text{Fe}$  over  $^{56}\text{Fe}$  in the above-ground plant organs without the roots (Table 4-2).

It is therefore hypothesized that roots were depleted in lighter iron isotopes during growth, as light iron isotopes from storage molecules in the roots or apoplast were transported preferentially into younger plant parts, probably involving an initial reduction step.

##### ***4.6.1.2 Fractionation during translocation of iron in strategy I plants***

With that isotope fractionation model during uptake in mind the distribution of iron isotopes between the different organs of bean plants can be discussed. It was previously observed that iron in leaves of soil-grown plants became increasingly enriched in the lighter isotopes from the oldest to the youngest leaf (Guelke and von Blanckenburg, 2007, chapter 2 of this thesis). The same pattern emerged in bean plants in the present study although plants were grown on Fe(III)-EDTA. This indicates that in strategy I plants the isotope fractionation patterns during both uptake and translocation do not differ depending on whether natural soil or an artificial solution is used as growth medium.

Iron isotope fractionation during uptake alone cannot be responsible for the observed patterns in the bean plants. Such an open-system fractionation during uptake was discussed in chapter 2. If an infinite iron pool was to supply the roots, and the iron isotope fractionation during uptake was also constant, the  $\delta^{56}\text{Fe}$  values in all parts of strategy I plants would be identical.

Such uniform compositions have never been observed in strategy I plants. Rather, during growth, iron in older leaves of bean evolved towards heavier and iron of new young leaves towards even lighter compositions. Newly grown fruits showed the lightest iron isotope composition with a  $\Delta^{56}\text{Fe}_{\text{plant-Fe(III)-EDTA}}$  of up to  $-2.5\text{‰}$  at the fourth harvest point. Therefore fractionation during translocation of iron is adding to the iron isotopic shift induced into strategy I plants during uptake. This scenario, called “fractionation during uptake and translocation as an open system” in chapter 2 can be seen as a series of Rayleigh steps supplying light iron from older into younger plant parts. A series of consecutive iron reduction steps lead to fractionation during growth of the plant. However, since the early grown parts of the plant do not contain sufficient iron amounts to supply the younger growth stages, fresh iron from uptake is continuously mixed into the plant, too. The combination of these two processes leads to a decrease of the  $\delta^{56}\text{Fe}$  value during growth of the plants, but due to binary mixing the resulting isotope effect will be smaller than if all iron in young leaves was supplied from older parts of the plant. Regardless of the actual details of the process, fractionation during translocation is the mechanism that best fits the decrease in  $\delta^{56}\text{Fe}$  from older to younger organs of strategy I plants. This effect can be demonstrated with a simple example. The amount of iron lost from the cotyledon and leaves 1-3 during growth was 737  $\mu\text{g}$  if not all iron was remobilized from the dying cotyledon and first leaf (Table 4-2). Iron contained in the fruits (fruit 1 and 2 including fruit shells) amounts to 1935  $\mu\text{g}$ , therefore about 38 % of the fruits’ iron has been retranslocated from the early plant parts. The residual 62 % originated from iron uptake via the roots. Now the possible iron isotopic composition of this fresh iron can be estimated if one assumes that old leaves are not supplied with fresh iron from uptake. The  $\delta^{56}\text{Fe}$  of the Fe which has been remobilized by the earlier leaves amounts to  $-0.41\text{‰}$  which is not as low as the  $\delta^{56}\text{Fe}$  of the fruits. The  $\delta^{56}\text{Fe}$  of the new iron taken up is determined with the assumption that all is transported qualitatively to the fruits according to:

$$\delta^{56}\text{Fe}_{\text{fruit}} = f_{\text{remobilized Fe}} \cdot \delta^{56}\text{Fe}_{\text{Fe remobilized}} + f_{\text{new Fe}} \cdot \delta^{56}\text{Fe}_{\text{new Fe}} \quad 4.2$$

with  $f$  being the fraction of remobilized (38 %) and fresh iron (62 %); and  $\delta^{56}\text{Fe}$  its respective iron isotopic composition. Total fruits (fruit 1+2 inclusive shells of fruit) have a  $\delta^{56}\text{Fe}_{\text{fruit}}$  of  $-1.8\text{‰}$ . This results in a  $\delta^{56}\text{Fe}_{\text{new Fe}}$  of  $-2.65\text{‰}$ . This value is only a very rough estimate as the correct iron amount being transferred to the fruits from older leaves can only be assumed and probably always new fresh Fe from uptake is mixed into the leaves during growth. Nevertheless it is demonstrated that the iron isotopic composition of the fruits is a mixture of fresh iron from uptake and remobilized iron from older leaves.

Which mechanisms during translocation may potentially be responsible for the fractionation of iron isotopes? Changes of the binding form and redox state of iron are expected to result in isotope fractionation whenever they are not quantitative as has been presented in section 4.3. According to the processes during iron translocation in plants, an enrichment of the lighter iron isotopes can occur during reduction of iron in the root apoplast, while the heavier iron isotopes can be concentrated in the oxidized and precipitated iron pool in the apoplast leading to even lighter iron in the ferrous iron pool which is taken up by the strategy I plant. Fractionation of iron isotopes can also occur during release of iron into xylem vessels where it is transported as Fe(III) or uptake into leaf tissues where iron has to be reduced for transport across the plasma membrane. Non-quantitative oxidative phytoferritin fixation during storage would result in light residual Fe(II)-NA. Also ligand exchange and change of the redox state during loading of iron to the phloem, transport inside it or unloading from the phloem can cause iron isotope fractionation. As it has been shown that iron is transported as Fe<sup>2+</sup> into the cell's vacuole and is stored probably as Fe(III)-complexes (Kim et al., 2006), it can be assumed that the mobilization of iron involves a reduction step and can therefore result in isotope fractionation favoring a relative accumulation of lighter iron isotopes in the soluble iron pool. Especially when the plant enters the generative growth phase, root activity usually decreases, so elements become retranslocated to sink tissues like the seeds or fruits. In summary it is concluded that fruits contain iron that mainly originates from light iron upon reduction in the root apoplast and from light remobilized iron from older leaves.

### **4.6.2 Iron isotope fractionation in strategy II plants**

#### ***4.6.2.1 Fractionation during uptake of iron in strategy II plants***

Mass balance (equation 4.1) showed that iron of total oat plants was around 0.54 ‰ lighter than the Fe(III)-EDTA solution (Table 4-2) at all growth stages. This is in contrast to the finding of the first study on iron isotope fractionation in higher plants (Guelke and von Blanckenburg, 2007; chapter 2 of this thesis), where iron in strategy II plants appeared to be similar or even slightly heavier than to the iron isotope composition of the iron assumed to be plant-available in the soil substrate, but consistent with Fe isotope data of a potential alpine strategy II plant (above ground biomass) determined by Kiczka et al. (2010b) with a  $\delta^{56}\text{Fe}$  of approx. -1 ‰ compared to the cortex which consists mainly of apoplastic iron. The main difference between these studies was the type of growth medium and therefore the iron



availability. In Guelke and von Blanckenburg (2007) plants were grown on two soil substrates, a sandy Cambisol and a loamy Stagni-Haplic Luvisol. Iron solubility is as low as  $10^{-10}$  M in these kinds of soils (Briat and Lobreaux, 1997). The concentration of iron from Fe(III)-EDTA in the growth medium of the present study was far higher than that of the free iron pool in the soils. Hence, plants in the growth solution were supplied with sufficient iron and therefore had no reason to induce their plant-specific iron mobilization strategies. Therefore it is likely that oat plants grown on a Fe(III)-EDTA nutrient solution reduce iron and take up the resulting  $\text{Fe}^{2+}$ . In addition strategy II plants exude phytosiderophores but their amounts are not as large as in strategy II plants grown on soil, because upregulating of the strategy-specific processes only occurs when plants suffer from Fe-deficiency (Grusak and DellaPenna, 1999). In the Kiczka et al. (2010b) study the potential strategy II plant *Agrostis* grew on a natural soil as well, but the authors attributed the very high Fe concentration of the roots to a high apoplastic Fe pool and therefore to the sufficient supply with iron.

In the present study one can assume a binary mixing in the oat plants, with iron being taken up by both the reductive pathway and as Fe(III)-PS. As shown in section 4.6.1 reduction of iron in the nutrient solution can lead to an enrichment of the light iron isotopes which were more prone to subsequent uptake. This iron represents the first component of the binary mixture. The second component is the fractionation occurring when oat plants exude phytosiderophores into the nutrient solution which then compete with EDTA for iron. As the Fe(III)-PS complex as a whole is too big for mass-dependent isotope fractionation (relative mass differences are too small), the Fe(III)-PS membrane transport process should not result in any further fractionation. More likely is that the fractionation occurs when ligands and chelates are exchanged. The direction of the reaction is determined by the stability constant of the respective complexes.

Siderophores form multi-dentate and very stable complexes with dissolved Fe(III), with stability constants up to  $\sim 10^{50}$  (Hider, 1984). Fe(III)-EDTA has a stability constant of  $\sim 10^{25}$ . In an aqueous solution where both chelates are present at the same concentration, the more stable chelator will bind the metal. Therefore, when phytosiderophores are exuded into the nutrient solution, Fe(III)-EDTA dissociates and the more stable Fe(III)-PS complex forms which is subsequently taken up by YS1-type membrane transporters that mediate root uptake by the cotransport of metal-phytosiderophores with protons (Curie et al., 2001; Schaaf et al., 2004).

The described ligand exchange process was predicted to entail isotope fractionation. The principle is that the sense of direction of equilibrium isotope fractionation depends on bonding environment, where the heavier iron isotopes are favoured by the complex with the strongest bonds (Urey, 1947; Schauble, 2004). Wiederhold et al. (2006) and Dideriksen et al., (2008) have shown that heavy iron isotopes are enriched in Fe(III) complexed by organic ligands. Therefore during ligand exchange Fe(III)-PS is expected to obtain a heavier iron isotope composition than the Fe(III)-EDTA as the stability constant of Fe(III)-PS is higher. In the oat plants, this heavy Fe(III) is mixed with the light Fe(II) released during reduction of Fe(III)-EDTA.

The iron isotope composition of the roots of oat plants supports this hypothesis. Roots were enriched in the light iron isotopes by 0.5 to 0.6 ‰ compared to the Fe(III)-EDTA regardless of the point of harvest. The reductive pathway into the plasma membrane led to an enrichment of the lighter iron isotopes in ferrous iron as explained above (section 4.6.1). But the reductase activity of roots in strategy II plants was not as high as that of strategy I plants as it comprises only a constitutive reductase which cannot be upregulated. Hence the binary iron mixture was shifted towards the phytosiderophore pathway, which binds Fe(III) from Fe(III)-EDTA or from precipitated FePO<sub>4</sub> or Fe(OH)<sub>3</sub>.

##### ***4.6.2.2 Fractionation during translocation of iron in strategy II plants***

In contrast to the bean plants, all parts of the oat plants had similar  $\delta^{56}\text{Fe}$  values at all growth stages. Furthermore, the iron isotope ratios of roots were identical to those of the above-ground tissues and remained constant during growth. It is therefore concluded that iron isotope fractionation is the same during growth and even if iron is remobilized from the roots this does not lead to fractionation. This finding points to differences in the way of how iron is translocated within strategy I and II plants.

As described in section 4.3 no consensus exists on the fate of the imported Fe(III)-PS complex in strategy II plants. Current thinking is that strategy I plants may more frequently change the redox state of Fe during translocation, while in strategy II plants, iron remains to a larger extent in its ferric form, also during ligand exchange. These differences potentially result in the substantial differences in the distribution of stable iron isotopes between these two plant types as found in this study.

## 4.7 Conclusions and potential applications

The principle conclusions of this study are:

1) The bulk strategy I plant bean was enriched by up to 1.25 ‰, the above-ground plant by up to 1.75 ‰ in the lighter iron isotopes compared to the nutrient solution, which confirms the hypothesis of Guelke and von Blanckenburg (2007, also chapter 2 of this thesis) that the reductive uptake pathway induced by these plants leads to iron isotope fractionation preferring the light isotopes. During growth of the bean plant older leaves and roots evolved towards being more enriched in the heavier iron isotopes whereas new young leaves were more enriched in the lighter iron isotopes. It is proposed that the observed distribution of iron isotopes in different plant organs is due to iron isotope fractionation during reduction of iron before membrane transport or chelate exchange which is relevant at uptake as well as during remobilization of iron from storage pools, such as reduction of apoplastic iron or non-quantitative oxidative phytoferritin fixation.

2) Iron in the bulk strategy II plant oat was 0.4 ‰ lighter than Fe(III)-EDTA of the nutrient solution. This fractionation is in contrast to the previous results obtained during growth on soil substrates where isotope fractionation was minor (Guelke and von Blanckenburg, 2007; also chapter 2 of this thesis). The difference can be explained by the influence of iron speciation in the growth media. In the Fe(III)-EDTA solution strategy II plants were well-fed with iron and the specific acquisition system was not upregulated. Therefore, under these conditions even strategy II plants were at least in part supplied by the constitutive system of iron reduction and uptake in the ferrous form (favouring light iron isotopes), and in part by Fe(III)-PS uptake (favouring heavy iron isotopes). In soil, in contrast, a larger fraction of phytosiderophores were exuded and most iron was taken up as Fe(III)-PS.

3) In the strategy II plant oat all parts of the plants and the roots exhibited a similar iron isotope composition that also did not change significantly during growth. Thus, these iron isotope observations allow to support the hypothesis that translocation mechanisms differ (under iron sufficient conditions) between strategy I and II plants. According to this hypothesis, strategy I plants more frequently change the redox state of iron during translocation, while in strategy II plants, iron may remain to a larger extent in its ferric form, also during ligand exchange.

The above conclusions clearly need further investigation, but, nevertheless, the stable iron isotope variations observed in plants contribute considerably to the understanding of iron

cycling processes in the environment and in individual organisms. In addition the potential of stable iron isotopes as a tool of tracing iron fluxes within plants has been demonstrated. Up to now radiolabelled iron ( $^{55}\text{Fe}$  or  $^{59}\text{Fe}$ ) has been used to trace iron and even to image it (Brown et al. 1965). These studies have focused on the uptake and breakdown of synthetic or natural chelates, as well as on the shoot translocation rates of the iron supplied by those compounds (e.g. Reid and Crowley, 1984; Roemheld and Marschner, 1986; Crowley et al., 1992; Johnson et al., 2002; Cesco et al., 2004). The current study demonstrates that stable isotopes too present an excellent tool to trace biogeochemical pathways of iron which possibly complements studies employing radiotracers. Stable iron isotopes can be used in two different ways: fractionation and tracer studies, the latter employing an enriched stable iron isotope label. Both approaches permit to follow the natural cycles of iron and to study metabolic processes. In the present study fractionation studies on a strategy I and a strategy II plant grown with artificial chelates demonstrate that redox processes and differences in the iron fluxes within plants employing different Fe acquisition systems can be mapped out. In addition it is shown that uptake mechanisms of the strategy II plant oat depend on the iron availability and therefore the type of growth substrate. These findings suggest that fractionation studies with stable iron isotopes will become a complementary tool in the study of iron uptake and translocation in plants as suggested recently by Álvarez-Fernández (2006) and Baxter (2009).

## **5 Deciphering mechanisms of iron acquisition and retranslocation in maize using stable iron isotope fractionation**

### **5.1 Aim of the study**

The aim of this chapter is to report the results and a preliminary interpretation of using stable iron isotopes to investigate the specific processes of iron metabolism of strategy II plants. The following questions will be addressed: (1) Does the Fe isotope signature of maize depend on the kind of Fe substrate? (2) Are translocation mechanisms in strategy II plants indeed different to those of strategy I plants? (3) Does (re-)translocation of iron in strategy II plants take place only under iron-deficiency or also under iron-sufficient conditions? (4) Is iron only remobilized from the root apoplast but also from older leaves? (5) What mechanism is relevant for the remobilisation of iron?

Different experiments were conducted together with scientists of the University of Hohenheim from the Institute for Plant Nutrition. We chose maize as a strategy II plant and grew it in pots filled with nutrient solution in a climate chamber. Iron was added either as Fe(III)–EDTA or as Fe(III)–phytosiderophores, depending on the experiment. Plants were cultured under Fe-sufficient and –deficient conditions and the apoplastic iron was removed from the roots for some of the experiments according to Bienfait (Bienfait et al., 1985). In addition maize was grown on a soil substrate of which the isotopic composition of the iron which is most likely available for plants was determined (chapter 3 of this thesis). This part of the study was conducted at the Institute for Biological Production Systems at the Leibniz Universität Hannover.

### **5.2 Materials and Methods**

#### **5.2.1 Experiments**

An overview for all experiments can be found in Table 5-1.

### Experiment 1: Maize sequential harvest

The intention of experiment 1 was to investigate how the stable iron isotope signatures of different parts of maize plants change during growth when grown on a nutrient solution supplemented with Fe(III)-EDTA and when grown on iron deficient conditions.

Maize (*Zea mays*) seeds (cv. UH002) were germinated in the dark between filter papers soaked with a CaSO<sub>4</sub>-saturated solution for 4 days and transferred to a half-strength nutrient solution not containing any iron. After one day, seedlings were transferred to a full-strength nutrient solution with +Fe conditions (see section 5.2.2). 18 days after sowing, plants were partially harvested (T0). Remaining plants were exposed to +Fe or -Fe conditions and harvested on day 22 (T1) and day 24 (T2) (Figure 5.1). Apoplastic iron was removed according to Bienfait et al. (1985) but not measured. Stems were not harvested.

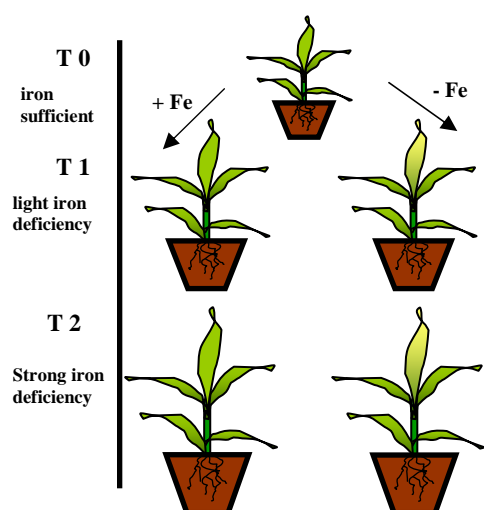


Figure 5.1 Experimental design of Experiment 1.

### Experiment 2: Maize supplied with phytosiderophores from wheat 1

The intention of experiment 2 was to resolve the stable iron isotope signature of different parts of maize plants when grown on a nutrient solution supplemented with Fe(III)-phytosiderophores to see if Fe isotope fractionation in strategy II plants depends on the form of iron supply in the nutrient solution.

Wheat (*Triticum aestivum*) plants (cv. Thomy) were germinated in quartz sand moistened with a CaSO<sub>4</sub>-saturated solution. After 7 days the seedlings (50 per pot) were transferred to 1 L pots containing an iron-free full-strength nutrient solution.

7 days after germination of wheat, maize seeds (cv. UH002) were germinated in the dark between filter papers soaked with a CaSO<sub>4</sub>-saturated solution for 4 days. Five plants were transferred to 1 L pots containing a half-strength nutrient solution without iron.

From day 7 after maize germination, Fe-starved wheat plants were allowed to exude phytosiderophores (PS) in 1 L freshly prepared iron-free nutrient solution for five hours, starting two hours after the onset of light. The produced exudates-enriched nutrient solution was supplemented with 3 μM FeCl<sub>3</sub>. Five maize plants were directly subjected to 950 mL of this solution until the next day. This procedure was repeated for 4 days. Afterwards maize plants were divided into the +Fe and –Fe treatment. +Fe plants continued growing in the exudates-containing nutrient solution treatment. –Fe plants continued growing on an iron-free nutrient solution. All plants were harvested 4 days later.

In addition maize was grown under the same conditions with a nutrient solution supplemented with Fe(III)-EDTA and another that was iron-free.

### Experiment 3: Maize plants for Bienfait solution (Fe(III)-EDTA)

The intention of experiment 3 was to find out if apoplastic and symplastic iron in the roots differ in their iron isotope signature when maize is grown in a nutrient solution supplied with Fe(III)-EDTA in order to discover if fractionation occurs only during reduction or also during passage across the plasma membrane. Another aim is to find out if there is remobilization from the apoplastic iron pool when plants get iron-deficient and what mechanism could play a role during remobilization.

Maize seeds (cv. UH002) were germinated in the dark between filter papers soaked with a CaSO<sub>4</sub>-saturated solution for 4 days. Five plants were transferred to 1 L pots containing the half-strength nutrient solution without iron. After 3 days seedlings were transferred to a full-strength nutrient solution with +Fe conditions. Ten days past germination, the plants were subjected to +Fe and –Fe conditions for 6 days. Before harvest, roots were transferred to 0.5 mM CaSO<sub>4</sub> for 10 minutes. Apoplast-bound iron was removed from the roots according to the method of Bienfait et al. (1985): CaSO<sub>4</sub> was replaced by a solution containing 0.5 mM

Ca(NO<sub>3</sub>)<sub>2</sub>, 10 mM MES buffer (2-(*N*-morpholino) ethanesulfonic acid) (pH 5.5) and 1.5 mM dipyridin (= 2.2 'bipyridyl). After an exposure of one minute in this solution, Na-dithionate was added to a final concentration of 12.5 mM. This caused a reduction of all accessible Fe(III) precipitates. Fe<sup>2+</sup> was then complexed by dipyridin to form a violet-coloured complex. Before the addition of dipyridin and during the reaction time (10 minutes) the reaction solution was kept free of oxygen by continuous aeration with N<sub>2</sub>. The Fe concentration and iron isotope composition of the Bienfait solutions and that of maize plant organs was then determined.

### Experiment 4: Maize supplied with phytosiderophores from wheat, <sup>58</sup>Fe tracer experiment

The intention of experiment 4 was to find out if iron is retranslocated from older into younger plant parts under Fe-deficiency and under non-deficient conditions. A <sup>58</sup>Fe enriched nutrient solution was used as a tracer and from the binary mixing between <sup>58</sup>Fe enriched iron and unspiked seed Fe it is possible to figure out if iron is retranslocated. Additionally the measured δ<sup>56</sup>Fe values which are not influenced by the spiked iron show what mechanisms play a role during remobilization.

Wheat (*Triticum aestivum*) plants (cv. Thomy) were germinated in quartz sand moistened with a CaSO<sub>4</sub>-saturated solution and 6 days old seedlings (50 per pot) were transferred to 1 L pots containing an iron-free full-strength nutrient solution.

Six days after germination of wheat, maize seeds (cv. UH002) were germinated in the dark between filter papers soaked with a CaSO<sub>4</sub>-saturated solution for 4 days. Five plants were transferred to 1 L pots containing a half-strength iron-free nutrient solution.

From day 8 after maize germination, Fe-starved wheat plants were allowed to exude PS in 1 L freshly prepared iron-free nutrient solution for five hours, starting two hours after the onset of light. The obtained exudates-enriched nutrient solution was enriched with 1 mM Ca(NO<sub>3</sub>)<sub>2</sub>, 0.4 mM K<sub>2</sub>SO<sub>4</sub> and 3 μM <sup>58</sup>Fe labeled FeCl<sub>3</sub> and mixed gently. Five maize plants were directly subjected to 1 L of this solution until the next day. This procedure was repeated for 3 days. Afterwards maize plants were divided into the +Fe and -Fe treatment. However, to neglect allelopathic effects all plants remained exposed to the nutrient solution containing wheat exudates. Therefore, the exudates-enriched nutrient solution was divided before supplementing with FeCl<sub>3</sub>. All plants were harvested 6 days later.



Experiment 5: Plant growth on a soil substrate

The intention of experiment 5 was to resolve the stable iron isotope signature of different parts of maize plants when grown on soil to see if Fe isotope fractionation in strategy II plants depends on the form of iron supply in the growth medium.

Eight seeds of maize (*Zea mays*, cv. UH002) were planted in 3x 5 L pots filled with 4.4 L of a Stagni-Haplic Luvisol ( $\text{pH}_{\text{H}_2\text{O}} = 7.8$ ). Plants grew in a daylight climate chamber with a temperature of 16 – 18 °C and were watered with deionised water whenever required. Plants were harvested at three growth stages. The first harvest took place after 21 days when plants had four fully grown leaves (first pot, the other two remained growing), the second harvest was done after 42 days when plants had six leaves and after 54 days plants were harvested when they had seven fully grown leaves. Eight plants were harvested, respectively, cleaned with deionised water and separated into roots, stem and the different leaves. Roots were cleaned especially careful to remove any adherent soil particles. Plants were dried in an oven for at least 3 days at 80 °C after which their dry weight was determined. Finally the plant parts were ground to mince and homogenize them. The original seeds were subjected to the same procedure.

Table 5-1 Overview experiments

Experiment	Substrate	Addition	Conditions
1	nutrient solution	Fe(III)-EDTA	+Fe, -Fe
2	nutrient solution	Fe(III)-EDTA and FeCl <sub>3</sub> + phytosiderophores from wheat	+Fe, -Fe
3	nutrient solution	Fe(III)-EDTA	+Fe, -Fe
4	nutrient solution	FeCl <sub>3</sub> + phytosiderophores from wheat	+Fe, -Fe
5	soil		+Fe

**5.2.2 Nutrient solution**Environmental conditions for growth experiments

Plant culture experiments were conducted in a climate chamber with 60 % humidity, a light intensity of ~200  $\mu\text{mol photons/m}^2\text{s}$  at plant height, and a 16/8 h (24/20°C) day-night regime.

### Composition of nutrient solution

All plants were grown in an aerated, non-sterile nutrient solution consisting of 2.0 mM  $\text{Ca}(\text{NO}_3)_2$ , 0.7 mM  $\text{K}_2\text{SO}_4$ , 0.5 mM  $\text{MgSO}_4$ , 0.1 mM  $\text{KCl}$ , 0.1 mM  $\text{KH}_2\text{PO}_4$ , 0.5  $\mu\text{M}$   $\text{MnSO}_4$ , 0.5  $\mu\text{M}$   $\text{ZnSO}_4$ , 0.2  $\mu\text{M}$   $\text{CuSO}_4$ , 0.01  $\mu\text{M}$   $(\text{NH}_4)_6\text{Mo}_7\text{O}_{24}$ , and 1  $\mu\text{M}$   $\text{H}_3\text{BO}_3$ . If not stated otherwise Fe-sufficient (+Fe) treatments were supplemented with 100  $\mu\text{M}$  Fe(III)-EDTA and the nutrient solution was changed every 2-3 days. In experiment 1, 3 and 4 apoplastic iron was removed according to Bienfait et al. (1985).

### Preparation of the nutrient solution for $^{58}\text{Fe}$ tracer experiment (experiment 4)

For the  $^{58}\text{Fe}$  tracer experiment, 10 mg of  $^{58}\text{Fe}$  enriched metal pieces were purchased (*Chemotrade*, 92.8 % isotopic enrichment, Ref: Certificate of analysis, No. 26-01-58-3197, isotopic distribution:  $^{54}\text{Fe}$ : 0.05 %,  $^{56}\text{Fe}$ : 0.55 %,  $^{57}\text{Fe}$ : 6.6 %,  $^{58}\text{Fe}$ : 92.8 %), and completely dissolved in 6 M HCl. The resulting solution was diluted to a concentration of 570 ppm Fe.

As the preparation of the nutrient solution required 52.65 mg  $\text{FeCl}_3$  and 0.16 % of the contained iron in the nutrient solution should be  $^{58}\text{Fe}$  to assure that the obtained  $\delta^{58}\text{Fe}$  was high enough to detect binary mixing between spiked and unspiked iron ( $\delta^{58}\text{Fe}$  about 450 ‰) and the  $\delta^{56}\text{Fe}$  of the nutrient solution was not influenced, 0.033 ml spiked Fe solution (equalling 18.8  $\mu\text{g}$  Fe) was given to 0.053 g  $\text{FeCl}_3$  dissolved in 3.9 mL concentrated HCl and the solution was shaken to homogenize.

### **5.2.3 SPAD value**

In experiment 1 and 2 the SPAD value was determined after harvest. The SPAD value determines the relative chlorophyll content by measuring the absorbance of the leaf in two wavelength regions. Chlorophyll has absorbance peaks at 400-500 nm and 600-700 nm with no transmittance in the near-infrared region. Using these two transmittances a SPAD-meter calculates a numerical SPAD value which is proportional to the amount of chlorophyll present in the leaf. This amount is closely related to the nutritional status of the plant. When plants suffer from iron-deficiency the chlorophyll synthesis is affected and therefore the SPAD value decreases.

## 5.2.4 Sample decomposition and iron separation

All sample preparation and iron chromatographic separation were carried out following the procedures described in chapters 2 to 4. Separate equipment was used for samples in the  $^{58}\text{Fe}$  tracer experiment (experiment 4) to avoid contamination. Total procedural iron blanks were measured yielding about 50 ng. This was less than 1 % of the processed Fe and was considered to be insignificant.

## 5.2.5 Iron isotope measurements

The iron isotope compositions of the Fe(III)-EDTA and  $\text{FeCl}_3$  solutions and the different plant parts were determined with the use of a multiple-collector inductively coupled plasma mass spectrometer (MC-ICP-MS; Neptune, *ThermoFinnigan*) following the methods described in chapter 4.

The natural iron isotope ratios determined in this study are expressed relative to the IRMM-014 standard (Institute of Reference Material and Measurement, Geel, Belgium), of which the isotopic composition is close to that of rocks at the Earth's surface (Schoenberg and von Blanckenburg, 2006, and others), as:

$$\delta^{56}\text{Fe}/[\text{‰}] = \left[ \left( \frac{{}^{56/54}\text{Fe}_{\text{sample}}}{{}^{56/54}\text{Fe}_{\text{IRMM-014}}} \right) - 1 \right] \cdot 10^3 \quad 5.1$$

Similarly, results from the  $^{58}\text{Fe}$  tracer experiment are also expressed in permil deviation from the natural ratios as  $\delta^{58}\text{Fe}$ :

$$\delta^{58}\text{Fe}/[\text{‰}] = \left[ \left( \frac{{}^{58/54}\text{Fe}_{\text{sample}}}{{}^{58/54}\text{Fe}_{\text{IRMM-014}}} \right) - 1 \right] \cdot 10^3 \quad 5.2$$

The isotopic difference between plant organs and the nutrient solution or soil are expressed as  $\Delta^{56}\text{Fe}_{\text{plant-nutrient solution}} = \delta^{56}\text{Fe}_{\text{plant}} - \delta^{56}\text{Fe}_{\text{nutrient solution}}$  5.3

or the equivalent equation with  $^{58}\text{Fe}$ . But it has to be born in mind that while  $\delta^{56}\text{Fe}$  describes mass-dependent stable isotope fractionation,  $\delta^{58}\text{Fe}$  quantifies the contribution of the added tracer  $^{58}\text{Fe}$  relative to the natural  $^{56}\text{Fe}$ . Because the amounts of  $^{58}\text{Fe}$  added to the nutrient solution increased the natural amount of  $^{58}\text{Fe}$  by 450 ‰, the small mass-dependent shift in the  $^{58}\text{Fe}/^{54}\text{Fe}$  ratio that accompanies the reactions are negligible and can be ignored.

Within each analytical session the internal laboratory standard JM (Johnson & Matthey, Fe Puratronic wire) was measured to test the accuracy of the measurements. During the course of this study the measured Fe isotope composition of the JM standard was  $\delta^{56}\text{Fe} = 0.431 \pm$

0.046 ‰,  $\delta^{57}\text{Fe} = 0.633 \pm 0.079$  ‰ and  $\delta^{58}\text{Fe} = 0.88 \pm 0.38$  ‰ ( $2\sigma$ ,  $n = 209$ ), which agrees with previous measurements ( $\delta^{56}\text{Fe} = 0.423 \pm 0.046$  ‰,  $\delta^{57}\text{Fe} = 0.624 \pm 0.073$  ‰ and  $\delta^{58}\text{Fe} = 0.83 \pm 0.41$  ‰) given by Schoenberg and von Blanckenburg (2005).

The reproducibility of replicate measurements and chemical replicates of the samples processed in this study was determined according to Schoenberg and von Blanckenburg (2005). It was found to be 0.11 ‰ ( $2\sigma$ ;  $n=6$ ) for the  $\delta^{56}\text{Fe}$  of chemical replicates and 0.07 ‰ for replicate measurements ( $2\sigma$ ;  $n=220$ ). For the  $\delta^{58}\text{Fe}$  it was found to be 0.40 ‰ ( $2\sigma$ ,  $n=14$ ) for replicate measurements. These values are slightly inferior to that obtained by Schoenberg and von Blanckenburg (2005).

## 5.3 Results

### 5.3.1 Experiment 1: Maize sequential harvest

The relative chlorophyll content in the different maize leaves, illustrated by the SPAD value, is displayed in Figure 5.2. Plants grown under iron-deficient conditions (–Fe plants) had lower SPAD values in the younger leaves than +Fe plants.

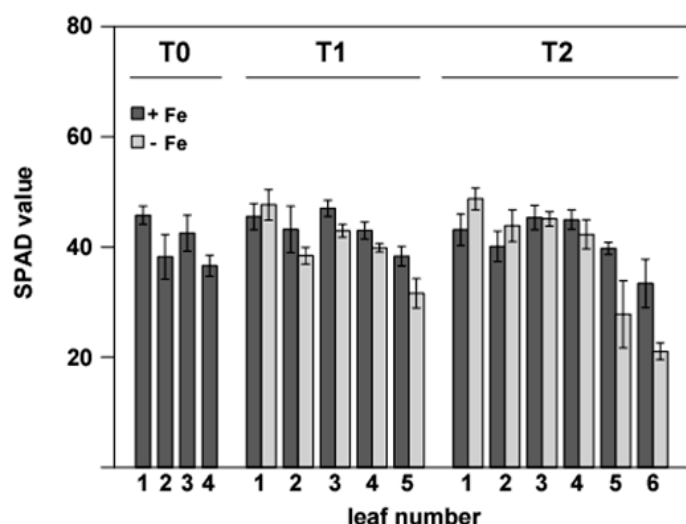


Figure 5.2 Relative chlorophyll content of the maize leaves of experiment 1.

All +Fe plant parts had iron concentrations expected for green plant parts (Table 5-2). Roots and younger leaves of –Fe plants obtained less than 50 ppm iron, which was beyond the

minimum supply and denoted Fe deficiency in the maize plants (Marschner, 1995). The dry mass of the –Fe plants’ roots was lower than that of the +Fe plants at the same harvest point.

All parts of the maize plants were enriched in the lighter iron isotopes compared to the Fe(III)-EDTA of up to 2.3 ‰ (Figure 5.3, Table 5-2). Iron in leaf 1 (the cotyledon) was 0.4 to 0.7 ‰ heavier than the roots, this isotopic difference increased during growth. Iron became increasingly lighter from the oldest to the youngest leaf. This trend is visible at every harvest point regardless of the iron status. However, the +Fe plants obtained lighter iron than the –Fe plants. The reproducibility between the different pots was poor. Because stems were not harvested the calculation of the plant’s total iron isotope composition from mass balance was not possible. However, the complete iron isotope composition  $\Delta^{56}\text{Fe}_{\text{plant-nutrient solution}}$  without apoplastic roots iron and stems of maize plants accounted to –0.9 ‰ for T 0, –1.2 ‰ for T1 (+Fe), –1 ‰ for T1 (–Fe), –1.4 ‰ for T2 (+Fe) and –0.9 ‰ for T2 (–Fe) (horizontal bars in Figure 5.3).

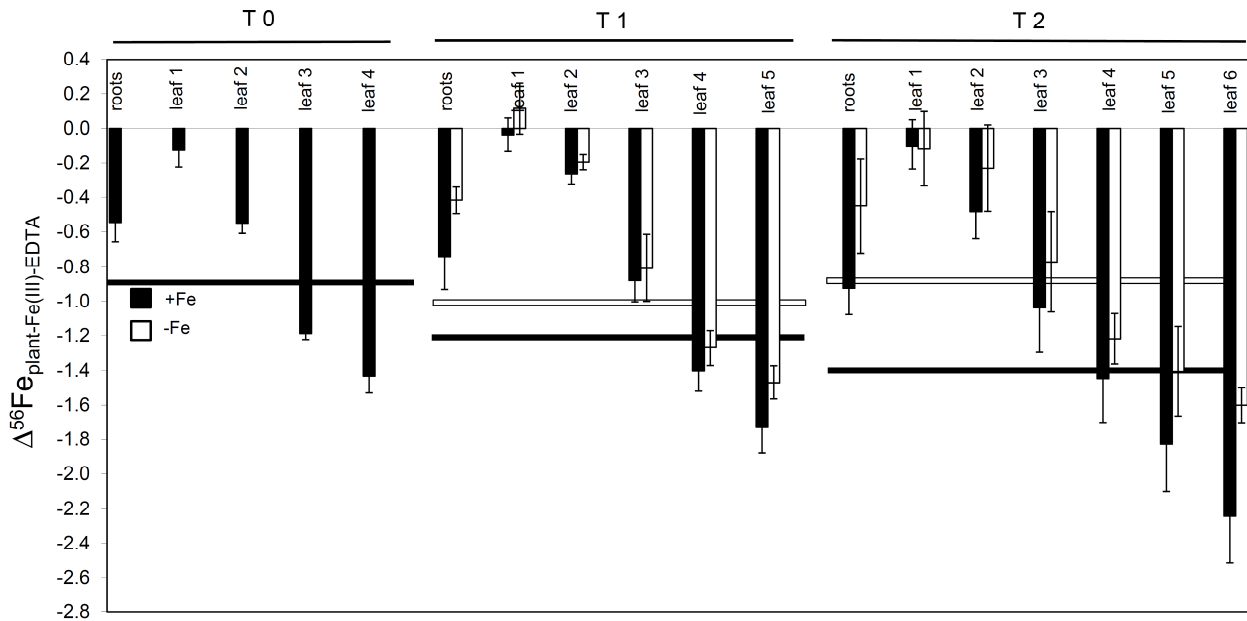


Figure 5.3 Mean  $\Delta^{56}\text{Fe}_{\text{plant-nutrient solution}}$  of four pots of experiment 1. Horizontal lines: composition of the complete plant without apoplastic iron and stems. Error bars denote the standard reproducibility of the mean of four pots.

### 5.3.2 Experiment 2: Maize supplied with phytosiderophores from wheat

In the younger leaves 3 and 4 the SPAD value, representing the chlorophyll content, was lower in the –Fe plants than in the +Fe plants grown on both types of nutrient media. This effect was more pronounced in the plants grown on Fe(III)-EDTA, however (Figure 5.4).

Organs of –Fe plants showed similar dry weights than those of +Fe plants grown in both types of nutrient media, but plants grown on FeCl<sub>3</sub>-PS obtained higher dry masses than plants grown on Fe(III)-EDTA (Table 5-3). Iron concentrations were higher in the +Fe plants than in the –Fe plants and lower in plants grown on FeCl<sub>3</sub>-PS than in plants grown on Fe(III)-EDTA. The iron content of roots was higher in plants grown on FeCl<sub>3</sub>-PS whereas the iron content of the leaves was higher in plants grown on Fe(III)-EDTA.

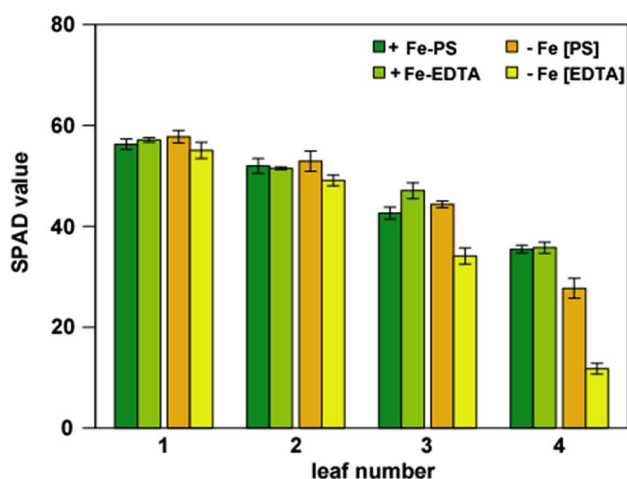


Figure 5.4 Relative chlorophyll content of the maize leaves of experiment 2.

The  $\Delta^{56}\text{Fe}_{\text{plant-nutrient solution}}$  values are illustrated in Figure 5.5. The horizontal lines represent the iron isotopic composition of complete plants including apoplastic iron. Iron in total plants grown on FeCl<sub>3</sub>-PS was unfractionated compared to that of the nutrient solution, regardless of the iron status of the plants. In contrast, plants grown on Fe(III)-EDTA were enriched in the lighter iron isotopes compared to the nutrient solution by –0.5 ‰ (+Fe plants) and by –0.2 ‰ (–Fe plants).

In the FeCl<sub>3</sub>-fed plants iron evolved towards increasingly lighter compositions during growth. Roots of +Fe plants were enriched in the heavier iron isotopes by 0.3 ‰ compared to the nutrient solution; leaf 1 had a similar iron isotope composition as the nutrient solution and the stem and leaves 2 to 4 were enriched in the lighter iron isotopes compared to the nutrient

solution. Under iron-deficient conditions all leaves and the stem obtained heavier iron than those of +Fe plants. Roots of +Fe and –Fe plants obtained identical iron isotope compositions. The Fe(III)-EDTA fed plants showed similar iron isotope patterns as in experiment 1, iron in leaves became increasingly lighter during growth and +Fe plants obtained lighter iron than –Fe plants. The values of the plants grown in the different pots did not reproduce exactly and therefore the standard deviation was very high. However, it can be recognized that in contrast to the first experiment the  $\delta^{56}\text{Fe}$  of leaf 1 was lower as that of roots, regardless of the iron status.

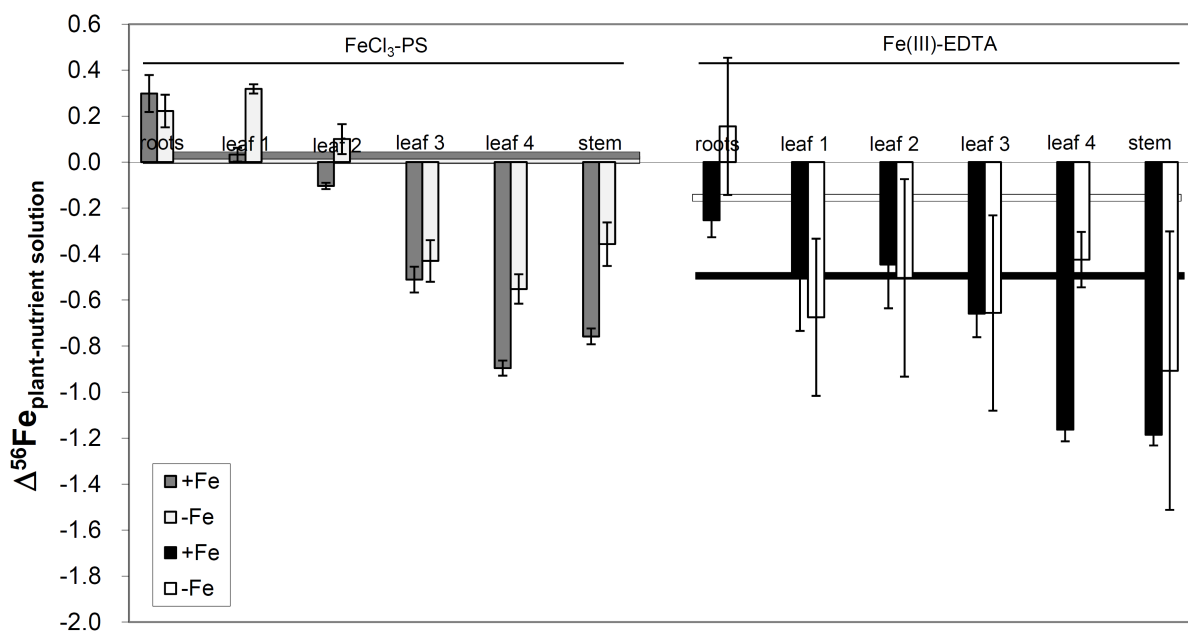


Figure 5.5 Mean  $\Delta^{56}\text{Fe}_{\text{plant-nutrient solution}}$  of four pots of experiment 2. Horizontal lines: composition of the complete plants. Error bars denote the standard reproducibility of the mean of four pots.

### 5.3.3 Experiment 3: Maize plants for Bienfait solution (Fe(III)-EDTA)

In the third experiment apoplastic iron was removed from roots according to Bienfait et al. (1985) and the iron concentrations and  $\delta^{56}\text{Fe}$  values were determined in the roots (containing symplastic iron) and in the Bienfait solutions (containing apoplastic iron). The Bienfait solutions of +Fe plants contained 700 ppm iron, those of –Fe plants contained 210 ppm iron (Table 5-4). Roots had an iron concentration of about 150 ppm when grown under iron sufficient conditions and of only 40 ppm when grown under iron-deficient conditions. Leaves and stem of +Fe plants yielded iron concentrations expected for green plant parts (Marschner,

1995) with 90-190 ppm. Leaf 1 had the highest iron concentration with 189 in pot 1 and 154 ppm in pot 2. The -Fe plants, however, yielded lower iron concentrations which were mostly less than 50 ppm, which was beyond the minimum supply and denoted Fe deficiency in the maize plants (Marschner, 1995). Only leaf 1 had higher Fe concentrations with 73 and 83 ppm.

The  $\Delta^{56}\text{Fe}_{\text{plant-nutrient solution}}$  values of all parts of the maize plants are illustrated in Figure 5.6. Mass balance shows that iron of complete +Fe maize plants was 0.6 ‰ lighter than the iron in the Fe(III)-EDTA and that of -Fe plants was only 0.1 ‰ lighter than Fe(III)-EDTA (Table 5-4, horizontal bars in Figure 5.6). Iron of the Bienfait solutions of +Fe plants was 0.6 ‰ lighter than that of the Fe(III)-EDTA and apoplastic and symplastic roots' iron obtained similar iron isotope compositions. Iron of the Bienfait solutions of -Fe plants was 0.2 ‰ heavier than that of Fe(III)-EDTA. Again, symplastic roots' iron showed similar values as the apoplastic iron.  $\Delta^{56}\text{Fe}$  values of the Bienfait solutions and root samples differed substantially between the two pots. Leaf 1 was virtually unfractionated compared to the nutrient solution and during growth iron of the subsequent leaves and the stem became increasingly lighter. The youngest leaf 4/5 incorporated iron which was 1.2 ‰ lighter than the Fe(III)-EDTA. Leaves 1 and 2 of -Fe plants obtained lighter iron than in the +Fe plants, whereas iron of leaves 3 and 4 as well as that of the stem was heavier in -Fe plants.

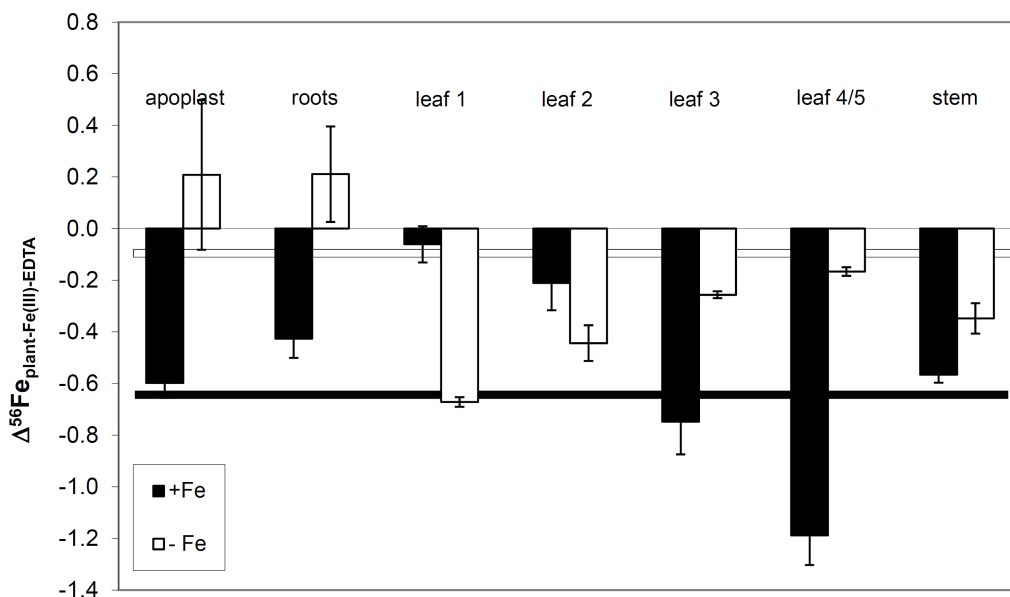


Figure 5.6 Mean  $\Delta^{56}\text{Fe}_{\text{plant-nutrient solution}}$  of two pots of experiment 3. Horizontal lines: composition of the complete plants. Error bars denote the standard reproducibility of the mean of two pots.



### 5.3.4 Experiment 4: Maize supplied with phytosiderophores from wheat, $^{58}\text{Fe}$ tracer experiment

Organs of  $-Fe$  plants obtained similar dry weights as that of  $+Fe$  plants, but iron concentrations and iron contents were higher in the  $+Fe$  plants than in the  $-Fe$  plants (Table 5-5). As the younger leaves of the  $-Fe$  plants contained more than 50 ppm iron, iron deficiency can be excluded. The iron concentration of  $+Fe$  plant roots was 309 and 356 ppm, which was higher as that of leaves as apoplastic iron was not removed.

Mass balance calculations revealed that iron of complete maize plants grown under Fe-sufficient conditions was unfractionated compared to that of the nutrient solution (Figure 5.7). Within the  $+Fe$  plants the distribution of iron isotopes was not uniform. Roots yielded the same  $\delta^{56}\text{Fe}$  as the nutrient solution whereas leaves 1, 2 and 3 were enriched in the heavier iron isotopes with a  $\Delta^{56}\text{Fe}$  of 0.48, 0.39 and 0.18 ‰, respectively. The stem and leaves 4 and 5 obtained lighter iron than the nutrient solution ( $\Delta^{56}\text{Fe}$  of  $-0.18$  ‰ for stem,  $-0.17$  ‰ for leaf 4 and  $-0.37$  ‰ for leaf 5) (Table 5-5).

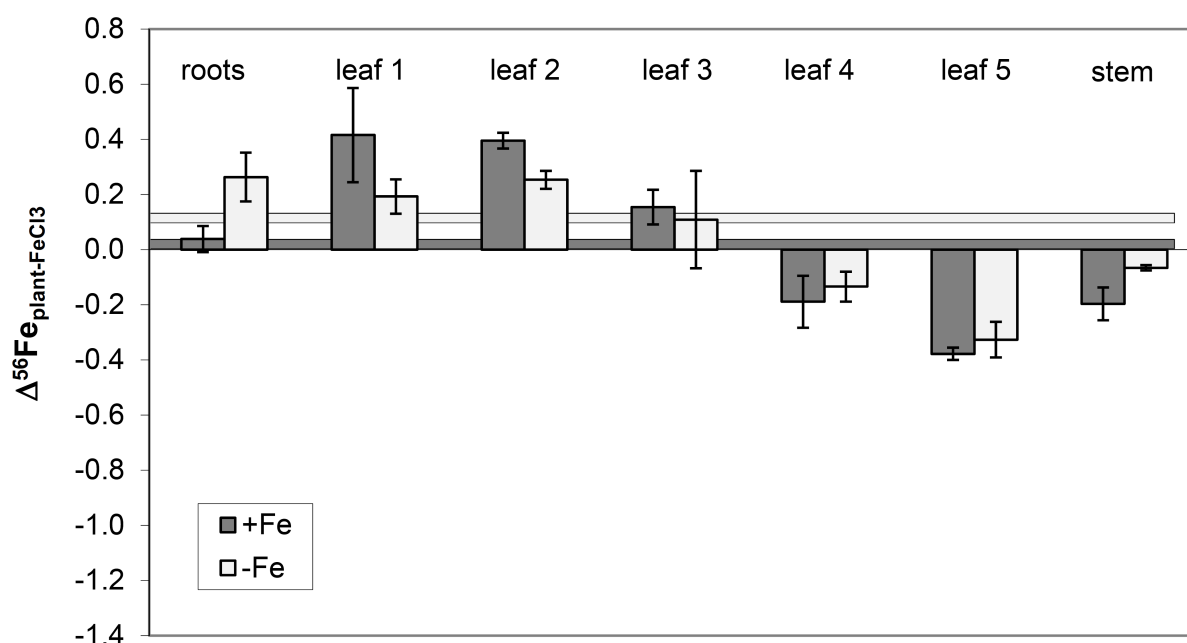


Figure 5.7 Mean  $\Delta^{56}\text{Fe}_{\text{plant-nutrient solution}}$  of two pots. Horizontal lines: composition of the complete plants. Error bars denote the standard reproducibility of the mean of two pots.

Complete maize plants grown under Fe-deficient conditions were only slightly enriched in the heavier iron isotopes compared to the nutrient solution with  $+0.1$  ‰. Iron of the roots and of

the first three leaves was heavier than the nutrient solution by 0.25, 0.21, 0.26 and 0.11 ‰, whereas leaves 4 and 5 and the stem obtained lighter iron than the nutrient solution ( $\Delta^{56}\text{Fe}$  of  $-0.06$  ‰ for stem,  $-0.12$  ‰ for leaf 4 and  $-0.30$  ‰ for leaf 5). The trend for the  $\Delta^{56}\text{Fe}$  was identical between  $-Fe$  and  $+Fe$  plants. However, the isotopic difference to the nutrient solution was larger in  $+Fe$  plants.

In addition to the  $\Delta^{56}\text{Fe}$  values the  $\Delta^{58}\text{Fe}$  values were determined as well. The nutrient solution spiked with  $^{58}\text{Fe}$  yielded a  $\delta^{58}\text{Fe}$  of 458.4 ‰ (Table 5-5). Mass balance calculations showed that iron of complete  $+Fe$  plants was depleted by about 30 ‰ and that of  $-Fe$  plants was depleted by about 100 ‰ compared to the nutrient solution. This depletion reveals that there was unspiked iron in all parts of the plants (Figure 5.8).

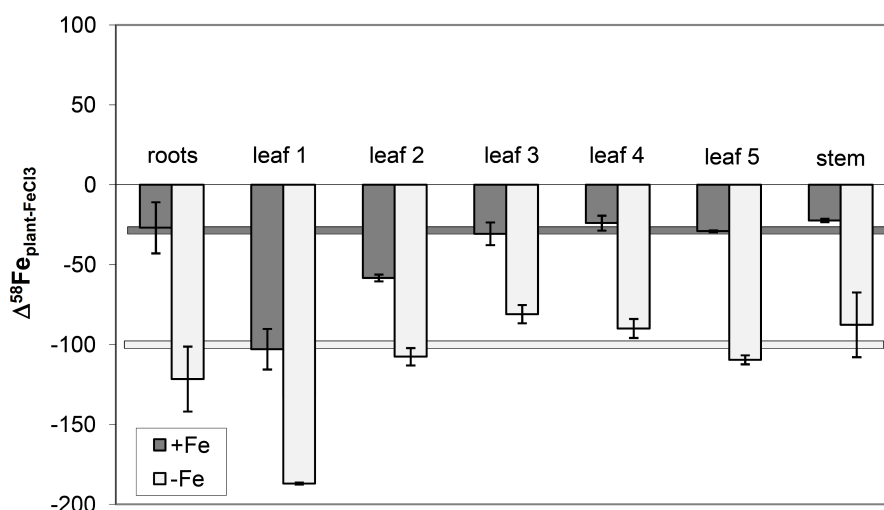


Figure 5.8 Mean  $\Delta^{58}\text{Fe}_{\text{plant-nutrient solution}}$  of two pots of experiment 4. Horizontal lines: composition of the complete plants. Error bars denote the standard reproducibility of the mean of two pots.

This unspiked iron can merely result from seed iron as the plants only obtained a nutrient solution enriched in  $^{58}\text{Fe}$ . This explanation is supported by the following calculation: maize seeds contained 23  $\mu\text{g/g}$  iron with a  $\delta^{56}\text{Fe}$  of  $-0.14$  ‰ (Table 5-2) which results in a natural  $\delta^{58}\text{Fe}$  of approximately  $-0.28$  ‰, as iron isotope fractionation is mass-dependent. Maize seeds had a weight of 200 mg which results in an iron content of 4.6  $\mu\text{g}$ . As five maize seeds were grown in one pot, the sum of iron from all plant organs in one pot contained 23  $\mu\text{g}$  seed iron. The total iron content of the plants in the pot 1 was 403  $\mu\text{g}$  for  $+Fe$  plants and 114  $\mu\text{g}$  for  $-Fe$  plants (sum of the iron content of all plant organs given in Table 5-5). The total iron content of

the plants in pot 2 was 420  $\mu\text{g}$  for +Fe plants and 96  $\mu\text{g}$  for –Fe plants. Given that 23  $\mu\text{g}$  of this total iron is sourced in the seeds, 380  $\mu\text{g}$  iron in +Fe plants of pot 1 was derived from the spiked nutrient solution (94.3 %). In –Fe plants 91  $\mu\text{g}$  iron was derived from the spiked nutrient solution (79.8 %). In +Fe plants of pot 2 397  $\mu\text{g}$  iron was derived from the spiked nutrient solution (94.5 %). In –Fe plants 73  $\mu\text{g}$  iron was derived from the spiked nutrient solution (76.0 %). With binary mixing it is now possible to calculate the  $\delta^{58}\text{Fe}_{\text{total plant}}$  with  $f$  being the fraction of seed iron and iron from nutrient solution, respectively and  $\delta^{58}\text{Fe}$  their respective isotopic composition:

$$\delta^{58}\text{Fe}_{\text{total plant}} = f \cdot \delta^{58}\text{Fe}_{\text{seed}} + (1-f) \cdot \delta^{58}\text{Fe}_{\text{nutrient solution}} \quad 5.4$$

This results in a  $\delta^{58}\text{Fe}_{\text{total plant}}$  for pot 1, +Fe plants of 432.26 ‰ (measured: 430.22 ‰; Table 5-5), for –Fe plants 365.74 ‰ (measured: 352.87 ‰; Table 5-5) and for pot 2, +Fe plants of 433.17 ‰ (measured: 424.92 ‰; Table 5-5) and for –Fe plants 348.22 ‰ (measured: 355.26 ‰; Table 5-5). The deviations of the calculated values from the measured values might result from uncertainties from iron concentrations and dry weights of seeds, and propagated errors of  $\delta^{58}\text{Fe}$  of the different plant organs.

With mass balance (equation 5.4) it is possible to calculate the fraction of seed Fe in every plant organ of the maize plants (Figure 5.9).

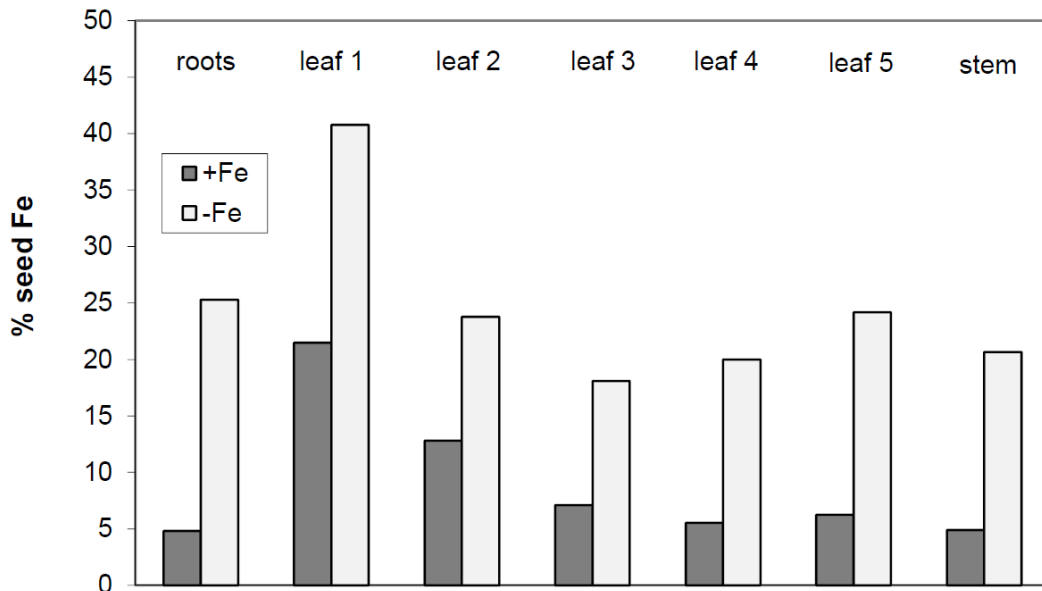


Figure 5.9 Mean fraction of seed Fe in the different plant organs of maize plants of experiment 4 in %.

It can be recognized that +Fe plants contain a less percentage of seed Fe as –Fe plants. Roots and leaves 3-5 as well as the stem of +Fe plants contain around 5 % seed Fe, whereas leaf 1 contains more than 20 % and leaf 2 about 13 % seed Fe.

Roots and leaf 2-5 as well as the stem of –Fe plants contain between 20-25 % seed Fe, leaf 1 holds more than 40 %.

### 5.3.5 Experiment 5: Maize grown on a soil substrate

Roots of maize plants grown on the soil substrate showed very high iron concentrations at all three points of harvest. This might be due to a high apoplastic iron pool. All plant organs at the first and second point of harvest yielded iron concentrations typical for green plant parts (Marschner, 1995); however, at the third point of harvest the stem and leaves 2 to 6 showed a decrease in the iron concentration whereas the first leaf contained nearly 300  $\mu\text{g/g}$  more iron than at the first and second harvest point (Table 5-6).

In chapter 3 the isotopic composition  $\delta^{56}\text{Fe}$  of the iron which is most likely to be available for plant nutrition in the Stagni-Haplic Luvisol soil substrate where maize plants grew on, was shown to be  $-0.27\text{‰}$ . As the same number of plants as well as all organs of the plants were harvested in all experiments, it was possible to calculate the iron content of the different plant parts as basis of a mass balance. This shows that complete plants obtained the same iron isotope composition within the 2 standard deviation at the three times of harvest with a  $\delta^{56}\text{Fe}$  of  $-0.05$ ,  $-0.03$  and  $-0.01\text{‰}$ , respectively (Figure 5.10). Therefore the  $\Delta^{56}\text{Fe}_{\text{plant-soil}}$  for complete maize plants was reproduced with approximately  $0.25\text{‰}$  at all three points of harvest.

The obtained  $\delta^{56}\text{Fe}$  values of the different organs of the maize plants covered a small range of about  $0.5\text{‰}$ . Original seeds showed a slight enrichment of the light iron isotopes compared to IRMM-014 (Table 5-6).

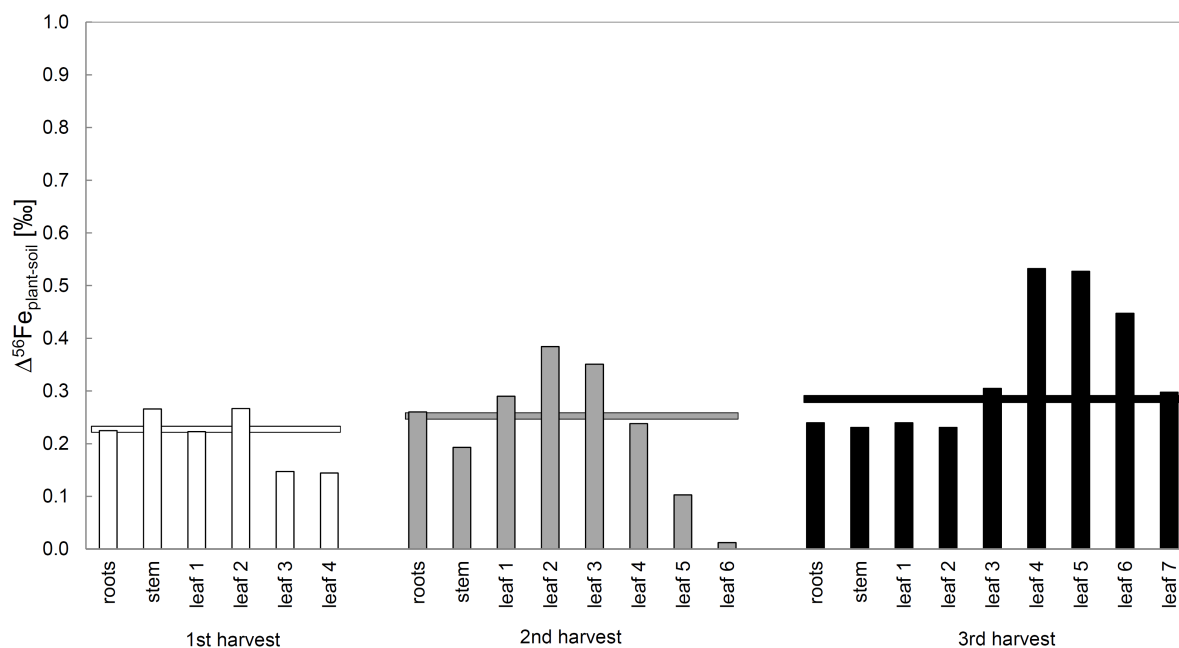


Figure 5.10  $\Delta^{56}\text{Fe}_{\text{plant-soil}}$  of maize plant parts of experiment 5. Horizontal lines:  $\Delta^{56}\text{Fe}$  of total plant. The 2 standard deviation of replicate measurements amounts to 0.07 ‰ in  $\delta^{56}\text{Fe}$ .

The  $\Delta^{56}\text{Fe}_{\text{plant-soil}}$  values for the maize plants are illustrated in Figure 5.10. It can clearly be seen that during growth younger leaves were enriched in the heavier iron isotopes. Within 2 standard deviations (see section 5.2.5) roots and stems had the identical iron isotope composition at all three points of harvest. In contrast iron of leaves 1 and 2 evolved towards heavier compositions from the first to the second, but to lighter compositions from the second to the third harvest point. In parallel the  $\Delta^{56}\text{Fe}$  values increased in leaves 3 and 4 from the first to the third harvest point whereas in the new grown leaves 5 and 6 at the second harvest point the  $\Delta^{56}\text{Fe}$  value was lower than in all leaves harvested earlier. Again, these leaves also became increasingly enriched in the heavier iron isotopes by up to 0.45 ‰ from the second to the third harvest point. The new grown seventh leaf at the third harvest point contained iron that was enriched in the heavy isotopes by 0.3 ‰ compared to the plant-available soil iron.

## 5.4 Discussion

### 5.4.1 Isotope fractionation during acquisition of iron

The SPAD value as well as the iron concentrations of maize in the **first experiment** (maize sequentially harvested when grown on the Fe(III)-EDTA –supplemented nutrient solution) of this study provided evidence that plants suffered from iron deficiency. The complete iron isotope composition  $\Delta^{56}\text{Fe}_{\text{plant-nutrient solution}}$  (without apoplastic iron in roots and iron in stems) of these maize plants revealed an enrichment in the lighter iron isotopes compared to the Fe(III)-EDTA at all growth stages. This finding points at a fractionation favouring the lighter iron isotopes which occurs during acquisition of iron by maize plants. A similar finding was reported in chapter 4 for oat grown on a Fe(III)-EDTA-supplemented nutrient solution. Under non-limiting iron supplies, iron uptake of all plants is mediated via a constitutive acquisition system that consists of a membrane-bound ferric reductase which is linked to a divalent metal ion transporter and an ATP-driven proton extrusion pump. This is similar to the “strategy I” iron acquisition of plants but cannot be upregulated under iron-stress. Hence maize plants of experiment 1 probably enzymatically reduced iron of Fe(III)-EDTA but almost certainly this ferrous iron could not be quantitatively taken up by the membrane ion transporter. The reduction of iron has been shown to fractionate iron isotopes if it is not quantitative, favouring the lighter iron isotopes in the ferrous species (e.g. Welch et al., 2003; Anbar et al., 2005; Crosby et al., 2007). Probably the residual ferrous iron in the apoplast was oxidized and precipitated as  $\text{Fe}(\text{OH})_3$  or  $\text{FePO}_4$ . This precipitation is likely to be quantitative and therefore caused no additional fractionation. Thus, the apoplastic iron pool was enriched in the light iron isotopes. In addition maize exuded phytosiderophores which could bind precipitated Fe(III) in the apoplast. This chelation process favours the heavier iron isotopes as has been shown by Dideriksen et al. (2008) or Brantley et al. (2004). PS can compete with EDTA for iron as ligands and chelates can be exchanged, the direction of the reaction is determined by the stability constant of the respective complexes. Siderophores form multi-dentate and very stable complexes with dissolved Fe(III), with stability constants up to  $\sim 10^{50}$  (Hider, 1984). Fe(III)-EDTA has a stability constant of  $\sim 10^{25}$ . As the heavier iron isotopes are favoured by the complex with the strongest bonds (Urey, 1947, Schauble, 2004), Fe(III)-PS is expected to obtain a heavier iron isotope composition than the Fe(III)-EDTA or precipitated iron. Fe(III)-PS could be taken up easily by YS1-type membrane transporters that mediate root uptake by the cotransport of metal-phytosiderophores with protons (Curie et al., 2001; Schaaf et al.,

2004). As the Fe(III)-PS complex as a whole is too large to cause any detectable fractionation (relative mass differences are too small), the Fe(III)-PS membrane transport process should not result in any further fractionation. Thus a binary mixing occurred in the maize plants, with iron being taken up by the reductive pathway (light Fe) and as Fe(III)-PS (heavy Fe).

As iron of complete +Fe plants of experiment 1 became increasingly light during growth (Figure 5.3), it is obvious that the apoplast was not depleted in light iron isotopes. This is due to the exchange of the nutrient solution every two days. Thus a very light iron pool could have been developed. In contrast, under iron-deficiency, plants accelerate their specific iron acquisition strategies; hence strategy II plants exuded a larger amount of phytosiderophores into the nutrient solution. As no new iron diffused into the apoplast, the apoplastic light iron pool was depleted, as precipitated Fe(III) was bound to PS. Therefore iron of -Fe plants became increasingly enriched in the heavier iron isotopes from the second to the third point of harvest.

In the **second experiment** (maize supplied with phytosiderophores from wheat 1) the SPAD value revealed that -Fe plants suffered from iron deficiency. Wheat phytosiderophores complexed Fe(III) from FeCl<sub>3</sub> which resulted in the absence of fractionation as complexation was quantitative. During uptake of Fe(III)-PS into the maize plants no isotope fractionation is assumed as the complex is too large to cause any detectable mass-dependant isotope fractionation. FeCl<sub>3</sub>-PS is an efficient form of Fe supply as the Fe(III)-PS complex can be easily taken up.

In contrast, plants grown on Fe(III)-EDTA were enriched in the lighter iron isotopes compared to the nutrient solution which was more distinct in +Fe than in -Fe plants and similar to the enrichment of light isotopes in maize plants of experiment 1. As explained in the context of experiment 1 this might be due to a larger fraction of enzymatically reduced iron.

The similarity of the  $\delta^{56}\text{Fe}$  values obtained for the Bienfait solutions and roots of maize of the **third experiment** (maize plants for Bienfait solution (Fe(III)-EDTA) demonstrates that iron isotope fractionation has to occur before membrane transport, supporting the hypothesis of a preferential enzymatically reduction of light iron isotopes in the apoplast and the development of a light apoplastic Fe pool. As remaining Fe(III)-EDTA in the apoplast was probably washed out during cleaning of roots, only the isotope composition of that iron which was reduced once and then precipitated in the apoplast was measured. Complete +Fe plants were enriched

in the light iron isotopes, similar to that of experiment 1 and 2 (plants fed with Fe(III)-EDTA supplemented nutrient solution). Under iron-deficient conditions no new iron diffused into the apoplast, therefore the apoplastic iron pool was likely to be depleted in the light isotopes (Rayleigh fractionation model) during remobilization of iron.

Mass balance calculations with  $\delta^{56}\text{Fe}$  values revealed that iron of complete maize plants grown under Fe-sufficient and deficient conditions in **experiment 4** (maize supplied with phytosiderophores from wheat,  $^{58}\text{Fe}$  tracer experiment) was unfractionated compared to that of the FeCl<sub>3</sub>-PS nutrient solution. This is similar to the finding in experiment 2. Therefore it is concluded that uptake of iron in the presence of phytosiderophores does not lead to isotope fractionation.

Complete maize plants grown on soil (**experiment 5**) were enriched in the heavier iron isotopes. These plants probably had to exude more phytosiderophores as plants grown on Fe(III)-EDTA, as the constitutive acquisition system was not sufficient to avoid iron deficiency. Exuded phytosiderophores complexed the Fe(III) from the rhizosphere which was bound there to poorly-crystalline iron oxyhydroxides or to organic complexes. This binding could have resulted in an enrichment of the heavier iron isotopes as shown in chapter 3 of this thesis, and the Fe(III)-PS complex enriched in the heavy iron isotopes, was transported into the plant.

It can be concluded that the direction and extent of iron isotope fractionation during acquisition of iron in maize plants depends on the form of iron supply and therefore on iron availability.

### **5.4.2 Isotope fractionation during (re-)translocation of iron**

In all experiments it was observed that stable iron isotopes distributed unequally between the different organs of maize plants indicating that (re-)translocation of iron in maize leads to iron isotope fractionation.

It has been proposed that reduction causes the uptake of light iron in the roots of maize plants grown on the Fe(III)-EDTA-supplied nutrient solution and that chelation to phytosiderophores in the rhizosphere of maize plants grown on soil favours the heavier iron isotopes (see 5.4.1).

Ferrous iron which has been taken up by the root cells of maize plants grown on the Fe(III)-EDTA-supplied nutrient solution (experiments 1,2 and 3) had to be chelated by nicotianamine



(NA) in the root cells. As NA can chelate both, Fe(II) and Fe(III) (von Wirén et al., 1999), it is likely that iron was present as Fe(II)-NA in the root cells when it was taken up via the reductive pathway. For transport in the xylem to other plant tissues iron had to be oxidized before it was bound to citrate (Tiffin, 1966) to be transported in the xylem as a Fe(III)-citrate complex. If this oxidation was not quantitative iron isotope fractionation could occur, favouring the heavier iron isotopes in the ferric species. It has been stated recently that older leaves receive their iron from the xylem whereas younger leaves receive their iron from the phloem (Morrissey and Guerinot, 2009). This finding could explain why the first leaf of maize plants of experiments 1 and 3 obtained heavier iron than the respective roots. However, iron of the first leaf of experiment 4 was also heavier than the roots although iron has been taken up as Fe(III)-PS and it is therefore proposed that iron stayed in the ferric form and only changed its ligands (Hell and Stephan, 2003). However, currently no consensus exists on the fate of the imported Fe(III)-PS complex in strategy II plants. Fe(III) might just be chelated by NA as a default mechanism until it is channelled into further transport, storage sites or functional target molecules (Hell and Stephan, 2003). When chelate exchange for the transport in the xylem takes place it is likely that iron isotope fractionation occurs, favouring the heavier iron isotopes in the complex with the stronger bonds. If Fe(III)-citrate has a higher stability constant as Fe(III)-NA an enrichment of the heavier iron isotopes in the xylem could have occurred which were then transported into the first leaf. As it has been shown that iron is transported as Fe<sup>2+</sup> into the cells vacuole and is stored probably as Fe(III)-complexes (Kim et al., 2006), it can be assumed that the mobilization of iron involves a reduction step and can therefore result in isotope fractionation favouring a relative accumulation of lighter iron isotopes in the soluble iron pool. This would explain the depletion in lighter iron isotopes during growth, as light iron isotopes from storage molecules in vacuoles or plastids were likely to be transported preferentially into younger plant parts, probably involving an initial reduction step. Similar scenarios have been proposed for iron translocation in strategy I plants in chapter 4 of this thesis. This negates the hypothesis of different translocation mechanisms in strategy I and II plants (chapter 2 and 4 of this thesis), at least for maize grown in nutrient solutions.

The  $\delta^{58}\text{Fe}$  values of **experiment 4** (maize supplied with phytosiderophores from wheat, <sup>58</sup>Fe tracer experiment) revealed that unspiked seed iron was present in all leaves of +Fe and -Fe plants, regardless if grown before or after the separation in the +/- treatment. This is an evidence that maize retranslocated iron, regardless of the iron status. The amount of

apoplastic iron is likely to be small, as plants were only shortly grown. As younger leaves were enriched in  $^{54}\text{Fe}$  over  $^{56}\text{Fe}$  compared to the nutrient solution, remobilization of iron probably involves reduction of iron, even under Fe-sufficient conditions.

The trend of decreasing  $\delta^{56}\text{Fe}$  in +Fe maize leaves was the same in all nutrient-solution-experiments and neither depended on the form of Fe supply, the supply of additional PS, nor the removal of apoplastic iron. This indicates that translocation mechanisms are always the same in maize plants grown in nutrient solutions.

In **experiment 5** (maize grown on soil) the  $\delta^{56}\text{Fe}$  values differed in the various organs of maize plants at the three points of harvest. This is in contrast to what was found in oat plants grown on Fe(III)-EDTA (chapter 4 of this thesis). Mass balance showed that at all three harvest points maize plants had the same total iron isotope composition. This suggests that always the same fractionation mechanism occurred during acquisition of iron, whereas inside the plant, different translocation mechanisms of iron probably led to a partitioning of iron isotopes. During growth younger leaves were enriched in the heavier iron isotopes. This trend is totally opposite from that found in maize grown on nutrient solution and that found in bean grown on Fe(III)-EDTA (chapter 4 of this thesis) and points to diverse mechanisms of translocation in strategy I and II plants on soil. The results also indicate that translocation mechanisms of maize differ between soil and nutrient solution as growth medium which lead to a different distribution of iron isotopes inside the plants.

At the moment it is not clear what exactly these differences are, as many details in iron metabolism in plants are still unclear (Morrissey and Guerinot, 2009), but different numbers of redox changes and chelation processes are likely.

### 5.5 Conclusion

This chapter reports the results and a preliminary interpretation of using stable iron isotopes to investigate the specific processes of iron metabolism of maize as a representative of strategy II plants. The obtained results reveal that the direction and extent of iron isotope fractionation during acquisition of iron by maize plants depends on the form of iron supply and therefore on iron availability. It is also shown that stable iron isotope fractionation is an indicator for iron (re-)translocation in maize plants. It is demonstrated that iron was retranslocated regardless of the iron status of the plants. This retranslocation process involved at least one

reduction step and transport of remobilized iron from leaf to leaf. Mostly light Fe developed during growth probably due to a change in redox states during translocation

The translocation mechanisms in maize grown on soil seem to be different to that of maize grown on nutrient solution and to that of strategy I plants when grown on soil. It is hypothesized that, depending on the kind of Fe supply, strategy I and II plants probably have different numbers of redox cycles and chelation changes during iron translocation.

## 5.6 Tables

Table 5-2 All data of experiment 1

time	iron status	pot/repetition	plant part	dry mass [mg]	Fe concentration [ $\mu\text{g/g}$ ]	Fe content [ $\mu\text{g}$ ]	$\delta^{56}\text{Fe}$ [‰]	$\Delta^{56}\text{Fe}_{\text{plant-nutrient solution}}$	mean $\Delta^{56}\text{Fe}$	SD
			EDTA				0.214			
			seeds		23		-0.136			
T 0	+Fe	1	roots	689	91	63	-0.317	-0.531		
		2	roots	578	85	49	-0.226	-0.440	<b>-0.452</b>	<b>0.207</b>
		3	roots	714	64	46	0.041	-0.173		
		4	roots	585	71	41	-0.449	-0.663		
		1	leaf 1	114	89	10	-0.007	-0.221		
		2	leaf 1	119	76	9	0.187	-0.027	<b>-0.025</b>	<b>0.214</b>
		3	leaf 1	123	52	6	0.486	0.272		
		4	leaf 1	116	69	8	0.090	-0.124		
		1	leaf 2	233	71	17				
		2	leaf 2	239	64	15		lost	<b>-0.338</b>	<b>0.298</b>
		3	leaf 2	275	53	15	0.087	-0.127		
		4	leaf 2	240	48	12	-0.335	-0.549		
		1	leaf 3	605	83	50	-0.938	-1.152		
		2	leaf 3	634	62	39	-0.954	-1.168	<b>-1.104</b>	<b>0.132</b>
		3	leaf 3	668	55	37	-0.694	-0.908		
		4	leaf 3	580	35	20	-0.976	-1.190		
		1	leaf 4	903	106	96	-1.170	-1.384		
		2	leaf 4	714	69	49	-1.187	-1.401	<b>-1.386</b>	<b>0.134</b>
		3	leaf 4	939	66	62	-1.001	-1.215		
		4	leaf 4	711	70	50	-1.329	-1.543		
T 1	+Fe	1	roots	1180	132	156	-0.305	-0.519		
		2	roots	1400	86	120	-0.630	-0.844	<b>-0.656</b>	<b>0.227</b>
		3	roots	1360	47	64	-0.640	-0.854		
		4	roots	1440	58	84	-0.193	-0.407		
		1	leaf 1	90	104	9	0.187	-0.027		
		2	leaf 1	110	154	17	0.060	-0.154	<b>-0.035</b>	<b>0.096</b>
		3	leaf 1	110	70	8	0.294	0.080		
		4	leaf 1	140	65	9	0.174	-0.040		
		1	leaf 2	230	60	14	-0.106	-0.320		
		2	leaf 2	230	81	19	0.025	-0.189	<b>-0.262</b>	<b>0.059</b>
		3	leaf 2	250	43	11	-0.084	-0.298		
		4	leaf 2	200	90	18	-0.026	-0.240		
		1	leaf 3	630	88	55	-0.755	-0.969		
		2	leaf 3	640	97	62	-0.533	-0.747	<b>-0.878</b>	<b>0.124</b>
		3	leaf 3	690	77	53	-0.784	-0.998		
		4	leaf 3	660	96	63	-0.583	-0.797		
		1	leaf 4	1740	81	140	-1.248	-1.462		
		2	leaf 4	1730	65	112	-1.308	-1.522	<b>-1.402</b>	<b>0.116</b>
		3	leaf 4	1730	67	116	-1.043	-1.257		
		4	leaf 4	1780	75	133	-1.151	-1.365		

5 Deciphering mechanisms of iron acquisition and retranslocation in maize

Table 5-2 continuation

time	iron status	pot/repetition	plant part	dry mass [mg]	Fe concentration [ $\mu\text{g/g}$ ]	Fe content [ $\mu\text{g}$ ]	$\delta^{56}\text{Fe}$ [‰]	$\Delta^{56}\text{Fe}_{\text{plant-nutrient solution}}$	mean $\Delta^{56}\text{Fe}$	SD
T 0	+Fe	1	leaf 5	1610	74	120	-1.478	-1.692	<b>-1.729</b>	<b>0.149</b>
		2	leaf 5	1770	63	112	-1.558	-1.772		
		3	leaf 5	1320	60	80	-1.335	-1.549		
		4	leaf 5	1560	95	149	-1.690	-1.904		
T 1	-Fe	1	roots	1090	38	42	-0.100	-0.314	<b>-0.416</b>	<b>0.077</b>
		2	roots	1400	33	46	-0.268	-0.482		
		3	roots	1260	58	73	-0.183	-0.397		
		4	roots	1270	37	47	-0.256	-0.470		
		1	leaf 1	70	89	6	0.179	-0.035	<b>0.115</b>	<b>0.147</b>
		2	leaf 1	90	90	8	0.500	0.286		
		3	leaf 1	110	86	9	0.398	0.184		
		4	leaf 1	70	98	7	0.240	0.026		
		1	leaf 2	220	72	16	0.027	-0.187	<b>-0.027</b>	<b>0.288</b>
		2	leaf 2	250	70	18	0.014	-0.200		
		3	leaf 2	260	82	21	lost			
		4	leaf 2	240	83	20	0.520	0.306		
		1	leaf 3	570	83	47	-0.608	-0.822	<b>-0.807</b>	<b>0.193</b>
		2	leaf 3	640	104	67	-0.850	-1.064		
		3	leaf 3	590	88	52	-0.516	-0.730		
		4	leaf 3	650	94	61	-0.395	-0.609		
		1	leaf 4	1600	109	174	-1.102	-1.316	<b>-1.270</b>	<b>0.101</b>
		2	leaf 4	1750	56	98	-1.166	-1.380		
		3	leaf 4	1650	74	122	-0.934	-1.148		
		4	leaf 4	1750	80	140	-1.022	-1.236		
1	leaf 5	1250	41	51	-1.241	-1.455	<b>-1.468</b>	<b>0.095</b>		
2	leaf 5	1430	35	50	-1.364	-1.578				
3	leaf 5	1370	38	51	-1.134	-1.348				
4	leaf 5	1460	34	50	-1.278	-1.492				
T 2	+Fe	1	roots	1970	61	120	-0.737	-0.951	<b>-1.062</b>	<b>0.283</b>
		2	roots	1670	59	99	-0.647	-0.861		
		3	roots	1710	59	101	-0.743	-0.957		
		4	roots	1810	90	163	-1.267	-1.481		
		1	leaf 1	120	86	10	-0.003	-0.217	<b>-0.103</b>	<b>0.154</b>
		2	leaf 1	90	104	9	0.330	0.116		
		3	leaf 1	120	83	10	0.011	-0.203		
		4	leaf 1	110	122	13	0.104	-0.110		
		1	leaf 2	250	66	17	-0.527	-0.741	<b>-0.515</b>	<b>0.181</b>
		2	leaf 2	230	60	14	-0.230	-0.444		
		3	leaf 2	190	73	14	-0.101	-0.315		
		4	leaf 2	250	71	18	-0.345	-0.559		
		1	leaf 3	650	92	60	-0.924	-1.138	<b>-1.037</b>	<b>0.156</b>
		2	leaf 3	510	63	32	-0.697	-0.911		
		3	leaf 3	540	82	44	-0.683	-0.897		
		4	leaf 3	680	85	58	-0.989	-1.203		

## 5 Deciphering mechanisms of iron acquisition and retranslocation in maize

Table 5-2 continuation

time	iron status	pot/repetition	plant part	dry mass [mg]	Fe concentration [ $\mu\text{g/g}$ ]	Fe content [ $\mu\text{g}$ ]	$\delta^{56}\text{Fe}$ [‰]	$\Delta^{56}\text{Fe}_{\text{plant-nutrient solution}}$	mean $\Delta^{56}\text{Fe}$	SD	
T 2	+Fe	1	leaf 4	2070	82	169	-1.247	-1.461	<b>-1.445</b>	<b>0.260</b>	
		2	leaf 4	1500	80	119	-1.070	-1.284			
		3	leaf 4	1600	93	148	-1.014	-1.228			
		4	leaf 4	1970	78	153	-1.591	-1.805			
		1	leaf 5	2670	62	166	-1.775	-1.989	<b>-1.826</b>	<b>0.255</b>	
		2	leaf 5	2410	73	175	-1.382	-1.596			
		3	leaf 5	2820	89	250	-1.408	-1.622			
		4	leaf 5	2520	88	221	-1.885	-2.099			
	1	leaf 6	1800	51	92	-2.148	-2.362	<b>-2.257</b>	<b>0.213</b>		
	2	leaf 6	2620	74	193	-1.753	-1.967				
	3	leaf 6	2590	54	140	-2.027	-2.241				
	4	leaf 6	2360	62	145	-2.245	-2.459				
	T 2	-Fe	1	roots	1490	38	56	-0.605	-0.819	<b>-0.449</b>	<b>0.271</b>
			2	roots	1340	37	49	-0.132	-0.346		
			3	roots	1520	42	64	0.036	-0.178		
			4	roots	1320	31	41	-0.239	-0.453		
1			leaf 1	2020	75	151	-0.200	-0.414	<b>-0.117</b>	<b>0.215</b>	
2			leaf 1	2300	86	198	0.093	-0.121			
3			leaf 1	2000	82	165	0.197	-0.017			
4			leaf 1	1890	84	159	0.297	0.083			
1			leaf 2	120	41	5	-0.293	-0.507	<b>-0.248</b>	<b>0.219</b>	
2			leaf 2	100	63	6	0.067	-0.147			
3			leaf 2	120	73	9	0.209	-0.005			
4			leaf 2	100	72	7	-0.118	-0.332			
1			leaf 3	230	63	15	-0.767	-0.981	<b>-0.784</b>	<b>0.295</b>	
2			leaf 3	260	75	19	-0.315	-0.529			
3			leaf 3	250	75	19	-0.322	-0.536			
4			leaf 3	230	78	18	-0.878	-1.092			
1			leaf 4	690	36	25	-1.076	-1.290	<b>-1.119</b>	<b>0.252</b>	
2			leaf 4	690	55	38	-0.835	-1.049			
3			leaf 4	690	71	49	-0.578	-0.792			
4			leaf 4	530	53	28	-1.129	-1.343			
1			leaf 5	1940	25	48	-1.489	-1.703	<b>-1.276</b>	<b>0.357</b>	
2			leaf 5	1900	34	65	-1.061	-1.275			
3			leaf 5	1860	40	75	-0.616	-0.830			
4			leaf 5	1580	40	63	-1.083	-1.297			
1	leaf 6	970	21	20	-1.470	-1.684	<b>-1.600</b>	<b>0.101</b>			
2	leaf 6	1270	27	34	-1.474	-1.688					
3	leaf 6	1350	40	53	-1.277	-1.491					
4	leaf 6	1270	35	44	-1.322	-1.536					

## 5 Deciphering mechanisms of iron acquisition and retranslocation in maize

Table 5-3 All data of experiment 2

Fe medium	iron status	pot/repetition	plant part	dry mass [g]	Fe concentration [µg/g]	Fe content [µg]	$\delta^{56}\text{Fe}$ [‰]	$\Delta^{56}\text{Fe}_{\text{plant-nutrient solution}}$	mean $\Delta^{56}\text{Fe}$	SD
							0.147			
			EDTA				-0.445			
			50mMFeCl3-PS							
Fe(III)-PS	+Fe	1	roots	0.23	1262	290	-0.070	0.375		
		2	roots	0.25	1376	351	-0.109	0.336	<b>0.290</b>	<b>0.079</b>
		3	roots	0.24	1283	301	-0.239	0.206		
		4	roots	0.26	1260	326	-0.203	0.242		
		1	leaf 1	0.04	252	10	-0.439	0.006		
		2	leaf 1	0.04	388	14	-0.379	0.066	<b>0.024</b>	<b>0.033</b>
		3	leaf 1	0.04	324	12	-0.413	0.032		
		4	leaf 1	0.03	345	12	-0.454	-0.009		
		1	leaf 2	0.07	242	17	-0.542	-0.097		
		2	leaf 2	0.08	350	27	-0.559	-0.114	<b>-0.112</b>	<b>0.014</b>
		3	leaf 2	0.08	297	23	-0.576	-0.131		
		4	leaf 2	0.08	338	26	-0.552	-0.107		
		1	leaf 3	0.14	197	28	-0.916	-0.471		
		2	leaf 3	0.15	280	43	-0.944	-0.499	<b>-0.519</b>	<b>0.056</b>
		3	leaf 3	0.15	250	38	-1.045	-0.600		
		4	leaf 3	0.22	266	57	-0.952	-0.507		
		1	leaf 4/5	0.22	138	30	-1.318	-0.873		
		2	leaf 4/5	0.22	170	37	-1.344	-0.899	<b>-0.904</b>	<b>0.033</b>
		3	leaf 4/5	0.22	168	36	-1.396	-0.951		
		4	leaf 4/5	0.22	173	38	-1.338	-0.893		
1	stem	0.23	172	39	-1.219	-0.774				
2	stem	0.25	200	50	-1.170	-0.725	<b>-0.766</b>	<b>0.034</b>		
3	stem	0.21	215	46	-1.253	-0.808				
4	stem	0.27	190	51	-1.203	-0.758				
Fe(III)-PS	-Fe	1	roots	0.23	300	68	-0.125	0.320		
		2	roots	0.28	305	86	-0.254	0.191	<b>0.214</b>	<b>0.071</b>
		3	roots	0.27	339	91	-0.270	0.175		
		4	roots	0.26	247	65	-0.273	0.172		
		1	leaf 1	0.03	171	6		lost		
		2	leaf 1	0.04	218	8	-0.112	0.333	<b>0.310</b>	<b>0.020</b>
		3	leaf 1	0.04	198	7	-0.147	0.298		
		4	leaf 1	0.03	198	7	-0.147	0.298		
		1	leaf 2	0.07	145	10	-0.272	0.173		
		2	leaf 2	0.08	186	15	-0.362	0.083	<b>0.092</b>	<b>0.065</b>
		3	leaf 2	0.08	183	14	-0.349	0.096		
		4	leaf 2	0.08	147	12	-0.431	0.014		
		1	leaf 3	0.15	89	13	-1.006	-0.561		
		2	leaf 3	0.18	75	13	-0.801	-0.356	<b>-0.438</b>	<b>0.089</b>
		3	leaf 3	0.16	102	17	-0.890	-0.445		
		4	leaf 3	0.17	86	14	-0.836	-0.391		
		1	leaf 4/5	0.37	42	15	-1.055	-0.610		
		2	leaf 4/5	0.45	51	23	-0.930	-0.485	<b>-0.560</b>	<b>0.064</b>
		3	leaf 4/5	0.38	46	17	-1.061	-0.616		
		4	leaf 4/5	0.37	44	16	-0.974	-0.529		
1	stem	0.30	29	9	-0.793	-0.348				
2	stem	0.37	38	14	-0.711	-0.266	<b>-0.365</b>	<b>0.095</b>		
3	stem	0.34	32	11	-0.798	-0.353				
4	stem	0.33	26	9	-0.939	-0.494				

## 5 Deciphering mechanisms of iron acquisition and retranslocation in maize

Table 5-3 continuation

Fe medium	iron status	pot/repetition	plant part	dry mass [g]	Fe concentration [ $\mu\text{g/g}$ ]	Fe content [ $\mu\text{g}$ ]	$\delta^{56}\text{Fe}$ [‰]	$\Delta^{56}\text{Fe}_{\text{plant-nutrient solution}}$	mean $\Delta^{56}\text{Fe}$	SD
Fe(III)-EDTA	+Fe	1	roots	0.39	895	352	-0.134	-0.281	<b>-0.253</b>	<b>0.074</b>
		2	roots	0.37	992	369	-0.193	-0.340		
		3	roots	0.38	708	271	-0.072	-0.219		
		4	roots	0.40	873	353	-0.024	-0.171		
		1	leaf 1	0.04	115	4	-0.707	-0.854	<b>-0.495</b>	<b>0.239</b>
		2	leaf 1	0.03	87	3	-0.229	-0.376		
		3	leaf 1	0.03	114	4	-0.229	-0.376		
		4	leaf 1	0.04	114	4	-0.229	-0.376		
		1	leaf 2	0.09	77	7	-0.532	-0.679	<b>-0.445</b>	<b>0.191</b>
		2	leaf 2	0.08	104	8	-0.376	-0.523		
		3	leaf 2	0.08	93	8	-0.143	-0.290		
		4	leaf 2	0.09	93	8	-0.143	-0.290		
		1	leaf 3	0.22	71	15	-0.529	-0.676	<b>-0.659</b>	<b>0.103</b>
		2	leaf 3	0.19	105	20	-0.643	-0.790		
		3	leaf 3	0.21	92	20	-0.480	-0.627		
		4	leaf 3	0.21	88	18	-0.396	-0.543		
		1	leaf 4/5	0.61	61	37	-1.046	-1.193	<b>-1.163</b>	<b>0.051</b>
		2	leaf 4/5	0.53	90	48	-1.039	-1.186		
		3	leaf 4/5	0.58	72	42	-0.940	-1.087		
		4	leaf 4/5	0.61	69	42	-1.038	-1.185		
1	stem	0.44	34	15	-1.093	-1.240	<b>-1.186</b>	<b>0.046</b>		
2	stem	0.44	43	19	-0.985	-1.132				
3	stem	0.38	38	14	-1.021	-1.168				
4	stem	0.44	39	17	-1.056	-1.203				
Fe(III)-EDTA	-Fe	1	roots	0.38	263	101	0.072	-0.075	<b>0.155</b>	<b>0.298</b>
		2	roots	0.41	279	113	0.160	0.013		
		3	roots	0.39	284	111	0.737	0.590		
		4	roots	0.36	265	94	0.238	0.091		
		1	leaf 1	0.04	86	3	-0.520	-0.667	<b>-0.675</b>	<b>0.341</b>
		2	leaf 1	0.04	89	3	-0.874	-1.021		
		3	leaf 1	0.04	96	4	-0.191	-0.338		
		4	leaf 1	0.04			lost			
		1	leaf 2	0.09	103	9	-0.277	-0.424	<b>-0.504</b>	<b>0.429</b>
		2	leaf 2	0.09	83	8	-0.985	-1.132		
		3	leaf 2	0.10	76	7	-0.082	-0.229		
		4	leaf 2	0.09	76	7	-0.083	-0.230		
		1	leaf 3	0.23	36	8	-0.979	-1.126	<b>-0.629</b>	<b>0.351</b>
		2	leaf 3	0.23	61	14	-0.395	-0.542		
		3	leaf 3	0.25	42	11	-0.154	-0.301		
		4	leaf 3	0.21	31	7	-0.400	-0.547		
		1	leaf 4/5	0.35	17	6	lost		<b>-0.424</b>	<b>0.121</b>
		2	leaf 4/5	0.50	20	10	-0.138	-0.285		
		3	leaf 4/5	0.40	17	7	-0.347	-0.494		
		4	leaf 4/5	0.33	17	6	-0.347	-0.494		
1	stem	0.40	8	3	-1.580	-1.727	<b>-0.907</b>	<b>0.605</b>		
2	stem	0.44	8	3	-0.854	-1.001				
3	stem	0.46	7	3	-0.303	-0.450				
4	stem	0.40	7	3	-0.303	-0.450				



## 5 Deciphering mechanisms of iron acquisition and retranslocation in maize

Table 5-4 All data of experiment 3

Fe medium	iron status	pot/rep	EDTA (2007) plant part	dry mass [mg]	Fe concentra tion [µg/g]	Fe content [µg]	$\delta^{56}\text{Fe}$ [‰]	$\Delta^{56}\text{Fe}_{\text{plant-nutrient solution}}$	mean $\Delta^{56}\text{Fe}$	SD
Fe(III)-EDTA	+Fe	1	root apoplast			750	-0.496	-0.643	<b>-0.594</b>	<b>0.069</b>
		2	root apoplast			639	-0.399	-0.546		
		1	roots	463	170	78	-0.331	-0.478	<b>-0.423</b>	<b>0.078</b>
		2	roots	326	138	45	-0.221	-0.368		
		1	leaf 1	46	189	9	0.046	-0.101	<b>-0.058</b>	<b>0.061</b>
		2	leaf 1	24	154	4	0.132	-0.014		
		1	leaf 2	109	105	11	-0.142	-0.289	<b>-0.239</b>	<b>0.071</b>
		2	leaf 2	65	105	7	-0.042	-0.189		
		1	leaf 3	260	101	26	-0.697	-0.844	<b>-0.745</b>	<b>0.140</b>
		2	leaf 3	165	105	17	-0.499	-0.645		
		1	leaf 4/5	470	94	44	-1.135	-1.282	<b>-1.185</b>	<b>0.137</b>
		2	leaf 4/5	372	93	35	-0.942	-1.088		
		1	stem	462	123	57	-0.423	-0.570	<b>-0.562</b>	<b>0.011</b>
		2	stem	315	104	33	-0.407	-0.554		
Fe(III)-EDTA	-Fe	1	root apoplast			202	0.191	0.044	<b>0.295</b>	<b>0.355</b>
		2	root apoplast			222	0.692	0.546		
		1	roots	400	28	11	0.201	0.054	<b>0.214</b>	<b>0.227</b>
		2	roots	354	53	19	0.521	0.374		
		1	leaf 1	36	73	3	-0.510	-0.657	<b>-0.668</b>	<b>0.015</b>
		2	leaf 1	34	83	3	-0.532	-0.679		
		1	leaf 2	82	55	4	-0.253	-0.400	<b>-0.461</b>	<b>0.086</b>
		2	leaf 2	96	83	8	-0.374	-0.521		
		1	leaf 3	187	24	4	-0.103	-0.250	<b>-0.255</b>	<b>0.007</b>
		2	leaf 3	237	46.9	11	-0.113	-0.260		
		1	leaf 4/5	212	14	3	-0.021	-0.168	<b>-0.172</b>	<b>0.005</b>
		2	leaf 4/5	297	22.6	7	-0.028	-0.175		
		1	stem	316	6.9	2	-0.266	-0.413	<b>-0.362</b>	<b>0.072</b>
		2	stem	287	10.5	3	-0.164	-0.311		

Table 5-5 All data of experiment 4

Fe medium	iron status	pot/repetition	plant part	dry mass [g]	Fe concentration		$\delta^{56}\text{Fe}$ [‰]	$\Delta^{56}\text{Fe}_{\text{plant-nutrient solution}}$ [‰]		mean $\Delta^{56}\text{Fe}$ [‰]	SD	$\delta^{58}\text{Fe}$ [‰]	$\Delta^{58}\text{Fe}_{\text{plant-nutrient solution}}$ [‰]		mean $\Delta^{58}\text{Fe}$ [‰]	SD	
					[ $\mu\text{g/g}$ ]	content [ $\mu\text{g}$ ]		nutrient solution [‰]	plant solution [‰]				nutrient solution [‰]	plant solution [‰]			
Nährlösung FeCl <sub>3</sub>																	
Nährlösung Fe+Spike																	
Fe(III)-PS	+Fe	1	roots	676	309	209	0.331	0.017	0.033	0.7	436.4	-22.0	-29.0	9.9			
		2	roots	577	356	205	0.363	0.049	0.022	458.4	422.3	-36.1	-29.0	9.9			
		1	leaf 1	34	295	10	0.695	0.381	0.136	359.9	346.7	-98.5	-105.1	9.4			
		2	leaf 1	33	263	9	0.887	0.573	0.013	399.7	401.4	-58.7	-57.9	1.2			
		1	leaf 2	92	284	26	0.699	0.404	0.011	425.9	431.9	-32.5	-29.5	4.3			
	2	leaf 2	91	293	27	0.718	0.169	0.062	433.1	437.2	-25.3	-23.2	2.9				
	1	leaf 3	199	254	50	0.483	0.185	0.012	429.8	429.4	-28.6	-28.8	0.3				
	2	leaf 3	202	277	56	0.499	0.185	0.038	436.0	436.7	-22.4	-22.1	0.6				
	1	leaf 4	298	171	51	0.096	-0.218	-0.174	342.5	342.5	-115.9	-124.6	12.3				
	2	leaf 4	278	206	57	0.184	-0.130	0.253	325.1	325.1	-133.3	-124.6	12.3				
Fe(III)-PS	-Fe	1	roots	687	58	40	0.602	0.288	0.206	271.5	271.5	-186.9	-187.1	0.3			
		2	roots	714	33	23	0.531	0.217	0.045	349.5	354.0	-108.9	-106.7	3.2			
		1	leaf 1	30	139	4	0.488	0.174	0.258	375.5	379.6	-82.9	-80.9	2.9			
		2	leaf 1	32	129	4	0.552	0.238	0.088	366.8	372.0	-91.6	-89.0	3.7			
		1	leaf 2	97	142	14	0.589	0.275	0.036	347.6	350.7	-110.8	-109.3	2.2			
	2	leaf 2	95	143	14	0.556	0.242	0.013	350.7	350.7	-107.7	-109.3	2.2				
	1	leaf 3	217	92	20	0.365	0.051	0.061	363.7	363.7	-94.7	-87.6	10.1				
	2	leaf 3	219	92	20	0.490	0.176	0.005	378.0	378.0	-80.4	-87.6	10.1				
	1	leaf 4	302	76	23	0.215	-0.099	-0.124	342.5	342.5	-115.9	-124.6	12.3				
	2	leaf 4	289	63	18	0.164	-0.150	0.253	325.1	325.1	-133.3	-124.6	12.3				
1	leaf 5	51	56	3	0.003	-0.311	-0.301	347.6	347.6	-110.8	-109.3	2.2					
2	leaf 5	81	55	4	0.022	-0.292	0.013	350.7	350.7	-107.7	-109.3	2.2					
1	stem	354	29	10	0.250	-0.064	-0.061	363.7	363.7	-94.7	-87.6	10.1					
2	stem	379	34	13	0.256	-0.058	0.005	378.0	378.0	-80.4	-87.6	10.1					

Table 5-6 All data of experiment 5

number of harvest	plant part	dry weight [g]	Fe concentration [ $\mu\text{g/g}$ ]	Fe content [ $\mu\text{g}$ ]	$\delta^{56}\text{Fe}$ [‰]	2SD [‰] <sup>1</sup>	$\Delta^{56}\text{Fe}_{\text{plant-soil}}$ [‰]
<i>1<sup>st</sup> harvest</i>	seeds	0.20	23	4.6	-0.136	0.070	
	roots	0.14	1129	156	-0.045	0.070	0.225
	stem	0.20	92	18	-0.004	0.070	0.266
	leaf 1	0.09	167	16	-0.047	0.070	0.223
	leaf 2	0.20	108	22	-0.003	0.070	0.267
	leaf 3	0.21	104	22	-0.123	0.070	0.147
<i>2<sup>nd</sup> harvest</i>	leaf 4	0.05	101	5	-0.126	0.070	0.144
	roots	0.20	1082	216	-0.010	0.070	0.260
	stem	0.97	169	164	-0.077	0.070	0.193
	leaf 1	0.11	127	14	0.020	0.070	0.290
	leaf 2	0.21	184	39	0.114	0.070	0.384
	leaf 3	0.36	143	51	0.081	0.070	0.351
	leaf 4	0.65	129	83	-0.032	0.070	0.238
<i>3<sup>rd</sup> harvest</i>	leaf 5	0.50	113	56	-0.167	0.070	0.103
	leaf 6	0.04	147	6	-0.258	0.070	0.012
	roots	0.28	1116	317	-0.030	0.070	0.240
	stem	2.77	40	111	-0.039	0.070	0.231
	leaf 1	0.14	460	63	-0.030	0.070	0.240
	leaf 2	0.17	97	17	-0.039	0.070	0.231
	leaf 3	0.64	71	45	0.035	0.070	0.305
	leaf 4	0.87	83	72	0.262	0.070	0.532
leaf 5	1.95	77	151	0.257	0.070	0.527	
leaf 6	1.54	75	116	0.177	0.070	0.447	
leaf 7	0.30	62	19	0.028	0.070	0.298	

<sup>1</sup> given as the 2 standard deviation reproducibility of replicate measurements



## 6 References

- Allegre, C., Manhès, G., and Lewin, E., 2001. Chemical composition of the Earth and the volatility control on planetary genetics. *Earth and Planetary Science Letters* **185**, 49-69.
- Álvarez-Fernández, A., 2006. Application of stable isotopes in plant iron research. In: Barton, L. L. and Abadía, J. (Eds.), *Iron nutrition in plants and rhizospheric microorganisms*. Springer, Dordrecht.
- Anbar, A. D., Roe, J. E., Barling, J., and Neelson, K. H., 2000. Nonbiological fractionation of iron isotopes. *Science* **288**, 126-128.
- Anbar, A. D., 2004. Iron stable isotopes: beyond biosignatures. *Earth and Planetary Science Letters* **217**, 223-236.
- Anbar, A. D., Jarzecki, A. A., and Spiro, T. G., 2005. Theoretical investigation of iron isotope fractionation between  $\text{Fe}(\text{H}_2\text{O})_{(6)}^{(3+)}$  and  $\text{Fe}(\text{H}_2\text{O})_{(6)}^{(2+)}$ : Implications for iron stable isotope geochemistry. *Geochimica Et Cosmochimica Acta* **69**, 825-837.
- Anbar, A. D. and Rouxel, O., 2007. Metal stable isotopes in paleoceanography. *Annual Review of Earth and Planetary Sciences* **35**, 717-746.
- Balci, N., Bullen, T. D., Witte-Lien, K., Shanks, W. C., Motelica, M., and Mandernack, K. W., 2006. Iron isotope fractionation during microbially stimulated Fe(II) oxidation and Fe(III) precipitation. *Geochimica Et Cosmochimica Acta* **70**, 622-639.
- Barker, S., Greaves, M., and Elderfield, H., 2003. A study of cleaning procedures used for foraminiferal Mg/Ca paleothermometry. *Geochemistry Geophysics Geosystems* **4**, 8407.
- Baxter, I., 2009. Ionomics. Studying the social network of mineral nutrients. *Current Opinion in Plant Biology* **12**, 381-386.
- Beard, B. L., Johnson, C. M., Cox, L., Sun, H., Neelson, K. H., and Aguilar, C., 1999. Iron isotope biosignatures. *Science* **285**, 1889-1892.
- Beard, B. L., Johnson, C. M., Skulan, J. L., Neelson, K. H., Cox, L., and Sun, H., 2003. Application of Fe isotopes to tracing the geochemical and biological cycling of Fe. *Chemical Geology* **195**, 87-117.
- Beard, B. L. and Johnson, C. M., 2004. Fe isotope variations in the modern and ancient earth and other planetary bodies. In: *Geochemistry of Non-Traditional Stable Isotopes. Reviews in Mineralogy & Geochemistry*. Mineralogical Society of America and Geochemical Society, Washington, **55**, 319-357.
- Becker, R., Fritz, E., and Manteuffel, R., 1995. Subcellular-Localization and Characterization of Excessive Iron in the Nicotianamine-Less Tomato Mutant Chloronerva. *Plant Physiology* **108**, 269-275.
- Belshaw, N. S., Zhu, X. K., Guo, Y., and O'Nions, R. K., 2000. High precision measurement of iron isotopes by plasma source mass spectrometry. *International Journal of Mass Spectrometry* **197**, 191-195.

## 6 References

---

- Berggren, D. and Mulder, J., 1995. The role of organic matter in controlling aluminum solubility in acidic mineral soil horizons. *Geochimica Et Cosmochimica Acta* **59**, 4167-4180.
- Bertrand, I. and Hinsinger, P., 2000. Dissolution of iron oxyhydroxide in the rhizosphere of various crop species. *Journal of Plant Nutrition* **23**, 1559-1577.
- Bienfait, H. F., Vandenberg, W., and Meslandmul, N. T., 1985. Free Space Iron Pools in Roots - Generation and Mobilization. *Plant Physiology* **78**, 596-600.
- Bienfait, H. F. and Scheffers, M. R., 1992. Some Properties of Ferric Citrate Relevant to the Iron Nutrition of Plants. *Plant and Soil* **143**, 141-144.
- Black, J. R., Epstein, E., Rains, W. D., Yin, Q-Z., and Casey, W. H., 2008. Magnesium isotope fractionation during plant growth. *Environmental Science and Technology* **42**, 7831-7836.
- Boccio, J. R. and Iyengar, V., 2003. Iron deficiency - Causes, consequences, and strategies to overcome this nutritional problem. *Biological Trace Element Research* **94**, 1-31.
- Bolou Bi, E. B., Poszwa, A., and Vigier, N., 2008. Experimental determination of magnesium isotope fractionation during higher plant growth. *Geophysical Research Abstracts* **10**, A08852.
- Borggaard, O. K., 1988. Phase identification by selective dissolution techniques. In: Stucki, J. W., Goodman, B. A., and Schwertmann, U. (Eds.), *Iron in soils and clay minerals*. D. Reidel, Dordrecht, 83-97.
- Borggaard, O. K., 1992. Dissolution of poorly crystalline iron-oxides in soils by EDTA and oxalate. *Zeitschrift Fuer Pflanzenernaehrung und Bodenkunde* **155**, 431-436.
- Bradford, G. R., Bair, F. L., and Hunsaker, V., 1971. Trace and major element contents of soil saturation extracts. *Soil Science* **112**, 225-230.
- Brantley, S. L., Liermann, L., and Bullen, T. D., 2001. Fractionation of Fe isotopes by soil microbes and organic acids. *Geology* **29**, 535-538.
- Brantley, S. L., Liermann, L. J., Guynn, R. L., Anbar, A., Icopini, G. A., and Barling, J., 2004. Fe isotopic fractionation during mineral dissolution with and without bacteria. *Geochimica Et Cosmochimica Acta* **68**, 3189-3204.
- Briat, J. F., Curie, C., and Gaymard, F., 2007. Iron utilization and metabolism in plants. *Current Opinion in Plant Biology* **10**, 276-282.
- Briat, J. F. and Lobreaux, S., 1997. Iron transport and storage in plants. *Trends in Plant Science* **2**, 187-193.
- Brown, A. L., Yamaguchi, S., and Leal-Diaz, J., 1965. Evidence for translocation of iron in plants. *Plant Physiology* **40**, 35-38.
- Bughio, N., Takahashi, M., Yoshimura, E., Nishizawa, N. K., and Mori, S., 1997. Light-dependent iron transport into isolated barley chloroplasts. *Plant and Cell Physiology* **38**, 101-105.
- Bullen, T. D., White, A. F., Childs, C. W., Vivit, D. V., and Schulz, M. S., 2001. Demonstration of significant abiotic iron isotope fractionation in nature. *Geology* **29**, 699-702.

- Buss, H. L., Mathur, R., White, A. F., and Brantley, S. L., 2010. Phosphorus and iron cycling in deep saprolite, Luquillo Mountains, Puerto Rico. *Chemical Geology* **269**, 52-61.
- Butler, I. B., Archer, C., Vance, D., Oldroyd, A., and Rickard, D., 2005. Fe isotope fractionation on FeS formation in ambient aqueous solution. *Earth and Planetary Science Letters* **236**, 430-442.
- Canfield, D. E., Thamdrup, B., and Hansen, J. W., 1993. The Anaerobic Degradation of Organic-Matter in Danish Coastal Sediments - Iron Reduction, Manganese Reduction, and Sulfate Reduction. *Geochimica Et Cosmochimica Acta* **57**, 3867-3883.
- Campbell, D. J. and Beckett, P. H. D., 1988. The soil solution in a soil treated with digested sewage sludge. *Journal of Soil Science* **39**, 283-298.
- Cenki-Tok, B., Chabaux, F., Lemarchand, D., Schmitt, A. D., Pierret, M. C., Viville, D., Bagard, M. L., and Stille, P., 2009. The impact of water-rock interaction and vegetation on calcium isotope fractionation in soil- and stream waters of a small forested catchment (the Strengbach case). *Geochimica Et Cosmochimica Acta* **73**, 2215-2228.
- Cesco, S., Rombolà, A. D., Tagliavini, M. Varanini, Z., and Pinton, R., 2004. Use of Fephtosiderophores by Citrus species. *Proceedings of the XII International Symposium on Iron Nutrition in Plants*, Tokyo, Japan, p. 122.
- Chaney, R. L., Brown, J. C., and Tiffin, L. O., 1972. Obligatory Reduction of Ferric Chelates in Iron Uptake by Soybeans. *Plant Physiology* **50**, 208-213.
- Chaney, R. L., 1989. Kinetics of ferric chelate reduction by roots of iron deficient peanut. *Acta Botanica Neerlandica* **38**, 155-163.
- Cheah, S. F., Kraemer, S. M., Cervini-Silva, J., and Sposito, G., 2003. Steady-state dissolution kinetics of goethite in the presence of desferrioxamine B and oxalate ligands: implications for the microbial acquisition of iron. *Chemical Geology* **198**, 63-75.
- Chapman, J. B., Weiss, D. J., Shan, Y., and Lehmburger, M., 2009. Iron isotope fractionation during leaching of granite and basalt by hydrochloric and oxalic acids. *Geochimica Et Cosmochimica Acta* **73**, 1312-1324.
- Chasteen, N. D., 1998. Ferritin. Uptake, Storage and release of iron. In: Sigel, A. (Ed.), *Metal ions in biological systems: Iron transport and storage in microorganisms, plants, animals*. Dekker, New York.
- Cohen, C. K., Fox, T. C., Garvin, D. F., and Kochian, L. V., 1998. The role of iron-deficiency stress responses in stimulating heavy-metal transport in plants. *Plant Physiology* **116**, 1063-1072.
- Cornell, R. M. and Schwertmann, U., 2003. *The iron oxides - structure, properties, reactions, occurrence and uses*. VGH, Weinheim, Germany.
- Croal, L. R., Johnson, C. M., Beard, B. L., and Newman, D. K., 2004. Iron isotope fractionation by Fe(II)-oxidizing photoautotrophic bacteria. *Geochimica Et Cosmochimica Acta* **68**, 1227-1242.

## 6 References

---

- Crosby, H. A., Roden, E. E., Johnson, C. M., and Beard, B. L., 2007. The mechanisms of iron isotope fractionation produced during dissimilatory Fe(III) reduction by *Shewanella putrefaciens* and *Geobacter sulfurreducens*. *Geobiology* **5**, 169-189.
- Crowley, D. E., Roemheld, V., Marschner, H. and Szaniszlo, P. J., 1992. Root-microbial effects on plant iron uptake from siderophores and phytosiderophores. *Plant and Soil* **142**, 1-7.
- Curie, C., Panaviene, Z., Loulergue, C., Dellaporta, S. L., Briat, J. F., and Walker, E. L., 2001. Maize yellow stripe1 encodes a membrane protein directly involved in Fe(III) uptake. *Nature* **409**, 346-349.
- Curie, C. and Briat, J. F., 2003. Iron transport and signaling in plants. *Annual Review of Plant Biology* **54**, 183-206.
- Curie, C., Cassin, G., Couch, D., Divol, F., Higuchi, K., Le Jean, M., Misson, J., Schikora, A., Czernik, P., and Mari, S., 2009. Metal movement within the plant: contribution of nicotianamine and yellow stripe 1-like transporters. *Annals of Botany* **103**, 1-11.
- Dauphas, N. and Rouxel, O., 2006. Mass spectrometry and natural variations of iron isotopes. *Mass Spectrometry Reviews* **25**, 515-550.
- Dideriksen, K., Baker, J. A., and Stipp, S. L. S., 2008. Equilibrium Fe isotope fractionation between inorganic aqueous Fe(III) and the siderophore complex, Fe(III)-desferrioxamine B. *Earth and Planetary Science Letters* **269**, 280-290.
- Dixon, J. B. and Weed, S. B. (Eds), 1989. *Minerals in soil environments*. Soil Science Society of America., 2nd ed. Madison, Wi.
- Dultz, S., 2002. Effect of parent material and weathering on feldspar content in different particle size fractions from forest soils in NW Germany. *Geoderma* **106**, 63-81.
- Eckhardt, U., Marques, A. M., and Buckhout, T. J., 2001. Two iron-regulated cation transporters from tomato complement metal uptake-deficient yeast mutants. *Plant Molecular Biology* **45**, 437-448.
- Edison, E. S., Bajel, A., and Chandy, M., 2008. Iron homeostasis: new players, newer insights. *European Journal of Haematology* **81**, 411-424.
- Eide, D., Broderius, M., Fett, J. and Guerinot, M. L. 1996. A novel iron-regulated metal transporter from plants identified by functional expression in yeast. *Proceedings of the Natural Academy of Science USA* **93**, 5624-5628.
- Emmanuel, S., Erel, Y., Matthews, A., and Teutsch, N., 2005. A preliminary mixing model for Fe isotopes in soils. *Chemical Geology* **222**, 23-34.
- Engels, C. and Marschner, H., 1992. Root to shoot translocation of macronutrients in relation to shoot demand in maize (*Zea-Mays* L) grown at different root zone temperatures. *Zeitschrift Für Pflanzenernaehrung Und Bodenkunde* **155**, 121-128.



- Engrand, C., McKeegan, K. D., Leshin, L. A., Herzog, G. F., Schnabel, C., Nyquist, L. E., and Brownlee, D. E., 2005. Isotopic compositions of oxygen, iron, chromium, and nickel in cosmic spherules: Toward a better comprehension of atmospheric entry heating effects. *Geochimica Et Cosmochimica Acta* **69**, 5365-5385.
- Essington, M. E., 2004. *Soil and water chemistry: an integrative approach*. CRC Press, Boca Raton.
- Fantle, M. S. and DePaolo, D. J., 2004. Iron isotopic fractionation during continental weathering. *Earth and Planetary Science Letters* **228**, 547-562.
- Goodman, B. A. and Dekock, P. C., 1982. Mossbauer Studies of Plant Materials. 1. Duckweed, Stocks, Soybean and Pea. *Journal of Plant Nutrition* **5**, 345-353.
- Grusak, M. A. and DellaPenna, D., 1999. Improving the nutrient composition of plants to enhance human nutrition and health. *Annual Review of Plant Physiology and Plant Molecular Biology* **50**, 133-161.
- Guelke, M. and von Blanckenburg, F., 2007. Fractionation of stable iron isotopes in higher plants. *Environmental Science & Technology* **41**, 1896-1901.
- Guerinot, M. L. and Yi, Y., 1994. Iron - Nutritious, Noxious, and Not Readily Available. *Plant Physiology* **104**, 815-820.
- Guerinot, M. L. and Salt, D. E., 2001. Fortified foods and phytoremediation. Two sides of the same coin. *Plant Physiology* **125**, 164-167.
- Haese, R. R., 2000. The reactivity of iron. In: Schulz, H. D. and Zabel, M. (Eds.), *Marine Geochemistry*. Springer, Heidelberg, 233-261.
- Halliday, A. N., Lee, D. C., Christensen, J. N., Walder, A. J., Freedman, P. A., Jones, C. E., Hall, C. M., Yi, W., and Teagle, D., 1995. Recent Developments in Inductively-Coupled Plasma Magnetic-Sector Multiple Collector Mass-Spectrometry. *International Journal of Mass Spectrometry and Ion Processes* **146**, 21-33.
- Halliday, A. N., Lee, D. C., Christensen, J. N., Rehkamper, M., Yi, W., Luo, X. Z., Hall, C. M., Ballentine, C. J., Pettke, T. and Stirling, C., 1998. Applications of multiple collector-ICPMS to cosmochemistry, geochemistry, and paleoceanography. *Geochimica Et Cosmochimica Acta* **62**, 919-940.
- Hell, R. and Stephan, U. W., 2003. Iron uptake, trafficking and homeostasis in plants. *Planta* **216**, 541-551.
- Heron, G., Crouzet, C., Bourg, A. C. M., and Christensen, T. H., 1994. Speciation of Fe(II) and Fe(III) in Contaminated Aquifer Sediments Using Chemical-Extraction Techniques. *Environmental Science & Technology* **28**, 1698-1705.
- Hider, R. C., 1984. Siderophore Mediated Absorption of Iron. *Structure and Bonding* **58**, 25-87.
- Hill, P. S. and Schauble, E. A., 2008. Modeling the effects of bond environment on equilibrium iron isotope fractionation in ferric aquo-chloro complexes. *Geochimica Et Cosmochimica Acta* **72**, 1939-1958.
- Hoefs, J., 2009. *Stable Isotope Geochemistry*. Springer, Berlin.

## 6 References

---

- Horn, I. and von Blanckenburg, F., 2007. Investigation on elemental and isotopic fractionation during 196 nm femtosecond laser ablation multiple collector inductively coupled plasma mass spectrometry. *Spectrochimica Acta Part B-Atomic Spectroscopy* **62**, 410-422.
- Hotz, K., 2009. *Understanding the message of iron isotopes in the human body*. Dissertation, ETH Zürich: Diss. ETH No. 18376.
- Icopini, G. A., Anbar, A. D., Ruebush, S. S., Tien, M., and Brantley, S. L., 2004. Iron isotope fractionation during microbial reduction of iron: The importance of adsorption. *Geology* **32**, 205-208.
- Inoue, K., Hiradate, S., and Takagi, S., 1993. Interaction of Mugineic Acid with Synthetically Produced Iron-Oxides. *Soil Science Society of America Journal* **57**, 1254-1260.
- Johnson, C. M., Skulan, J. L., Beard, B. L., Sun, H., Nealson, K. H., and Braterman, P. S., 2002. Isotopic fractionation between Fe(III) and Fe(II) in aqueous solutions. *Earth and Planetary Science Letters* **195**, 141-153.
- Johnson, G. V., López, A., and La Valle Foster, N., 2002. Reduction and transport of Fe from siderophores. *Plant and Soil* **241**, 27-33.
- Johnson, C. M., Beard, B. L., and Albarède, F., 2004a. Overview and general concepts. In: *Geochemistry of Non-Traditional Stable Isotopes. Reviews in Mineralogy & Geochemistry*. Mineralogical Society of America and Geochemical Society, Washington, **55**, 1-24.
- Johnson, C. M., Beard, B. L., Roden, E. E., Newman, D. K., and Nealson, K. H., 2004b. Isotopic constraints on biogeochemical cycling of Fe. In: *Geochemistry of Non-Traditional Stable Isotopes. Reviews in Mineralogy & Geochemistry*. Mineralogical Society of America and Geochemical Society, Washington, **55**, 359-408.
- Johnson, C. M., Roden, E. E., Welch, S. A., and Beard, B. L., 2005. Experimental constraints on Fe isotope fractionation during magnetite and Fe carbonate formation coupled to dissimilatory hydrous ferric oxide reduction. *Geochimica Et Cosmochimica Acta* **69**, 963-993.
- Johnson, C. M. and Beard, B. L., 2006. Fe isotopes: an emerging technique in understanding modern and ancient biogeochemical cycles. *GSA Today* **16**, 4-10.
- Johnson, C. M., Beard, B. L., and Roden, E. E., 2008. The iron isotope fingerprints of redox and biogeochemical cycling in modern and ancient earth. *Annual Review of Earth and Planetary Sciences* **36**, 457-493.
- Kalinowski, B. E., Liermann, L. J., Brantley, S. L., Barnes, A., and Pantano, C. G., 2000. X-ray photoelectron evidence for bacteria-enhanced dissolution of hornblende. *Geochimica Et Cosmochimica Acta* **64**, 1331-1343.
- Kiczka, M., Wiederhold, J. G., Frommer, J., Kraemer, S. M., Bourdon, B., and Kretzschmar, R., 2010a. Iron isotope fractionation during proton- and ligand-promoted dissolution of primary phyllosilicates. *Geochimica Et Cosmochimica Acta* **74**, 3112-3128.

- 
- Kiczka, M., Wiederhold, J. G., Frommer, J., Kraemer, S. M., Bourdon, B., and Kretzschmar, R., 2010b. Iron isotope fractionation during Fe uptake and translocation in alpine plants. *Environmental Science and Technology* **44**, 6144-6150.
- Kim, S. A., Punshon, T., Lanzirotti, A., Li, L. T., Alonso, J. M., Ecker, J. R., Kaplan, J., and Gueriot, M. L., 2006. Localization of iron in Arabidopsis seed requires the vacuolar membrane transporter VIT1. *Science* **314**, 1295-1298.
- Kim, S. A. and Gueriot, M. L., 2007. Mining iron: Iron uptake and transport in plants. *Febs Letters* **581**, 2273-2280.
- Kraemer, S. M., 2004. Iron oxide dissolution and solubility in the presence of siderophores. *Aquatic Science* **66**, 3-18.
- Krayenbuehl, P. A., Walczyk, T., Schoenberg, R., von Blanckenburg, F., and Schulthess, G., 2005. Hereditary hemochromatosis is reflected in the iron isotope composition of blood. *Blood* **105**, 3812-3816.
- Kushnir, S., Babiychuk, E., Storozhenko, S., Davey, M. W., Papenbrock, J., De Rycke, R., Engler, G., Stephan, U. W., Lange, H., Kispal, G., Lill, R., and Van Montagu, M., 2001. A mutation of the mitochondrial ABC transporter Sta1 leads to dwarfism and chlorosis in the Arabidopsis mutant starik. *Plant Cell* **13**, 89-100.
- La Force, M. J. and Fendorf, S., 2000. Solid-phase iron characterization during common selective sequential extractions. *Soil Science Society of America Journal* **64**, 1608-1615.
- Larbi, A., Morales, F., Lopez-Millan, A. F., Gogorcena, Y., Abadia, A., Moog, P. R., and Abadia, J., 2001. Technical advance: Reduction of Fe(III)-chelates by mesophyll leaf disks of sugar beet. Multi-component origin and effects of Fe deficiency. *Plant and Cell Physiology* **42**, 94-105.
- Le Jean, M., Schikora, A., Mari, S., Briat, J. F., and Curie, C., 2005. A loss-of-function mutation in AtYSL1 reveals its role in iron and nicotianamine seed loading. *Plant Journal* **44**, 769-782.
- Lindsay, W. L. and Schwab, A. P., 1982. The chemistry of iron in soils and its availability to plants. *Journal of Plant Nutrition* **5**, 821-840.
- Loeppert, R. H. and Inskip, W. P., 1996. Iron. In: Sparks, D. L. (Ed.), *Methods of soil analysis*. Part 3 Chemical methods Soil Science Society of America, Madison, WI, USA, 639-664.
- Lovley, D. R. and Phillips, E. J. P., 1988. Novel mode of microbial energy-metabolism. Organic-carbon oxidation coupled to dissimilatory reduction of iron or manganese *Applied and Environmental Microbiology* **54**, 1472-1480.
- Marschner, H., Roemheld, V., and Kissel, M., 1986. Different Strategies in Higher-Plants in Mobilization and Uptake of Iron. *Journal of Plant Nutrition* **9**, 695-713.
- Marschner, H., 1995. *Mineral Nutrition of higher plants*. Academic Press, London.

## 6 References

---

- Martell, A. E., Motekaitis, R. J., Fried, A. R., Wilson, J. S., and MacMillan, D. T., 1975. Thermal decomposition of EDTA, NTA and nitrilotrimethylenephosphonic acid in aqueous-solution. *Canadian Journal of Chemistry-Revue Canadienne de Chimie* **53**, 3471-3476.
- Meda, A. R., Scheuermann, E. B., Prechsl, U., Erenoglu, B. E., Schaaf, G., Hayen, H., Weber, G., and von Wirén, N., 2007. Iron acquisition by phytosiderophores contribute to cadmium tolerance. *Plant Physiology* **143**, 1761-1773.
- Mikutta, C., Wiederhold, J. G., Chirpka, O. A., Hofstetter, T. B., Bourdon B., and von Gunten, U., 2009. Iron isotope fractionation and atom exchange during sorption of ferrous iron to mineral surfaces. *Geochimica Et Cosmochimica Acta* **73**, 1795-1812.
- Mori, S., 1998. Iron transport in graminaceous plants. In: *Metal ions in biological systems: Iron transport and storage in microorganisms, plants, animals*. Dekker, New York, Vol. **35**, 215-237.
- Morrissey, J. and Guerinot, M. L., 2009. Iron uptake and Transport in plants: The good, the bad and the ionome. *Chemical Reviews* **109**, 4553-4567.
- Moynier, F., Pichat, S., Pons, M.-L., Fike, D., Balter, V., and Albarède, F., 2009. Isotopic fractionation and transport mechanisms of Zn in plants. *Chemical Geology* **267**, 125-130.
- Myers, C. R. and Nealson, K. H., 1988. Microbial reduction of manganese oxides-interactions with iron and sulphur. *Geochimica Et Cosmochimica Acta* **52**, 2727-2732.
- Niederbudde, E. A. and Schwertmann, U., 1980. Clay mineralogy of soils. *Geologisches Jahrbuch* **D39**, 99-114.
- Noordmann, J., 2008. *Lebensmittelauthentifizierung mit stabilen Eisenisotopen*. Diploma Thesis, Leibniz Universität Hannover, Germany.
- Ohno, T., Shinohara, A., Kohge, I., Chiba, M., and Hirata, T., 2004. Isotopic analysis of Fe in human red blood cells by multiple collector-ICP-mass spectrometry. *Analytical Sciences* **20**, 617-621.
- Opfergelt, S., Cardinal, D., Henriot, C., Andre, L., and Delvaux, B., 2006a. Silicon isotope fractionation between plant parts in banana: In situ vs. in vitro. *Journal of Geochemical Exploration* **88**, 224-227.
- Opfergelt, S., Cardinal, D., Henriot, C., Draye, X., Andre, L., and Delvaux, B., 2006b. Silicon isotopic fractionation by banana (*Musa* spp.) grown in a continuous nutrient flow device. *Plant and Soil* **285**, 333-345.
- Page, B. D., Bullen, T. D., and Mitchell, M. J., 2008. Influences of calcium availability and tree species on Ca isotope fractionation in soil and vegetation. *Biogeochemistry* **88**, 1-13.
- Pich, A., Manteuffel, R., Hillmer, S., Scholz, G., and Schmidt, W., 2001. Fe homeostasis in plant cells: Does nicotianamine play multiple roles in the regulation of cytoplasmic Fe concentration? *Planta* **213**, 967-976.
- Poitrasson, F. and Freydier, R., 2005. Heavy iron isotope composition of granites determined by high resolution MC-ICP-MS. *Chemical Geology* **222**, 132-147.

- 
- Poitrasson, F., 2007. Does planetary differentiation really fractionate iron isotopes? *Earth and Planetary Science Letters* **256**, 484-492.
- Poitrasson, F., Viers, J., Martin, F., and Braun, J. J., 2008. Limited iron isotope variations in recent lateritic soils from Nsimi, Cameroon: Implications for the global Fe geochemical cycle. *Chemical Geology* **253**, 54-63.
- Polyakov, V. B., 1993. On ideality of isotope mixture in solids. *Russian Journal of Physical Chemistry* **67**, 422-425.
- Polyakov, V. B. and Mineev, S. D., 2000. The use of Mossbauer spectroscopy in stable isotope geochemistry. *Geochimica Et Cosmochimica Acta* **64**, 849-865.
- Powell, P. E., Cline, G. R., Reid, C. P. P., and Szaniszlo, P. J., 1980. Occurrence of hydroxamate siderophore iron chelators in soils. *Nature* **287**, 833-834.
- Rayleigh, L., 1902. On the distillation of binary mixtures. *Philosophical Magazine* **4**, 521-537.
- Reichard, P. U., Kraemer, S. M., Frazier, S. W., and Kretzschmar, R., 2005. Goethite dissolution in the presence of phytosiderophores: Rates, mechanisms, and the synergistic effect of oxalate. *Plant and Soil* **276**, 115-132.
- Reid, C. P. P. and Crowley, D. E., 1984. Utilization of iron by oat when supplied as ferrated synthetic chelate or as ferrated hydroxamate siderophore. *Journal of Plant Nutrition* **7**, 437-447.
- Robinson, N. J., Procter, C. M., Connolly, E. L., and Guerinot, M. L., 1999. A ferric-chelate reductase for iron uptake from soils. *Nature* **397**, 694-697.
- Rodriguez-Castrillon, J. A., Moldovan, M., Alonso, J. I. G., Lucena, J. J., Garcia-Tome, M. L., and Hernandez-Apaolaza, L., 2008. Isotope pattern deconvolution as a tool to study iron metabolism in plants. *Analytical and Bioanalytical Chemistry* **390**, 579-590.
- Roe, J. E., Anbar, A. D., and Barling, J., 2003. Nonbiological fractionation of Fe isotopes: evidence of an equilibrium isotope effect. *Chemical Geology* **195**, 69-85.
- Roemheld, V. and Marschner, H., 1986. Evidence for a Specific Uptake System for Iron Phytosiderophores in Roots of Grasses. *Plant Physiology* **80**, 175-180.
- Roemheld, V. and Schaaf, G., 2004. Iron transport in plants: Future research in view of a plant nutritionist and a molecular biologist. *Soil Science and Plant Nutrition* **50**, 1003-1012.
- Rosman, K. J. R. and Taylor, P. D. P., 1998. Isotopic compositions of the elements 1997. *Journal of Analytical Atomic Spectrometry* **13**, 45N-55N.
- Sah, R. N. and Mikkelsen, D. S., 1986. Effects of Anaerobic Decomposition of Organic-Matter on Sorption and Transformations of Phosphate in Drained Soils. 2. Effects on Amorphous Iron Content and Phosphate Transformation. *Soil Science* **142**, 346-351.

## 6 References

---

- Sattelmacher, B., Horst, W. J., and Becker, H. C., 1994. Factors That Contribute to Genetic-Variation for Nutrient Efficiency of Crop Plants. *Zeitschrift Für Pflanzenernährung Und Bodenkunde* **157**, 215-224.
- Sattelmacher, B., 2001. Tansley review no. 22 - The apoplast and its significance for plant mineral nutrition. *New Phytologist* **149**, 167-192.
- Schaaf, G., Ludewig, U., Erenoglu, B. E., Mori, S., Kitahara, T., and von Wirèn, N., 2004. ZmYS1 functions as a proton-coupled symporter for phytosiderophore- and nicotianamine-chelated metals. *Journal of Biological Chemistry* **279**, 9091-9096.
- Schauble, E. A., Rossman, G. R., and Taylor, H. P., 2001. Theoretical estimates of equilibrium Fe-isotope fractionations from vibrational spectroscopy. *Geochimica Et Cosmochimica Acta* **65**, 2487-2497.
- Schauble, E. A., 2004. Applying stable isotope fractionation theory to new systems. In: *Geochemistry of Non-Traditional Stable Isotopes. Reviews in Mineralogy & Geochemistry*. Mineralogical Society of America and Geochemical Society, Washington, **55**, 65-101.
- Schmidt, W., 1999. Mechanisms and regulation of reduction-based iron uptake in plants. *New Phytologist* **141**, 1-26.
- Schoenberg, R. and von Blanckenburg, F., 2005. An assessment of the accuracy of stable Fe isotope ratio measurements on samples with organic and inorganic matrices by high-resolution multicollector ICP-MS. *International Journal of Mass Spectrometry* **242**, 257-272.
- Schoenberg, R. and von Blanckenburg, F., 2006. Modes of planetary-scale Fe isotope fractionation. *Earth and Planetary Science Letters* **252**, 342-359.
- Schuth, S., Mansfeldt, T., Overesch, M., Greef, K., Hindersmann, I., and Münker, C. 2009. Iron isotope fractionation in soil suspensions at controlled redox conditions. *Geochimica Et Cosmochimica Acta* **73**, A1186.
- Schwertmann, U., 1973. Use of Oxalate for Fe Extraction from Soils. *Canadian Journal of Soil Science* **53**, 244-246.
- Schwertmann, U., 1991. Solubility and dissolution of iron oxides. *Plant and Soil* **130**, 1-25.
- Severmann, S., Johnson, C. M., Beard, B. L., and McManus, J., 2006. The effect of early diagenesis on the Fe isotope compositions of porewaters and authigenic minerals in continental margin sediments. *Geochimica Et Cosmochimica Acta* **70**, 2006-2022.
- Singh, A., Kaur, N. and Kosman, D. J., 2007. The metalloreductase Fre6p in Fe-Efflux from the yeast vacuole. *Journal of Biological Chemistry* **282**, 28619-28626.
- Skulan, J. L., Beard, B. L., and Johnson, C. M., 2002. Kinetic and equilibrium Fe isotope fractionation between aqueous Fe(III) and hematite. *Geochimica Et Cosmochimica Acta* **66**, 2995-3015.
- Staubwasser, M., von Blanckenburg, F., and Schoenberg, R., 2006. Iron isotopes in the early marine diagenetic iron cycle. *Geology* **34**, 629-632.

- 
- Stephan, U. W. and Scholz, G., 1993. Nicotianamine - Mediator of Transport of Iron and Heavy-Metals in the Phloem. *Physiologia Plantarum* **88**, 522-529.
- Stephan, U. W., Schmidke, I., Stephan, V. W., and Scholz, G., 1996. The nicotianamine molecule is made-to-measure for complexation of metal micronutrients in plants. *Biometals* **9**, 84-90.
- Strasser, O., Kohl, K., and Roemheld, V., 1999. Overestimation of apoplastic Fe in roots of soil grown plants. *Plant and Soil* **210**, 179-187.
- Stuerup, S., Hansen, H. R., and Gammelgaard, B., 2008. Application of enriched stable isotopes as tracers in biological systems: a critical review. *Analytical and Bioanalytical Chemistry* **390**, 541-554.
- Taiz, L. and Zeiger, E., 2002. *Plant Physiology*. Sinauer Associates, Sunderland, MA.
- Takagi, S., Nomoto, K., and Takemoto, T., 1984. Physiological Aspect of Mugineic Acid, a Possible Phytosiderophore of Gramineous Plants. *Journal of Plant Nutrition* **7**, 469-477.
- Taylor, P. D. P., Maeck, R., and Debievre, P., 1992. Determination of the absolute isotopic composition and atomic-weight of a reference sample of natural iron. *International Journal of Mass Spectrometry and Ion Processes* **121**, 111-125.
- Taylor, P. D. P., Maeck, R., Hendrickx, F., and Debievre, P., 1993. The Gravimetric Preparation of Synthetic Mixtures of Iron Isotopes. *International Journal of Mass Spectrometry and Ion Processes* **128**, 91-97.
- Tessier, A., Campbell, P. G. C., and Bisson, M., 1979. Sequential Extraction Procedure for the Speciation of Particulate Trace-Metals. *Analytical Chemistry* **51**, 844-851.
- Terry, N. and Abadia, J., 1986. Function of iron in chloroplasts. *Journal of Plant Nutrition* **9**, 609-646.
- Teutsch, N., von Gunten, U., Porcelli, D., Cirpka, O. A., and Halliday, A. N., 2005. Adsorption as a cause for iron isotope fractionation in reduced groundwater. *Geochimica Et Cosmochimica Acta* **69**, 4175-4185.
- Tiffin, L. O., 1966. Iron Translocation. 2. Citrate/Iron Ratios in Plant Stem Exudates. *Plant Physiology* **41**, 515-518.
- Thompson, A., Ruiz, J., Chadwick, O. A., Titus, M., and Chorover, J., 2007. Rayleigh fractionation of iron isotopes during pedogenesis along a climate sequence of Hawaiian basalt. *Chemical Geology* **238**, 72-83.
- Tripa, C. E., Pellin, M. J., Savina, M. R., Davis, A. M., Lewis, R. S., and Clayton, R. N., 2002. Fe isotopic compositions of presolar SiC mainstream grains. *Lunar Planetary Science*, XXXIII: 1975.
- Urey, H. C., 1947. The thermodynamic properties of isotopic substances. *Journal of the Chemical Society* **5**, 562-581.
- Vert, G., Grotz, N., Dedaldechamp, F., Gaymard, F., Guerinot, M. L., Briata, J. F., and Curie, C., 2002. IRT1, an Arabidopsis transporter essential for iron uptake from the soil and for plant growth. *Plant Cell* **14**, 1223-1233.

## 6 References

---

- Viers, J., Oliva, P., Nonell, A., Gelabert, A., Sonke, J. E., Freydier, R., Gainville, R., and Dupre, B., 2007. Evidence of Zn isotopic fractionation in a soil-plant system of a pristine tropical watershed (Nsimi, Cameroon). *Chemical Geology* **239**, 124-137.
- Voelkening, J. and Papanastassiou, D. A., 1989. Iron isotope anomalies. *Astrophysical Journal* **347**, L43-L46.
- von Blanckenburg, F., von Wirén, N., Guelke, M., Weiss, D. J., and Bullen, T., 2009. Fractionation of metal stable isotopes by higher plants. *Elements* **5**, 375-380.
- von Wirén, N., Klair, S., Bansal, S., Briat, J. F., Khodr, H., Shioiri, T., Leigh, R. A., and Hider, R. C., 1999. Nicotianamine chelates both Fe-III and Fe-II. Implications for metal transport in plants. *Plant Physiology* **119**, 1107-1114.
- Walczyk, T. and von Blanckenburg, F., 2002. Natural iron isotope variations in human blood. *Science* **295**, 2065-2066.
- Walczyk, T. and von Blanckenburg, F., 2005. Deciphering the iron isotope message of the human body. *International Journal of Mass Spectrometry* **242**, 117-134.
- Waters, B. M., Blevins, D. G., and Eide, D. J., 2002. Characterization of FRO1, a pea ferric-chelate reductase involved in root iron acquisition. *Plant Physiology* **129**, 85-94.
- Wedepohl, K. H., 1995. The composition of the continental crust. *Geochimica Et Cosmochimica Acta* **59**, 1217-1232.
- Weiss, D. J., Mason, T. F. D., Zhao, F. J., Kirk, G. J. D., Coles, B. J., and Horstwood, M. S. A., 2005. Isotopic discrimination of zinc in higher plants. *New Phytologist* **165**, 703-710.
- Weiss, D. J., Rehkämper, M., Schoenberg, R., McLaughlin, M., Kirby, J., Campbell, P. G. C., Arnold, T., Chapman, J., Peel, K., and Gioia, S., 2008. Application of nontraditional stable-isotope systems to the study of sources and fate of metals in the environment. *Environmental Science and Technology* **42**, 655-664.
- Welch, S. A., Beard, B. L., Johnson, C. M., and Braterman, P. S., 2003. Kinetic and equilibrium Fe isotope fractionation between aqueous Fe(II) and Fe(III). *Geochimica Et Cosmochimica Acta* **67**, 4231-4250.
- Weyer, S. and Schwieters, J., 2003. High precision Fe isotope measurements with high mass resolution MC-ICP-MS. *International Journal of Mass Spectrometry* **226**, 355-368.
- Weyer, S., Anbar, A. D., Brey, G. P., Munker, C., Mezger, K., and Woodland, A. B., 2005. Iron isotope fractionation during planetary differentiation. *Earth and Planetary Science Letters* **240**, 251-264.
- WHO, 2003. The World Health report 2002. *Midwifery* **19**, 72-73.
- Wiederhold, J. G. and von Blanckenburg, F., 2002. Iron isotope variations in a complete natural soil catena with lateral iron mobilization and reprecipitation. *Geochimica Et Cosmochimica Acta* **66**, A834.



- 
- Wiederhold, J. G., Kraemer, S. M., Teutsch, N., Borer, P. M., Halliday, A. N., and Kretzschmar, R., 2006. Iron isotope fractionation during proton-promoted, ligand-controlled, and reductive dissolution of goethite. *Environmental Science & Technology* **40**, 3787-3793.
- Wiederhold, J. G., Teutsch, N., Kraemer, S. M., Halliday, A. N., and Kretzschmar, R., 2007a. Iron isotope Fractionation during pedogenesis on redoximorphic soils. *Soil Science Society of America Journal* **71**, 1840-1850.
- Wiederhold, J. G., Teutsch, N., Kraemer, S. M., Halliday, A. N., and Kretzschmar, R., 2007b. Iron isotope fractionation in oxic soils by mineral weathering and podzolization. *Geochimica Et Cosmochimica Acta* **71**, 5821-5833.
- Wiegand, B. A., Chadwick, O. A., Vitousek, P. M., and Wooden, J. L., 2005. Ca cycling and isotopic fluxes in forested ecosystems in Hawaii. *Geophysical Research Letters* **32**, L11404.
- Wiesli, R. A., Beard, B. L., and Johnson, C. M., 2004. Experimental determination of Fe isotope fractionation between aqueous Fe(II), siderite and "green rust" in abiotic systems. *Chemical Geology* **211**, 343-362.
- Woodhead, J. D., 2006. Isotope ratio determination in the earth and environmental sciences: Developments and applications in 2004/2005. *Geostandards and Geoanalytical Research* **30**, 187-196.
- Yang, X. E., Chen, W. R., and Feng, Y., 2007. Improving human micronutrient nutrition through biofortification in the soil-plant system: China as a case study. *Environmental Geochemistry and Health* **29**, 413-428.
- Young, E. D., Galy, A., and Nagahara, H., 2002. Kinetic and equilibrium mass-dependent isotope fractionation laws in nature and their geochemical and cosmochemical significance. *Geochimica Et Cosmochimica Acta* **66**, 1095-1104.
- Zhang, C. D., Roemheld, V., and Marschner, H., 1996. Remobilization of iron from primary leaves of bean plants grown at various iron levels. *Journal of Plant Nutrition* **19**, 1017-1028.
- Ziegler, E. E. and Filer, L. J., 1996. *Present knowledge in nutrition*, 7th ed. Washington, DC: ILSI Press.



---

## Lebenslauf

**Monika Stelling, geb. Gülke**

monika.stelling@googlemail.com

---

### PERSÖNLICHE ANGABEN

geboren am 10. November 1979 in Hannover

deutsche Staatsangehörigkeit

verheiratet, ein Kind

---

### SCHULBILDUNG

1986-1990      Grundschule Hannover-Ahlem

1990-1992      Orientierungsstufe Hannover-Ahlem

1992-1999      Wilhelm-Raabe-Schule Hannover

Abschluss: Allgemeine Hochschulreife (Abitur)

---

### HOCHSCHULAUSSCHULUNG

1999-2000      Leibniz Universität Hannover, Studiengang: Chemie

2000-2005      Leibniz Universität Hannover, Studiengang: Geowissenschaften

Abschluss: Diplom-Geowissenschaftlerin (Dipl.-Geow.)

2005-2010      Leibniz Universität Hannover, Promotion Geowissenschaften

---

### BERUFLICHE TÄTIGKEIT

2010-            wissenschaftliche Angestellte am Institut für Mineralogie und Geochemie  
des Karlsruher Instituts für Technologie (KIT)

2005-2009      wissenschaftliche Angestellte am Institut für Mineralogie  
der Leibniz Universität Hannover

---

### ELTERNZEIT

2009            Elternzeit

## Publikationen

**Guelke, M.**, von Blanckenburg, F., Staubwasser, M., Schoenberg, R. & Stuetzel, H. (2010) Determining the stable iron isotope signature of plant-available iron in soils. *Chemical Geology*, 277 (3-4), 269-280.

von Blanckenburg, F., von Wirén, N., **Guelke, M.**, Weiss, D. & Bullen, T. (2009) Fractionation of metal stable isotopes by higher plants. *Elements*, 5 (6), 375-380.

**Guelke, M.** & von Blanckenburg, F. (2007) Fractionation of stable iron isotopes in higher plants. *Environmental Science & Technology*, 41 (6), 1896-1901.

## Tagungsbeiträge

**Guelke, M.**, Scheuermann E., von Blanckenburg F., von Wirén N. & Schoenberg R. (2007) Stable isotope fingerprinting of iron metabolism in higher plants. *Geochimica Et Cosmochimica Acta* 71 (15), A362 (Goldschmidt Conference Abstract Supplement).

**Guelke M.**, von Blanckenburg F., Schoenberg, R. & Staubwasser, M. (2006) Iron isotope fractionation in higher plants, *EOS Trans.* 87 (52), AGU Fall Meet. Suppl., Abstract H1310-14C.

**Guelke, M.**, von Blanckenburg, F., Schoenberg, R. & Stuetzel, H. (2006) Discrimination of stable Fe isotopes in strategy I and II plants. 13th International Symposium on Iron Nutrition and Interactions in Plants, July 3-7, 2006 - Montpellier, France.

**Guelke, M.**, von Blanckenburg, F. & Schoenberg R. (2006) Discrimination of stable iron isotopes in higher plants. Beiheft zum *European Journal of Mineralogy* - DMG Conference Abstracts 18, 51.

**Guelke, M.**, von Blanckenburg F., Schoenberg, R. & Stuetzel, H. (2005) Iron isotope fractionation in higher plants. *Schriftenreihe der Deutschen Gesellschaft für Geowissenschaften*, 39, 143.